This is to certify that the

dissertation entitled

Factors Affecting Deterioration of Transverse Cracks
In Jointed Reinforced Concrete Pavement (JRCP)

presented by

Zafar Iqbal Raja

has been accepted towards fulfillment
of the requirements for

_____Ph.D.___ degree in Civil & Env. Engineering

Major professor

Date August 2, 1991

O-12771

PLACE IN RETURN BOX to remove this checkout from your record.
TO AVOID FINES return on or before date due.

DATE DUE	DATE DUE	DATE DUE
MAR 1 5 1994		
MAR 1 5 1994		
MAR 1 3 1995		
AUG C 5 2008		
11 07 08		

MSU is An Affirmative Action/Equal Opportunity Institution

FACTORS AFFECTING DETERIORATION OF TRANSVERSE CRACKS

IN JOINTED REINFORCED CONCRETE PAVEMENT (JRCP)

BY

ZAFAR IQBAL RAJA

A DISSERTATION

submitted to

Michigan State University

in partial fulfillment of the requirements

for the degree of

DOCTOR OF PHILOSOPHY

Department of Civil and Environmental Engineering

1991

ABSTRACT

FACTORS AFFECTING DETERIORATION OF TRANSVERSE CRACKS
IN JOINTED REINFORCED CONCRETE PAVEMENT (JRCP)

By

Zafar Iqbal Raja

Transverse cracks in Jointed Reinforced Concrete
Pavement (JRCP) deteriorate due to loss of aggregate
interlock load transfer capacity. This thesis presents a
synthesis of factors that may reduce aggregate interlock
load transfer and describes the design, conduct, and results
of experimental research conducted to evaluate the relative
effects of several material and design factors on transverse
crack deterioration in JRCP. The work involved the
collection and analysis of load transfer data from cracks
that have been induced in a series of large-scale reinforced

concrete slab test specimens and are subjected to repeated applications of loads simulating the passage of heavy truck traffic.

The test variables selected for the study included type of coarse aggregate, gradation of coarse aggregate, treatment of coarse aggregate (virgin, recycled, and blend), amount of slab tension and foundation support.

Results obtained show that the slabs cast using crushed limestone and natural gravel graded to meet Michigan Department of Transportation (MDOT) specification 6A (1.5-in. [4-cm] top size, coarser gradation) performed comparably while specimens cast using similarly graded slag deteriorated much more rapidly. It has also been observed that the use of more finely graded gravels meeting MDOT specification 17A (1.0-in. [2.5-cm] top size, finer gradation) resulted in a performance only slightly poorer than that of the larger gravel. Test results also indicate that the specimens cast using 100% recycled gravel concrete (6A Gradation) or a blend of recycled gravel concrete (6A Gradation) and large crushed limestone (MDOT Gradation 4A: 2.5-in. [6-cm] top size) performed only slightly better than the slag specimen.

It was observed that increase in the amount of slab tension significantly decreased the load transfer efficiency and endurance. Test results also suggest that the amount of temperature steel currently used in Michigan JRCP (0.16% by area of concrete) may be insufficient to endure the combined effects of repeated truck traffic and environmental loads.

Finally, the test results indicate that transverse crack load transfer efficiency and endurance increases with increases in foundation stiffness.

To my Parents,

my wife Ameelia , and

daughters Hina and Nida

ACKNOWLEDGEMENTS

TABLE OF CONTENTS

LIST OF TABLES

LIST OF FIGURES

CHAPTER I

INTRODUCTION

1.1 Problem Statement

Jointed reinforced concrete pavement (JRCP) typically develops transverse cracks over the first several years of its service life as contractions of the slab (caused by combinations of drying and thermal shrinkage) are restrained by friction between the slab and supporting layers. Transverse cracks may also be initiated by combinations of curling, warping, and load-related stresses. Most JRCP designs rely on *grain* or *aggregate interlock* to transfer shear loads across these cracks. These cracks deteriorate with time and traffic due to loss of aggregate interlock load transfer capacity.

The loss of aggregate interlock due to opening of these cracks permits increased slab deflections, and the infiltration of water and intrusion of incompressibles into the cracks. These, in turn, lead to pumping and crack deterioration through faulting and spalling. Continued pumping eventually leads to a loss of support beneath the

1

slabs, which greatly increases load-related stresses in the slab and can result in fatigue cracking. Thus, transverse cracks must exhibit good long-term load transfer characteristics to minimize the development and severity of distresses described above.

It was recently observed that some of the recently-constructed JRCP in Michigan were exhibiting rapid transverse crack deterioration (spalling and faulting), which may lead to increased maintenance requirements and shortened service lives [1]. These newer JRCP contained important design modifications including, most notably, use of small-sized recycled concrete aggregates, and an open-graded untreated aggregate base course [2]. A preliminary evaluation of the causes of rapid deterioration of these cracks indicated that a combination of poor aggregate interlock (due to use of small-sized recycled concrete aggregate), increased slab tension (due to the open-graded base course and improperly functioning load transfer dowel bars at transverse joints), high deflections (due to soft support) and heavy traffic may be the major causes of crack deterioration. Many of these factors have not yet been evaluated in the context of JRCP transverse crack performance. The relative impacts of the above factors on JRCP transverse crack performance need to be quantified and documented to develop improved design guidelines and specifications for future JRCP design and construction.

1.2 Objective

The overall objective of this study is to advance the state-of-the-knowledge on the subject of aggregate interlock load transfer across transverse cracks in JRCP. The specific purpose of this comparative laboratory study was to estimate the effects of several material and design variables on the aggregate interlock load transfer characteristics of transverse cracks in JRCP.

Specific objectives include:-

1. Identify factors that may affect deterioration of transverse cracks in JRCP.

2. Develop and execute a laboratory experiment to evaluate the impact of selected factors on the performance of transverse cracks in JRCP.

3. Recommend construction materials that provide good load transfer across transverse cracks.

4. Recommend design modifications to improve the overall performance of JRCP.

5. Recommend variables for additional testing.

1.3 Scope

This study incorporated examination of existing literature on the topic and a laboratory experiment involving collection and analysis of load transfer data from

the testing of a series of large-scale reinforced slab test specimens that are subjected to repeated applications of loads simulating the passage of heavy truck traffic.

An extensive review of literature of previous field and laboratory studies aimed at evaluation of aggregate interlock load transfer characteristics of transverse cracks and weakened-plane transverse joints was conducted to identify variables that significantly affect the load transfer through aggregate interlock. This information and recent Michigan Department of Transportation (MDOT) experience (as described above) was used as a basis for selection of the laboratory study factors.

Due to *financial* and *time restraints* a <u>single-factor comparative experimental design</u> was employed to obtain estimates of main effects only. This approach reduced the number of specimens that must be tested while quickly providing usable results and a solid foundation for future expansion of research.

CHAPTER II

BACKGROUND

2.1 Load Transfer Across Transverse Cracks

The ability of transverse cracks/joints to transfer load is a major factor in the structural performance of the crack or joint and the surrounding slabs. This ability, typically referred to as load transfer efficiency, can be described in different ways, including deflection load transfer efficiency and stress load transfer efficiency. Several formulae for computing load transfer efficiency have been adopted by various researchers; the definitions referred to in this thesis are presented below:

$$\%LT = d_{UL}/(d_{UL} + d_L) \times 100 \text{ [3]} \qquad (\text{Eq. } 2.1)$$

$$\%LT = 2 \times d_{UL}/(d_{UL} + d_L) \times 100 \text{ [4,5,21]} \qquad (\text{Eq. } 2.2)$$

where

$\%LT$ = percent load transfer

d_{UL} = deflection of unloaded side of the crack or joint

5

d_L = deflection of loaded side of the crack or joint

Note that in the first formula (Eq. 2.1), the maximum load transfer that can be achieved is 50%. This is obtained when the two slabs deflect an equal amount.

In this study, the following definition was used to compute the load transfer efficiency based on deflection. This formula was preferred for its conceptual simplicity and ease of application.

$$\%LTE = (d_{UL}/d_L) \times 100 \quad [23] \tag{Eq. 2.3}$$

where

   $\%LTE$ = percent load transfer efficiency

   d_{UL} = deflection of unloaded side of the crack or joint

   d_L = deflection of loaded side of the crack or joint

Note that in the above formula, the maximum theoretical load transfer that can be achieved is 100%. This is obtained when the two sides deflect an equal amount. On the other extreme, if the two sides move with complete independence, the load transfer efficiency would be zero.

Load transfer efficiency based on stress can be computed using formulae similar to those described above for load transfer based on deflection. Sutherland and Cashell [6] used the following definition to compute load transfer efficiency based on stress

$$E = (f_f - f_j)/(f_f - f_i) \quad [6]$$

(Eq. 2.4)

where

E = joint efficiency

f_f = stress for a given load applied at a free edge

f_j = stress for a given load applied at the crack
    or joint edge

f_i = stress for a given load applied at the slab
    interior

Most JRCP designs rely on aggregate or grain interlock
to achieve the necessary load transfer capacity across
transverse cracks. Deterioration of these cracks has been
shown to be strongly related to loss of load transfer
efficiency. Therefore, a discussion of the mechanisms and
models of aggregate interlock is presented in the succeeding
paragraphs.

2.2 Aggregate Interlock Mechanism

Aggregate interlock is the simplest means of load
transfer; the protrusions in one fractured face mesh with
the recesses in the other to provide shear resistance along
the fractured face. At the time of crack development, the
vertical surfaces of the crack are usually rough and
irregular. The majority of the coarse aggregate particles
typically remain embedded in either of the crack faces. As a
wheel approaches a crack, differential vertical displacement

of the two slab fragments take place, causing the particles of one face of the crack to come into contact with the matrix of the other face. Further differential vertical movement is then restricted by the bearing and friction of the aggregate particles along the crack surface. A portion of the wheel load is "transferred" from one side of the crack to the other through the shear developed by the interlocking action of the aggregate particles at the fractured faces of the crack. This is commonly referred to as aggregate or "grain" interlock.

Substantial shear forces can be transmitted through this mechanism provided these cracks remain tight. JRCP typically contains a small amount of longitudinal reinforcement, often referred to as *temperature and shrinkage reinforcement*, to help to ensure that these cracks do not open appreciably.

2.3 Aggregate Interlock Models

Several models have been proposed to explain the aggregate interlock mechanism. One model [10] distinguishes between interlock due to *local roughness* and to *global roughness* of the crack face (Figure 2.1). It is postulated that local roughness (or micro texture) results from interlocking of the fine aggregate particles, which is principally a bearing or crushing action, and that global roughness (or macro texture) results from interlocking of coarse aggregate particles, principally a sliding and overriding action. Local roughness is believed to be
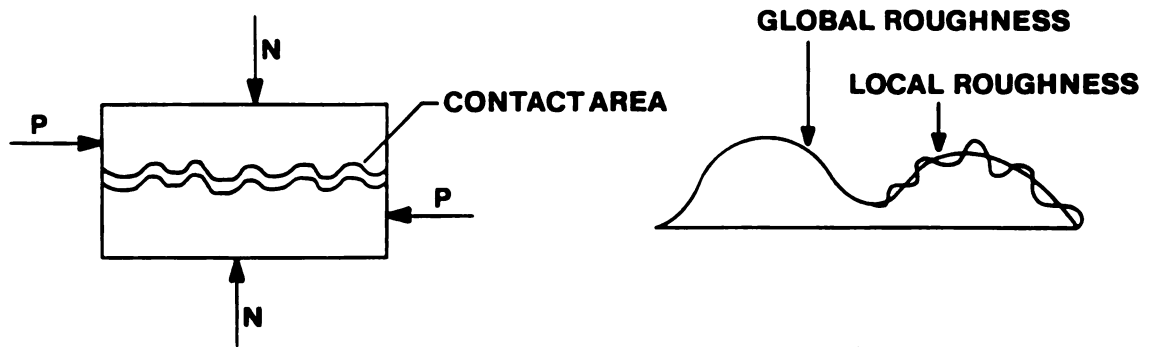
LOCAL-GLOBAL ROUGHNESS MODEL

Figure 2.1: Local/Global roughness model of aggregate interlock mechanism [10]

responsible for most aggregate interlock effects when crack widths are less than 0.01 inches. It is further postulated that the effects of local roughness predominate in the early loading cycles and that global roughness predominates in later cycles as crack widths increase and local roughness is reduced.

An alternative model proposes that aggregate interlock is due to the sliding resistance of two rigid surfaces. These surfaces have been represented by a sawtooth shape (Figure 2) [11] and by a series of parabolic segments [12].

A more recent model [13] suggests that concrete is a two-phase material of aggregate and cement matrix, which can be modelled as a distribution of rigid spheres of a range of sizes embedded to various depths within a deformable rigid-plastic matrix (Figure 2.3). In this model, shear forces are resisted by a combination of crushing and sliding of the rigid spheres into and over softer cement matrix; contact and interaction between spheres projecting from opposite crack face is not considered.

Millard and Johnson [14] devised a laboratory test to examine aggregate interlock and to determine whether any of the theoretical models could be verified. Their aggregate interlock test results do not support the local/global roughness and frictional sliding models. However, they found a fairly consistent agreement between the test results and the two-phase model. These researchers concluded that " *the aggregate interlock test results show that the two-phase model, involving a combination of crushing and sliding of the crack faces, is the most realistic one"* [14].
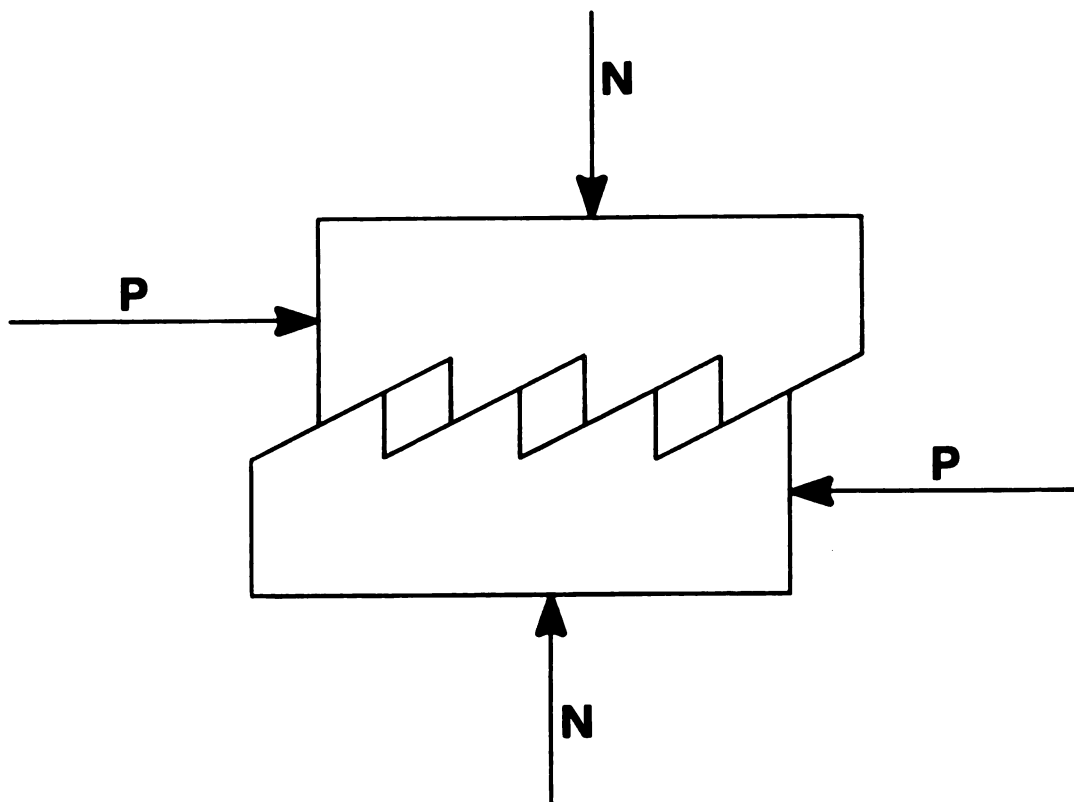
SHEAR-FRICTION MODEL

Figure 2.2: Frictional sliding model of aggregate interlock mechanism [11, 12]

CEMENT MATRIX   AGGREGATE SPHERE

GENERAL STRUCTURE OF CRACK PLANE
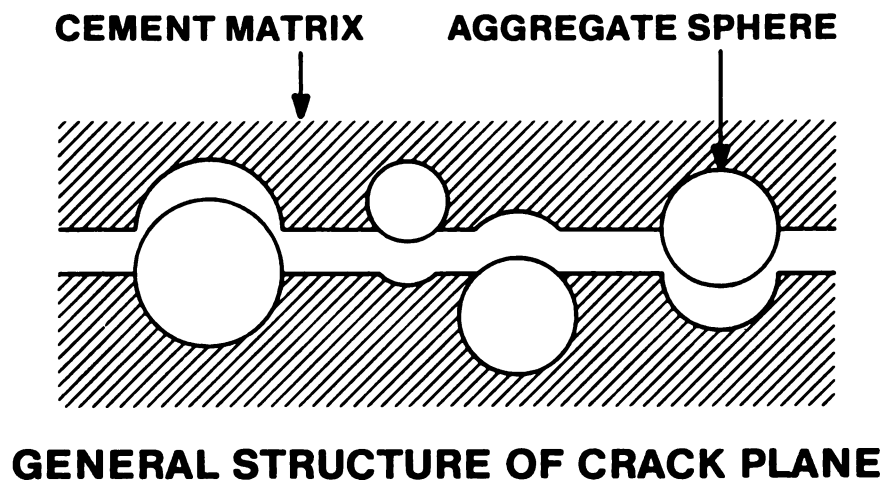
Figure 2.3: Two-phase model of aggregate interlock mechanism [13]

CHAPTER III

SUMMARY OF AGGREGATE INTERLOCK
LOAD TRANSFER RESEARCH

3.1 Aggregate Interlock Performance

An extensive review of the literature reveals that the development of load transfer through aggregate interlock has been studied by several researchers since the early 1900's. However, with the exception of a field study conducted by Michigan State Highway Department [3] to evaluate the aggregate interlock load transfer across reinforced transverse cracks, most of these previous studies were concerned with weakened-plane transverse joints. These previous studies have shown that a few variables predominantly affect development and endurance of load transfer through aggregate interlock. These variables include width of crack opening and texture of the crack face.

13

3.1.1 *Effect of the Width of Crack Opening*

The results of previous investigations have clearly established the *"width of crack opening"* as having the most pronounced effect on the load transfer capacity of transverse cracks/joints through aggregate interlock. Benkelman [3] showed that opening these cracks by as little as 0.03 inches produces a loss of load transfer of 50% (Figure 3.1). Colley and Humphrey [4] also observed a similar trend in their studies of aggregate interlock behavior (Figure 3.2). These researchers found that *"when test load, slab thickness, and subbase were held constant, joint effectiveness decreased as the joint opening was increased" [4]*. Nowlen [5] reported a loss of 45%-55%, for the same amount of opening, depending on maximum size of aggregate. Similarly, studies by Darter, et al [16] have shown that the drop in load transfer is from 20% to 60% for 0.03 inch openings depending upon the level of support provided by the foundation. A numerical study by Soroushian, et al [15] also indicated that the stiffness and ultimate strength of aggregate interlock decreases significantly with increases in crack width. This loss of load transfer capacity results from a loss of contact between the two slab fragments, requiring some differential vertical movement of the slab fragments before contact and bearing can take place.

Thus, for these cracks to exhibit good load transfer
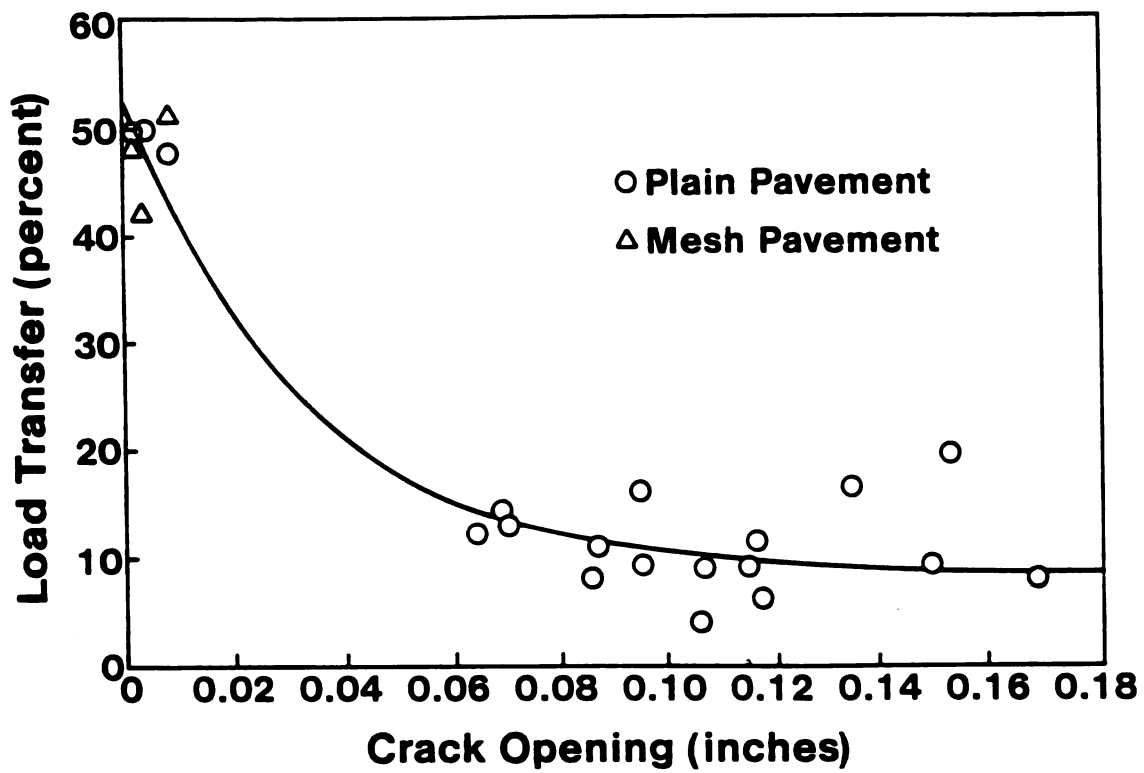
Figure 3.1: Relation of crack opening and per cent of load transferred (from Eq. 1) [3]
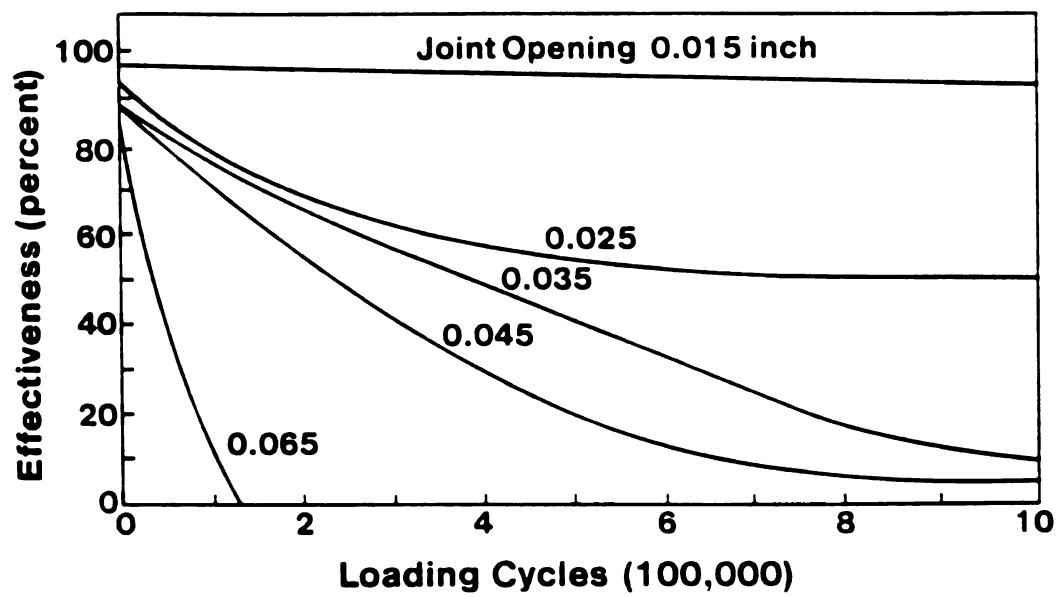
Figure 3.2: Influence of joint opening on effectiveness percent (from Eq. 2) [4]

characteristics, it is imperative that reinforcement must serve its intended purpose, i.e., *hold the fractured concrete in close interlock.*

The results of Benkelman's study effectively illustrated the impact of reinforcement on load transfer capacity of transverse cracks (Figure 3.3). This figure shows that a smaller percentage of load is transferred across cracks in plain concrete than across those in pavement containing reinforcement even during the summer months. Moreover, plain concrete cracks undergo a significant <u>drop</u> in load transfer from summer to fall due to the seasonal opening of these cracks while properly reinforced sections experience practically no loss of load transfer during the cold months. Thus, Benkelman concluded that *"when roughened edges of two slabs are held firmly together the aggregate interlock may be expected to function perfectly and permanently as a load-transfer medium"* [3].

3.1.2 *Effect of the Texture of the Crack Face*

The aggregate interlock load transfer capacity of transverse cracks/joints has been shown to be related to the texture of the crack face. The crack face texture is primarily a function of the type, size and number of the coarse aggregate particles, the maturity of the concrete at the time of fracture, and the strength of concrete. Angular, rough-surfaced aggregates (such as crushed stone) generally
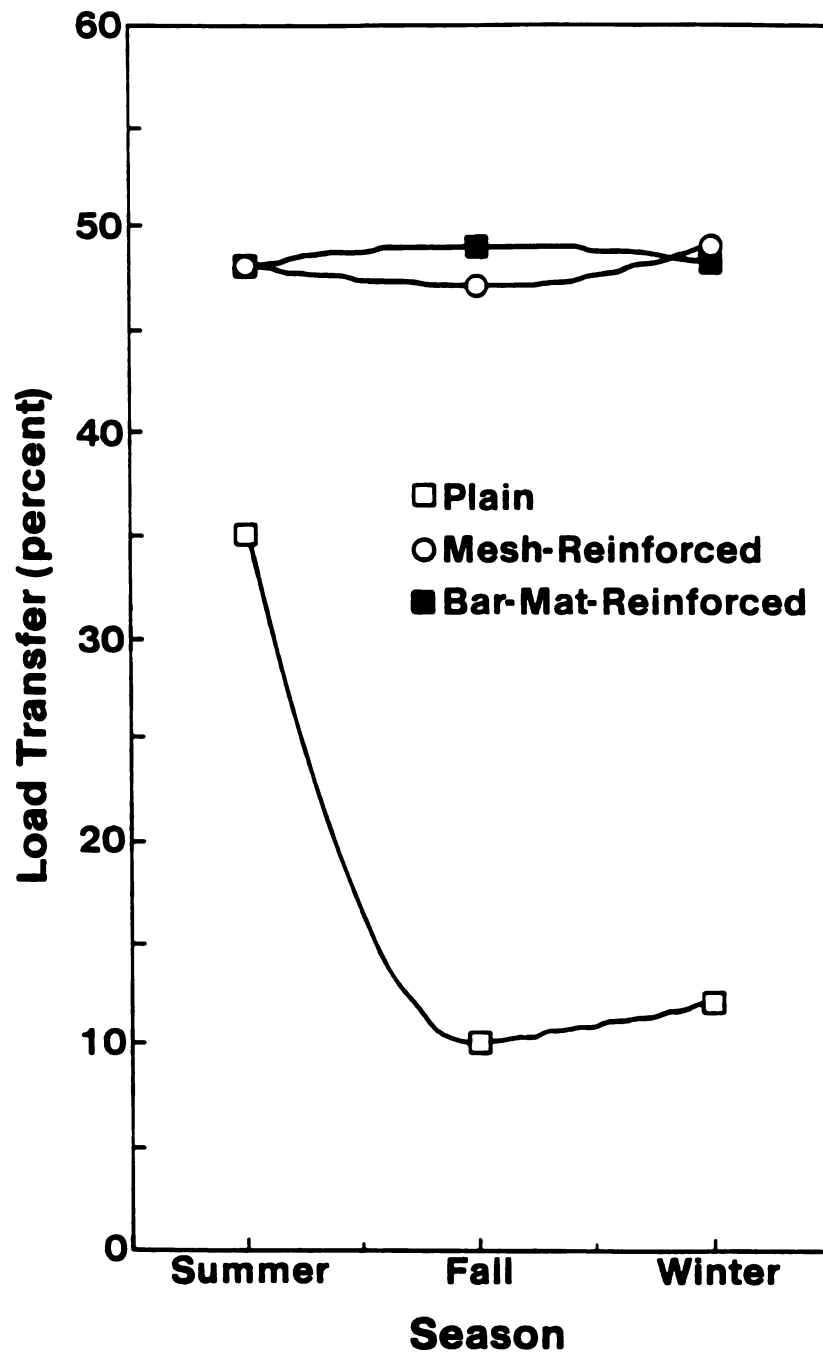
Figure 3.3: Illustration of restraining effect of reinforcement on load transfer capacity of transverse cracks, after [3]

provide better interlock and load transfer over narrow crack openings than rounded, smooth-surface aggregates (such as natural gravels). This contention is supported by the results of a study by Colley and Humphrey [4] which indicate that concretes made using crushed limestone and crushed gravel coarse aggregates had higher load transfer effectiveness values than those made with natural rounded gravels.

The key factor which determines the texture of the crack face is the *mode of concrete fracture*. Depending on the bond strength, concrete may fracture in two different ways i.e., fracture <u>around</u> the aggregate or fracture <u>through</u> the aggregate. When concrete fractures around the aggregate many pullouts of aggregate particles exist resulting in a rough interface. The results of the Nowlen study [5] show that early fracture (i.e., when the aggregate-paste bond is relatively weak) results in many pullouts. However, at later times of cracking concrete strength has increased, and pullouts are diminished because of higher aggregate-paste bond strengths resulting in more numerous aggregate fractures. The study concluded that *"for equal joint openings early fracture of the joint faces with resulting aggregate pullouts contributed to high effectiveness initially, and also to endurance of good effectiveness under repeated loads"* [5].

When coarse aggregate fractures occur during the crack formation, the advantages of angular, rough-surfaced aggregate are largely lost because fracture of aggregate

results in a smoother crack face. Sutherland and Cashell [6] found that concretes made using natural round gravel had better aggregate interlock load transfer characteristics than concretes made using similarly graded crushed limestone. They attributed the greater load transfer efficiency of the joints in concrete made using rounded gravel to develop aggregate projections along the crack face, which resulted from the poorer aggregate-paste bond which allowed aggregates to pull out of the matrix rather than fracture. Concretes made using crushed stone tended to crack through the aggregate, producing a smoother crack face and lower levels of interlock load transfer efficiency.

Sutherland and Cashell [6] and Nowlen [5] also studied the effect of coarse aggregate size on the performance of load transfer through aggregate interlock. The results of these studies agree that large coarse aggregates provide more interlock and higher load transfer efficiencies than small coarse aggregates, particularly for large joint openings (Figure 3.4 and 3.5). However, these figures also show that, although load transfer efficiency generally increases with increasing aggregate size, load transfer efficiency decreases very rapidly with increasing joint width, regardless of aggregate size. Sutherland and Cashell concluded that *"aggregate interlock was effective in stress control when the joints were closed or under compression, but that it was not dependable when the joints opened 0.037 in. or more irrespective of the type or maximum size of aggregate in concrete"* [6].
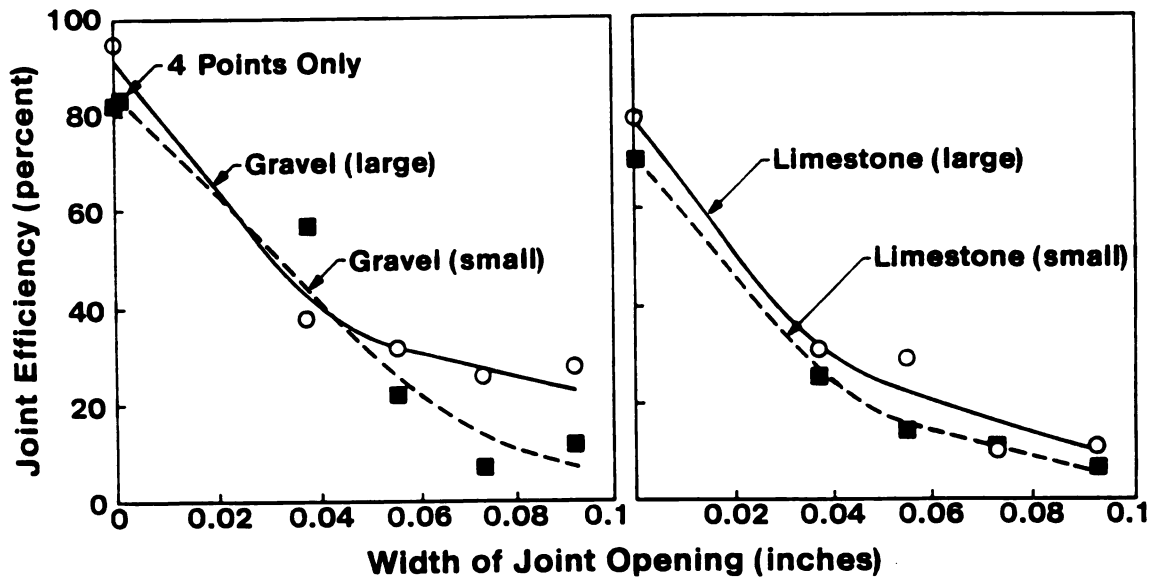
Figure 3.4: Effect of size of coarse aggregate on the relation between joint opening and joint efficiency [6]
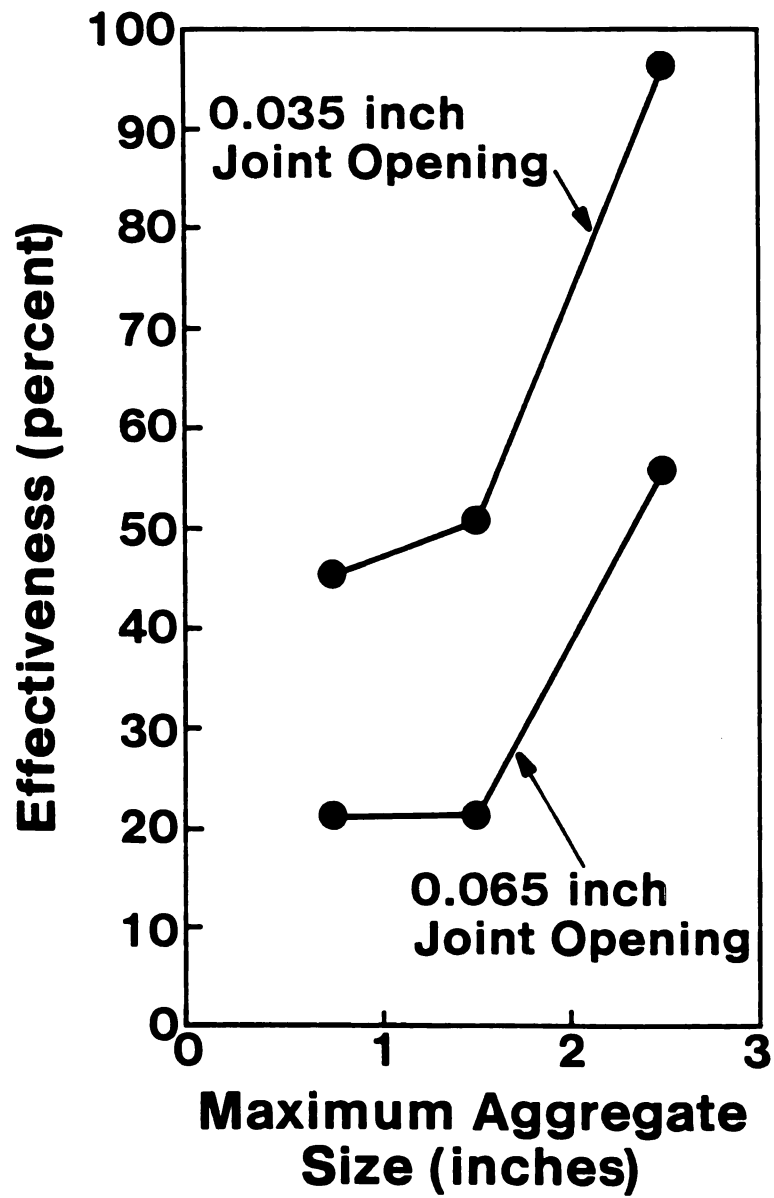
Figure 3.5: Influence of aggregate size on joint effectiveness [5]

The resistance of the crack faces against shear displacements is also affected by the compressive strength of concrete. Studies have shown that increasing the concrete compressive strength considerably increased the aggregate interlock stiffness and ultimate strength [14,15]. It was suggested that when increases in concrete compressive strength are due at least in part to increases in the matrix strength, resistance against contact area deformations is also larger so that higher shear stiffnesses are obtained.

3.2 Aggregate Interlock Endurance

Maintenance of adequate load transfer through aggregate interlock over a large number of heavy truck load applications is critical to the satisfactory long-term performance of JRCP. The interlocking features of cracks and joints can be worn through repeated slippage and abrasion of the two vertical faces under accumulated load applications. It follows that hard materials that are resistant to abrasion should provide good load transfer effectiveness longer than soft materials that abrade easily. Nowlen [5] confirmed the above contention through a study which found that the slabs built with aggregates with good abrasion resistance (Los Angeles Abrasion Loss Values (LA) = 17 and 28) were superior in effective endurance to slabs built with aggregates having poor abrasion resistance (LA = 46).

Colley and Humphrey [4] found that load transfer effectiveness decreases as the number of load applications

increases. They noted, however, that 90% of the decrease occurs during the first 500,000 load repetitions. These researchers introduced the concept of an Endurance Index, EI, which represents, the ability of a joint or crack to retain load transfer effectiveness under load repetitions. The following model was developed to predict Endurance Index as a function of the most significant variables in their test program:

$$EI = 230 \ h\sqrt{k}/Pw \qquad\qquad\qquad \text{(Eq. 4)}$$

where

EI = endurance index,

h = depth of roughened interface, in.,

k = foundation modulus, psi/in.,

P = wheel load, Ibs., and

w = joint opening, in.

The endurance index defined above is particularly sensitive to variations in foundation strength and joint openings, as shown in Figure 3.6 and 3.7. For example, increasing the k-value of the foundation from 90 to 450 psi/in., increases the endurance index by a factor of about 2.6 times for a 7 in. slab and about 2 times for a 9 in. slab. This increase in EI is due to the fact that strong foundation support reduces the magnitude of the differential vertical deflections, thereby allowing the application of
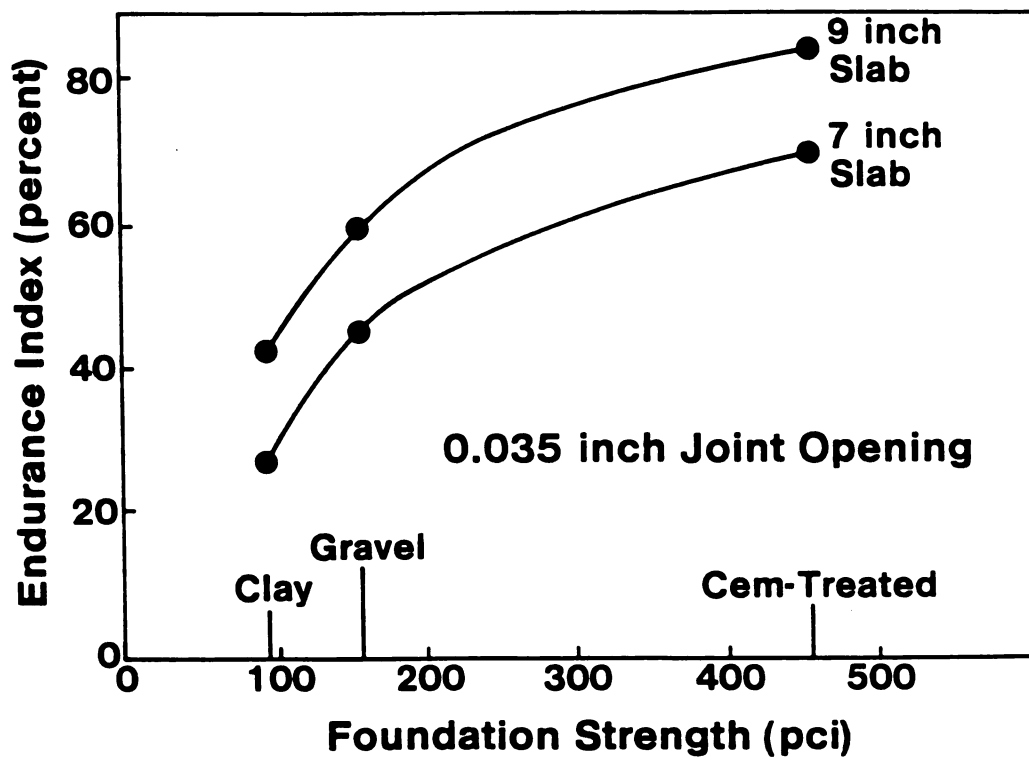
Figure 3.6: Effect of foundation strength on endurance index [4]

more load cycles to produce a given loss of interlock and load transfer. This finding was verified numerically by Ioannides and Korovesis [9]. Figure 3.7 shows that EI decreases as joint opening increases. For example, increasing the joint opening from 0.025 in. to 0.065 in. decreases the EI by a factor of about 6 for a 7 in. slab and by a factor of about 3 for a 9 in. slab.

3.3 Summary

In summary, studies conducted to date have indicated a large number of variables that may have some impact on the rate of deterioration of load transfer capacity through aggregate interlock of transverse cracks and joints in JRCP. Variables that significantly affect the load transfer through aggregate interlock include (but may not be limited to):

1. Width of crack opening

2. Restraining impact of reinforcement (% steel)

3. Type of coarse aggregate

4. Size of coarse aggregate

5. Paste-aggregate bond strength

6. Compressive strength of concrete

7. Hardness of coarse aggregate (abrasion resistance)

8. Applied load magnitude

9. Applied load repetitions

10. Foundation support

11. Depth of roughened interface (interlocking area)
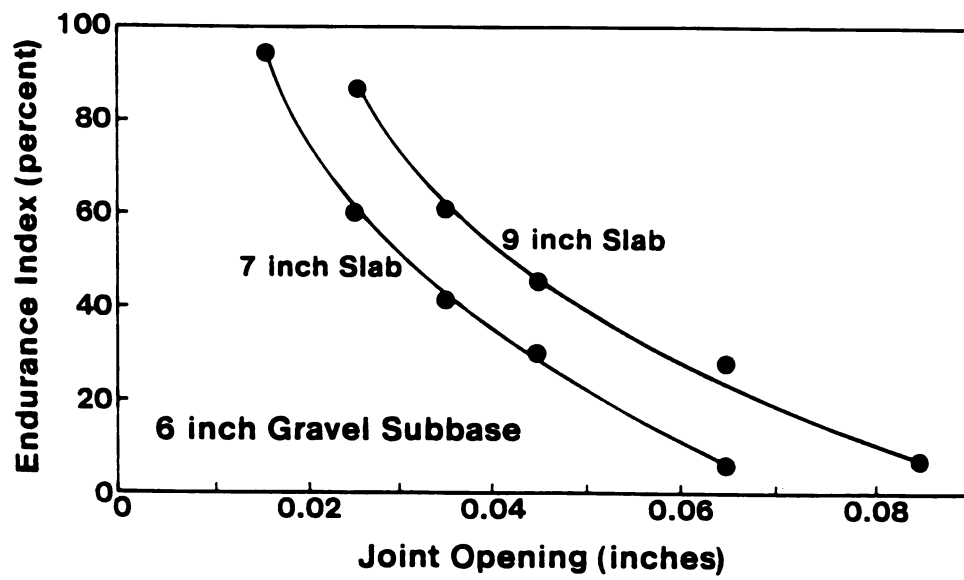
Figure 3.7: Effect of joint opening on endurance index [4]

CHAPTER IV

LABORATORY STUDY FACTORS

4.1 Research Needs

Past research efforts, with the exception of the Benkelman study [3], have been directed only at the evaluation of weakened-plane transverse joints. Transverse joints are designed to allow horizontal slab movements and are thus *different* in design and function from transverse cracks in JRCP, which contain steel reinforcement that is intended to hold these cracks tight and restrict horizontal movements. Because of these design and functional differences, different variables affect the performance of joints and cracks. For example, the opening and failure of reinforced cracks are influenced by the design and performance of the reinforcing steel. Abrasion and attrition of the aggregates, daily and seasonal temperature variations, as well as the presence of nonfunctional transverse joints (due to misaligned or corroded dowels or malfunctioning dowel assemblies), and the presence of expansion joints, can also produce excessive crack

28

movements. Many of these factors have not been evaluated in the context of transverse crack performance.

The performance of steel reinforcement in keeping JRCP transverse cracks from opening has historically been quite variable. While many JRCP cracks remain tight throughout the pavement design life, there have been many documented cases of steel rupture, suggesting that the coefficient of friction or interlock between the slab and subbase may be much higher than traditionally assumed values. For example, temperature reinforcement is typically designed to withstand the stresses that would be produced in the presence of a subbase friction coefficient of 1.5 to 2 without allowing excessive crack opening. However, some types of granular and stabilized bases have been found to produce much higher levels of friction or interlock with the paving slab [24]. This higher friction increases the slab and steel tension, which may cause permanent elongation or rupture of steel and opening of the transverse cracks. The above facts suggest that research efforts should be directed toward better characterization of the effects of slab tension and reinforcement on the performance of reinforced transverse cracks that are subjected to repeated heavy loads.

Another variable that merits further research is the effect of foundation support on crack load transfer capacity and endurance. A cracked slab supported on a fairly stiff foundation will experience little differential vertical movement across the cracks, even if they open substantially. However, pavements built upon softer or unstable foundations

can be expected to exhibit poor crack load transfer efficiency endurance. This factor is suspected of playing a major role in the rapid deterioration of cracks on at least one construction project [1]. Further research will help to quantify the role that foundation support plays in JRCP crack deterioration.

Previous research has not addressed some key issues which face pavement engineers today. For example, current pavement design often calls for the use of smaller top size aggregates (e.g., 3/4" or less) as part of an effort to improve pavement *durability*. However, rapid deterioration of transverse cracks has been observed in many recently-constructed JRCP containing *small-sized coarse aggregate* [1]. Cores taken at some of these projects have shown very straight vertical crack faces with very little roughness or meander. In many cases, the crack face has been ground almost to a sandpaper finish, indicating that very little, if any, mechanical interlock will exist across even a tight crack [1]. Such conditions reduce the vertical shear capacity of these cracks to near zero and can result in accelerated crack deterioration (i.e., spalling, faulting, and pumping) under repeated heavy traffic load applications. Additional research must be devoted to determining the role of aggregate top size and gradation in the deterioration of reinforced transverse cracks.

High-quality aggregates suitable for use in highway construction are in short supply at many locations. One source of potentially high-quality aggregates is the

recycling of the concrete pavements that are in need of reconstruction. Coarse aggregates produced by recycling old pavements are often crushed to smaller sizes to improve the durability of the new pavement (especially if the old pavement exhibited durability-related distresses). These aggregates may also exhibit very different bonding characteristics with the cement paste due to local variations in the water-cement ratio caused by the non uniform (and sometimes high) moisture absorption characteristics of these aggregates. Furthermore, these aggregates may fracture differently (and more readily) than natural aggregates, producing unusual crack face textures. A number of projects constructed using *small-sized recycled coarse aggregate* have developed transverse cracks that deteriorated rapidly [1]. Further study is needed to determine the effects of using various quantities of recycled concrete containing different types and gradations of virgin aggregate.

4.2 Research Variables

In light of the research need described above, a comparative laboratory study was undertaken to estimate the relative impacts of several material and design factors (Table 4.1) on the aggregate interlock load transfer characteristics of transverse cracks in JRCP.

A full-factorial, unreplicated experimental design using these variables and test levels would require 72 test

Table 4.1: Laboratory Study Factors

Variable	Test Level		
	1	2	3
MATERIAL FACTORS			
CA Type	Gravel	Limestone	Slag
CA Gradation	6A	17A	-
CA Treatment	Virgin	Recycled Blend	100% Recycled
DESIGN FACTORS			
Slab Tension	Typical	High	-
Foundation Support	100 psi/in	250 psi/in	-

Notes:

1. 6A gradation: (1.5-in. [4-cm] top size, coarser gradation)

2. 17A gradation: (1.0-in. [2.5-cm] top size, finer gradation)

3. Recycled blend: 50-50 blend of 6A recycled gravel concrete with 4A (2.5-in. [6-cm] top size) crushed limestone

4. 100% recycled gravel concrete - graded to meet MDOT 6A specification

5. Typical slab tension = 3500 lb/ft width [51 KN/m width] (coefficient of friction = 1.5)

6. High slab tension = 7000 lb/ft width [102 KN/m width] (coefficient of friction = 3.0)

specimens. Because of financial and time constraints, only 10 test specimens have been run to failure as of this writing. The 10 runs involved 8 different treatments from the 72 making up the complete factorial design. The data on different treatments allow for the estimation of main effects and no interactions, and the data from the replications provide an estimate of pure error. This fractional factorial approach was chosen to provide results that are usable and a foundation for further expansion of the research.

6A virgin gravel, typical slab tension and the foundation modulus of 100 psi/in were selected as nominal standard conditions because they represent typical field conditions. Thus, this treatment combination was chosen to be replicated for the purpose of estimating the pure error coming from fixed experimental conditions. Moreover, contrasts from other treatments relative to this control treatment were of special interest.

For material factors, the "reference" or "control" cell is the cell in matrix A (Figure 4.1) that calls for 6A virgin gravel. The results of all other material test factor combinations were compared to the results of this cell. For design factors, the control cell is the cell in matrix D (Figure 4.4) that calls for typical slab tension and a foundation modulus of 100 psi/in with the material combination being 6A virgin gravel. The results for all other design factors were compared to the results of this cell.

Figures 4.1 - 4.5 show the levels of the five factors being investigated through this experiment. Table 4.2 shows the treatment combinations and the order of the tests that were run. Because the test stand required modifications and recalibration after Test No. 6, it was necessary to block the experimental results. This blocking was not anticipated, and it caused a loss of one degree of freedom in the estimate of pure error. Detailed descriptions of the data analysis are presented in Chapter 6 and APPENDIX C.

MATRIX A

CA TYPE	GRAVEL	X
	LIMESTONE	X
	SLAG	X

Notes:

1. X = Test cell being tested under matrix A

2. All coarse aggregates conform to MDOT gradation 6A

3. Foundation modulus = 100 psi/in.

4. Slab tension = 3500 lb/ft width [51 KN/m width] (modelling an assumed coefficient of friction = 1.5, slab length = 41 ft [12.5 m], crack face depth = 9-in. [23-cm])

5. Longitudinal steel = 0.16% by area of concrete

Figure 4.1: Test matrix A

MATRIX B

CA GRADATION	6A	A
	17A	X

Notes:

1. A = Test cell first filled in matrix A

2. X = Test cell being tested under matrix B

3. Aggregate type gravel

4. Foundation modulus = 100 psi/in.

5. Slab tension = 3500 lb/ft width [51 KN/m width]
   (coefficient of friction = 1.5, slab length =
   41 ft [12.5 m], crack depth = 9-in. [23-cm])

6. Longitudinal steel = 0.16% by area of concrete

Figure 4.2: Test matrix B

MATRIX C

	VIRGIN	**A**
CA TREATMENT	**RECYCLED BLEND**	**X**
	100% RECYCLED	**X**

Notes:

1. A = Test cell first filled in matrix A

2. X = Test cell being tested under matrix C

3. Foundation modulus = 100 psi/in.

4. Slab tension = 3500 lb/ft width [51 KN/m width] (coefficient of friction = 1.5, slab length = 41 ft [12.5 m], crack face depth = 9-in. [23 cm])

5. Longitudinal steel = 0.16% by area of concrete

Figure 4.3: Test matrix C

MATRIX D

Slab Tension	Typical	X	X
	High	X	

Notes:

1. X = Test cell being tested under matrix D

2. Foundation modulus = 100 psi/in.

3. Typical Slab tension = 3500 lb/ft width [51 KN/m width] (coefficient of friction = 1.5, slab length = 41 ft [12.5 m], crack face depth = 9-in. [23-cm])

4. High Slab tension = 7000 lb/ft width [102 KN/m width] (coefficient of friction = 3.0, slab length = 41 ft [12.5 m], crack face depth = 9-in. [23-cm])

5. Longitudinal steel = 0.16% by area of concrete

6. Coarse aggregate, virgin gravel meeting MDOT specification 6A

Figure 4.4: Test matrix D

MATRIX E

Foundation	100 psi/in	D D
Modulus	250 psi/in	X

Notes:

1. D = Test cell first filled in matrix D

2. X = Test cell being tested under matrix E

3. Coarse aggregate, virgin gravel meeting MDOT specification 6A

4. Slab tension = 3500 lb/ft width [51 KN/m width] (coefficient of friction = 1.5, slab length = 41 ft [12.5 m], crack face depth = 9-in. [23-cm])

5. Longitudinal steel = 0.16% by area of concrete

Figure 4.5: Test matrix E

Table 4.2: Treatment combinations run in the experiment

Test		Material Factors			Design Factors	
No.	Block	Type	Gradation	Treatment	Tension	Foundation
1	1	Gravel	6A	Virgin	Typical	100 psi/in
2	1	Limestone	6A	Virgin	Typical	100 psi/in
3	1	Slag	6A	Virgin	Typical	100 psi/in
4	1	Gravel	17A	Virgin	Typical	100 psi/in
5	1	Gravel	6A	100% Recycled	Typical	100 psi/in
6	1	Gravel	6A	50-50 Blend	Typical	100 psi/in
7	2	Gravel	6A	Virgin	Typical	100 psi/in
8	2	Gravel	6A	Virgin	Typical	100 psi/in
9	2	Gravel	6A	Virgin	High	100 psi/in
10	2	Gravel	6A	virgin	Typical	250 psi/in

CHAPTER V

EXPERIMENTAL PROGRAM

5.1 Test Equipment

For this research it was necessary to develop equipment to apply repetitive loads of known magnitude across a transverse crack in a manner closely simulating field loading conditions. A test setup was developed similar to the apparatus used in the joint load transfer research conducted by Teller and Cashell in the 1950's [21], Colley and Humphrey in the 1960's [4], Ball and Childs, and Ciolko and Colley in the 1970's [18,19]. The test stand (shown in Figure 5.1 and 5.2) consists of three basic components and is described below.

5.1.1 *Test Specimen Loading System*

The test stand allows the application of a known repetitive load profile to the test specimen. This is accomplished using a pair of hydraulic actuators (11-kip

41
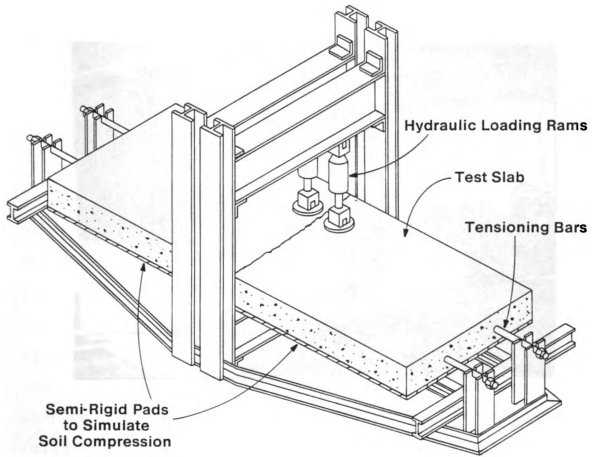
Figure 5.1: An isometric view of the test stand
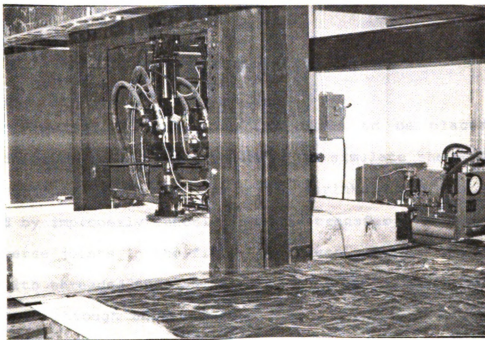
Figure 5.2: Test stand

[5000-kg] capacity) which react against a structural steel frame (see Figure 5.3). The load is transmitted to the test specimen by a pair of 12-in. [30-cm] diameter, 1.0-in. [2.54-cm] thick steel plates, each resting on a 1/4-in. [5/8-cm] contact rubber pad. The plates are positioned on each side of the crack with their centers 7-in. [18-cm] from the crack and 18-in. [46-cm] from the slab edge.

5.1.2 *Test Specimen Tensioning System*

The test stand allows the slabs to be placed in tension prior to and during testing to simulate the effects of resistance to thermal and drying shrinkage and restraint caused by improperly functioning load transfer dowel bars at transverse joints in the field. To induce tension, two steel rods with threaded ends anchored in each end of the slab are connected through threaded couplings to crossplates at the end columns (see Figure 5.4). Tightening the nuts on the threaded ends places the slab in tension; this tension is carried through steel at the transverse crack. This system also helps to reduce movement of the slabs under dynamic loads and helps to simulate the continuity of longer slabs in the field.

5.1.3 *Test Specimen Support System*

The test stand provides approximately uniform support for the specimen through the use of an artificial foundation
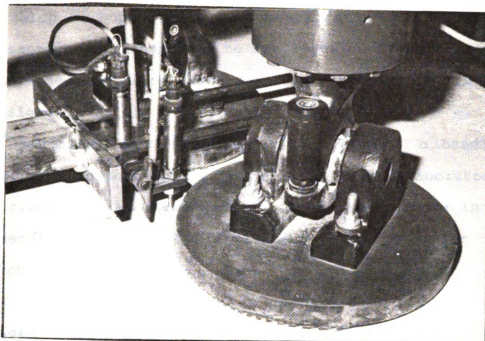
Figure 5.3: Test specimen loading system
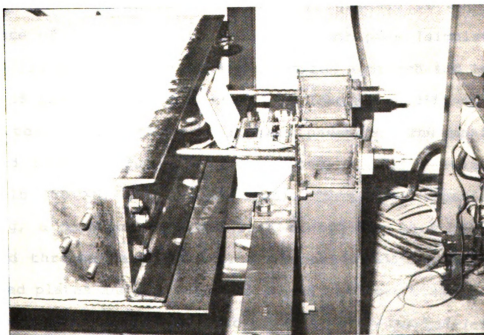
Figure 5.4: Test specimen tensioning system

(neoprene vibration isolation padding) resting on a steel plate which is supported by structural steel sections. The steel sections are connected to the reaction frame in such a way that the test frame absorbs the simulated truck loadings in tension.

In addition, test specimen casting frames, a handling frame (for transporting the large slabs in the laboratory), and a cracking frame (for inducing transverse cracks in the specimens) were designed, fabricated, and erected for this research work.

5.2 Load Simulation

5.2.1 *Loading due to Truck Traffic*

The hydraulic actuators were programmed to apply a sequence of load pulses to rubber contact pads (simulating 12 in. [30 cm] tire imprint areas) on the approach and leave sides of the crack to simulate field loading conditions for the outer wheel path of a highway pavement. The maximum applied load was 9000 lbs [40 KN] (one-half of a standard 18000-lb [80 KN] single-axle load). Throughout repetitive loading, a minimum sustained load of 500 lbs [2.3 KN] was applied through each actuator to maintain contact between the load plates and the slab throughout the test program.

A composite sinusoidal load profile was generated (using MTS T/RAC software) to simulate a wheel crossing the crack at 55 mph [88 km/hr]. To simulate a wheel approaching a

crack,
from
second
the st
simil
dynami
vices
improv
accos
movin
is rev
approa
load
repea
resul
allow

5

resul
resis
cause
trans
the t
heavy
subgr
dropp

crack, the load applied to the approach side is increased from the static load to the peak dynamic load in 0.0125 seconds. The load on the approach side is then reduced to the sustained load while the load on the departure side is simultaneously increased from the sustained load to the peak dynamic load in 0.0125 seconds. This cross-over interval of 0.0125 second would permit a tire making a 12-in. [30-cm] imprint and travelling 55 mph [88 km/hr] to move completely across the crack (see Figure 5.5). To simulate a wheel moving away from the crack, the load on the departure side is reduced to the sustained load in 0.0125 second while the approach load is held at the sustained load. The sustained load is then maintained for 0.175 second before the cycle is repeated. Thus, one full load cycle takes 0.2 second, resulting in a load application frequency of 5 Hz. This allows the application of 432,000 load cycles per day.

5.2.2 *Loading due to Environment*

Each test specimen is placed in tension just prior to testing to simulate the effects of foundation frictional resistance to thermal and drying shrinkage and restraint caused by improperly functioning load transfer dowel bars at transverse joints in the field. This slab tension may open the transverse cracks, exacerbating the effects of repeated heavy loads. The amount of tension was computed from subgrade drag theory for an assumed coefficient of frictional resistance of 1.5 and for a 9-in. thick [23-cm]

Load (lbs)

N
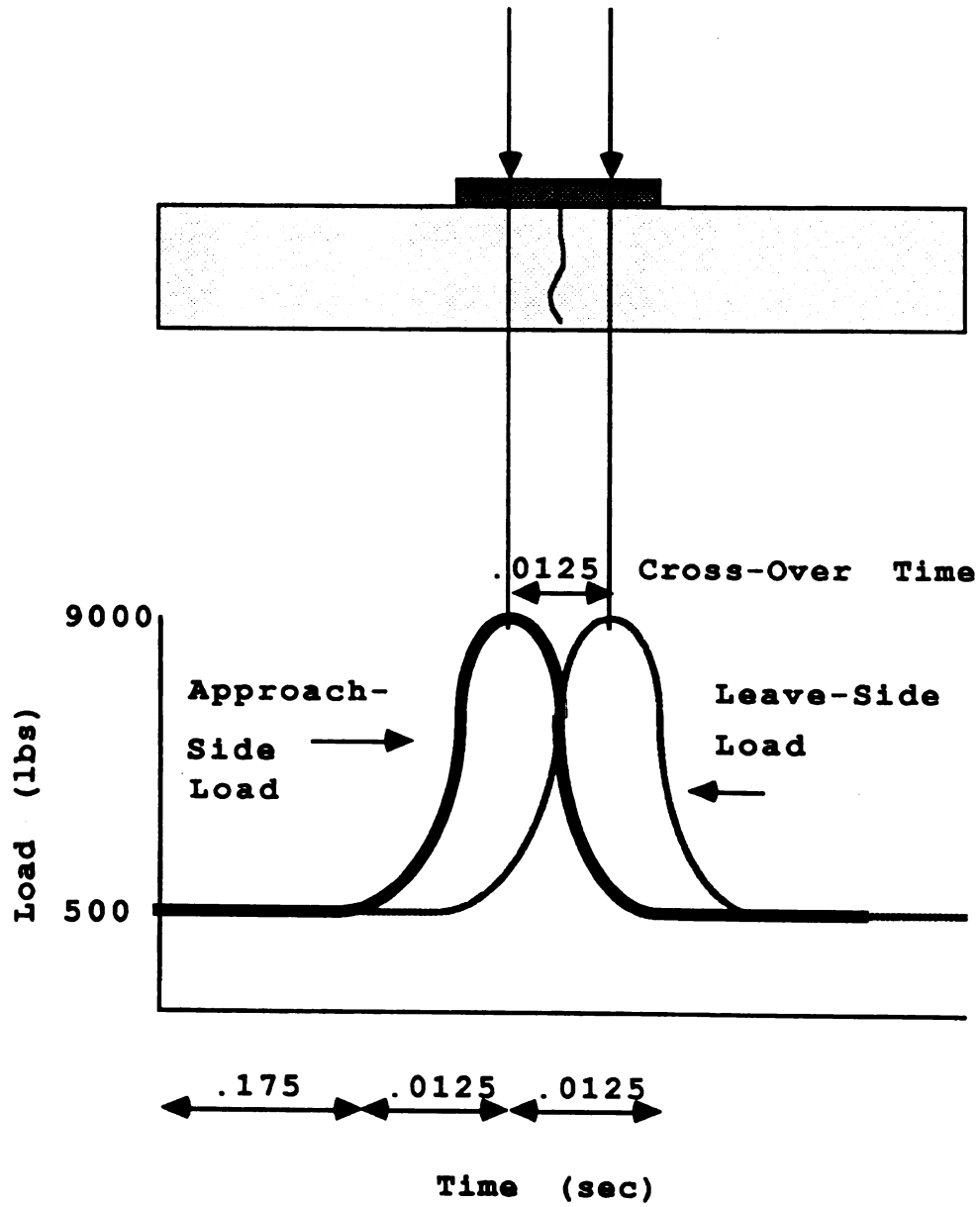
Figure 5.5: Load Profile

slab measuring 41 ft [12.5 m] in length by 4.5 ft [1.4 m] wide. A tension of approximately 16000 lbs [71.3 KN] (3500 lb/ft width) [51 KN/m width] was induced in the test specimens by adjusting the two tensioning bars embedded in each test specimen and monitoring tension bar strain with the strain gages. To study the effects of high amount of tension one specimen was tensioned to 32000 lbs [142.6 KN] (7000 lb/ft width) [102 KN/m width], simulating an assumed coefficient of frictional resistance of 3.0.

5.3 Instrumentation and Data Collection

Test specimens were instrumented for measurements of crack openings, deflections under loading, and tensile strains (tensioning). Instrument locations are shown in Figure 5.6. Gage plugs and a vernier caliper were used to monitor crack openings. Linearly variable deflection transducers (LVDT's) were used for measuring deflections on either side of the crack. General purpose CEA-series strain gages were used to measure strain in the tensioning bars, thereby monitoring the amount of tension in the specimen.

All testing and data collection operations were controlled using a 286-based personal computer equipped with a data acquisition system (Metrabyte I/O board and Labtech Notebook software). This system was connected directly to the hydraulic actuator control panel (MTS T/RAC controller) and signal conditioners. The arrangement, shown in Figure 5.7, allowed the coordinated control of both hydraulic
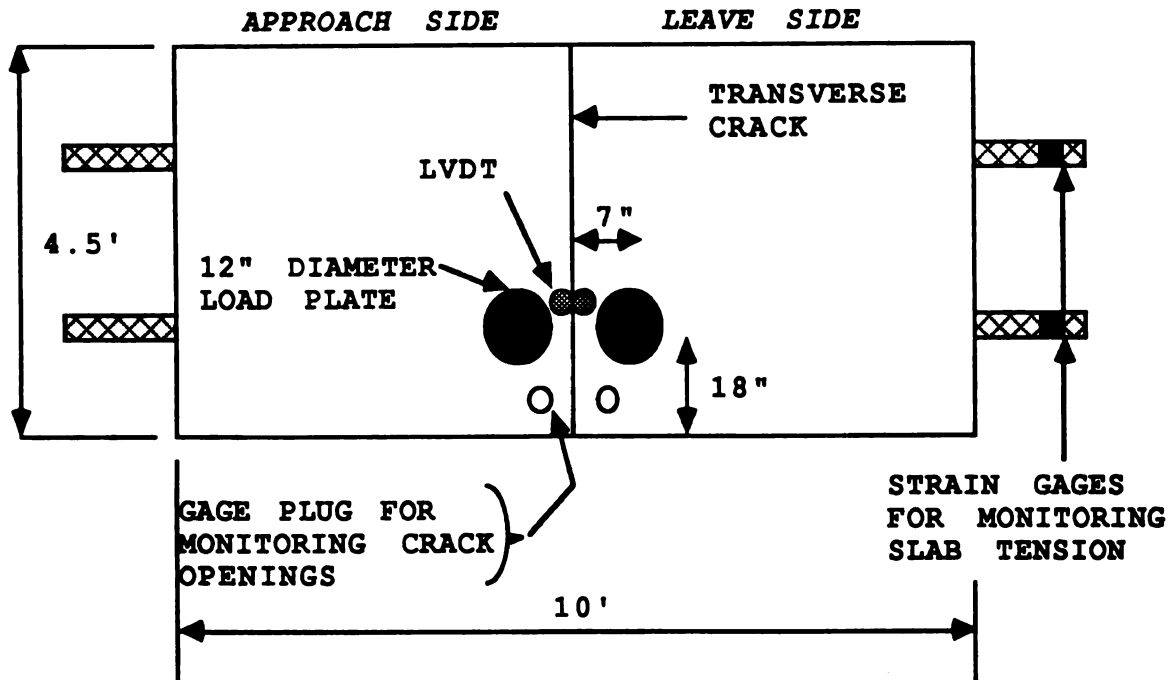
Figure 5.6: Test specimen instrumentation

286-PC


```
┌─────────────────────────────────────────────────────────┐
│   ┌─────────────────────────────────────────┐           │
│   │         MTS  T/RAC  SYSTEM               │           │
│   │   Test  Definition  &  Control  System   │◄──────────┼──
│   └─────────────────────────────────────────┘           │
│       ┌─────────────────────────────────┐               │
│       │      LABTECH  NOTEBOOK           │               │
│       │   Data  Acquisition  Software    │               │
│       └─────────────────────────────────┘               │
│   ┌─────────────────────────────────────────────────────┐
│   │ DAS-HRES  16  Bit  Analog  and  Digital  I/O  Board │
│   └─────────────────────────────────────────────────────┘
└─────────────────────────────────────────────────────────┘
```

T/RAC Controller

Command Generation and Feedback optimization Unit

LVDT Signal Conditioners

Analog Servocontrollers

LVDT'S

HYDRAULIC ACTUATORS
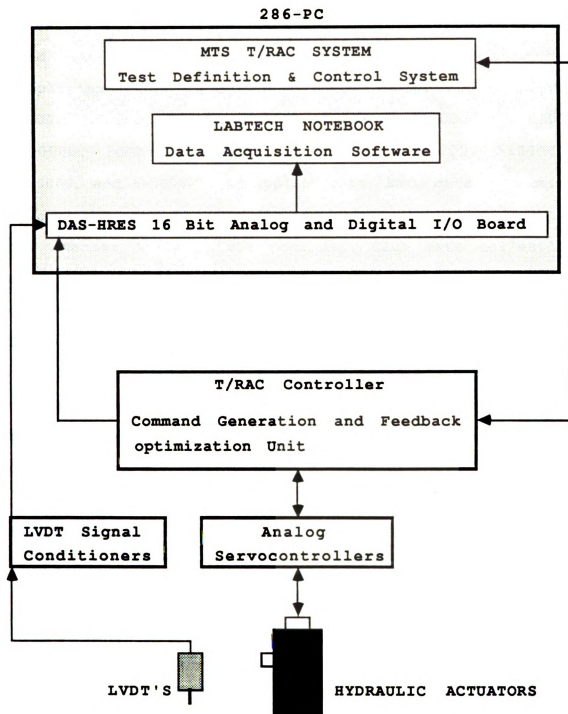
Figure 5.7: Test control and data acquisition setup

actuators, as well as the collection of load data from both actuators and deflection data from two external LVDT's. The load and deflection data were collected following the completion of 1, 1000, 2000, 5000, 10000, 20000, 50000, 100000, 300000, 600000, 900000, 1200000, 1500000, 1800000, 2400000, 3000000, 3600000, 4200000, 4800000, 5400000, 6000000, and 6600000 load applications. Each data collection channel was sampled 250 times per load cycle (about 1 sample per channel every 0.0008 seconds). Each data collection stage lasted one second (5 load cycles). This sampling rate and stage duration provided sufficiently close data points for plotting smooth curves and identifying peak loads and deflections (see Figure 5.8 and APPENDICES A and B). In this thesis, unless otherwise noted, all data pertaining to loads and relative deflections are based on the average of 5 sets of measurements.

5.4 Test Materials

5.4.1 *Artificial Foundation*

Each test specimen was provided approximately uniform support through the use of an artificial foundation (FABCEL vibration isolation padding rated at specific "k" values). Since it is difficult to reproduce foundation properties accurately and consistently using real granular materials and this can introduce variability in test results, it was decided to use artificial material for the foundation
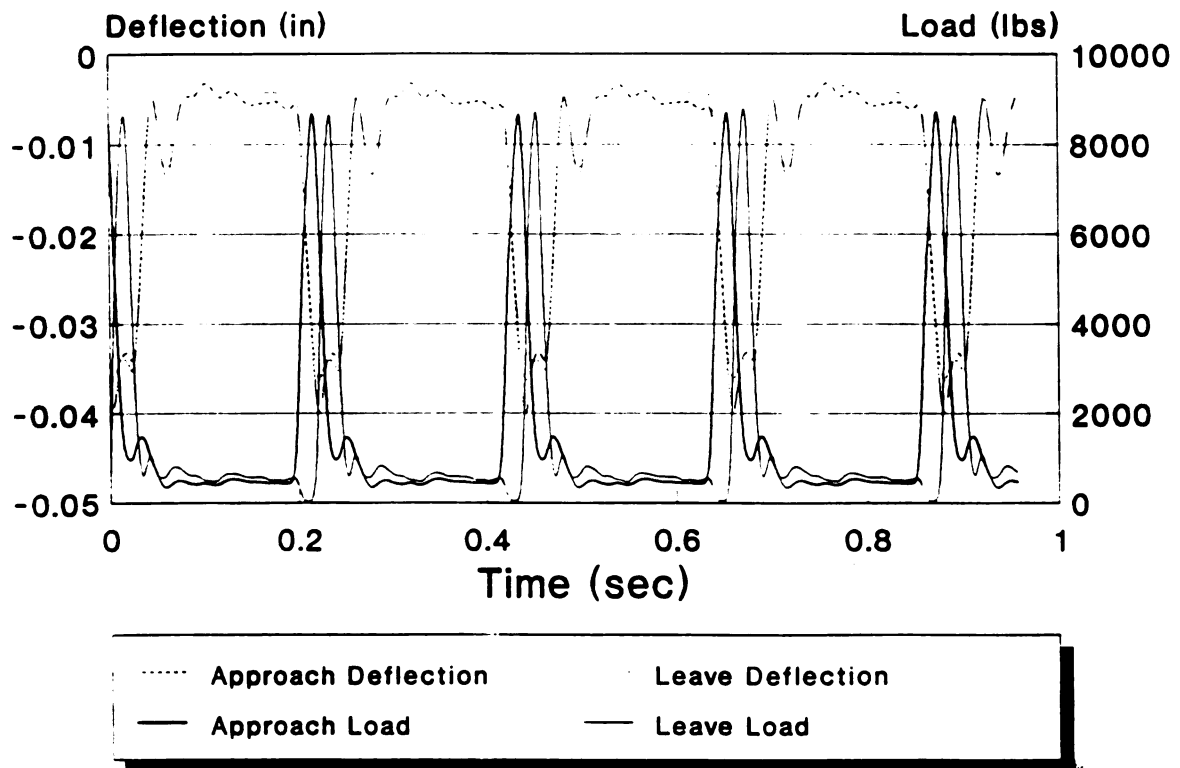
Figure 5.8: A plot of a data collection run

support. FABCEL is a high quality neoprene, molded into scientifically designed pads measuring 18" x 18" x 5/16" [46 cm x 46 cm x 3/4 cm]. The pad surfaces have molded recessed offset-cells to allow the neoprene to deform under load while maintaining lateral stability. Desired levels of foundation support are achieved by providing various thickness and type combinations of these pads. Three layers of FABCEL-25 were used to provide a foundation with a simulated modulus of subgrade reaction of approximately 100 psi/in [27 Kpa/m] under the entire test specimen. Two layers of FABCEL-25 were used under the high foundation specimen to simulate a modulus of subgrade reaction of approximately 250 psi/in [68 Kpa/m].

5.4.2 *Portland Cement Concrete Slabs*

The test specimens were PCC slabs measuring approximately 10 ft [12.5 m] long by 4.5 ft [1.4 m] wide and 9-in. [23-cm] thick at the crack. The cracks were of the plane-of-weakness type where load transfer is achieved solely by aggregate interlock. Each specimen contained 8 ft x 4 ft [2.8 m x 1.2 m] of smooth steel wire mesh reinforcment (0.16% by area of concrete longitudinally) placed 3-in. [7.5-cm] below the slab surface. This reinforcment was typical of the size, quantity and type used in Michigan JRCP construction.

The test program required the design of six concrete mixes for material factor specimens and four concrete mixes

for design factor specimens. Mix designs provided by MDOT (mortar voids method of proportioning) were used as a starting point for trial batching to reach a final mix design (target slump 2-3 inches, air content 6-7 percent). Type I portland cement was used in each mix (cement factor of approximately six sacks per cubic yard of concrete). Air entrainment was provided through the addition of Microair air-entraining admixture. Tables 5.1 and 5.2 show the mix characteristics and other properties of the test specimens. Figures 5.9 and 5.10 show the average age-strength relationship of compression cylinders cast from the same mixes as the test specimens.

Three types of virgin coarse aggregates were used in the concrete. One was natural gravel with rounded particles and smooth surfaces. The second aggregate was crushed limestone with angular edges and relatively rough surfaces. The third type was slag with rounded particles and rough surfaces. Physical characteristics of the three aggregates are shown in Table 5.3.

Two different coarse aggregate gradations were used, designated as MDOT specification 6A (1.5-in. [4-cm] top size, coarser gradation) and MDOT specification 17A (1.0-in. [2.5-cm] top size, finer gradation). The grading requirements for these designations along with actual gradations of the materials are given in Tables 5.4 and 5.5. Test specimens incorporating recycled concrete were produced by breaking and crushing slabs cast using 6A gravel in commercial crushers, and then sieving, grading and

Table 5.1: Mix characteristics and concrete

properties – material factor specimens

Test Specimens	Mix Proportions (oven-dry weights) CA:FA:WATER:CEMENT	Entrained Air %	Compressive Strength (28-days) psi
6A Virgin Gravel	1966:1079:235:554	6.4	5681
6A Virgin Limestone	1817:1240:245:560	5.4	5295
6A Virgin Slag	1808:1297:305:744	6.7	5954
17A Virgin Gravel	1878:1163:283:548	6.0	4294
100% Recycled	1559:1209:263:523	6.7	4780
50-50 Recycle Blend	1682:1137:272:545	6.7	5352

Note: All weights are in pounds

Table 5.2: Mix characteristics and concrete properties - design factor specimens

Test Specimens	Mix Proportions (oven-dry weights) CA:FA:WATER:CEMENT	Entrained Air %	Compressive Strength (28-days) psi
Typical Tension and Foundation	1814:1264:221:570	6.5	4125
Typical Tension and Foundation	1832:1238:217:549	7.4	3645
High Tension	1800:1238:234:563	6.8	4178
High Foundation	1791:1250:234:563	6.8	5837

Note: All weights are in pounds
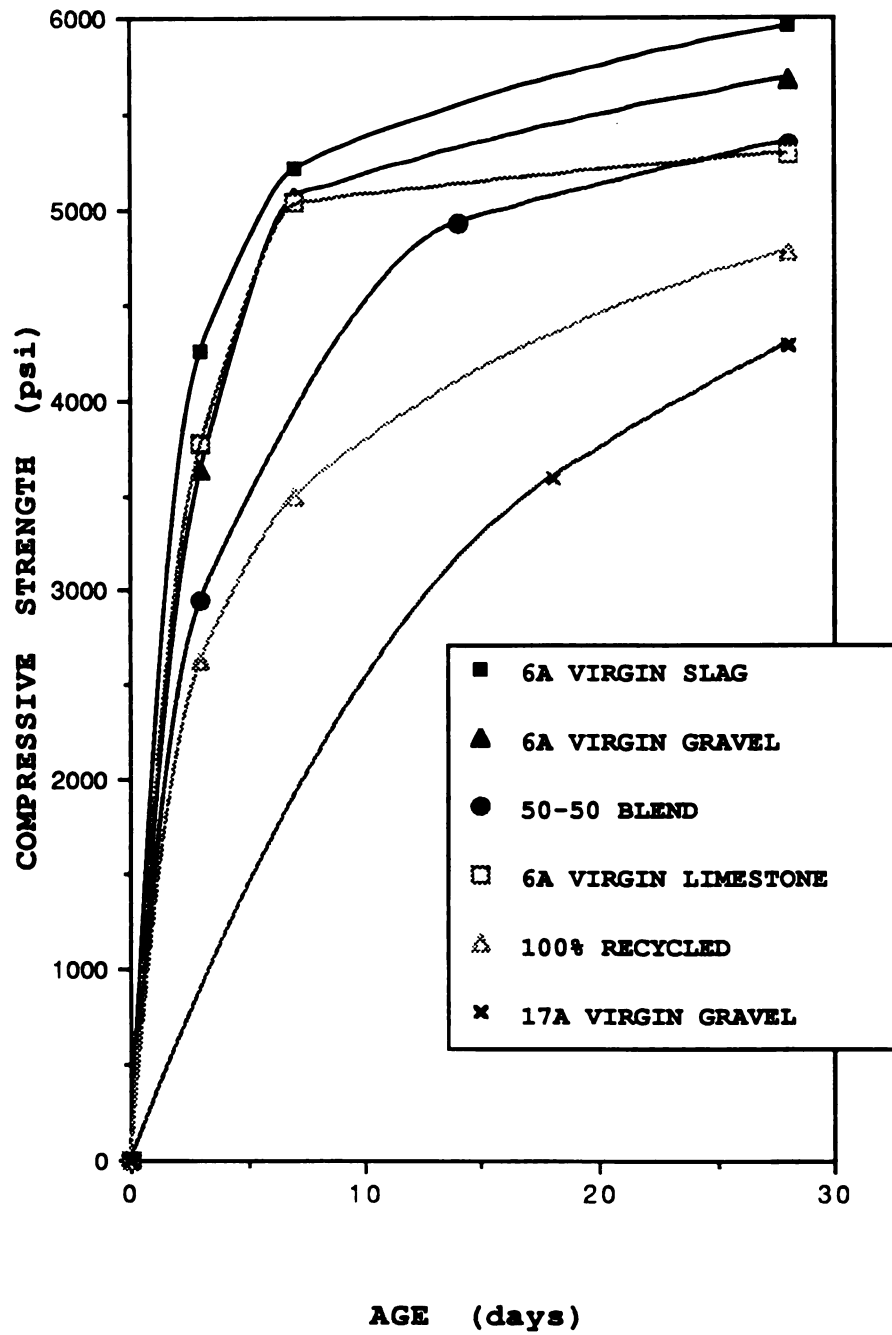
Figure 5.9: Strength-gain curves of the test specimens (material factors)
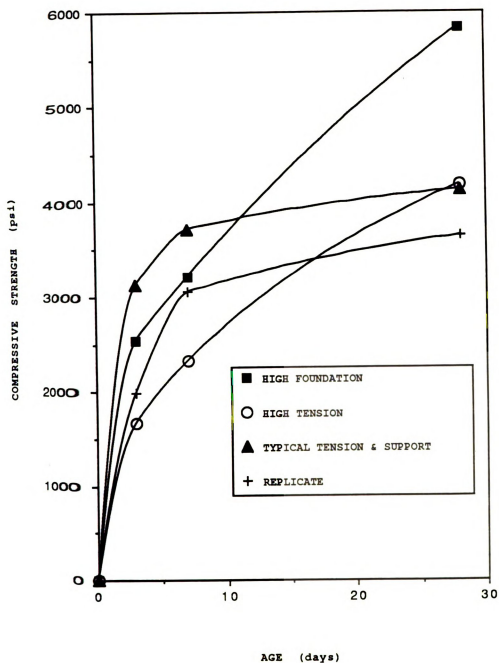
Figure 5.10: Strength-gain curves of the test specimens (design factors)

Table 5.3: Physical characteristics of concrete

aggregates

AGGREGATE	SPECIFIC GRAVITY	ABSORPTION (24hr) PERCENT
Sand	2.62	2.20
6A Virgin Gravel	2.61	0.90
4A/6A Virgin Limestone	2.60	0.66
6A Virgin Slag	2.41	3.71
17A Virgin Gravel	2.61	0.90
100% 6A Recycled Gravel	2.40	4.66
50-50 Recycle Blend	2.50	2.92

Note: Absorption capacity of sand for design factor
specimens = 1.05

Table 5.4: Coarse aggregate gradation of 6A material

SIEVE SIZE	TOTAL PERCENT PASSING				
	6A Spec	6A Limestone	6A Gravel	6A Slag	6A Recycled
1.5 in	100%	100	100	100	100
1.0 in	95-100%	98	98	100	97
1/2 in	30-60%	38*	38	60	42
No. 4	0-8%	2	4	2	4

Note: *Gradation test run in the lab show only 16% passing 1/2 in sieve for 6A crushed Limestone

Table 5.5: Coarse aggregate gradation of 17A material

SIEVE SIZE	TOTAL PERCENT PASSING	
	17A Spec	17A gravel
1.0 in	100%	100%
3/4 in	90-100%	100%
1/2 in	50-75%	56%
No. 4	0-8%	6%

5.5 T

5.

reblending this recycled material for use in test specimens. The 100% recycled test specimen was graded to meet MDOT specification 6A. The 50-50 recycled blend specimen contained coarse aggregate composed of a blend of 50% (by weight) recycled gravel concrete graded to meet MDOT specification 6A and 50% virgin crushed limestone graded to meet MDOT specification 4A (2.5-in. [6-cm] top size). The 4A gradation requirements and actual 4A material gradation are presented in Table 5.6.

5.5 Test Procedures

5.5.1 *Casting*

The concrete was mixed under careful laboratory control. First the coarse aggregates were sieved and blended (as required) to meet the appropriate gradation requirements. Then the coarse and fine aggregates were left in the laboratory to air dry. Tests were run to determine coarse and fine aggregate absorption capacities, unit weights and moisture contents. Trial batches were made to develop a final mix design for each test specimen. Prior to actual mixing, moisture contents of the aggregates were again determined to adjust the mix water.

The size of the test specimens and the capacity of the available drum mixers required mixing the concrete in a continuous stream of small batches to prevent the formation of cold joints. For each batch, one-half of coarse

Table 5.6: Coarse aggregate gradation of 4A material

SIEVE SIZE	TOTAL PERCENT PASSING	
	4A Spec	4A Limestone
2.5 in	100%	82
2.0 in	95-100%	47
1.5 in	65-90%	9
1.0 in	10-40%	2
1/2 in	0-20%	-
3/8 in	0-5%	-

aggregates, fine aggregates and water were blended first, followed by the addition of cement, the remaining one-half of the water (with air-entraining admixture), coarse aggregates and fine aggregates. The mixer was operated for five minutes after the addition of the final component.

Concrete was hauled to the structural steel form in wheel barrows, where it was consolidated with a shaft-type vibrator. Each specimen was cast according to a schedule that generally allowed testing to begin after 28 days of curing*. Specimens were cured in the laboratory under polyethelene sheets.

5.5.2 *Cracking*

The transverse crack was forced near midslab after approximately 18 hrs. of curing. A removable metal joint insert (1/4 in. x 1.0 in. [5/8 cm x 2.5 cm]) was used at the bottom of the 10-in. [25-cm] slab to form a plane-of-weakness at the midslab. The slab was cracked full-depth along the weakened plane by jacking one-half of

---

*The first two specimens (6A gravel and 6A limestone) were tested at 55 days and 52 days, respectively due to difficulties in getting the test program to operate properly. According to Troxell, Davis and Kelly [22] concrete made with 1.5-in. [4-cm] aggregates; 6 sacks cement per cu yd; and cured under standard conditions typically experiences a 9 percent gain in compressive strength between 28 and 55 days of curing. Thus, these specimens could have gained another 500 psi in compressive strength. However, actual increase in strength is expected to be less than this because of exposure to air after 28-days which may retard the hydration process due to drying.

the slab and frame while clamping the other half to the cracking frame. A hinge mounted on top of the casting frame assured a tensile mode of fracture.

5.5.3 *Loading*

After 28 days of curing, each test specimen was moved to the test stand while still in the structural channel casting form, which was equipped with lifting loops. The slabs were held securely in the form during cracking and transportation by short steel studs, which were welded to the insides of the form around its perimeter. After each specimen was placed and centered on the test stand, the casting form was removed. This procedure ensured that the temperature steel was not over stressed prior to loading.

Tension was induced in the specimens as described previously. LVDT's were then set to zero, the data acquisition system was initialized, and the repetitive loading was begun.

Load-deflection data were collected at the intervals described earlier. Each test was run until the temperature steel ruptured (see Figure 5.11). During the test, applied loads and slab tension were monitored and adjusted as needed.
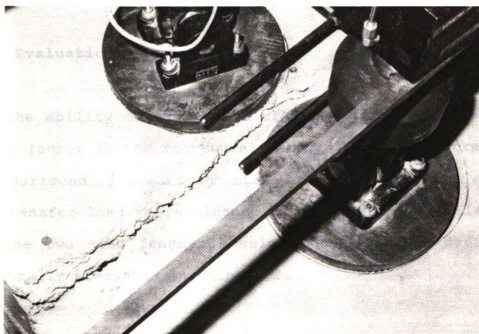
Figure 5.11: A view of a failed specimen

CHAPTER VI

DISCUSSION AND ANALYSIS OF TEST RESULTS

6.1 Evaluation of Load Transfer

The ability of transverse cracks to transfer load is a major factor in the structural performance of the crack and the surrounding slab fragments. In this study, the ability to transfer load was evaluated by comparing the deflections of the two slab fragments using the following definition originally presented in chapter 2:

$$\%LTE = (d_{UL}/d_L) \times 100 \, [23] \qquad\qquad (Eq. \ 2.3)$$

where

$\%LTE$ = percent load transfer efficiency

d_{UL} = deflection of unloaded side of the crack

d_L = deflection of the loaded side of the crack

Note that in the above formula, the maximum theoretical load transfer that can be achieved is 100%. This is obtained

when the two sides deflect an equal amount. On the other extreme, if the two sides move with complete independence, the load transfer efficiency would be zero.

6.2 Test Results - Material Factors

6.2.1 *Effect of Type of Coarse Aggregate*

The effect of coarse aggregate type on the aggregate interlock load transfer characteristics of transverse cracks was studied by comparing the performance of three test specimens, each containing a different type of coarse aggregate meeting the MDOT 6A gradation specifications. The three types of aggregates used were crushed limestone, gravel and slag. Figures 6.1 and 6.3 summarizes some of the test results for these materials. Detailed results are presented in APPENDIX A.

The results show that specimens containing crushed limestone and gravel coarse aggregates started with and retained higher load transfer efficiencies than the specimen containing slag coarse aggregate. This difference in performance is probably due to the different textures of the crack faces of these specimens, as illustrated in Figure 6.2. It is seen that the specimens containing crushed limestone and gravel have rougher crack faces (more large protrusions and macrotexture) than the specimen containing slag. This is due to the fact that slag aggregate apparently

Load Transfer Efficiency (%)

Thousands of Load Cycles

□ 6A VIRGIN GRAVEL + 6A VIRGIN LIMESTONE
* 6A VIRGIN SLAG
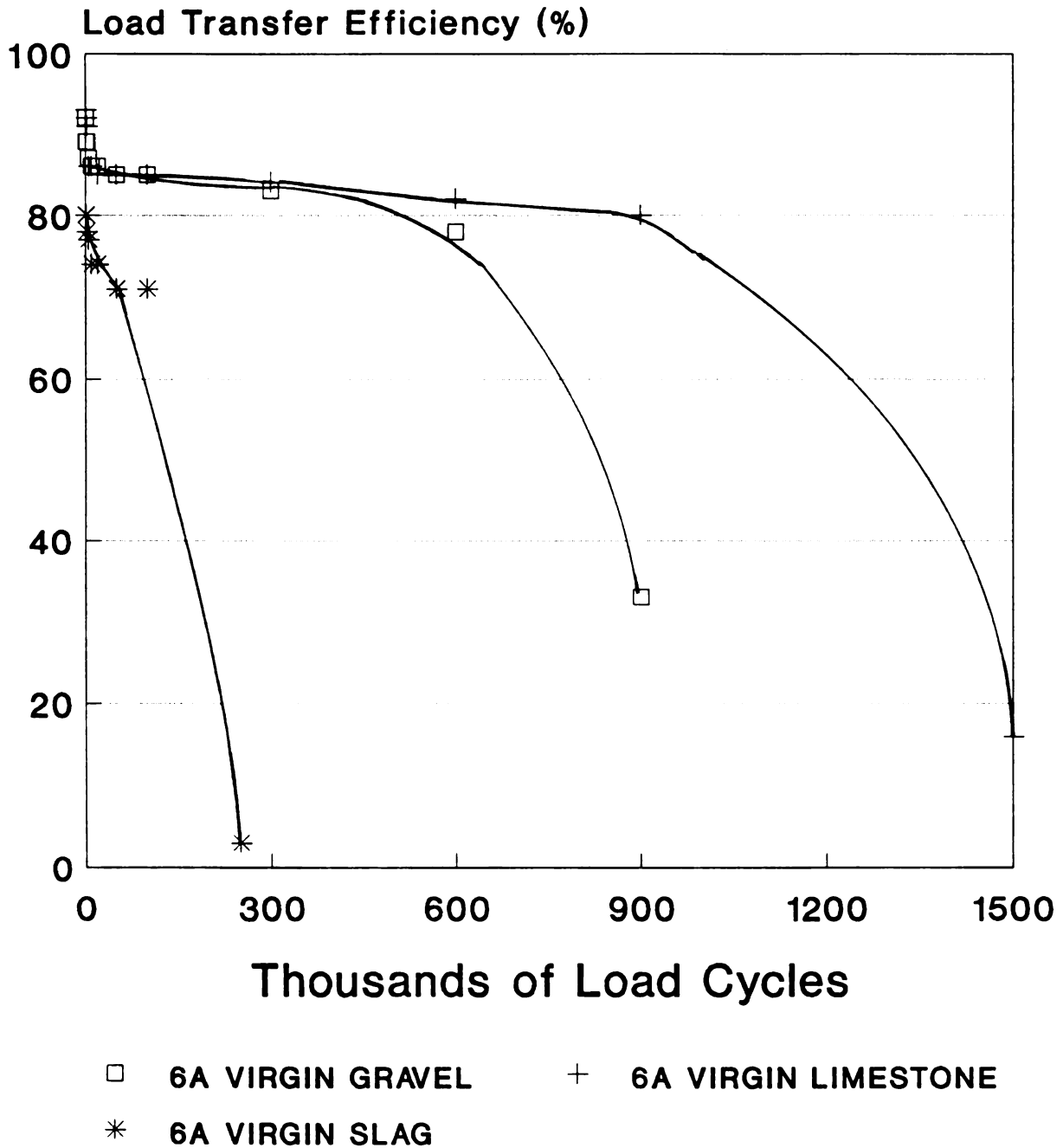
Figure 6.1: Effect of coarse aggregate type on the relation between LTE% and number of load cycles
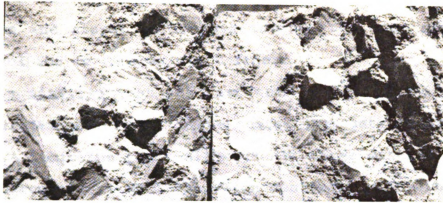
Crushed Limestone
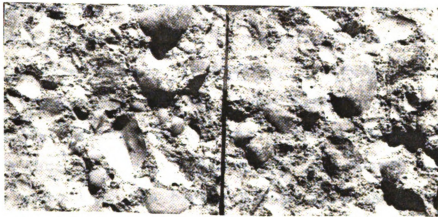
Gravel

Slag

Figure 6.2: Exposed crack faces of small test specimens, varying coarse aggregate type, 6A gradation materials

fractured at the time of crack development, whereas limestone and gravel pulled out through the loss of bond, thus resulting in rougher crack faces.

It is possible that the test results are biased due to slight differences in the three coarse aggregate gradations. Table 5.4 indicates that, although all three materials meet the requirements of MDOT gradation designation 6A, the slag is somewhat finer than either the limestone or gravel. It is also possible that the results were affected by the slight differences in mix designs[*] and strengths between the three test slabs (see Table 5.1). However, it seems most likely that the observed differences in performance (endurance of load transfer efficiency) are mainly due to differences in the crack face texture (see Figure 6.2) and coarse aggregate particle strengths. The highly porous slag particles were obviously of lower strength (see Tables 6.1 and 6.2) and produced crack faces with little macrotexture. These conclusions should be verified in future tests through the use of more comparably graded aggregates and identical curing conditions for each specimen.

Figure 6.3 shows the approach side peak deflections of the three test specimens after repeated loading. The crushed limestone specimen exhibited lower deflections than the gravel or slag at all times. Similarly, the gravel generally

---

[*] Recall that rough-textured, angular, elongated particles require more water to produce workable concrete than do smooth, rounded, compact aggregates. Thus, aggregate particles that are angular require more cement to maintain the same w/c ratio. Hence, slight differences in mix designs are unavoidable when using different types of coarse aggregate if workability and w/c ratio are to remain constant.

Table 6.1: Strength estimation of the three coarse aggregate types using flexural strength

CA TYPE	FLEXURAL STRENGTH (24 hrs) psi
Gravel	253
Limestone	261
Slag	187

Note: ASTM C78-84, Standard Test Method for Flexural Strength of Concrete (Using Simple Beam with Third-Point Loading)

Table 6.2: Strength evaluation of the three coarse aggregate types using Los Angeles (LA) test (ASTM Test Method C131-89)

CA Type	Percent Loss
Gravel	19
Limestone	31
Slag	39

Note: It is generally believed that the abrasion resistance of aggregate is mainly related to its strength. The Los Angeles (LA) test has been widely used as an *indicator* of the relative quality of coarse aggregate particles. The LA test is a measure of degradation of mineral aggregates of standard gradings resulting from a combination of actions including abrasion and attrition, impact, and grinding.

the fact that the 17A gravel test specimen was able to performed better than the slag. Although the temperature reinforcement eventually ruptured in all three cases, the crushed limestone concrete was able to endure a significantly higher number of load repetitions than the other two specimens. This better endurance is probably due at least in part to the relatively low deflections that are attributable to the angularity of the crushed particles, which increase the sliding resistance of the crack faces.

6.2.2 *Effect of Gradation of Coarse Aggregate*

The effect of coarse aggregate gradation on load transfer characteristics of transverse cracks was studied by comparing the results of two specimens, one cast using coarsely graded gravel (6A Gradation: 1.50-in. [4-cm] top size) and the other cast using more finely graded gravel (17A Gradation: 1.0-in. [2.5-cm] top size). The test results are summarized in Figure 6.4 (detailed results are presented in Appendix A). The results show that for initial loading cycles (up to 20,000 cycles) both test specimens performed comparably. As the number of load cycles increased, the load transfer efficiency of the 17A gravel test specimen dropped slightly. This is probably due to the relatively small size of coarse aggregates which, after initial attrition or abrasion of the crack faces, requires a larger vertical displacement of the two slab fragments to make contact and transfer load. However, this increase in looseness was not
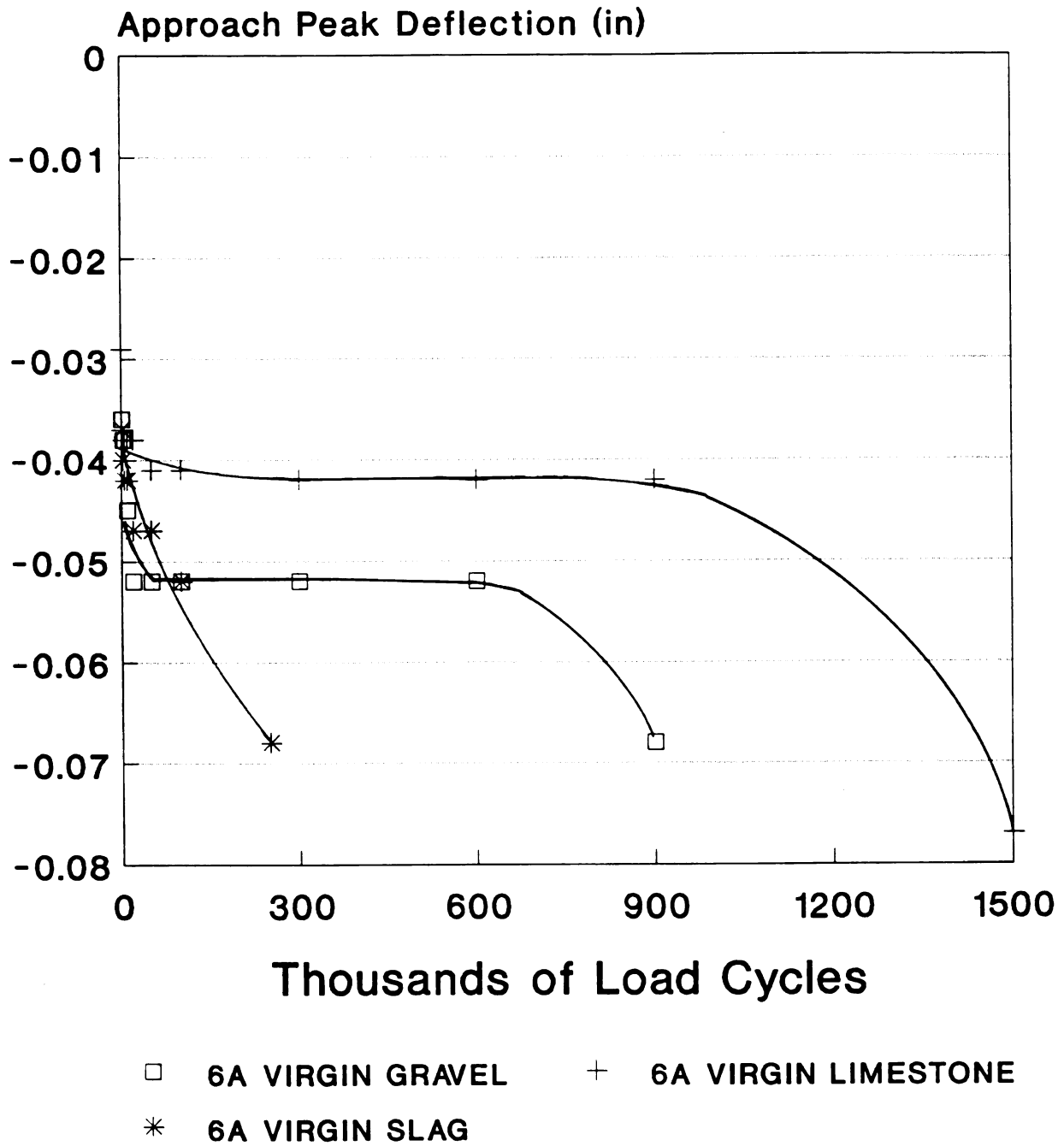
Figure 6.3: Effect of coarse aggregate type on the relation between approach-side peak deflection and number of load cycles
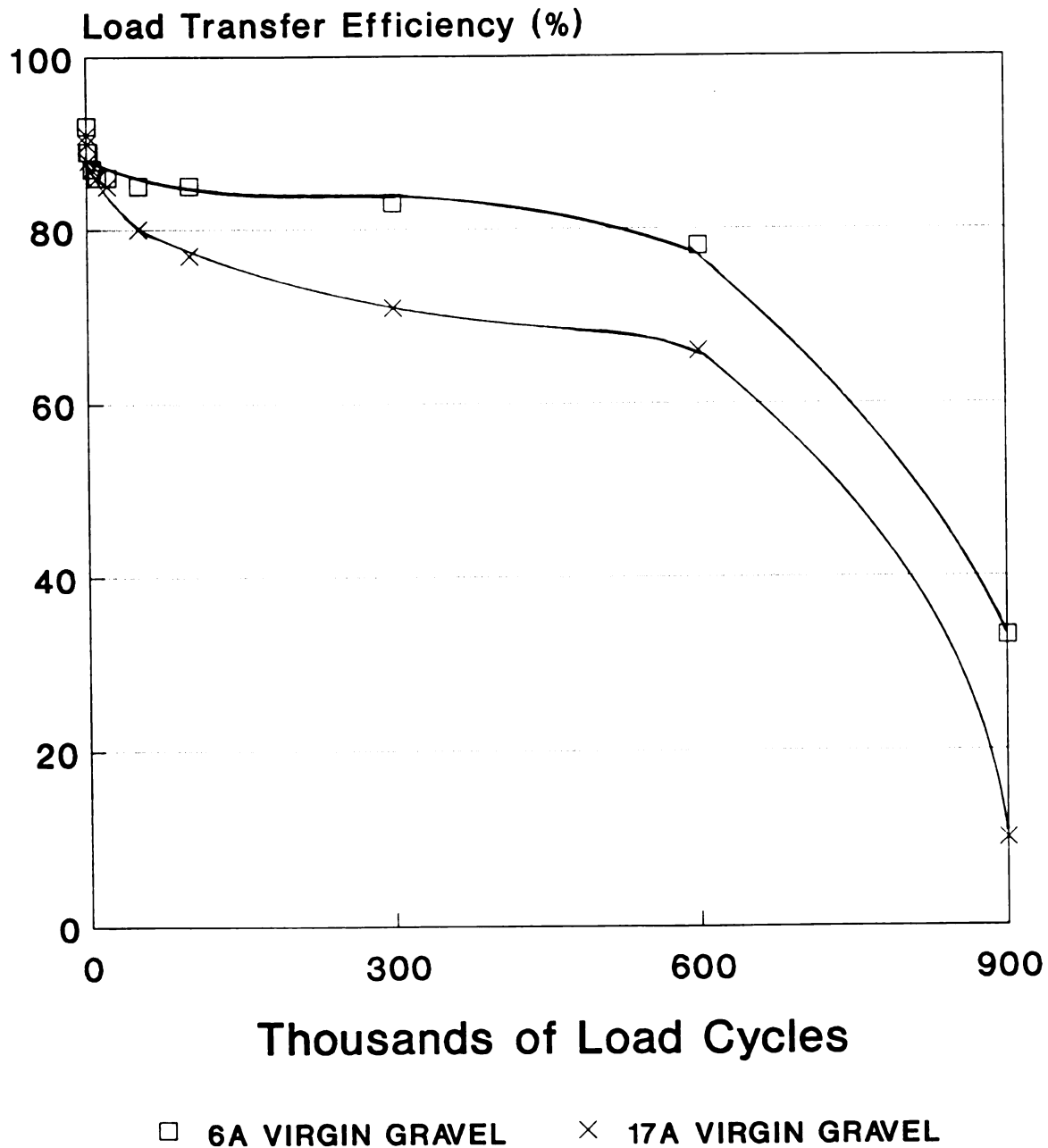
Figure 6.4: Effect of coarse aggregate gradation on the relation between LTE% and number of load cycles

large enough to produce immediate failure, as evidenced by the fact that the 17A gravel test specimen was able to endure a number of load cycles comparable to that of the 6A gravel test specimen before the steel reinforcement eventually ruptured.

These results agree with the results of Nowlen [5], who observed the following relationship between top size of coarse aggregate and load transfer efficiency for two different joint openings (weakened-plane transverse joint).

	Joint Opening (in)	
	0.035	0.065
Aggregate Top Size	Load Transfer Efficiency	
3/4"	45%	21%
1.5"	52%	23%
2.5"	96%	55%

It is seen that an increase in top size of coarse aggregate from 3/4-in. [2-cm] to 1.5-in. [4-cm] improved the effectiveness of the 0.035-in. [0.089-cm] joint by only 11 percent. Effectiveness of the 0.065-in. [0.165-cm] joint did not change significantly. Thus, the results of this and previous studies show that effect of top size of coarse aggregate is not pronounced in the range of 3/4-in. [2-cm]

to 1.5-in. [4-cm] top size.

6.2.3 *Effect of Treatment of Coarse Aggregate*

The effect of treatment of coarse aggregate on aggregate interlock load transfer characteristics of transverse cracks was studied by comparing the performance of three test specimens, each containing a different treatment of coarse aggregate. The three treatments of aggregates included virgin gravel aggregates (MDOT gradation 6A), 100% recycled gravel concrete aggregates (MDOT gradation 6A), and a 50-50 blend of recycled gravel concrete (MDOT gradation 6A) and large virgin limestone (MDOT gradation 4A) aggregates. Figure 6.5 summarizes the test results of these treatments (details are presented in Appendix A).

The results show that the specimen containing virgin coarse aggregates performed considerably better than the other two test specimens which contained recycled concrete as coarse aggregates. The examination of the crack faces of the 100% recycled specimen revealed that very few pull outs of aggregate particles existed (see Figure 6.6). The reason for this condition is probably related to the mode of fracture of recycled concrete aggregates. Coarse aggregates produced by recycling concrete consist of two materials (i.e., cement mortar and original aggregate) bonded together. At the time of crack development, recycled concrete aggregates apparently often fracture at the old

Load Transfer Efficiency (%)

Thousands of Load Cycles

□ 6A VIRGIN GRAVEL   +   100% 6A RECYCLED

✻ 50-50 RECYCLED BLEND
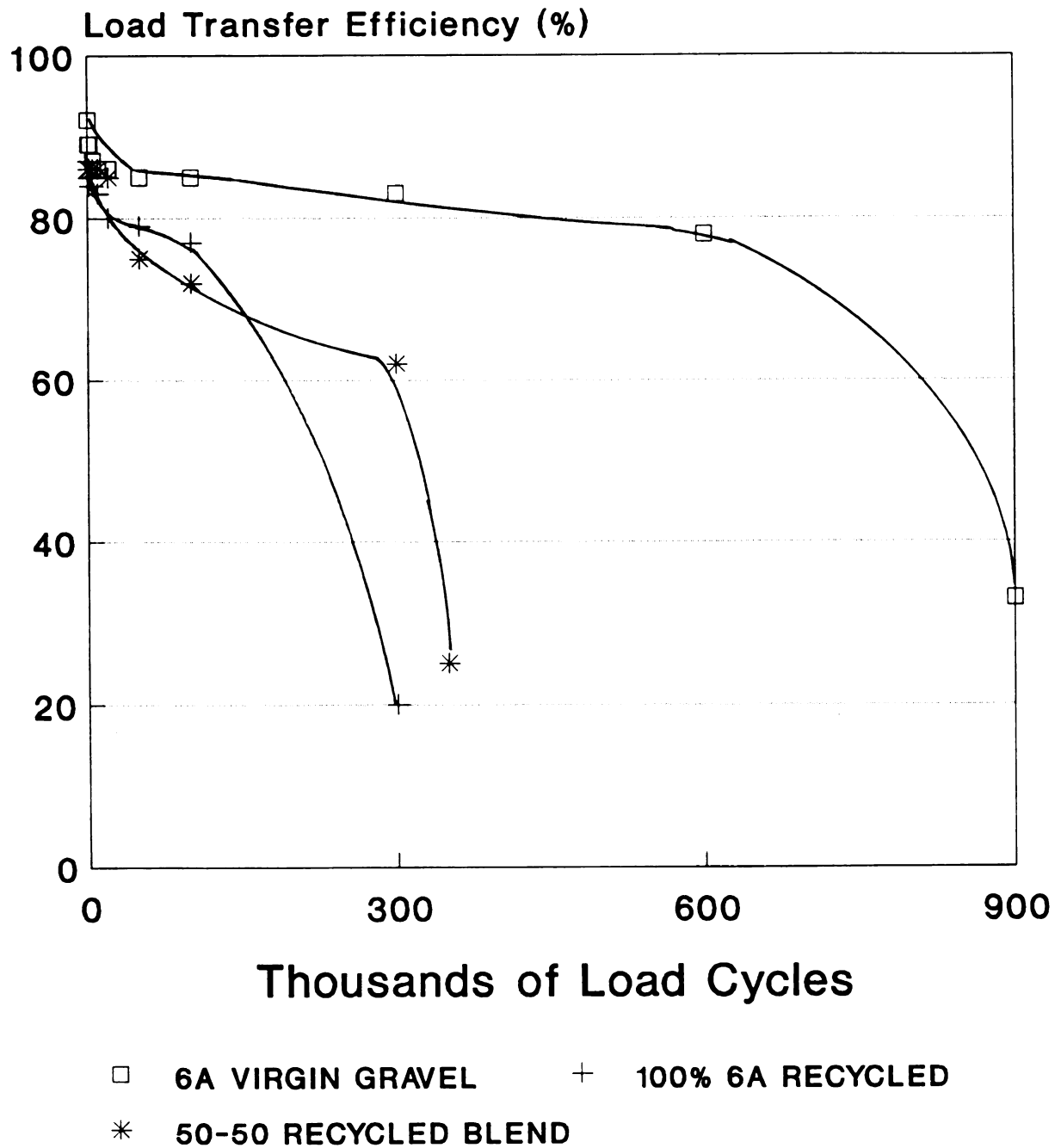
Figure 6.5: Effect of coarse aggregate treatment on the relation between LTE% and number of load cycles
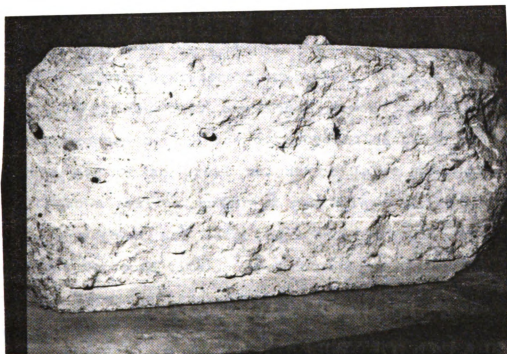
Figure 6.6: Exposed crack face of 100% recycled gravel concrete specimen after loading

bond interface, thus resulting in the above condition. Furthermore, the use of comparable quantities of recycled aggregate results in nearly a 50% reduction in the actual number of virgin coarse aggregate particles in the mix. If the shear transfer characteristics of the slab depend upon the number and quality of virgin aggregate particles at the crack interface, it stands to reason that concrete utilizing only recycled concrete aggregates may fare poorly.

The unexpected poor performance of 50-50 recycle blend specimen may also be attributable to a reduction in the number of virgin aggregate particles at the crack face (see Figure 6.7). Not only are there fewer virgin particles present because of the use of recycled concrete materials, but the use of an equal weight of large aggregate also results in a smaller number of particles (although the few that are present are large enough to provide significant interlock for some time). The distribution of particles that protrude from the crack face can be fairly widespread, as seen in Figure 6.7.

It should also be noted that during transportation of this specimen (50-50 recycle blend) from the cracking frame to the test stand, one of the lifting ropes broke, causing one end of the specimen to drop a distance of about 2-in. [5-cm]. This may have contributed to the observed performance since initial load transfer efficiency of this specimen was also low compared to all other specimens except one (6A virgin slag).

It is recommended that this test cell (50-50 recycled

Figure 6.7: Exposed crack face of 50-50 recycled blend specimen after loading

blend) should be replicated in future tests to determine whether the observed results were influenced by the handling of the specimen or were truly indicative of the performance of this mixture.

6.3 Test Results - Design Factors

6.3.1 *Effect of Slab Tension*

The effect of slab tension on aggregate interlock load transfer characteristics of transverse cracks was studied by comparing the performance of two test specimens (6A virgin gravel), one with an induced tension of 16000 lbs [71.3 KN] (3500 lb/ft width) [51 KN/m width] and the other with an induced tension of 32000 lbs [142.6 KN] (7000 lb/ft width) [102 KN/m width]. The amount of tension required was computed using subgrade drag theory, modelling assumed coefficients of frictional resistance of 1.5 and 3.0, respectively, for a 9-in. [23-cm] slab measuring 41 ft [12.5 m] in length by 4.5 ft [1.4 m] wide. The test results are summarized in Figure 6.8. Detailed results are presented in APPENDIX B.

The test results show that the specimen with lower tension started with and retained higher load transfer efficiencies than the specimen with higher slab tension. This difference in performance is probably due to the wider crack opening and consequent higher level of stresses and strains in longitudinal steel in the high tension specimen.
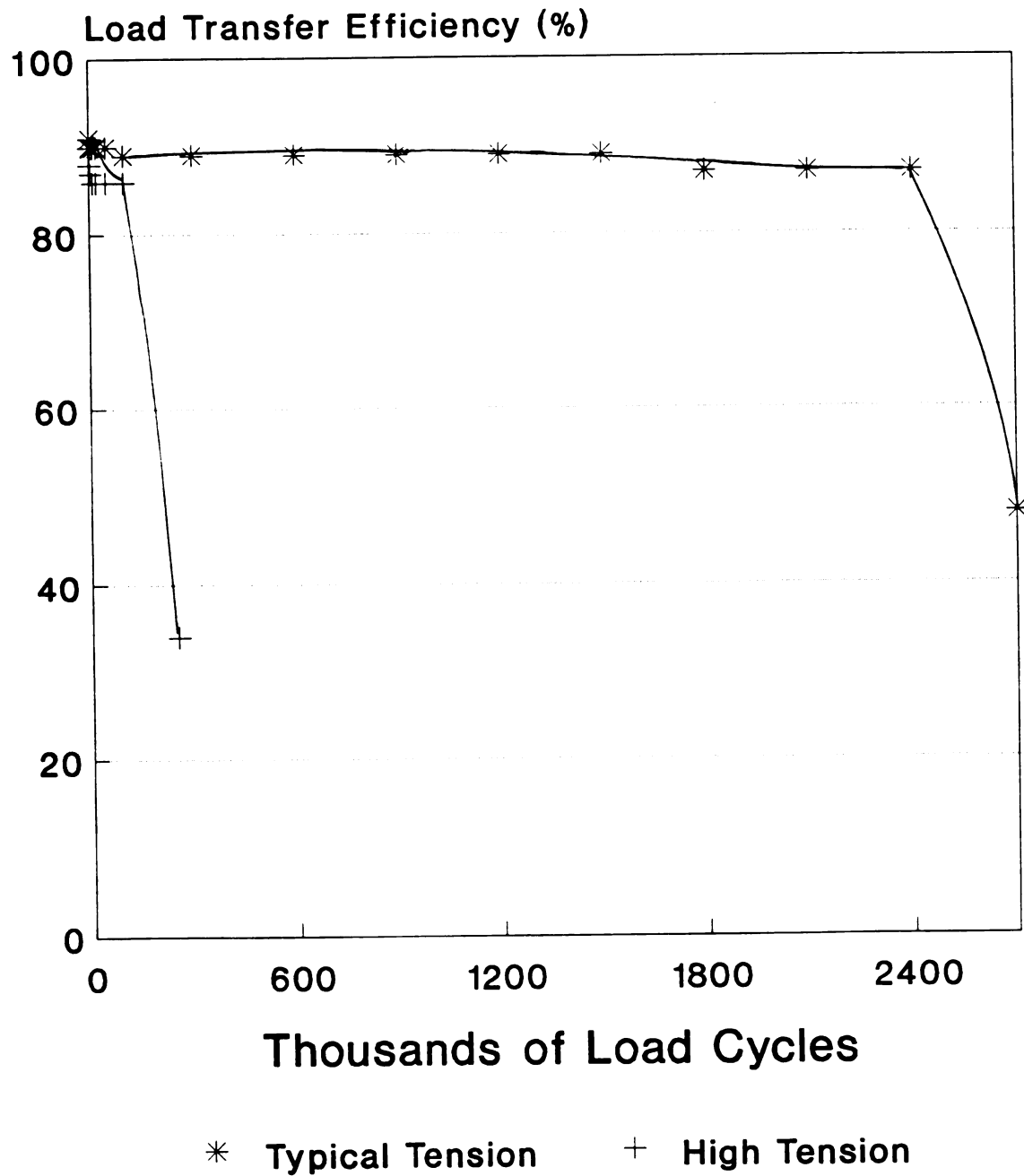
Figure 6.8: Effect of slab tension on the relation between LTE% and number of load cycles

The induction of 16000 lbs [71.3 KN] slab tension resulted in 0.015-in. [0.038-cm] crack width, whereas induction of 32000 lbs [142.6 KN] resulted in a 0.023-in. [0.058-cm] wide crack, an increase by a factor of 1.5. This increased crack opening may cause a partial loss of contact between the two crack faces, which, in turn, diminishes the bearing and crushing action of cement matrix. Thus, load is transferred solely through the sliding action of coarse aggregate particles. Hence, an increase in crack width results in an increase in looseness, requiring a vertical displacement of the loaded side of the slab to make contact and transfer load (see Figure 6.9). Analyses of the load-deflection data of the two specimens also shows the presence of significant looseness in the high tension specimen. Figure 6.10 illustrates the detrimental effects of increased looseness in the high tension specimen on its load transfer capacity. It is seen that at small loads, the load was not fully transferred to the unloaded slab fragment. This is due to lack of immediate contact of the two crack faces. However, with an increase in load, better contact was made between aggregate particles and the load transfer efficiency increased.

Moreover, presence of excessive looseness suggests that for a fraction of time longitudinal steel is picking up the shear and while doing so is also being bent to accommodate the vertical displacement of the loaded slab fragment before aggregate interlock becomes effective. The combined effect of high tensile stresses (due to high tension) and high
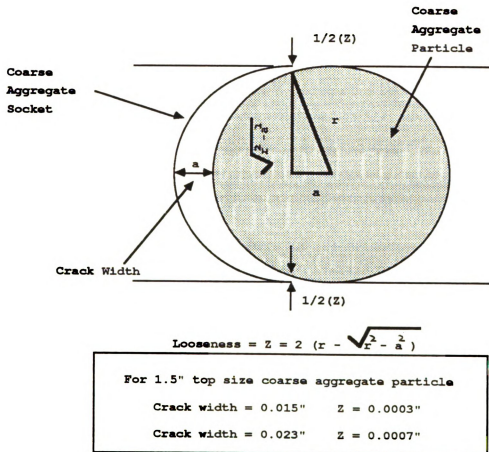
Figure 6.9: Aggregate looseness geometry [5]
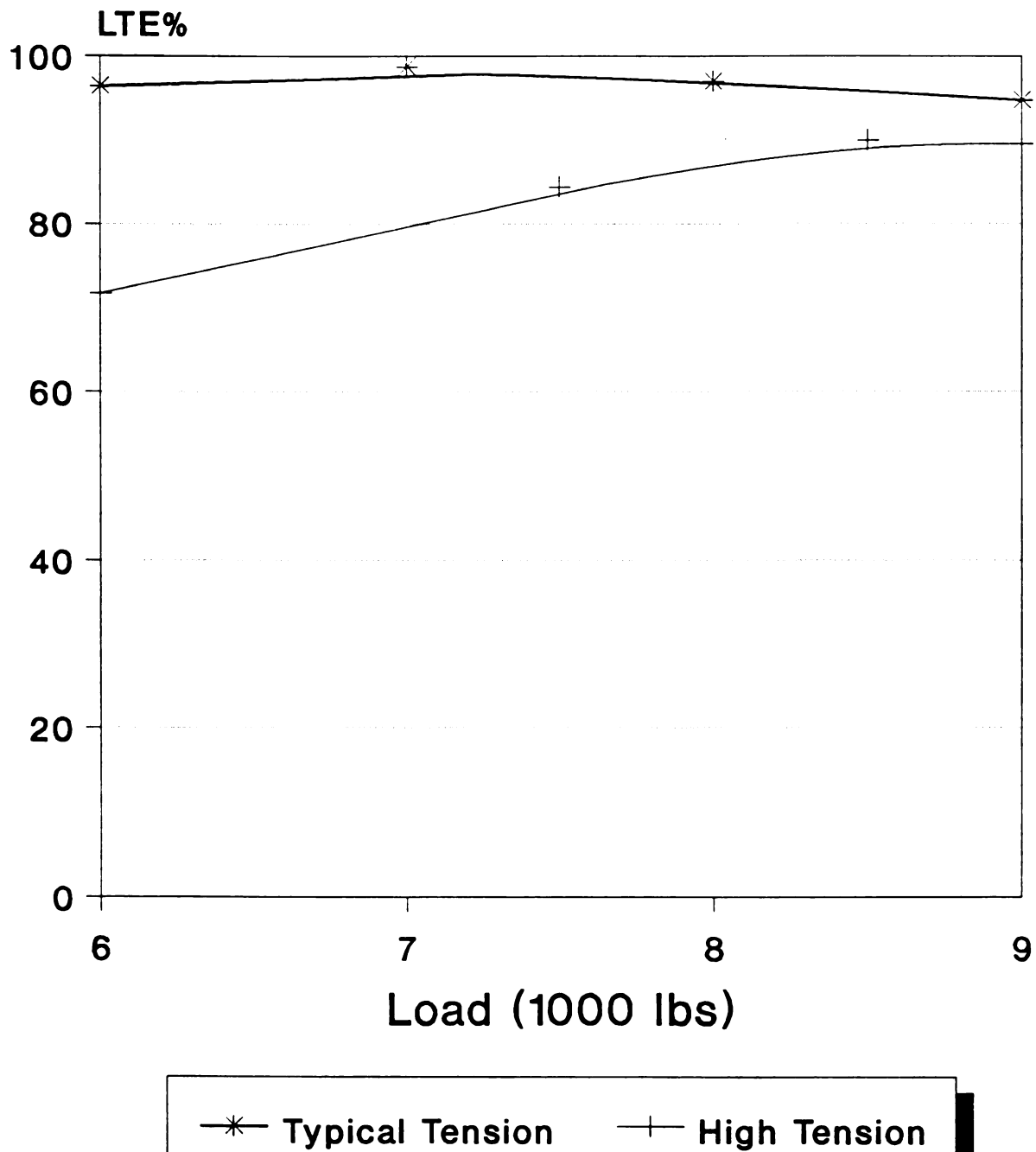
Figure 6.10: Effect of looseness on the relation between LTE% and load magnitude

shearing stresses (due to excessive looseness) under repeated heavy load applications may cause the accelerated rupture of steel. Note that the longitudinal steel in JRCP is not designed for shear loads.

6.3.2 *Effect of Foundation Support*

The effect of foundation support on the aggregate interlock load transfer characteristics of transverse cracks was studied by comparing the performance of two specimens (6A virgin gravel), one placed on three layers of FABCEL-25 simulating a modulus of subgrade reaction of approximately 100 psi/in [27 kPa/m], and the other placed on two layers of FABCEL-25 simulating a modulus of subgrade reaction of approximately 250 psi/in [68 kPa/m]. The test results are summarized in Figures 6.11 and 6.12. Detailed results are presented in APPENDIX B.

The results show that specimens placed on the stiffer foundation (250 psi/in [68 kPa/m]) started with and retained higher load transfer efficiency than the specimen placed on the relatively soft foundation (100 psi/in [27 kPa/m]). For example, the initial load transfer efficiencies (after application of load cycle # 1) of these specimens were 96% and 91% respectively. Load transfer efficiencies at the end of two million load cycles were 91% and 87% respectively.

The results also show that high foundation specimen was able to endure a considerably higher number of load cycles (6.6 million) compared to the low foundation modulus
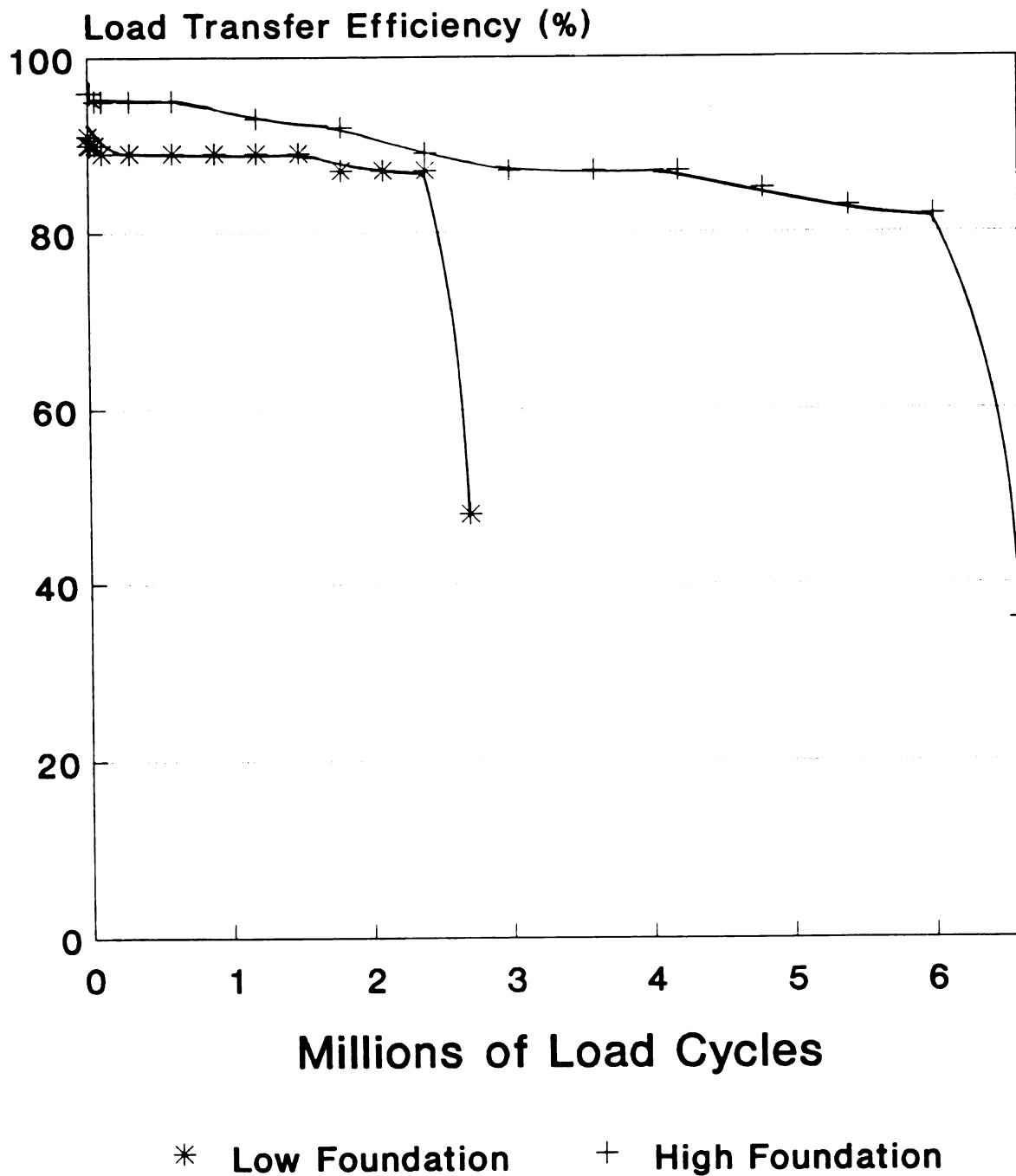
Figure 6.11: Effect of foundation support on the relation between LTE% and number of load cycles
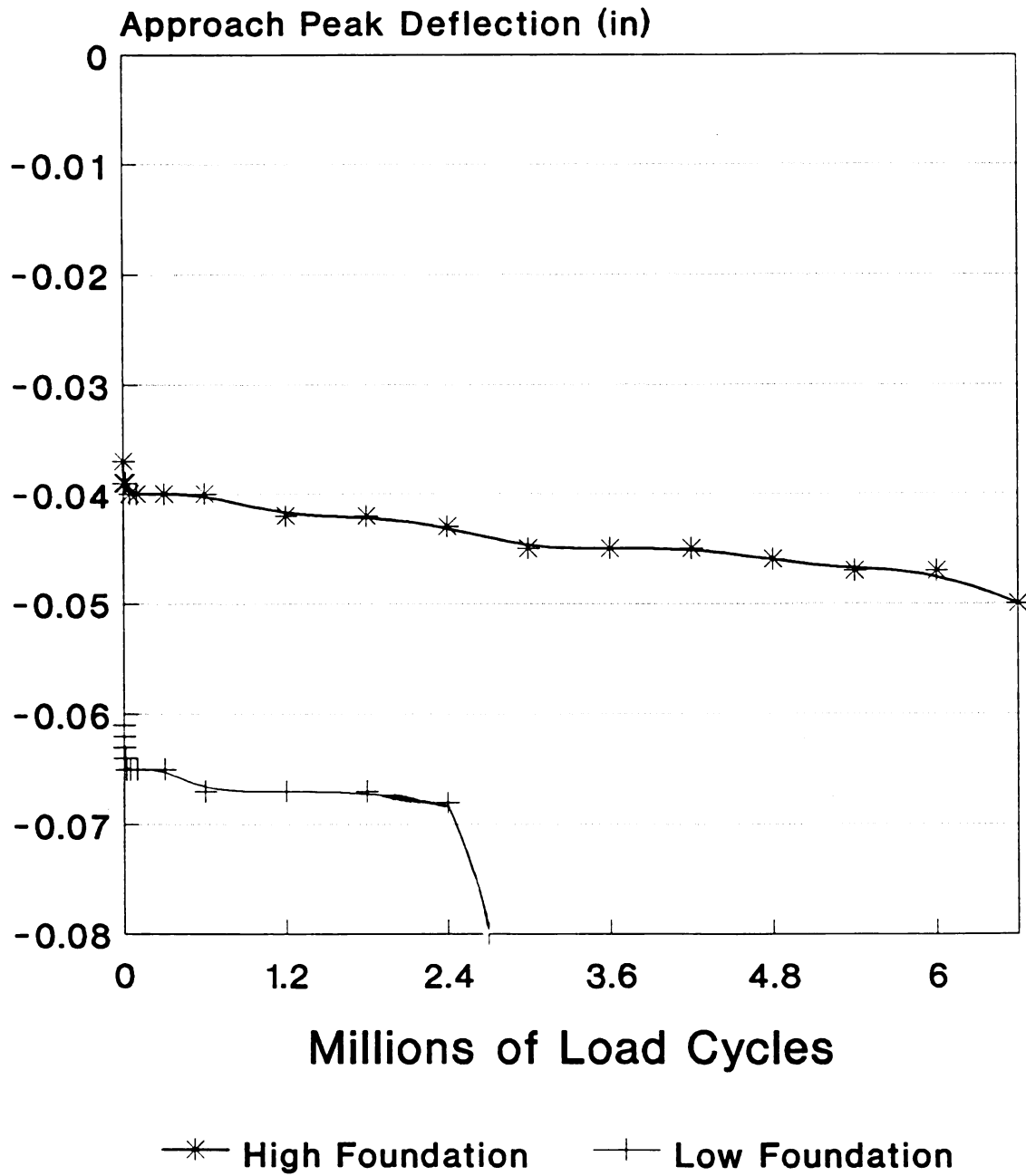
Figure 6.12: Effect of foundation support on the relation between approach-side peak deflection and number of load cycles

specimen (2.7 million). Thus, it is apparent that the added stiffness of the high foundation modulus specimen contributed significantly to the long-term aggregate interlock load transfer characteristics of the transverse crack. This increased endurance is due to the fact that strong foundation support reduces the magnitude of the peak and differential deflections, thereby allowing the application of more load cycles for any given loss of interlock and load transfer. Figure 6.12 shows the approach side peak deflections of the two test specimens after repeated loading. It is seen that the high foundation modulus specimen exhibited lower deflections than the low foundation modulus specimen at all times. Similarly, Table 6.3 shows that the high foundation modulus specimen experienced a lower magnitude of differential displacements at all times compared to the low foundation modulus specimen.

6.4 Development of a Model

One of the critical response variables in this testing program is the number of load cycles to failure (N). Based on the experience gained from other reliability studies and an examination of the load cycles to failure data generated from the 10 test runs, the N data were transformed by taking logarithms, resulting in the performance variable $Y = \text{Log}_{10} N$. An additive linear model was fit to the Y-data resulting in estimated effects for changes in the material and design

Table 6.3: Differential deflection data of the two specimens used in the evaluation of effect of foundation support

slab # / cycle #	differential deflection under peak load, mils	
	High Foundation	Low Foundation
1	1.62	5.30
1000	1.62	5.98
2000	1.64	6.13
5000	1.64	6.50
10000	1.64	6.60
20000	1.75	6.60
50000	1.98	6.36
100000	2.05	6.92
300000	2.05	6.93
600000	2.05	7.72
1200000	2.82	7.12
1800000	3.30	7.13
2400000	4.76	8.78
2700000	–	43.48[*]
3000000	5.60	
3600000	5.85	
4200000	5.98	
4800000	6.78	
5400000	7.98	
6000000	8.28	
6600000	31.63[*]	

Note: * = steel had ruptured

factor levels. The predictive model developed is presented below:

$$\text{Log}_{10} \ N = 6.48 + 0.23(\text{LS}) - 0.55(\text{SL}) - 0.41(\text{RB})$$
$$- 0.47(\text{R}) - 1.08(\text{HT}) + 0.34(\text{HF})$$

where

LS = 6A Virgin Limestone

SL = 6A Virgin Slag

RB = 50-50 Recycled Blend

R = 100% 6A Recycled Gravel

HT = High Tension (7000 lb/ft width)

HF = High Foundation (250 psi/in)

The formal analysis is presented in APPENDIX C. The estimate of the standard deviation of the pure error in Y is 0.064 which transforms to an estimated error of about 16% in measured cycles to failure. Not surprisingly, only extreme differences in cycles to failure, N, are statistically significant because the pure error is estimated with only one degree of freedom.

6.5 Equivalence of Performance

Maintenance of adequate load transfer through aggregate interlock over a large number of heavy truck load

applications is critical to the satisfactory long-term performance of JRCP. An Endurance Index, EI, concept may be used to describe the long-term transverse crack performance. In this study, Endurance Index (expressed as percentage) is arbitrarily defined as the ratio of the area under the curve of load transfer efficency, LTE%, versus logarithm of number of load cycles, Log_{10} N, to the corresponding area under the curve obtained by setting LTE = 100% for Log_{10} N = 8 (i.e., 100 million load cycles). The results are summarized in Figure 6.13. Detailed results are presented in APPENDIX D.

Figure 6.13 can be used to show equivalence of performance. It is seen that bars of approximately equal height indicate specimens with approximately equal endurance index values. For example, the high tension specimen and 6A virgin slag specimen exhibited comparable EI values i.e., 57 and 58 percent respectively. The reason for these low and comparable EI values is probably related to the inefficient functioning of the aggregate interlock mechanism in these two specimens. As pointed out earlier, significant looseness in the high tension specimen (caused by increased crack width due to high tensioning) prevented aggregate interlock from offering full resistance to the applied load. This resulted in lower load transfer efficiency and also subjected the longitudinal steel to higher level of stresses and strains. Similarly, in the 6A virgin slag specimen aggregate interlock mechanism was not effective in stress control due to lack of macrotexture and roughness at the crack face. Thus, it may be concluded that the effect of
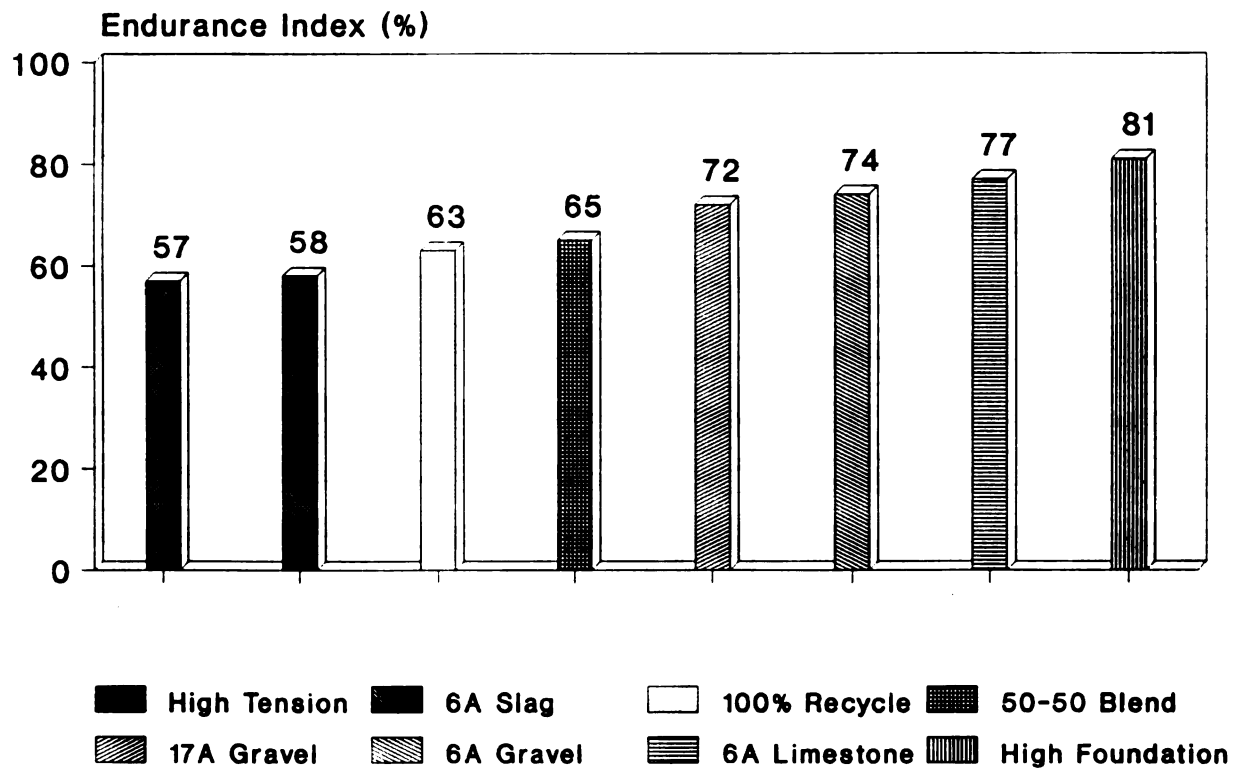
Endurance Index (%)

Figure 6.13: Equivalence of performance

increase in crack opening on aggregate interlock mechanism is same as that of fracture of coarse aggregate particles since in both instances, aggregate interlock mechanism is prevented from functioning at full efficiency.

A similar comparison can be made between the two recycled specimens. Figure 6.13 shows that 6A 100% recycled gravel specimen and 50-50 recycled blend specimen exhibited approximately comparable EI values i.e., 63 and 65 percent respectively. These low and approximately comparable EI values are also attributable to the inefficient functioning of aggregate interlock mechanism in these two specimens. The reasons for somewhat ineffective aggregate interlock mechanism were discussed previously. It was pointed out that very few pull outs of coarse aggregate particles existed at the crack interfaces of these specimens. However, note that the EI values for the recycled specimens are 9 to 14 percent higher than the EI value of 6A virgin slag specimen. This is due to the fact that crack face textures of the recycled specimens, though relatively smooth in the global sense, were somewhat rougher than the 6A virgin slag specimen (see Figures 6.2, 6.6 and 6.7).

6A virgin gravel specimen and 17A virgin gravel specimen exhibited approximately comparable EI values i.e., 74 and 72 percent respectively. This suggests that effect of coarse aggregate gradation is not significant in the range of 1.0-in. [2.54-cm] and 1.5-in. [4.0-cm] top size. However, note that these EI values are considerably higher than EI values of the four specimens discussed above. This

significant increase in EI is attributable to the fact that in virgin gravel specimens, gravel pulled out through the loss of bond (due to high particle strength, see Tables 6.1 and 6.2) thus resulting in crack faces with more protrusions and macrotexture. Figure 6.13 shows that, EI, further improves with the angularity of the coarse aggregate particles as evidenced by the EI value of 77 percent exhibited by 6A virgin crushed limestone specimen.

The most significant improvement in EI was observed when the stiffness of the foundation was increased from 100 psi/in [27 kpa/m] to 250 psi/in [68 kpa/m]. The EI values for these two specimens are 74 and 81 percent respectively. This increase in EI is due to the fact that strong foundation support reduces the magnitude of differential deflections, thereby allowing the application of more load cycles to produce a given loss of aggregate interlock and load transfer.

6.6 Discussion of Test Results

6.6.1 *Significance of Rougher Crack Face*

The results of this study show that aggregate interlock load transfer efficiency and endurance is strongly related to texture of the crack face. The crack face texture is primarily a function of type, number and size of coarse aggregate particles at the crack face and the mode of fracture. It was observed that specimens in which cracks

developed <u>around</u> the aggregate (virgin limestone and virgin gravel) developed higher initial load transfer efficiencies and were able to maintain this higher level over a considerably larger number of load cycles than specimens in which cracks developed through the aggregate (virgin slag and recycled slabs). The difference in performance is related to the texture of the crack face of these specimens as described previously. Specimens with rougher crack faces (virgin limestone and virgin gravel) exhibited lower approach-side peak deflections than specimens with relatively smooth crack faces (virgin slag and recycled). More importantly, specimens with rougher crack faces experienced much lower differential deflections (relative vertical displacements) than specimens with smooth crack faces. The magnitude of differential deflections of these specimens after various load cycles are tabulated in Table 6.4. It is seen that specimens with fracture <u>through</u> the aggregate had much higher (66% to 281%) initial differential deflections than specimens with fracture <u>around</u> the aggregate. The higher differential deflections of the two slab fragments results in higher level of shear stresses and strains in longitudinal steel. It is obvious that higher levels of strains and strain reversals would accelerate fatigue failure of longitudinal steel as is evidenced by the relatively small (and comparable) number of load cycles endured by the three specimens with smooth crack faces. Thus, it can be concluded that <u>rough crack interface (due to fracture around) is effective in controlling the magnitude</u>

Table 6.4: Differential deflection data - material factors

slab # / cycle #	differential deflection under peak load, mils					
	A	B	C	D	E	F
1	1.94	2.92	3.68	7.40	6.20	6.13
1000	3.28	3.93	4.56	7.40	6.20	6.13
2000	3.54	4.34	5.28	8.83	7.94	6.13
5000	5.03	4.74	5.28	9.82	8.50	6.83
10000	5.38	6.43	6.84	10.85	8.98	7.04
20000	5.64	7.52	7.20	12.30	10.58	8.38
50000	5.64	7.80	9.33	13.53	10.98	15.60
100000	6.32	7.80	12.15	14.84	12.55	17.90
250000	-	-	-	65.40*	-	-
300000	6.62	9.35	15.60		72.08*	22.73
350000	-	-	-			63.40*
600000	7.58	11.66	18.63			
900000	8.33	45.85*	83.64*			
1500000	64.73*					

Notes:

* = steel had ruptured
A = 6A virgin limestone
B = 6A virgin gravel
C = 17A virgin gravel
D = 6A virgin slag
E = 6A 100% recycled gravel
F = 50-50 recycled blend

<u>of peak as well as differential deflections</u> and thereby ensures that longitudinal steel is not subjected to a high level of stresses/strains and their reversals. This provides higher initial load transfer efficiency and better endurance.

The fact that crushed limestone performed the best among the three types of coarse aggregates does not necessarily means that this is always the case. Sutherland and Cashell [6] indicate that, for a given size (1.0-in. [2.5-cm] and 2.5-in. [6.3-cm], gravel performed better than crushed limestone. These researchers noted that crushed limestone fractured at the time of joint development (weakened-plane transverse joint). Thus, the advantages of angular, rough-surfaced crushed limestone aggregate particles were lost because fracture of aggregate results in a smooth crack face. Note that in this study crushed limestone was of good quality (see Table 6.1), thus, pulled out through the loss of bond.

The key factor which determines the mode of fracture is paste/aggregate bond strength at the time of crack development. Therefore, it is desirable to have paste/aggregate bond low at the time of fracture so that the crack passes around the aggregate resulting in a rough crack face. On the other hand, high paste/aggregate bond is required to keep coarse aggregate particles embedded in the cement matrix under repeated heavy truck traffic. The paste/aggregate bond generally increases with increase in concrete strength i.e., age of concrete. Thus, the age of

concrete at the time of crack development may play an important role in determining the texture of the crack face. In view of the above, it is recommended that in future experimentation different types of aggregates should be evaluated in the context of age of concrete at the time of cracking (effect of fracture delay).

6.6.2 *Effect of Aggregate Interlock Looseness*

The term looseness may be defined as conditions that prevent aggregate interlock from offering full resistance to applied load. Conditions which may affect the aggregate interlock looseness include top size of coarse aggregate particles, abrasion/attrition of coarse aggregate particles and sockets under repetitive loading, and opening of the crack due to thermal and drying shrinkage of the concrete. Aggregate interlock mechanism can function at full efficiency only after the looseness is taken up by load displacement of the slab fragments. Thus, the effect of looseness is to reduce the potential usefulness of the aggregate interlock mechanism by an amount proportional to the degree of looseness present at the crack interface. Figure 6.14 illustrates the above-described effect of looseness on load transfer capacity. This figure is drawn from the load-deflection data obtained for the high tension specimen after load cycle # 1. It is seen that, due to presence of significant looseness (caused by increased crack width due to high tension), the magnitude of differential
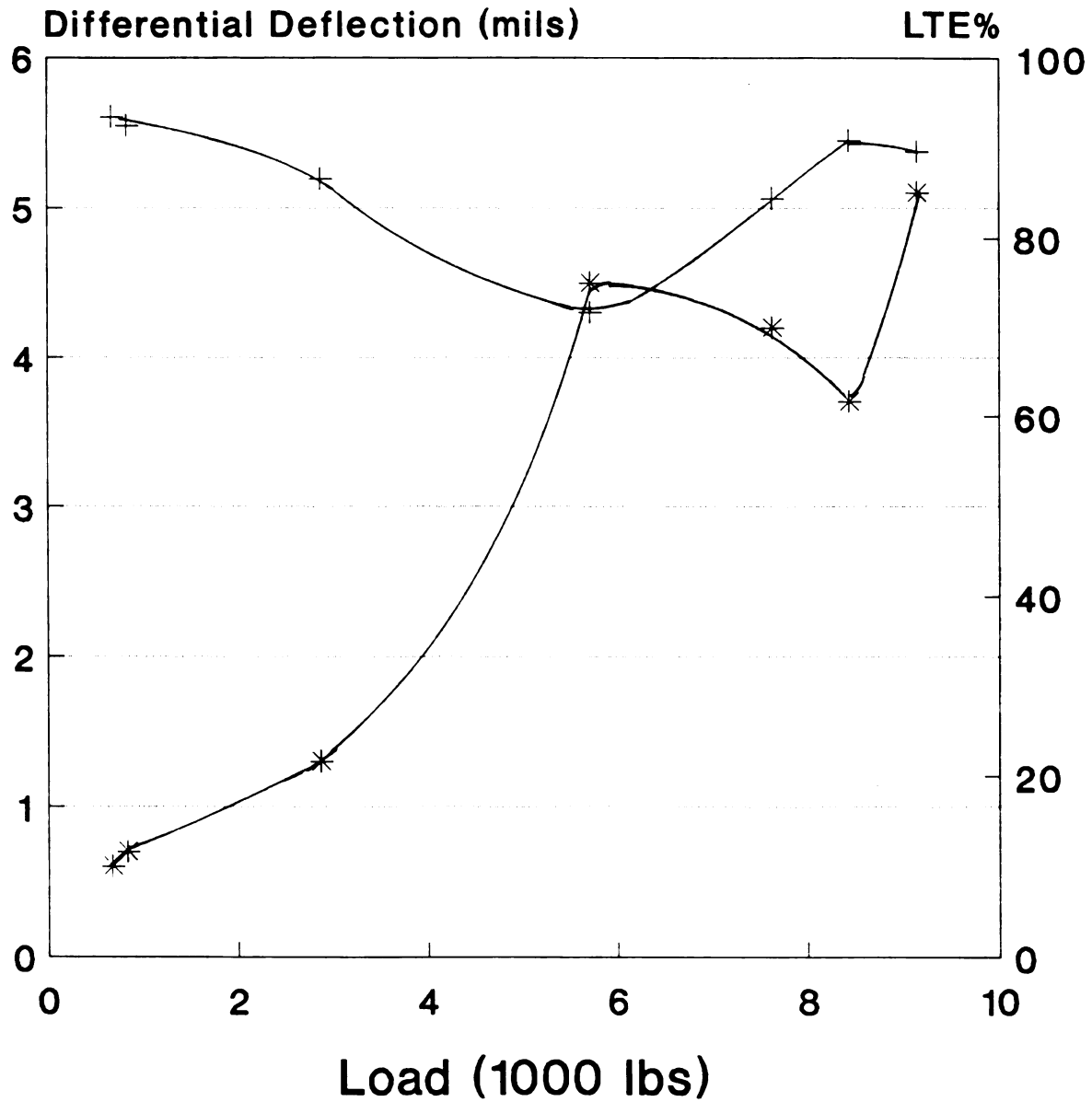
Figure 6.14: Illustration of effect of aggregate interlock looseness on load transfer capacity

deflections increases with increases in applied load. This increase in differential deflection is accompanied by a loss in load transfer capacity. However, after the looseness is taken up by load displacement of the slab fragments, the magnitude of differential deflection starts decreasing and the load transfer capacity begins to increase.

However, note that as the load approaches the peak load the magnitude of differential deflection starts increasing again and consequently the load transfer efficiency begins to drop. This suggests that this specimen experienced slippage of the two vertical faces under the action of the peak load. This is probably related to high tensioning of this specimen which resulted in increased crack width, which, in turn, pulled apart the coarse aggregate particles from their respective sockets. In view of the above, it is recommended that the effect of large top size aggregates (e.g., 2.5-in) on aggregate interlock load transfer characteristics of transverse cracks should be evaluated in future tests, particularly for large crack openings (high tension specimens).

6.6.3 *Effect of Repetitive Loading*

It was observed that aggregate interlock load transfer efficiency of transverse cracks decreases with increasing load cycles, as would be expected. This reduction in load transfer capacity is attributable to the increase in looseness at the crack face caused by wearing out of

interlocking features through repeated slippage of the two vertical faces under accumulated load applications. Generally, load transfer efficiency was observed to drop during initial load cycles, then typically remained approximately constant until the longitudinal steel began to yield, after which it dropped very sharply (due to opening of the crack).

The effect of repetitive loading on load transfer capacity is illustrated in Figure 6.15. This figure is drawn from the load-deflection data collected from 17A virgin gravel specimen. As stated earlier, small amounts of initial looseness existed in this specimen due to relatively smaller top size coarse aggregate (1.0-in. [2.54-cm]), as is seen from the top curve in Figure 6.15, though the effect is not prounounced. However, as the number of load cycles increased the magnitude of differential deflections also started increasing at a sharper rate (see curves for cycle #50,000). This increase in looseness produced decreases in load transfer capacity, as explained previously. As the number of load cycles further accumulated, the differential deflection curve (see curve for cycle # 100,000) shifted upward, indicating a significant increase in looseness, which in turn shifted the LTE curve further down. Note that LTE is now only 77% under the approach side peak load, a loss of approximately 15% from the initial 91% load transfer efficiency.

The fact that this specimen was able to endure approximately another 800,000 load cycles suggests that

Relative Deflection (in)   LTE%

Legend:
- ⊠ RD Cycle # 1
- ⊠ LTE% Cycle # 1
- ·■· RD Cycle # 50000
- ·■· LTE% Cycle # 50000
- ▽ RD Cycle # 100000
- ▽ LTE% Cycle # 100000
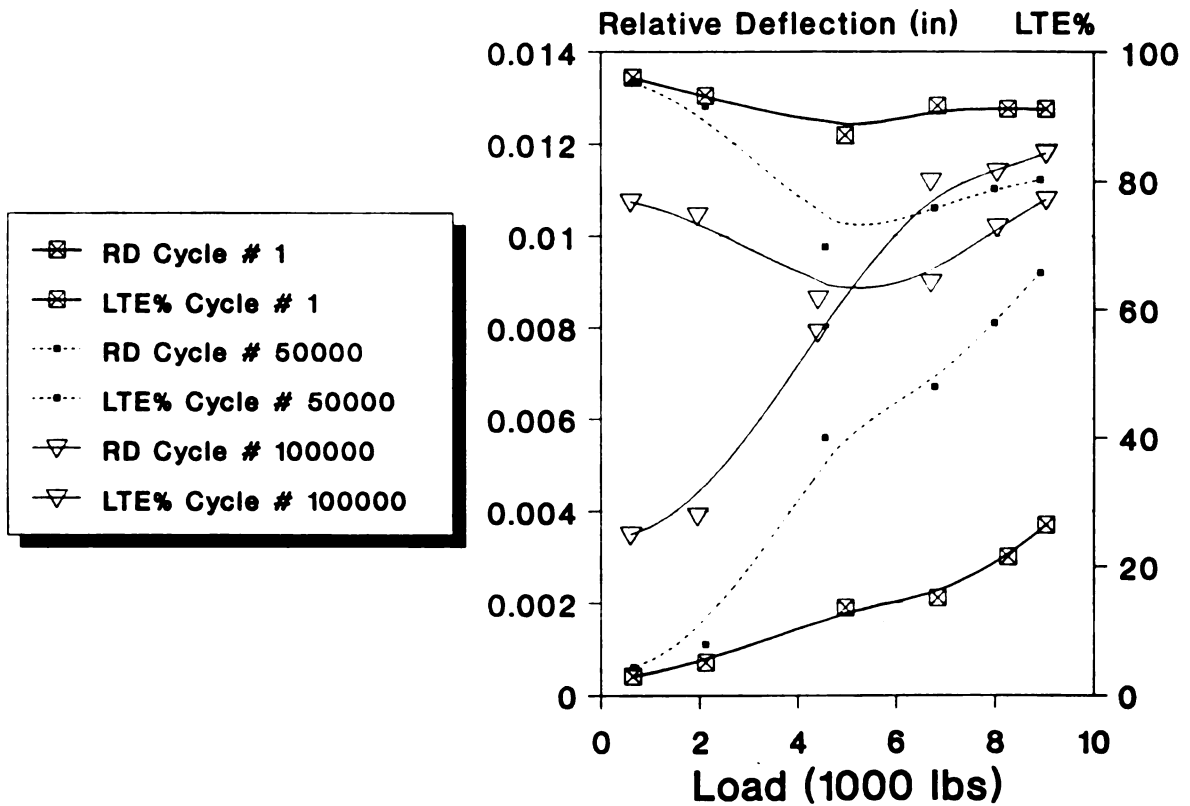
RD · Relative Deflection

Figure 6.15: Effect of repetitive loading on aggregate interlock load transfer (data from 17A virgin gravel specimen)

longitudinal steel had not begin to yield at this point i.e., there was no appreciable change in crack width. Thus, this increase in looseness is attributable to wearing out of the crack interface, more specifically, abrasion/attrition of the coarse aggregate particles and plastic deformation of the aggregate sockets (cement matrix) under repetitive heavy loads. From this description it is apparent that coarse aggregate particles with good abrasion and impact resistance and strong cement matrix should provide longer performance under accumulated heavy loading conditions. In view of the above, it is recommended that in future experimentation aggregates of different quality (source) should be evaluated e.g., limestone # 1 vs limestone # 2, gravel # 1 vs gravel # 2 etc.

6.6.4 *Design of Steel Reinforcement*

As stated earlier, for transverse cracks to exibit good load transfer characteristics, it is imperative that steel reinforcement must serve its intended purpose i.e., *hold the fractured concrete in close interlock*. The unexpected relatively early rupture of steel during this study indicates that current longitudinal steel quantities (0.16 percent by area of concrete) may be inadequate for the combined tension and shear loading conditions encountered in the field. It is realized that the laboratory test is rigorous in nature in that each specimen is under adverse loading conditions (i.e., combined tension and shear)

constantly, whereas in the field due to daily and seasonal temperature changes, tensile stress in longitudinal steel varies with cyclic opening and closing of transverse cracks. Moreover, the rate of application of wheel loads in the field varies and is generally much lower than 5 cycles per second applied in this study; thus, allowing the pavement structure to recover between load applications. Thus, laboratory test specimens were subjected to more severe loading conditions than those encountered in the field.

Nevertheless, rupture of steel during this study represents an need for developing improved reinforcement design procedure based on combined shear and tension failure criteria. Currently, in most design procedures the required amount of reinforcement in JRCP is determined by using subgrade drag theory i.e., area of steel is calculated to resist tensile stresses/strains that develop due to friction between the slab and the foundation. The shear stresses/strains caused by differential displacement of the two slab fragments are neglected. whereas, shear stresses and strains may become very high depending on *magnitude of the load*, *crack interface roughness* and *level of support* provided by the foundation. The cumulative effect of high shear stresses/strains and their reversals combined with tension, under accumulated heavy loads can result in shear-fatigue failure of the longitudinal steel.

The following calculations based on the results of this study illustrate the above point. We know from strength of materials that

Strain, ε = (Elongation)/(Original length)

$\qquad$ = $(\Delta_L)/L$ in/in

and the relation between the ultimate stress and strain is given by

Tensile Strain, ε_t = (Tensile Strength)/(Elastic Modulus)

$\qquad$ = F_y/E

Shear Strain, ε_s = (Shear Strength)/(Shear Modulus)

$\qquad$ = $0.6F_y/G$

where

$\qquad$ E = 29,000,000 psi, and

$\qquad$ G = 12,000,000 psi

In this study MDOT's standard welded smooth wire mesh (see Figure 6.16) was used in each of the specimens. The properties of the mesh are tabulated below:

- Area of longitudinal steel, A_{sl} = 0.172 in^2 [1.11 cm^2]
- Ultimate tensile strength = or > 75,000 psi
  [5273 kg/cm^2]
- Transverse steel spacing = 12-in. [30-cm]
- Cold rolled
- Carbon Content 0.6% - 0.8%

6" X 12" Standard Mesh

Transverse steel:
0.300-in.
diameter smooth
bars at
12 in. c/c

Longitudinal steel: 0.331-in. diameter smooth bars at 6 in. c/c
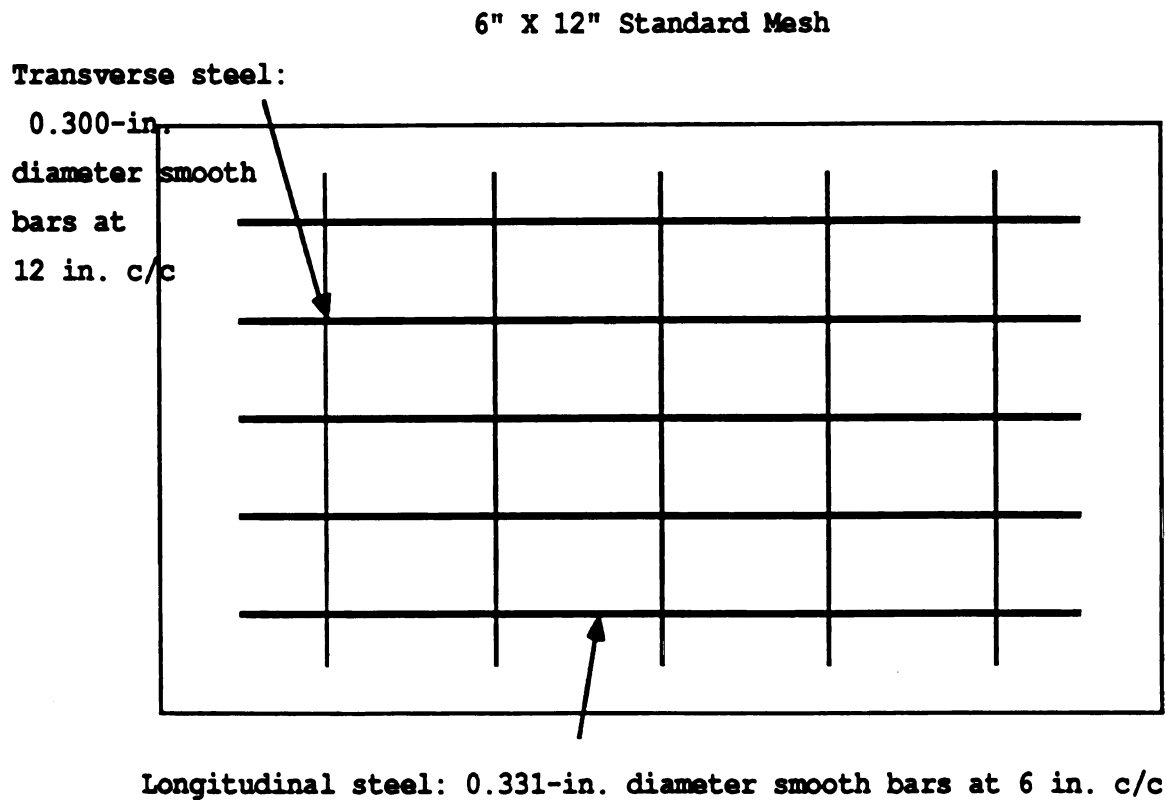
Figure 6.16: Details of 6"x12" wire mesh reinforcement

Using these numbers the ultimate strain capacities of
the longitudinal steel are:

Tensile Strain, ε_t = 0.00259 in/in, and

Shear Strain, ε_s = 0.00375 in/in

If it is assumed that all the stresses/strains are
taking place over the width of the crack only (i.e., no
debonding due to slippage between the steel and the
concrete), then the magnitude of applied shear strain,
computed for a crack opening of 0.015-in. [0.038-cm] and
minimum differential displacement of 1.94 mils observed
among all the data (see Table 6.4: virgin limestone, cycle #
1), equals 0.12933 in/in. This is far higher than the
ultimate shear strain capacity of the steel. Since the steel
had not ruptured at this point, this suggests that there is
some debonding/slippage taking place between the steel and
the concrete.

Assuming debonding/slippage is taking place along 12-in.
[30-cm] length of the longitudinal steel (i.e., center to
center spacing of transverse steel), it can be shown that
the crack may open 0.031-in. [0.079-cm] before steel
ruptures in tension, and that slab fragments may deflect
differentially up to 45 mils before steel is sheared. A look
at the **maximum** measured values (prior to steel rupture) of
crack openings (0.023-in. [0.058-cm]) and differential
displacements (22.73 mils) among all the specimens in this
study show that they were well short of these limiting

values.

This suggests that steel rupture was due to combined tension and shear fatigue. This contention is supported by the differential deflection data tabulated in Table 6.4. It is seen that the three specimens (6A virgin slag, 6A 100% recycled, and 50-50 recycled blend) in which steel ruptured at relatively low and comparable number of load cycles (about 300,000), exhibited considerably higher differential deflections throughout the course of their loading history; whereas the other three specimens (6A virgin limestone, 6A virgin gravel, and 17A virgin gravel) started with much lower differential deflections which started increasing generally after several hundred thousand load cycles. It is obvious that higher level of differential displacements (higher shear stresses/strains and their reversals) could not be sustained over a longer period of time as evidenced by the accelerated rupture of steel in the aforementioned three specimens.

In view of the above, further research is needed to establish a reinforcement design procedure based on a more comprehensive approach (combined tension and shear-fatigue) than the conventionally used simple approach based on the drag theory. One possible approach would be to develop fatigue curves for longitudinal steel, in terms of stress levels and number of load cycles required to cause failure at a certain given level. The relationship between stress level and number of load cycles may be shown on an S-N curve (see figure 6.17). Such a curve, presented on a log-log

$$F_n = S \left(\frac{N}{n}\right)^{\kappa}$$

Stress (log scale)

F_{n_1}

S

F_{n_2}

n_1 N n_2

Cycles to failure (log scale)
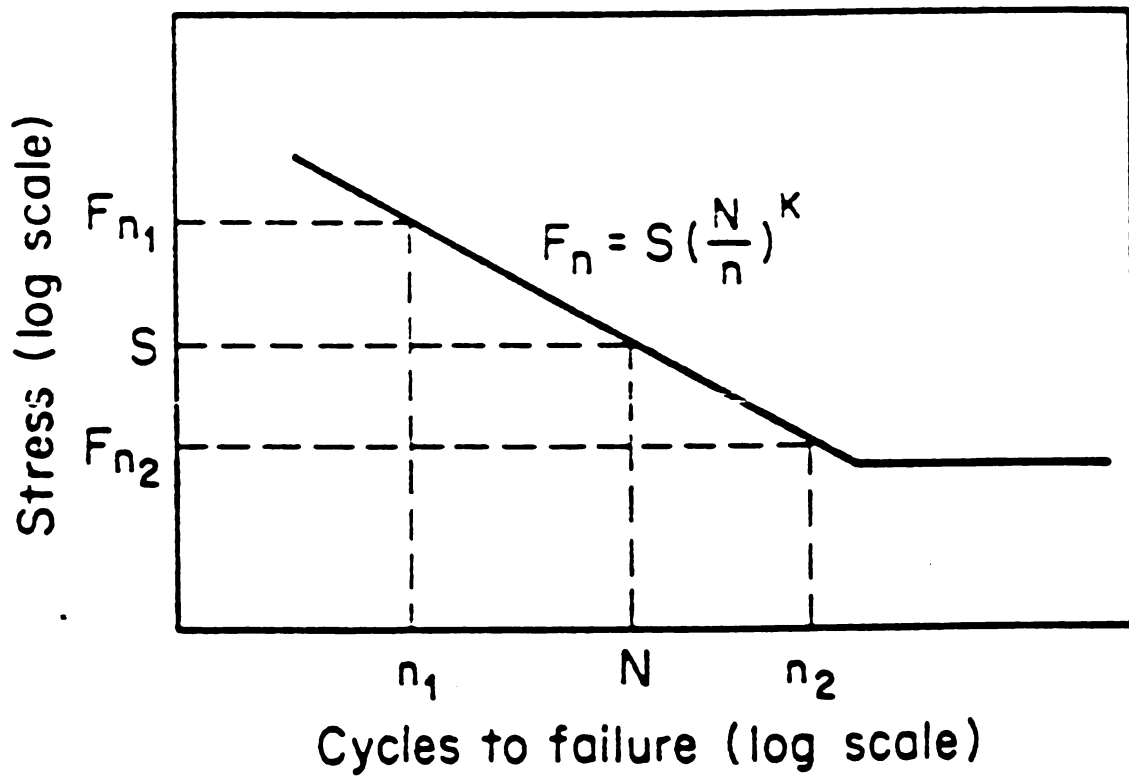
Figure 6.17: A typical S-N curve for steel [25]

basis, portrays the behavior of a specific structural steel detail for a given loading condition and can be expressed by [25]

$$F_n = S(N/n)^k$$

where

F_n = fatigue strength computed for failure at n cycles

S = stress which produced failure in N cycles

k = slope of the straight-line S-N curve

Such a relationship can be developed for JRCP longitudinal steel by conducting cyclic loading tests on laboratory specimens. The tests should be conducted so that the stress level during the course of loading remains constant for all specimens. The slope of the straight-line S-N curve can be obtained by varying the magnitude of stress level from specimen to specimen.

Once this relationship (for a typical type and quantity of longitudinal steel) has been developed, it can then be used to determine the fatigue limit of the longitudinal steel. This can be done by comparing the projected traffic (18000-lb [80-KN] single-axle loads) and the estimated stress level in the outer lane of the "to be constructed" pavement section. Since traffic and stress level, both increase with passage of time, Miner's hypothesis [25] may be used to analyze the fatigue behavior. For failure,

$$\Sigma(n_i/N_i) = (n_1/N_1) + (n_2/N_2) + \ldots = 1$$

where

n_i = number of stress cycles at stress level i

N_i = number of stress cycles to produce failure at stress level i

The use of above-described concepts in design of JRCP longitudinal steel would require development of a series of S-N curves representing different quantities of steel.

6.7 Summary

The overall objective of this study is to advance the state-of-the-knowledge on the subject of aggregate interlock load transfer across transverse cracks in JRCP. The specific purpose of this comparative laboratory study was to estimate the effects of several material and design factors on the aggregate interlock load transfer characteristics of transverse cracks in JRCP. The general concept of the study involved the application of repeated loads (simulating the passage of heavy truck traffic) across transverse cracks that have been induced in a series of large-scale reinforced concrete slab test specimens and the collection and analysis of load transfer data at several points during the testing of each specimen.

This laboratory study has provided valuable information on the characteristics of aggregate interlock load transfer mechanism. The major conclusions drawn from the results of this study are summarized in the next chapter along with recommendations for future experimentation.

CHAPTER VII

CONCLUSIONS AND RECOMMENDATIONS

7.1 Primary Conclusions

The following primary conclusions were drawn from the results of this laboratory study:

1. When the type of coarse aggregate (gravel, limestone or slag) was varied while holding all other variables approximately constant, load transfer efficiency and endurance was significantly higher for 6A limestone and 6A gravel than for 6A slag.

2. When all other variables were held constant, transverse crack load transfer efficiency and endurance decreased (but only slightly) when the coarse aggregate gradation was changed from 6A (1.5-in. top size) to 17A (1.0-in. top size).

3. The use of 100% recycled 6A gravel concrete as coarse aggregate decreased the load transfer efficiency and

p

t

6.

th

re

re

7.2

r

resu

t. A

reinfo

cycle

endurance considerably as compared to concrete made using virgin 6A gravel.

4. The use of the blend of 50% virgin 4A (2.5-in. top size) limestone and 50% recycled 6A gravel concrete as coarse aggregate decreased the load transfer efficiency and endurance considerably as compared to concrete made using virgin 6A gravel.

5. While holding all other variables approximately constant and increasing the amount of slab tension from typical (3500 lb/ft width) [51 KN/m width] to high (7000 lb/ft width) [102 KN/m width] resulted in a significant reduction in load transfer efficiency and endurance of transverse crack.

6. The use of a stiff foundation (k = 250 psi/in) increased the endurance of good load transfer efficiency under repeated load applications compared to the use of a relatively soft foundation (k = 100 psi/in).

7.2 Other Related Findings

The following observations were also made from the results of this laboratory study:

1. Aggregate interlock load transfer efficiency of reinforced transverse cracks decreases with increasing load cycle applications. It was observed that load transfer

3.

exc

cra

inte

func

taken

7.3

ag

Th

of this

efficiency (LTE) typically drops by 2 to 27 percent under repeated load applications until the longitudinal steel begins to yield, after which it drops sharply.

2. The aggregate interlock load transfer capacity of transverse cracks is related to the texture of the crack face. The crack face texture is primarily a function of the type, size, and number of coarse aggregate particles at the crack face and the mode of fracture. It was observed that specimens in which the cracks developed <u>around</u> the aggregate (i.e., virgin crushed stone and virgin gravel) developed higher initial load transfer efficiencies and were able to maintain this higher level over a considerably larger number of load cycles than specimens in which the crack developed <u>through</u> the aggregate (i.e., virgin slag and recycled aggregates).

3. The amount of aggregate interlock looseness (caused by excessive crack opening and/or attrition and wearing of crack interface) significantly affects the aggregate interlock efficiency and endurance, since it can only function at full efficiency only after the looseness is taken up by displacement of the slab.

7.3 Recommendations

The following recommendations are made from the results of this laboratory study:

1. The observed performance of the six specimens incorporating various material factors and the underlying reasons for differences in performance of these specimens suggest the use of a concrete mix that produces a rough crack interface (large protrusions and macrotexture). The key factor which determines the texture of the crack face is the mode of concrete fracture. The use of coarse aggregate particles with high tensile strength is recommended to ensure pullout of aggregate particles at the time of crack development. The results of this and some other previous studies suggest that large size, angular (rough-surfaced) coarse aggregate particles are beneficial in the preservation of aggregate interlock effectiveness (particularly for wide crack openings and high number of load repetitions). With regards to the use of recycled concrete as coarse aggregates, it is felt that increasing the number of virgin aggregate particles in a recycled blend may improve the performance of aggregate interlock. This can be verified in future experimentation by testing materials that have high percentages of large size virgin material (by weight) and/or by decreasing the top size of the virgin material to a gradation comparable to the recycled material.

2. Although the unexpected poor performance of the 50-50 recycled blend (6A recycled gravel concrete with 4A virgin limestone) concrete might be due to inadequate numbers of virgin coarse aggregate particles at the crack face or due

b

q

j

ne

ch

cor

Pra

4. S

crac

tsmo

coarse

top

aggreg

to slab handling difficulties, there is enough concern about the results of this particular specimen to recommend replicating the test in future experimentation.

3. One of the unexpected findings of this study is the relatively early rupture of steel in all six test specimens. Although this laboratory test is rigorous in nature in that each test specimen is under adverse loading conditions (i.e., combined tension and shear) constantly, it is possible that current longitudinal steel quantities (0.16% percent by area of concrete) are inadequate for the combined tension and shear loading conditions encountered in the field. Further testing should include variations of steel quantities. The results of this and any future testing can be used as a basis for recommending an increase in the quantity of "temperature and shrinkage" steel to keep cracks tighter and reduce deterioration. Development of a mechanistic reinforcement design procedure (as described in chapter 6) is suggested to replace or supplement the conventionally used design procedure based on the subgrade drag theory.

4. Several other factors are likely to affect transverse crack performance. These include type of steel reinforcement (smooth wire vs deformed wire), source or quality of virgin coarse aggregate (limestone # 1 vs limestone # 2 etc), large top size aggregates (e.g., 2.5-in [6.3-cm]) and aggregate/paste bond strength (effect of fracture delay).

These factors should also be considered in future testing.

5. Replicate test specimens should be prepared for most of these specimens that were tested during this study to determine the variability of the test results and help in identifying true differences in specimen performance. A preliminary statistical analysis is presented in APPENDIX C.

6. Based on recommendations 1-5, test matrices presented in Figures 7.1-7.5 are proposed for expanding the current test program. Note that these matrices accomplish the following three major goals:

- Provide replicate tests for selected cells to provide an better estimate of the blocking effect (as described in chapter 4 and APPENDIX C) and pure error. Testing a 6A virgin limestone specimen and a 50-50 recycled blend (see Figures 7.1 and 7.2) shall improve the precision of the estimate of the blocking effect. Moreover, the results of the 6A virgin limestone (under modified conditions) are needed to determine the effect of coarse aggregate source/quality (see Figure 7.1). Testing another 6A virgin gravel specimen (see Figure 7.1) shall increase the degree of freedom to two in the estimate of pure error. This will result in improved confidence levels in the statistical analysis.

- Consider additional test factors that are likely to play

important roles in the JRCP transverse crack performance (i.e., reinforcing steel quantities and type, age of concrete at the time of fracture, source or quality of aggregate, and a larger top size aggregate.

- Complete fractional factorial test matrices to identify possible interaction effects of selected test factors. It is felt that type of coarse aggregate and treatment of coarse aggregate are unlikely to interact. This contention is based on the examination of the crack faces of the recycled specimens, which revealed that very few pull outs of aggregate particles existed. It was pointed out previously, that use of comparable quantities of recycled aggregate (100% recycled specimen) and use of an equal weight of large aggregate (50-50 recycled specimen) results in a significant reduction in the actual number of virgin aggregate particles in the mix. Thus, various combinations of coarse aggregate type and treatment are unlikely to produce significant differences in performance. However. it is felt that performance of recycled specimens may be improved by having high percentages of large size virgin material (by weight) and/or by decreasing the top size of the virgin material to a gradation comparable to the recycled material. Yet, another possible approach would be to use recycled coarse aggregates produced by breaking and crushing slabs cast using a large top size virgin aggregates (e.g., MDOT gradation 10A/4A: 2.5-in. [6.35-cm] top size) (see Figure 7.2). Recycled aggregates thus obtained would contain

relatively large size virgin aggregate particles bonded to the old cement mortar, for a given gradation (e.g., 6A gradation).

PROPOSED MATRIX 1

	CA SOURCE (QUALITY)	
CA TYPE	**#1**	**#2**
GRAVEL	A D D M1	M1
LIMESTONE	A M1	M1

Notes:
1. A = Test cell run under matrix A (see Figure 4.1)
2. D = Test cell run under matrix D (see Figure 4.4)
3. M1 = Test cell being tested under proposed matrix 1
4. Foundation modulus = 100 psi/in
5. Typical slab tension = 3500 lb/ft [51 KN/m width] (coefficient of friction = 1.5, slab length = 41 ft [12.5 m], crack face depth = 9-in. [23-cm]
6. Longitudinal steel = 0.16% by area of concrete
7. All coarse aggregates conform to MDOT gradation 6A

Figure 7.1: Proposed test matrix 1

PROPOSED MATRIX 2

CA GRADATION	CA TREATMENT		
	VIRGIN	100% RECYCLED	50-50 BLEND
6A	A D D M1	C	C
17A	B		
10A/4A	M2	M2	M2

Notes:

1. A = Test cell run under matrix A (see Figure 4.1)
2. B = Test cell run under matrix B (see Figure 4.2)
3. C = test cell run under matrix C (see figure 4.3)
4. D = Test cell run under matrix D (see Figure 4.4)
5. M1 = Test cell first filled in proposed matrix 1
6. M2 = Test cell being tested under proposed matrix 2
7. Foundation modulus = 100 psi/in
8. Typical slab tension = 3500 lb/ft [51 KN/m width] (coefficient of friction = 1.5, slab length = 41 ft [12.5 m], crack face depth = 9-in. [23-cm]
9. Longitudinal steel = 0.16% by area of concrete
10. Aggregates type gravel
11. Treatments as defined in Table 4.1
12. 10A/4A gradation – top size = 2.5-in. [6.35-cm]

Figure 7.2: Proposed test matrix 2

PROPOSED MATRIX 3

STEEL TYPE	STEEL QUANTITY	SLAB TENSION	
		TYPICAL	HIGH
SMOOTH	TYPICAL	A D D M1	D
	HIGH	M3	M3
DEFORMED	TYPICAL	M3	M3
	HIGH	M3	M3

Notes:

1. A = Test cell run under matrix A (see Figure 4.1)

2. D = Test cell run under matrix D (see Figure 4.4)

3. M1 = test cell first filled in proposed matrix 1

5. M3 = Test cell being tested under proposed matrix 3

6. Foundation modulus = 100 psi/in

7. Typical slab tension = 3500 lb/ft [51 KN/m width] (coefficient of friction = 1.5, slab length = 41 ft [12.5 m], crack face depth = 9-in. [23-cm]

8 High slab tension = 7000 lb/ft width [102 KN/m width] (coefficient of friction = 3.0, slab length = 41 ft [12.5 m], crack face depth = 9-in. [23-cm]

9. Typical longitudinal steel = 0.16% by area of concrete

10. High longitudinal steel = 0.25% by area of concrete

11. Aggregates type gravel

Figure 7.3: Proposed test matrix 3

PROPOSED MATRIX 4

	AGE (days)	
CA SOURCE	1	7
GRAVEL # 1	A D D M1	M4
GRAVEL # 2	M4	M4

Notes:

1. A = Test cell run under matrix A (see Figure 4.1)

2. D = Test cell run under matrix D (see Figure 4.4)

3. M4 = Test cell being tested under proposed matrix 4

4. Foundation modulus = 100 psi/in

5. Typical slab tension = 3500 lb/ft [51 KN/m width] (coefficient of friction = 1.5, slab length = 41 ft [12.5 m], crack face depth = 9-in. [23-cm]

6. Longitudinal steel = 0.16% by area of concrete

7. All coarse aggregates conform to MDOT gradation 6A

Figure 7.4: Proposed test matrix 4

PROPOSED MATRIX 5

	FOUNDATION	
SLAB TENSION	100	250
TYPICAL	A D D M1	E
HIGH	D	M5

Notes:

1. A = Test cell run under matrix A (see Figure 4.1)

2. D = Test cell run under matrix D (see Figure 4.4)

3. M1 = Test cell first filled in proposed matrix 1

4. M5 = Test cell being tested under proposed matrix 5

5. Typical foundation modulus = 100 psi/in

6. High foundation modulus = 250 psi/in

7. Typical slab tension = 3500 lb/ft [51 KN/m width] (coefficient of friction = 1.5, slab length = 41 ft [12.5 m], crack face depth = 9-in. [23-cm]

8. High slab tension = 7000 lb/ft [102 KN/m width] (coefficient of friction = 3.0, slab length = 41 ft [12.5 m], crack face depth = 9-in. [23-cm]

9. Longitudinal steel = 0.16% by area of concrete

10. All coarse aggregates conform to MDOT gradation 6A

11. Aggregate type gravel

Figure 7.5: Proposed matrix 5

LIST OF REFERENCES

LIST OF REFERENCES

1. Darter, M. I., "Initial Evaluation of Michigan JRCP Crack Deterioration," a report prepared for Michigan Concrete Paving Association, December, 1988, Revised February, 1989, Mahomet, IL 61853.

2. McCarthy, G.J., and MacCreery, W.J., "Michigan Department of Transportation Recycles Concrete Freeways," Proceedings Third International Conference on Concrete Pavement Design and Rehabilitation, Purdue University, April 23-25, 1983, W. Lafayette, IN., pp. 643-647.

3. Benkelman, A.C., "Tests of Aggregate Interlock at Joints and Cracks," Engineering News Record, Vol. III, No. 8, August 24, 1933, New york, N.Y., pp. 227-232.

4. Colley, B.E., and Humphrey, H.A., "Aggregate Interlock at Joints in Concrete Pavements," Highway Research Record No. 189, Highway Research Board, National Research Council, Washington, D.C., 1967, pp. 1-18.

5. Nowlen, W.J., "Influence of Aggregate Properties on Effectiveness of Interlock Joints in Concrete Pavements," Journal of the PCA, Research and Development Laboratories, Vol. 10, No. 2, May 1968, pp. 2-8

6. Sutherland, E.C., and Cashell, H.D., "Structural Efficiency of Transverse Weakened-Plane Joints," Public Roads, Vol. 24, No. 4, April-May-June 1945.

7. Older, C., "Efficiency of Aggregate interlock in Concrete Roads," Engineering News Record, Vol. III, No. 8, November 23, 1933, New York, N.Y., pp 615-616.

8. Poblete, M., Valenzuela, R., and Salsilli, R., "Load Transfer in Undowelled Transverse Joints of PCC Pavements," Transportation Research Record 1207, Transportation Research Board, National Research Council, Washington, D.C. 1988.

9. Ioannides, A. M., and Korovesis, G. T., "Aggregate Interlock: Pure-Shear Load Transfer Mechanism," paper prepared for presentation at the 1990 Annual Meeting of the Transportation Research Board, Washington, D.C.

10. Laible, J. P., White, R. N., and Gergely, P., "Experimental Investigation of Siesmic Shear Transfer Across Cracks in Concrete Nuclear Containment Vessels," *Reinforced Concrete Structures in Siesmic Zones*. Detroit, American Concrete Institute, 1977. ACI Special Publication SP-53.

11. Jimenez, R., Gergely, P., and White, R. N., "Shear Transfer Across Cracks in Reinforced Concrete," Ithaca (N.Y.), Cornell University, August 1978, pp. 357. Report 78-4.

12. Fardis, M. N., and Bu yukozturk, o., "Shear Transfer Model for Reinforced Concrete," Proceedings of the American Society of Civil Engineers. Vol. 105, No. EM2. April 1979, pp. 225-275.

13. Walraven, J. C., "Fundamental Analysis of Aggregate Interlock," American Society of Civil Engineers, Journal of the Structural Division, Vol. 107, No. 11, November 1981, pp. 2245-2270.

14. Millard, S. G., and Johnson, R. P., "Shear Transfer Across Cracks in Reinforced Concrete Due to Aggregate Interlock and to Dowel Action," Magazine of Concrete

1
C
R

1
Ti
Co

20
Ev
Okl

21.
Dow
Hig

22.
and
Comp

Research, Vol. 36, No. 126, March 1984.

15. Soroushian, P., Obaseki, K., and Choi, K., "Analysis of Aggregate Interlock Behavior at Cracks in Reinforced Concrete," Magazine of Concrete Research, Vol. 40, No. 142, March 1988, pp. 43-49.

16. Darter, M.I., <u>Design of Zero-Maintainance Plain Jointed Pavements: Vol. 1.1 - Development of Design Procedures</u>, Contract Number DOT-FH-11-8474, Federal Highway Administration, Washington, D.C., June 1977.

17. Snyder, M. B., "Dowel Load Transfer Systems for Full-Depth Repairs of Jointed Portland Cement Concrete Pavements," Ph.D. Thesis, University of Illinois at Urbana-Champaign, 1988.

18. Ball, C. G., and Childs, L.D., "Tests of Joints for Concrete Pavements," Research and Development Bulletin RD026.01P, Portland Cement Association, Skokie, IL, 1975.

19. Ciolko, A. T., Nussbaum, P. J., and Colley, B. E., "Load Transfer of Dowel Bars and Star Lugs," Final Report, Construction Technology Laboratories, Skokie, IL, 1979.

20. Siriwat, C., "Development of a Test Facility for Evaluation of Concrete Pavement Joints," Ph.D. Thesis, Oklahoma State University, Stillwater, Oklahoma, 1987.

21. Teller, L.W., and Cashell, H.D., "Performance of Dowelled Joints Under Repetitive Loading," Bulletin 217, Highway Research Board, Washington, D.C., 1959.

22. Troxell, G.E., Davis, H.E., and Kelly, J.W., Composition and Properties of Concrete, second edition, McGraw-Hill Book Company, N.Y., 1968, pp 238-247.

23.Tabatabai, A. M., Barenberg, E. J., and Smith, R. E., "Longitudinal Joint Systems in Slip-Formed Pavements, Vol. II - Analysis of Load Transfer Systems for Concrete Pavements," Report No. FAA-RD-79-4, prepared for USDOT, FAA, 1979.

24. "Methods for Reducing Friction Between Concrete Slabs and Cement-Treated Subbases," an unpublished report by the Cement and Concrete Research Institute (a division of the Portland Cement Association) for the Federal Highway Administration, September 1971.

25. Gaylord, E. H., and Gaylord, C. N., Structural Engineering Handbook, second edition, McGraw-Hill Book Company, 1979, pp. 4-1 to 4-12.

26. Hanson, J. M., Burton, K. T., and Hognestad, E., "Fatigue Tests of Reinforcing Bars - Effect of Deformation Pattern," Journal of the PCA, Research and Development Laboratories, Vol. 10, No. 3, September 1968, pp. 2-13.

27. Snyder, M. B., "Dowel Load Transfer Systems for Full-Depth Repairs of Jointed Portland Cement Concrete Pavements," Ph.D. Thesis, University of Illinois at Urbana-Champaign, 1988.

28. Snyder, M. B., Reiter, M. J., Hall, K.T., Darter, M.I., Voigt, G.F., et. al., "Rehabilitation of Concrete Pavements
        Volume I   - Repair Rehabilitation Techniques
        Volume II   - Overlay rehabilitation Techniques
        Volume III - Concrete Pavement Evaluation and
                     Rehabilitation System
        Volume IV - Appendexis"
Final Report, Prepared for Federal Highway Administration, Department of Civil Engineering, University of Illinois at Urbana-Champaign, Urbana, Il, December 1987.

29. Darter, M.I., Becker, J., Snyder, M.B., and Smith, R.E., _Portland Cement Concrete Pavement Evaluation System (COPES)_, NCHRP Report No. 277, Transportation Research Board, 1984.

30. Paulay, T., and Loeber, P.J., "Shear Transfer by Aggregate Interlock," Shear in Reinforced Concrete, Detroit, American Concrete Institute, 1974, Special Publication SP-42, Vol. 1, pp. 1-16.

31. Christory, J.P., Nissoux, J. L., Orsat, P., and Verhee, F., "Load transfer Restoration at Joints," _Proceedings_ Fourth International Conference on Concrete Pavement Design and Rehabilitation, Purdue University, April 18-20, W. Lafayette, IN., pp. 1-18.

32. Gulden, W., and Brown, D., "Establishing Load Transfer in Existing Jointed Concrete Pavements," paper prepared for presentation at the 1985 Annual Meeting of the Transportation Research Board, Georgia Department of Transportation.

33. Kushing, J.W., and Fremont, W. O., "Design of Load Transfer Joints in Concrete Pavements," _Proceedings_ Vol. 20, Highway Research Board, Washington, D.C., 1940.

34. Bolourchi, Z., Temple, W. H., and Shah, S. C., Evaluation of Load Transfer Devices, Final Report, Report No. FHWA-2A-97, Federal Highway Administration, Washington, D.C., 1975.

35. Arnold, C. J., "Performance of Several Types of Corrosion Resistant Load Transfer Bars, for as much as 21 Years of Service in Concrete Pavements," Research Report No. R-1151, Michigan Department of State Highways and Transportation, Aug. 1980.

36. Peshkin, D. G., Smith, K. D., Darter, M. I., and Arnold, C. J., "Performance Evaluation of Experimental Pavement

Designs at Clare, Michigan," Transportation Research Record No. 1227, Transportation Research Board, National Research Council, Washington, D.C. 1989.

37. Kapernick, J. W., "Equipment for Studying Joint Performance in the Laboratory," Journal of the PCA, Research and Development Laboratories, Vol. 5, No. 2, May 1963.

38. Yoder, E. J., and Witczak, M. W., _Principles of Pavement Design_, second edition, John Wiley and sons, Inc., New York, new York, 1975.

39. _AASHTO Guide for the Design of Pavement Structures - 1986_, American Association of State Highway and Transportation Officials, Washington, D.C., 1986.

40. Neter, J., Wasserman, W., and Kutner, M. H., _Applied Linear Statistical Models_, second edition, Richard D. Irwin, Inc., Homewood, Illinois 60430, pp. 230-240.

41. _User Manual for LABTECH NOTEBOOK SYSTEMS_, version 5.0, Laboratory Technologies Corporation, Inc., Wilmington, MA, 1990.

42. _T/RAC OPERATORS GUIDE_, version 1.5.4, MTS Systems Corporation, Minneapolis, Minnesota, 1990.

43. _Annual Book of ASTM Standards_, Vols. 04.02 and 04.03, 1991.

44. Highter, W. H., and Moore, E. L., "Prediction of Rigid-Pavement Performance from Cumulative Deflection History," Transportation Research Record 633, Transportation Research Board, 1977.

left intentionally blank

left intentionally blank

APPENDIX A

LOAD-DEFLECTION HISTORIES OF TEST SPECIMENS

(MATERIAL FACTORS)
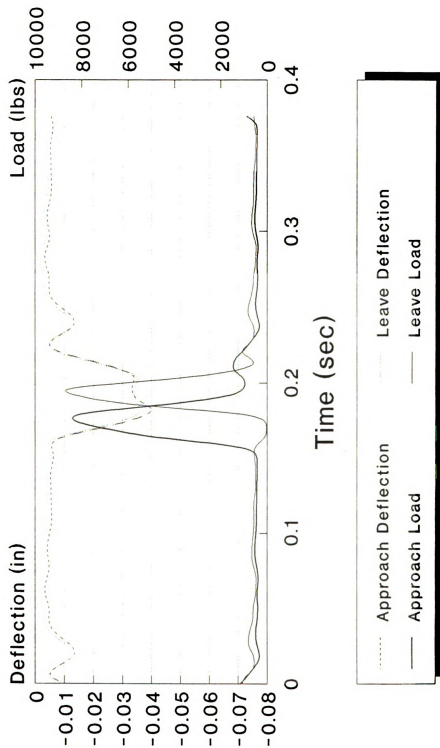
Figure A-1: Load and deflection curves for 6A virgin gravel slab after cycle # 1.

6A VIRGIN GRAVEL
CYCLE # 1000
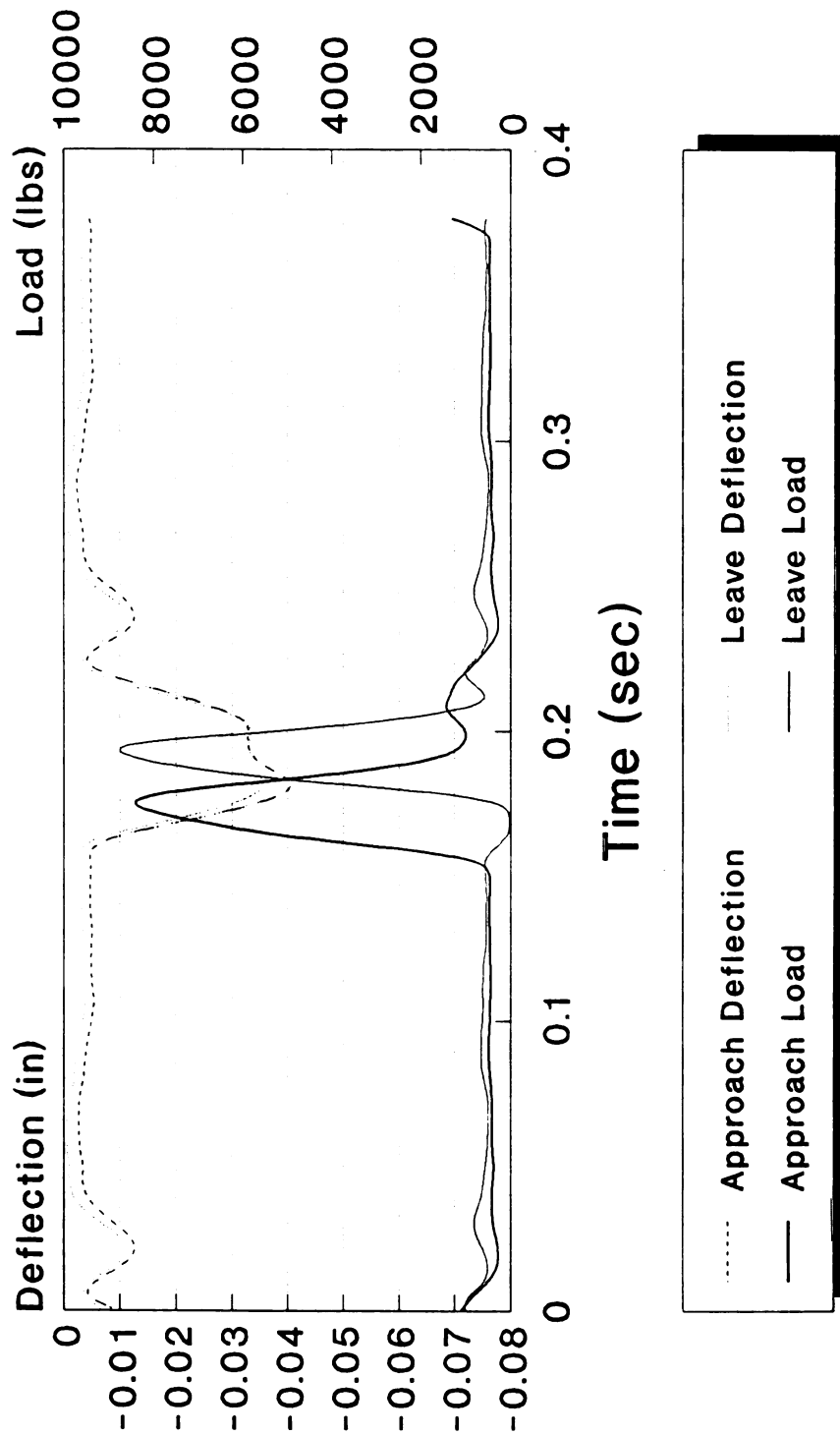
Figure A-2: Load and deflection curves for 6A virgin gravel slab after cycle # 1,000.

Figure A-3: Load and deflection curves for 6A virgin gravel slab after cycle # 2,000.
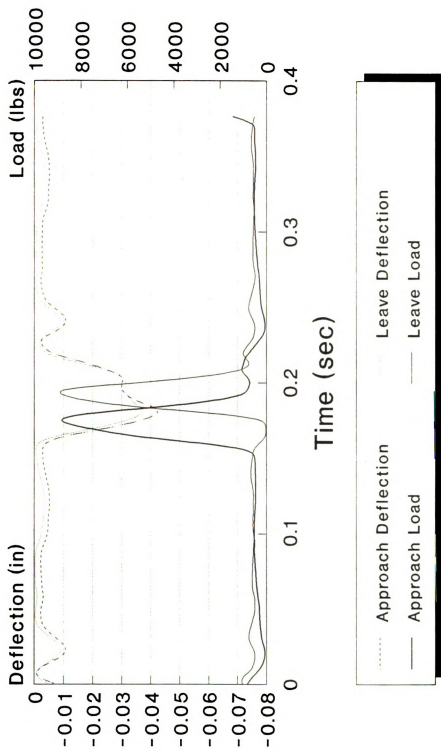
Figure A-4: Load and deflection curves for 6A virgin gravel slab after cycle # 5,000.
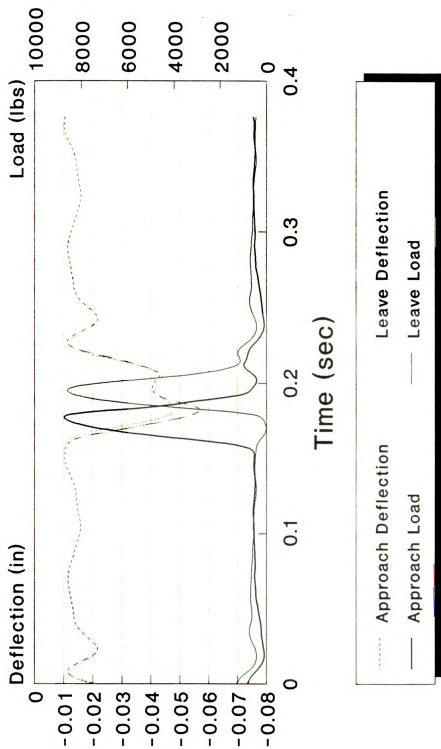
CA VIRGIN GRAVEL

Figure A-5: Load and deflection curves for 6A virgin gravel slab after cycle # 20,000.
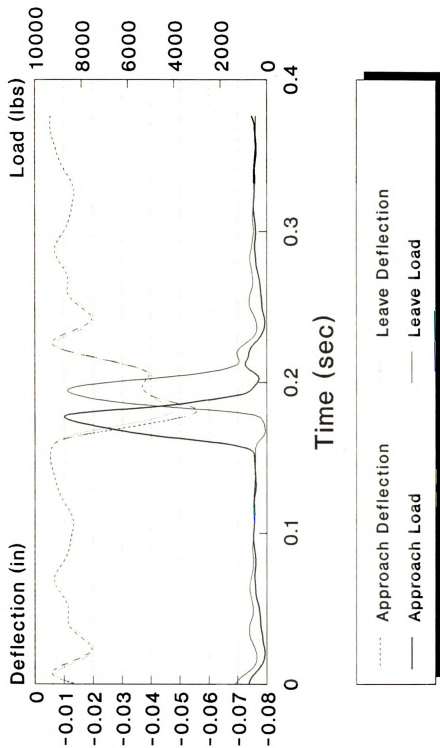
Figure A-6: Load and deflection curves for 6A virgin gravel slab after cycle # 50,000.

144
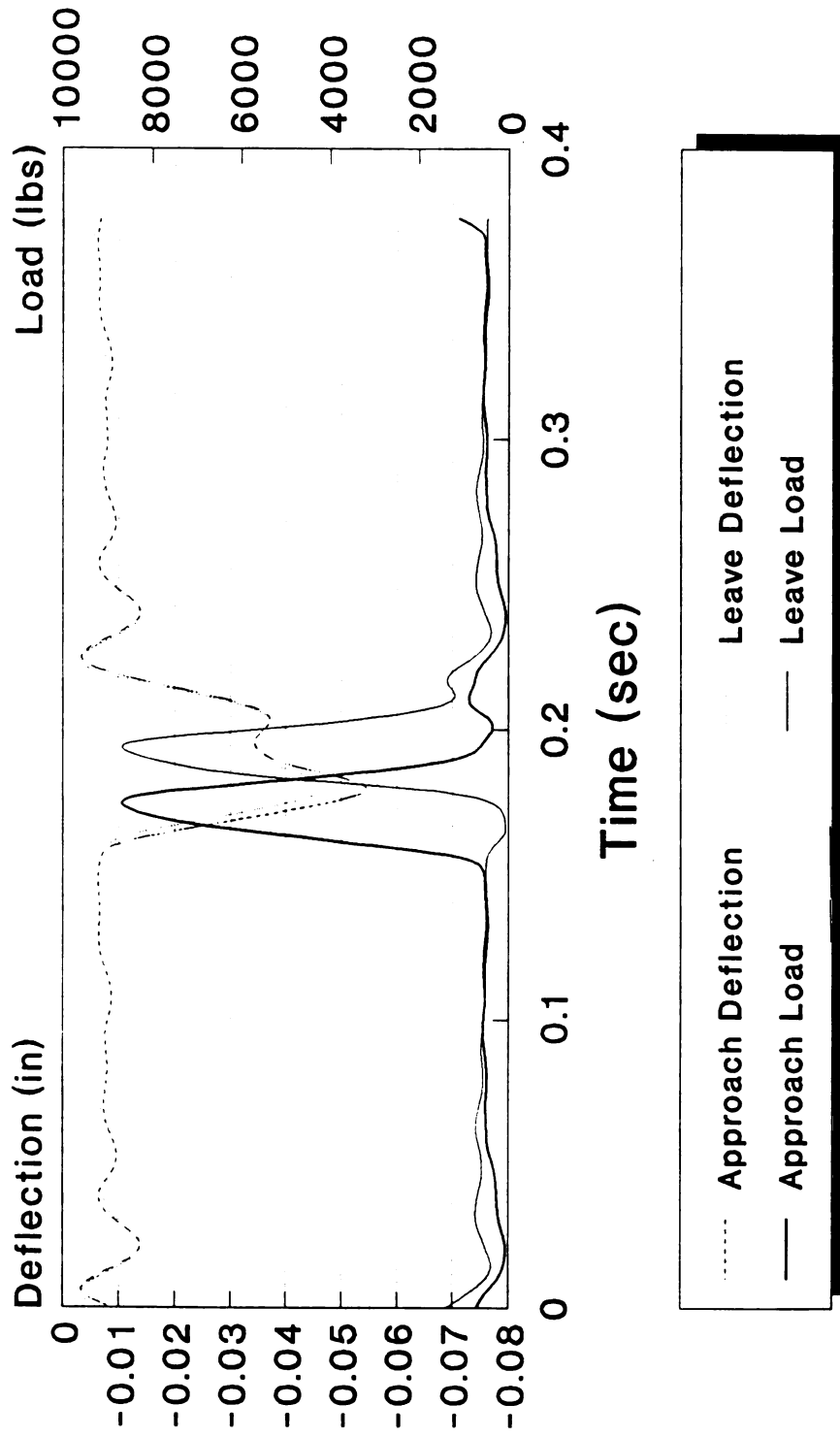
Figure A-7: Load and deflection curves for 6A virgin gravel slab after cycle # 100,000.

CANYON GRAVEL
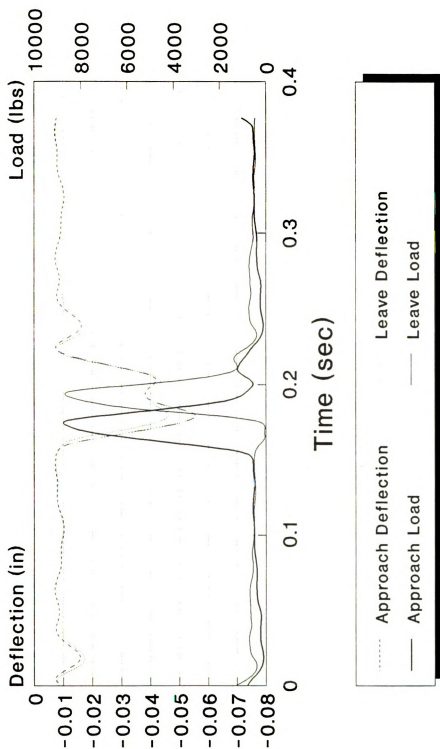
Figure A-8: Load and deflection curves for 6A virgin gravel slab after cycle # 300,000.

Figure A-9: Load and deflection curves for 6A virgin gravel slab after cycle # 600,000.
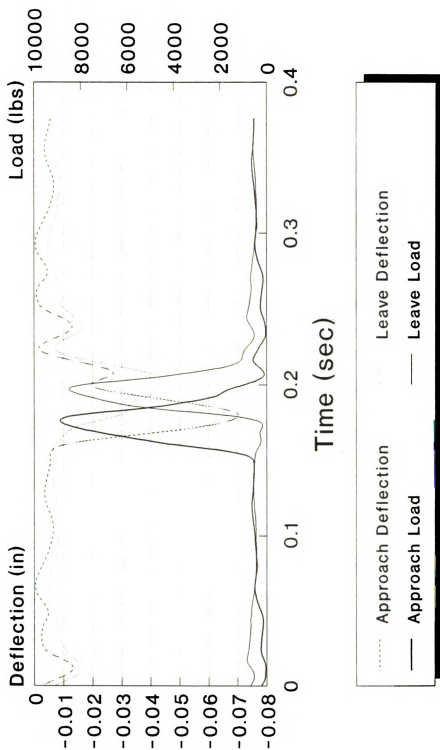
Figure A-10: Load and deflection curves for 6A virgin gravel slab after cycle # 900,000.

6A VIRGIN LIMESTONE
CYCLE # 1
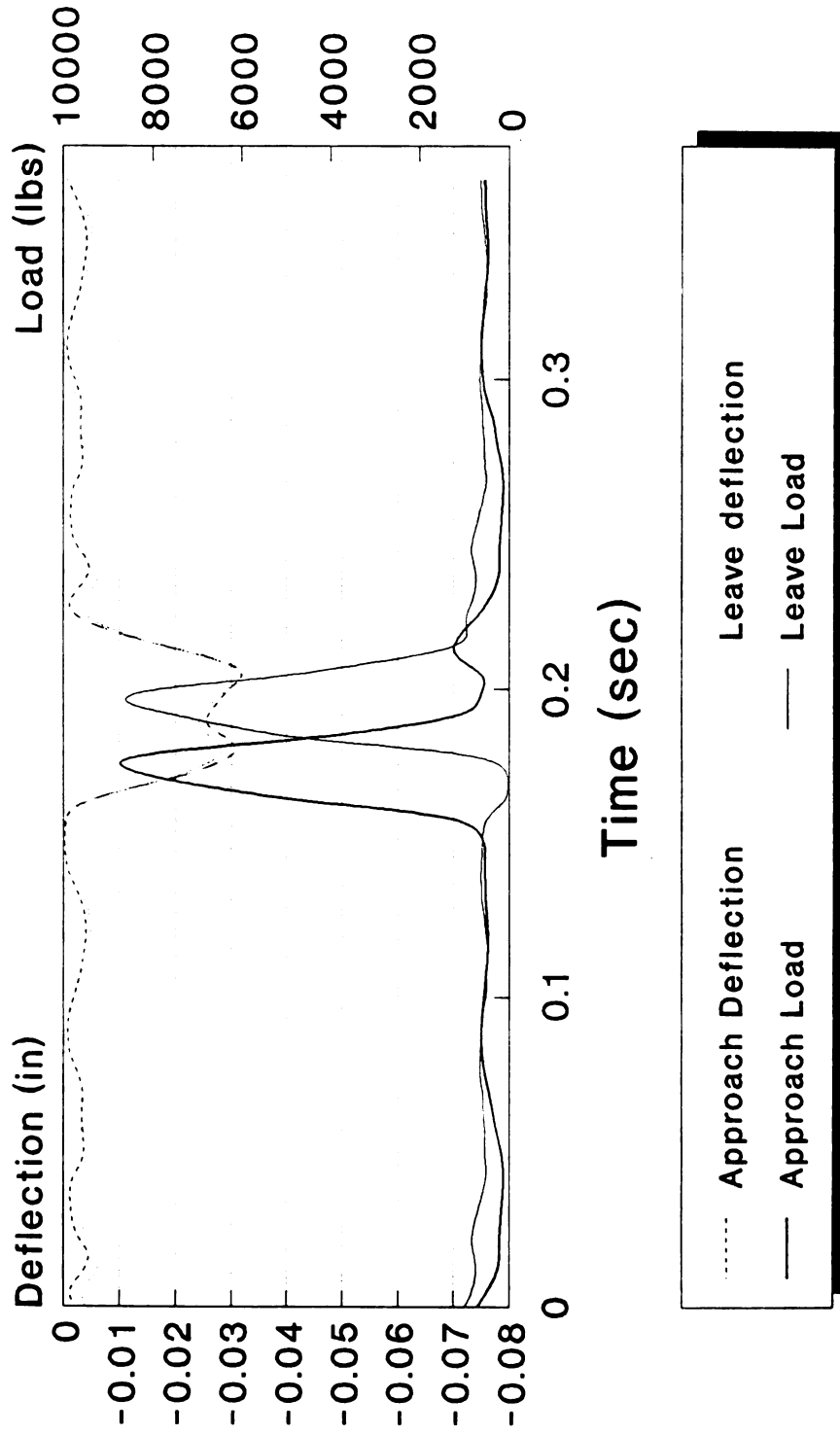
Figure A-11: Load and deflection curves for 6A virgin limestone slab after cycle # 1.
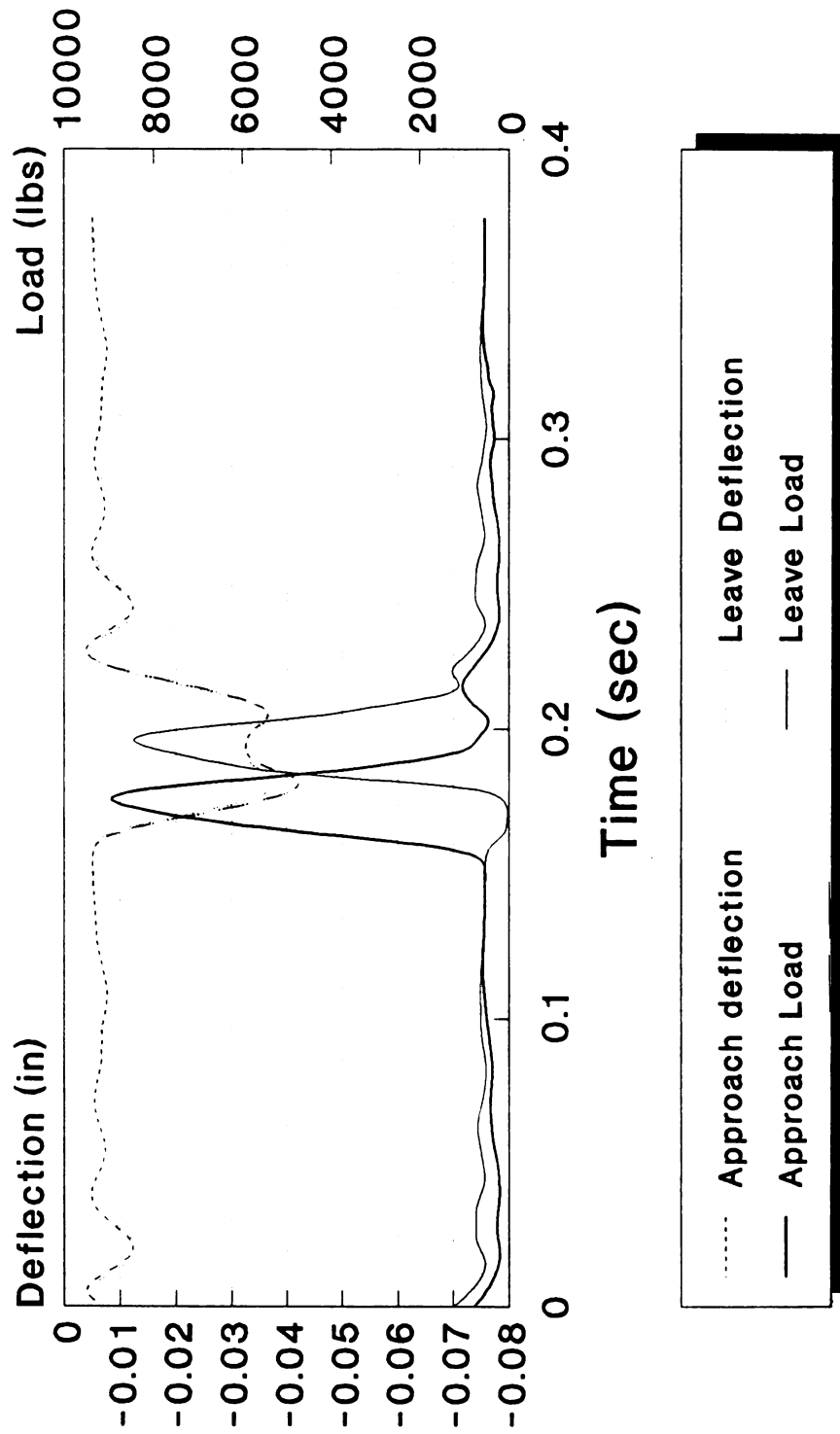
Figure A-12: Load and deflection curves for 6A virgin limestone slab after cycle # 1,000.

6A VIRGIN LIMESTONE
CYCLE # 2000

Deflection (in)

Load (lbs)

Time (sec)

Approach deflection
approach Load
Leave Deflection
Leave Load
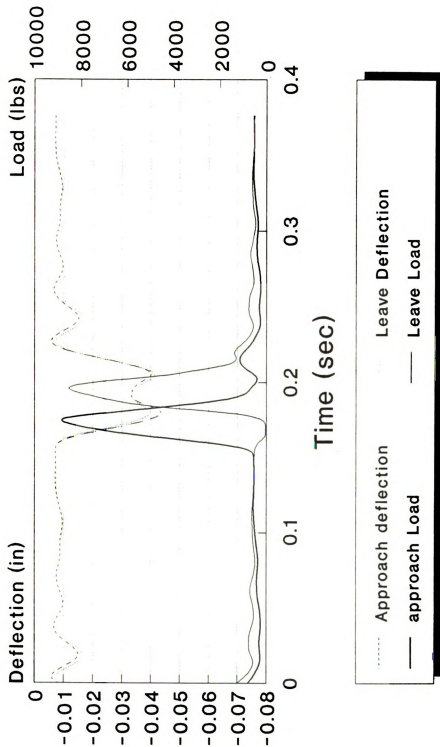
Figure A-13: Load and deflection curves for 6A virgin limestone slab after cycle # 2,000.

6A VIRGIN LIMESTONE
CYCLE # 5000

Deflection (in)

Load (lbs)

Time (sec)

..... Approach Deflection   — Leave Deflection

— Approach Load   — Leave Load
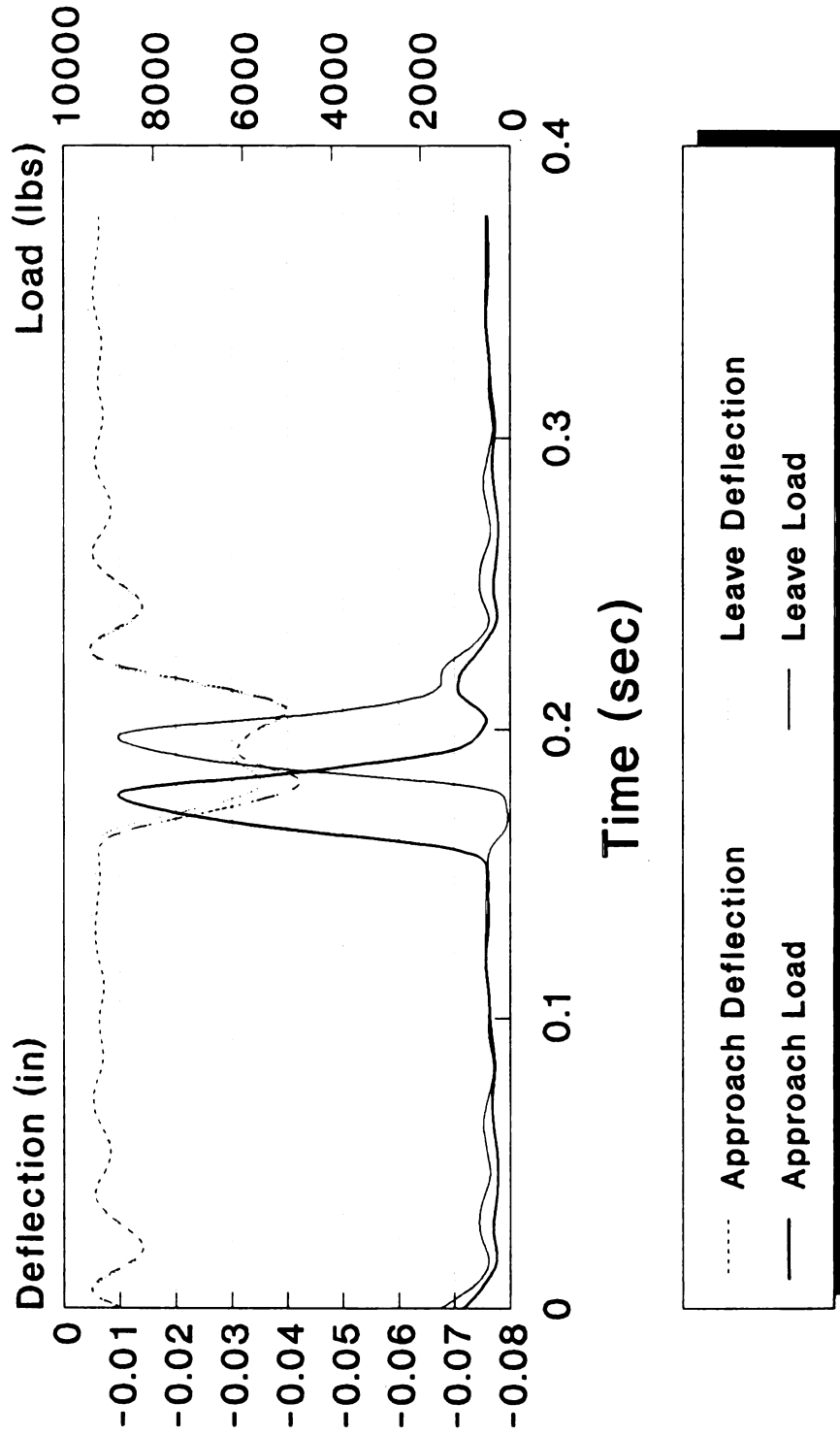
Figure A-14: Load and deflection curves for 6A virgin limestone slab after cycle # 5,000.
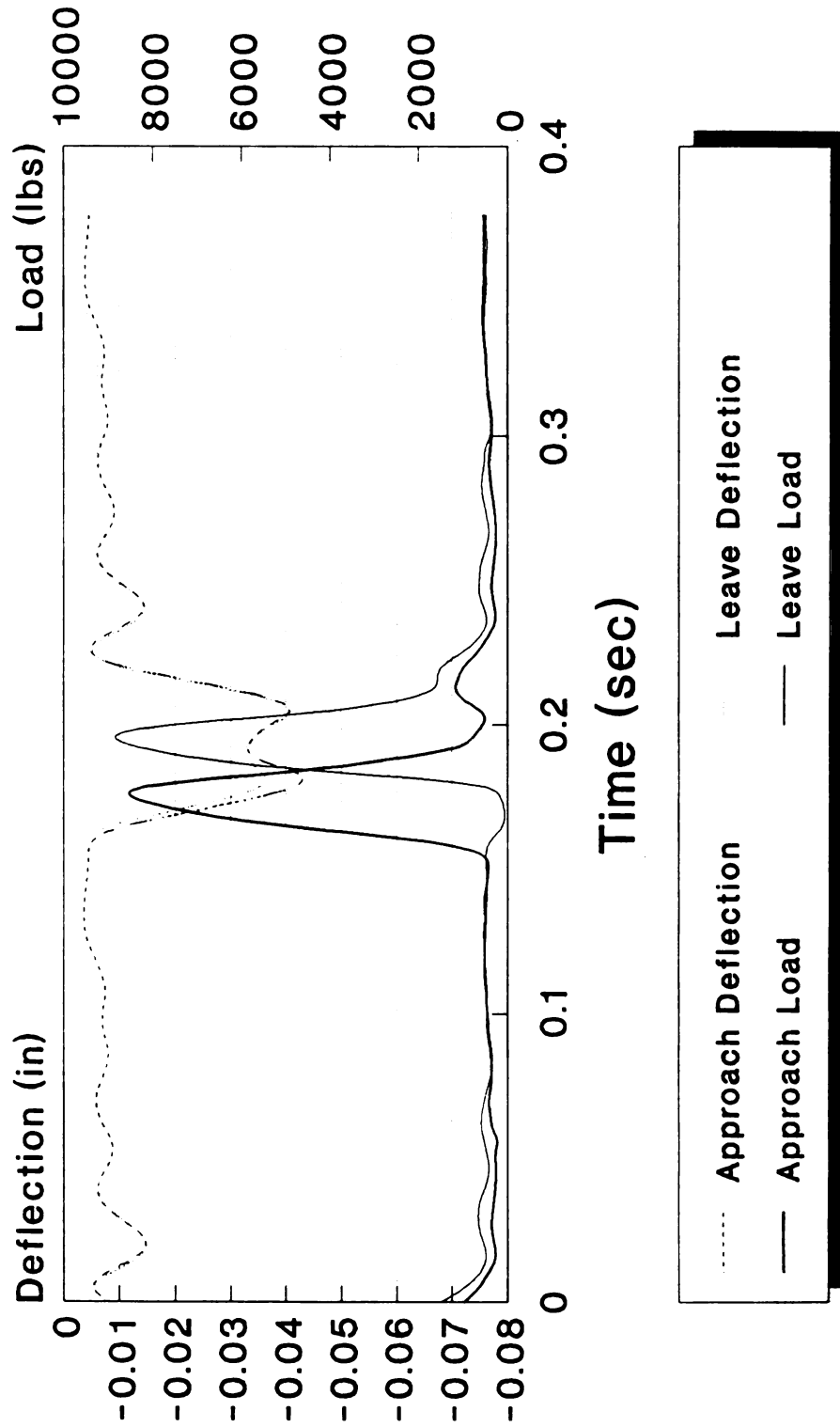
Figure A-15: Load and deflection curves for 6A virgin limestone slab after cycle # 10,000.
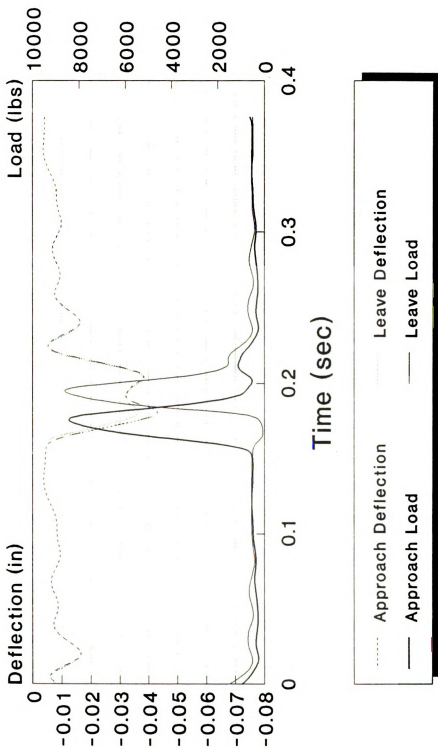
Figure A-16: Load and deflection curves for 6A virgin limestone slab after cycle # 20,000.
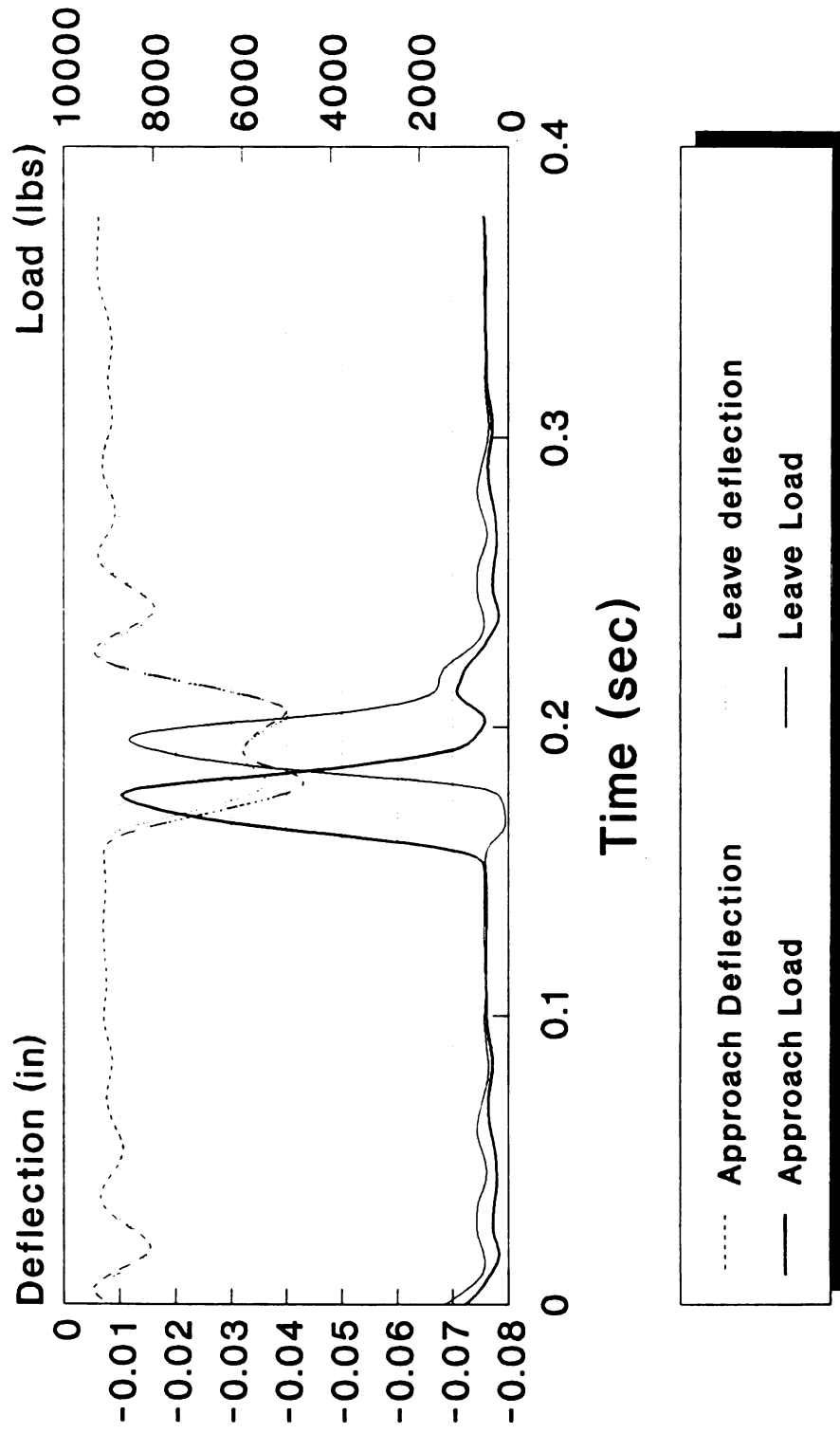
Figure A-17: Load and deflection curves for 6A virgin limestone slab after cycle # 50,000.
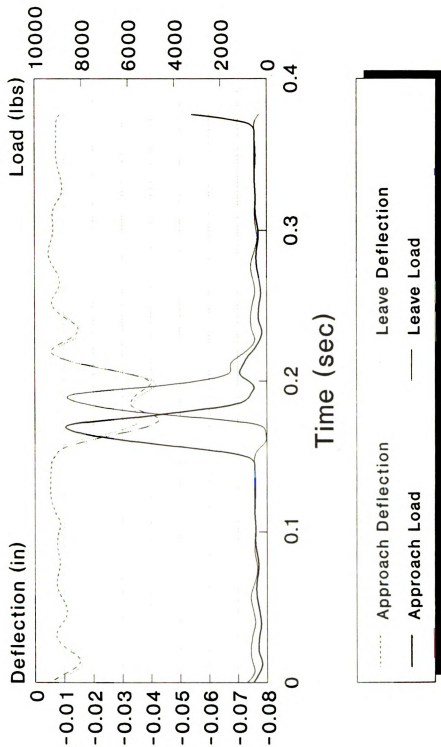
Figure A-18: Load and deflection curves for 6A virgin limestone slab after cycle # 100,000.
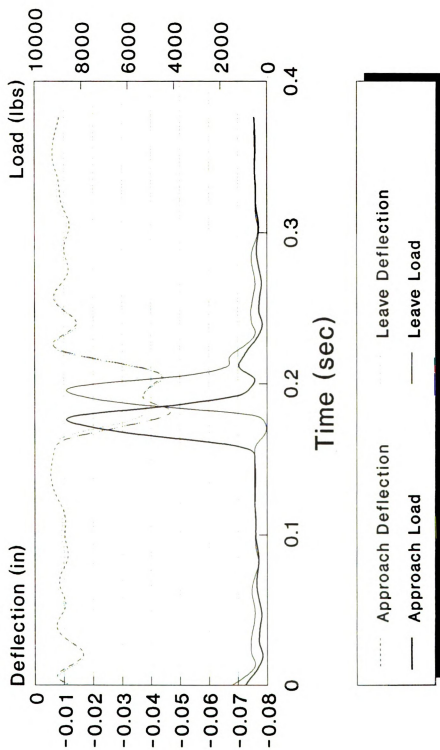
Figure A-19: Load and deflection curves for 6A virgin limestone slab after cycle # 300,000.
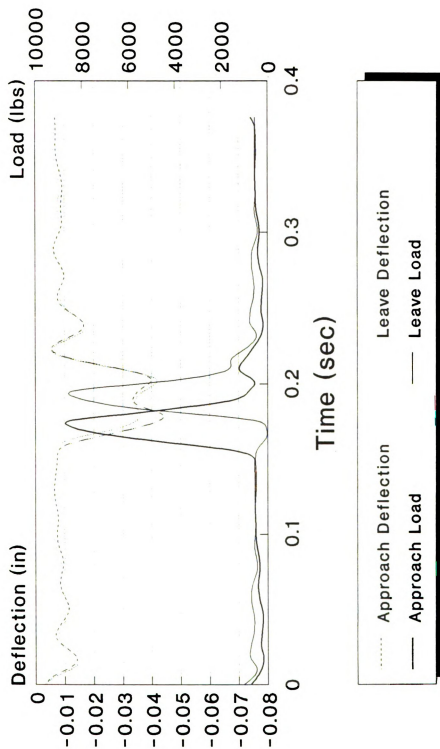
Figure A-20: Load and deflection curves for 6A virgin limestone slab after cycle # 600,000.
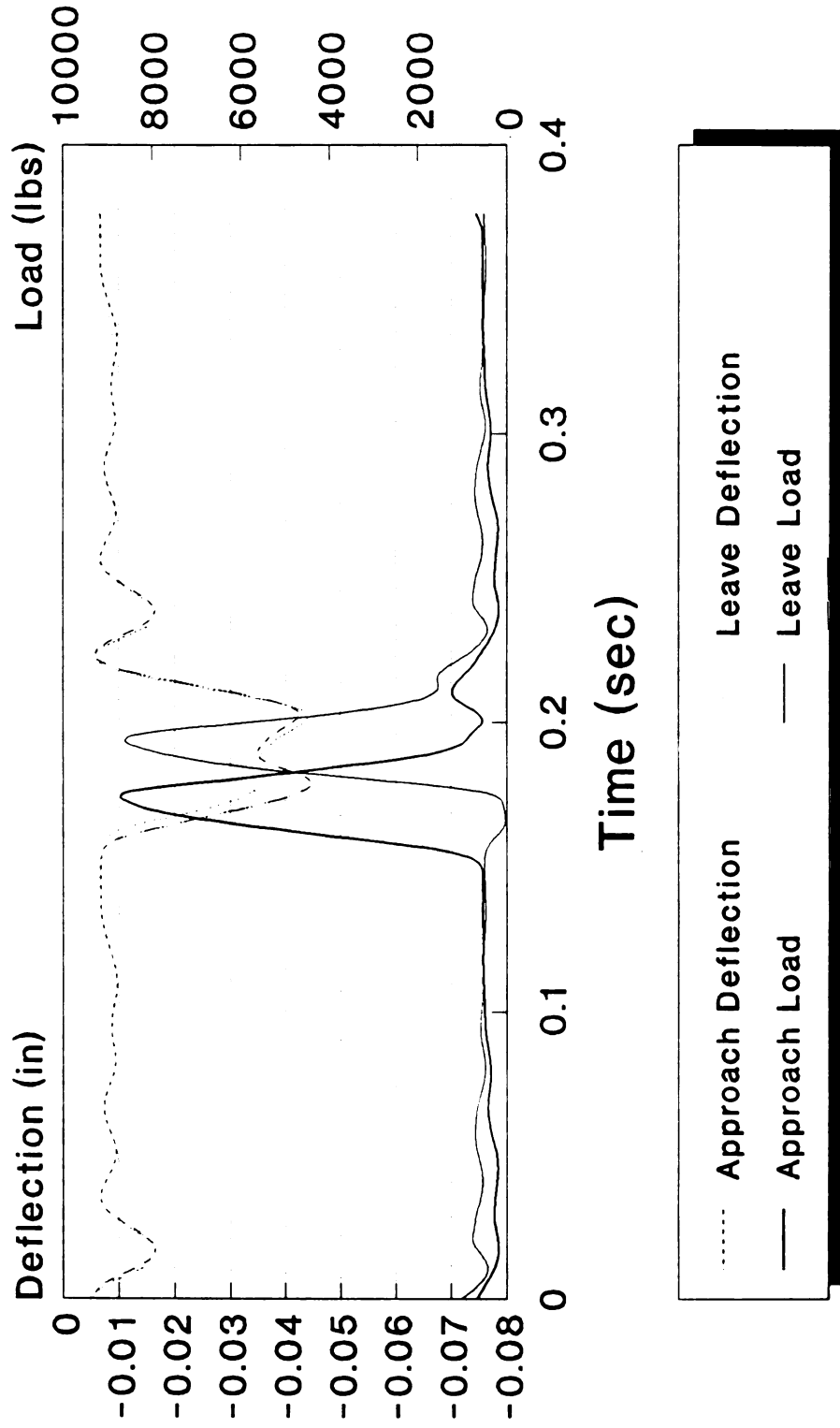
Figure A-21: Load and deflection curves for 6A virgin limestone slab after cycle # 900,000.

6A VIRGIN LIMESTONE
CYCLE # 1,500,000
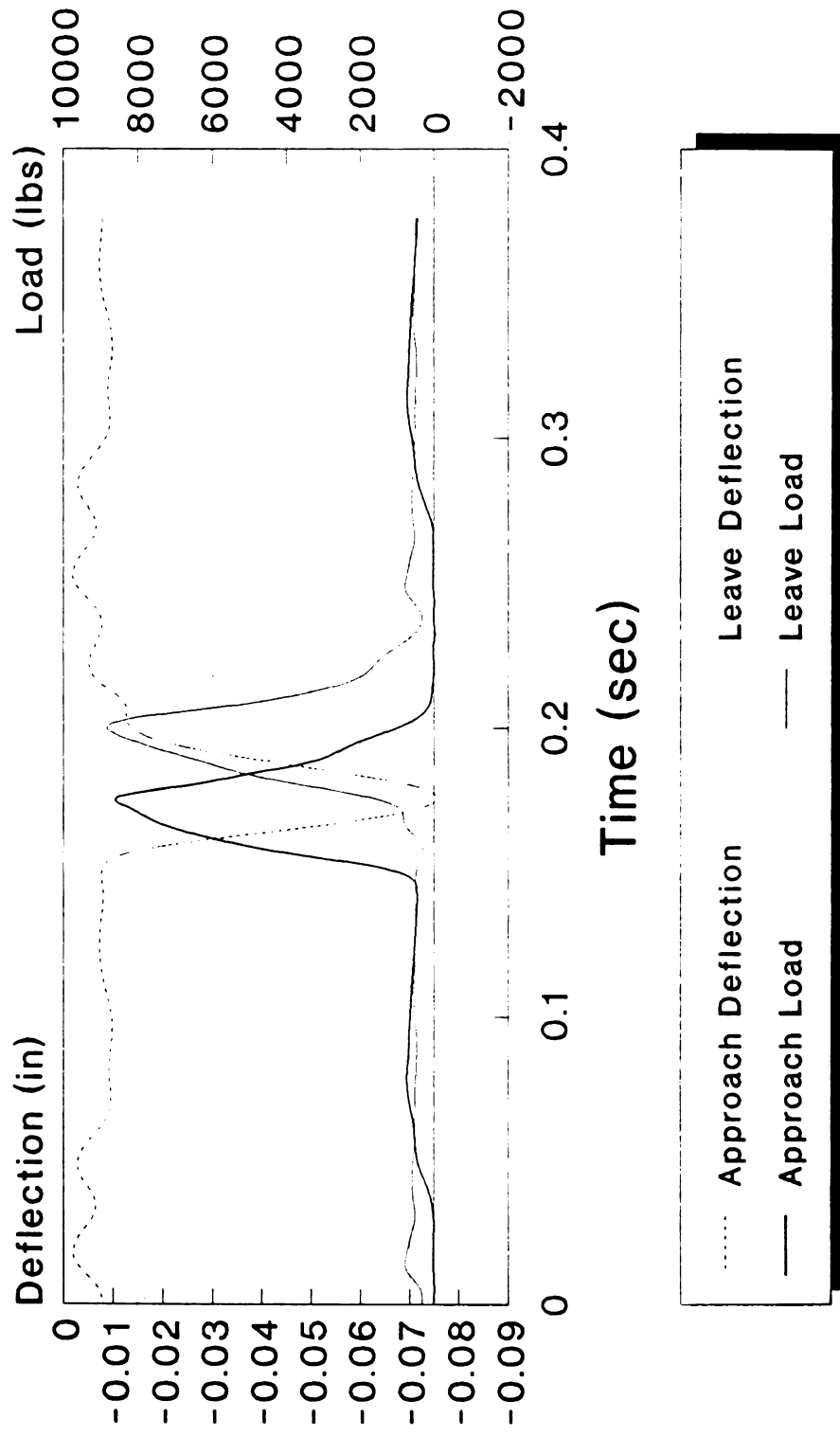
Figure A-22: Load and deflection curves for 6A Virgin limestone after cycle # 1,500,000.

6A VIRGIN SLAG
CYCLE # 1
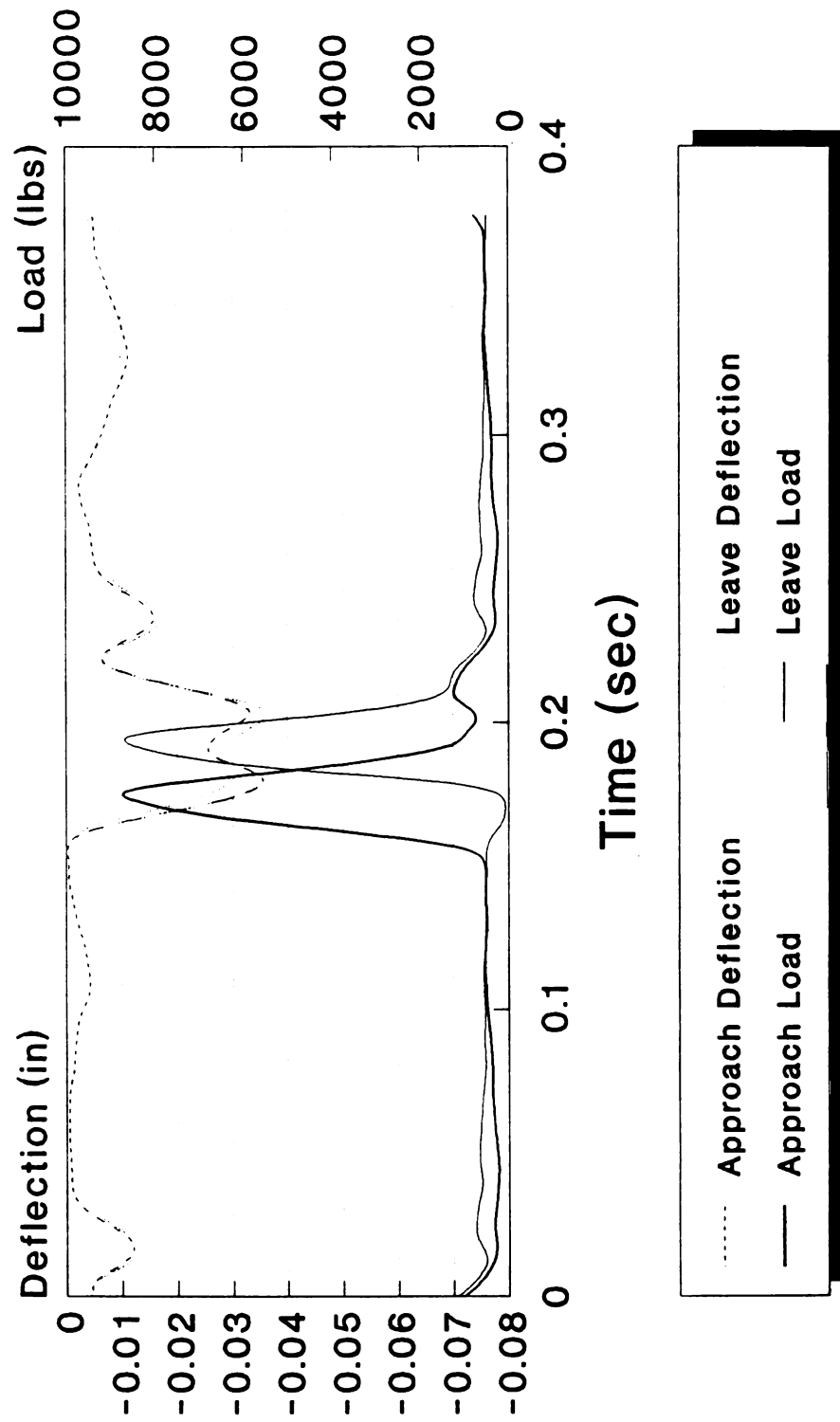
Figure A-23: Load and deflection curves for 6A virgin slag after cycle # 1.

6A VIRGIN SLAG
CYCLE # 1000
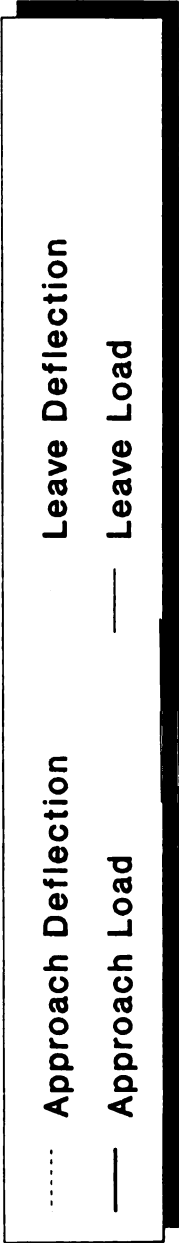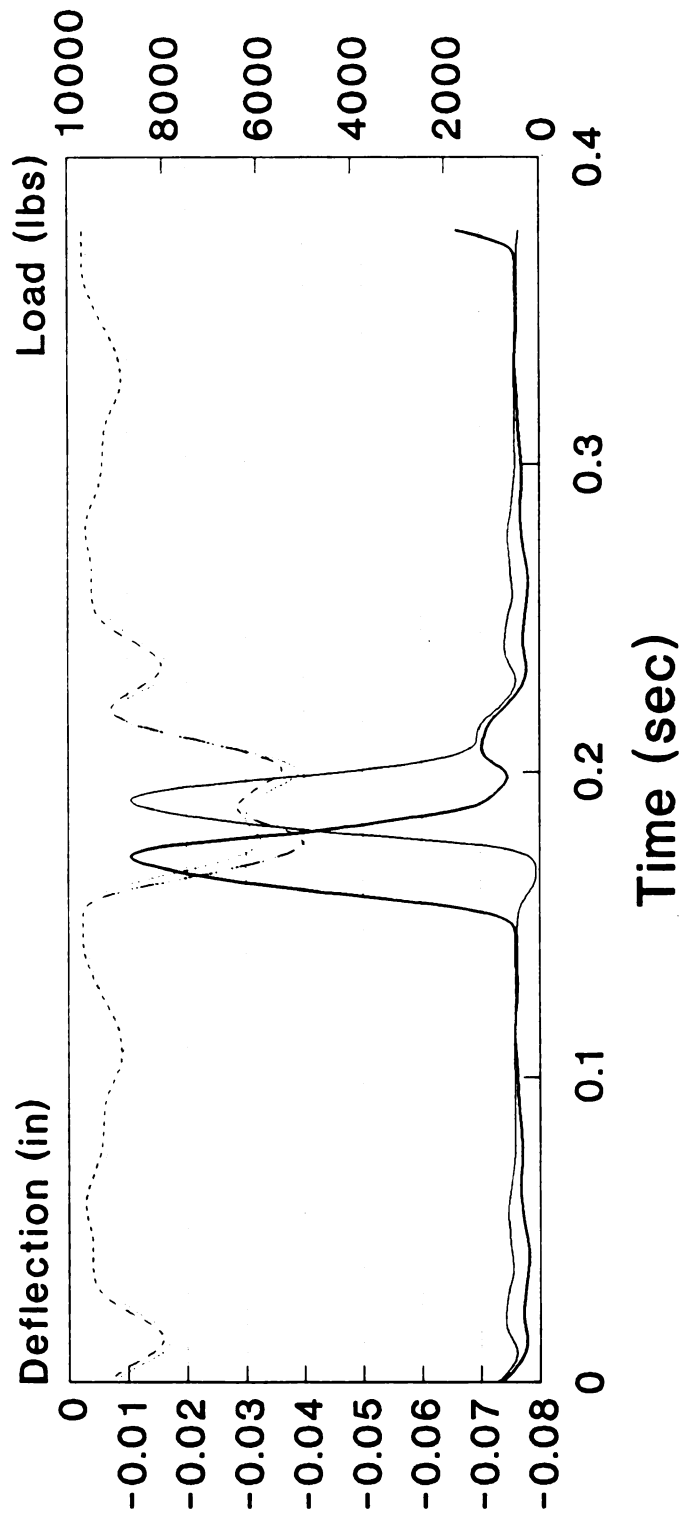
Figure A-24: Load and deflection curves for 6A virgin slag after cycle # 1,000.

162

Figure A-25: Load and deflection curves for 6A virgin slag after cycle # 2,000.

6A VIRGIN SLAG
CYCLE # 5000
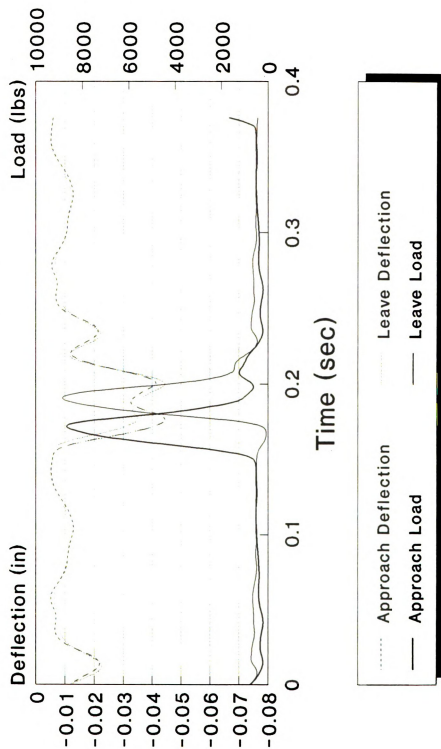
Figure A-26: Load and deflection curves for 6A virgin slag after cycle # 5,000.
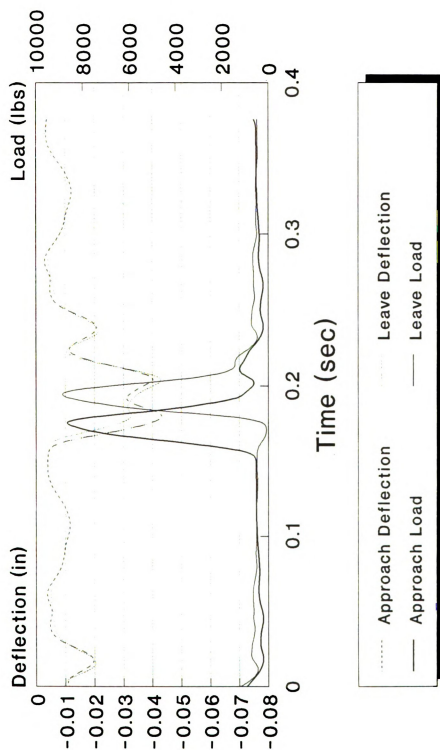
Figure A-27: Load and deflection curves for 6A virgin slag after cycle # 10,000.
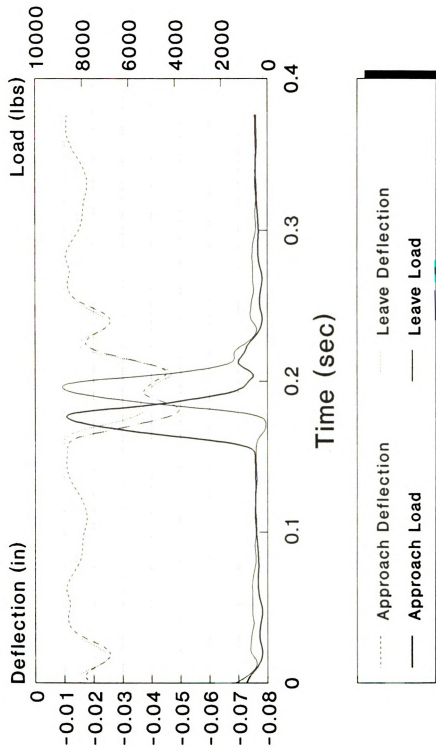
Figure A-28: Load and deflection curves for 6A virgin slag after cycle # 20,000.
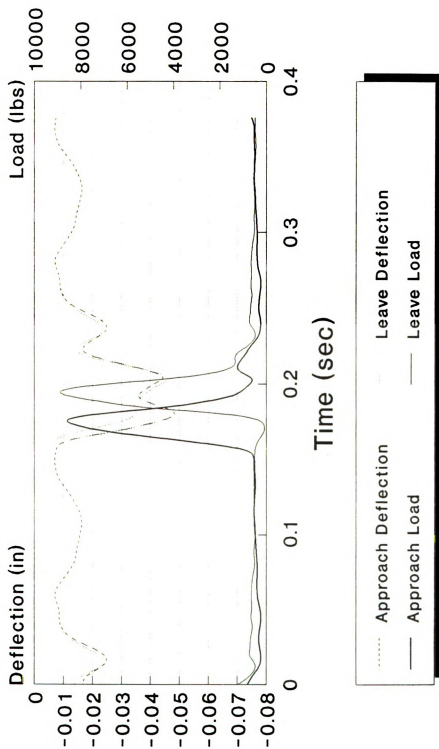
Figure A-29: Load and deflection curves for 6A virgin slag after cycle # 50,000.
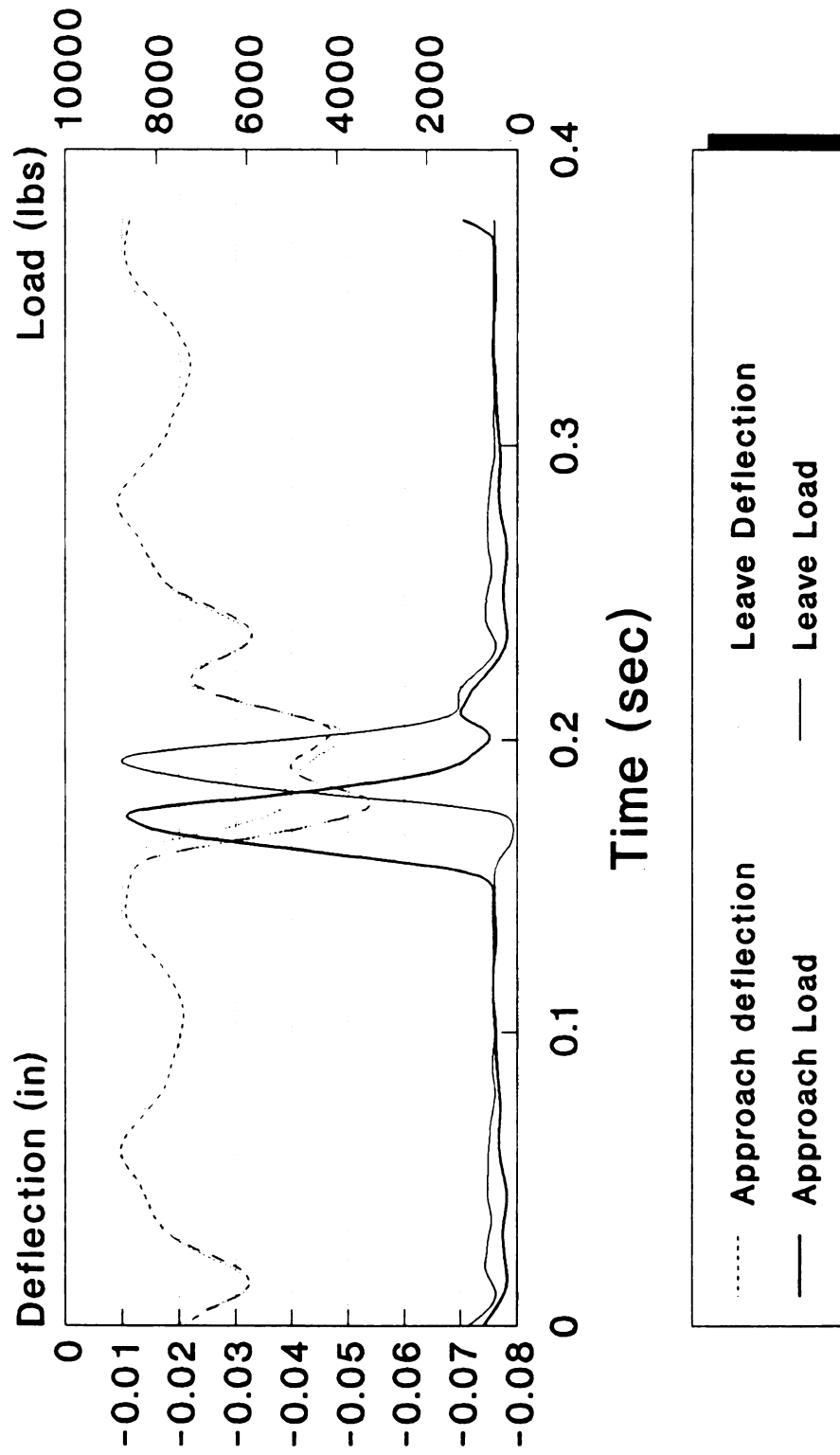
Figure A-30: Load and deflection curves for 6A virgin slag after cycle # 100,000.
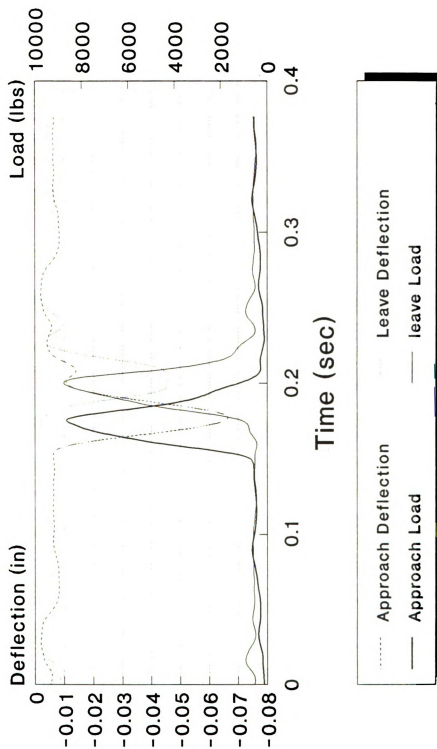
Figure A-31: Load and deflection curves for 6A virgin slag after cycle # 250,000.
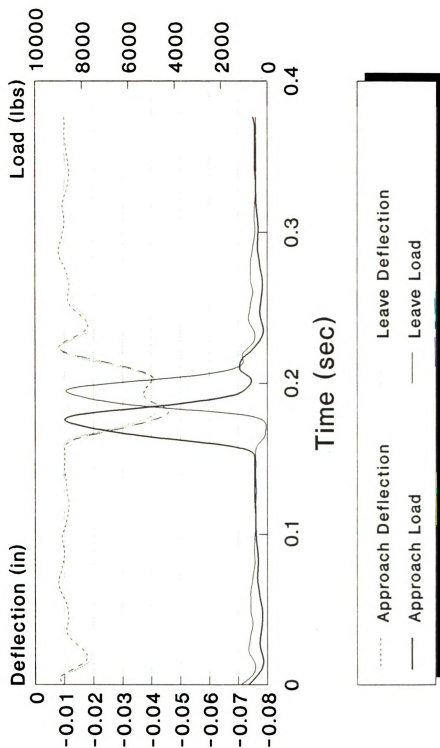
Figure A-32: Load and deflection curves for 17A virgin gravel after cycle # 1.

17A VIRGIN GRAVEL
CYCLE # 1000
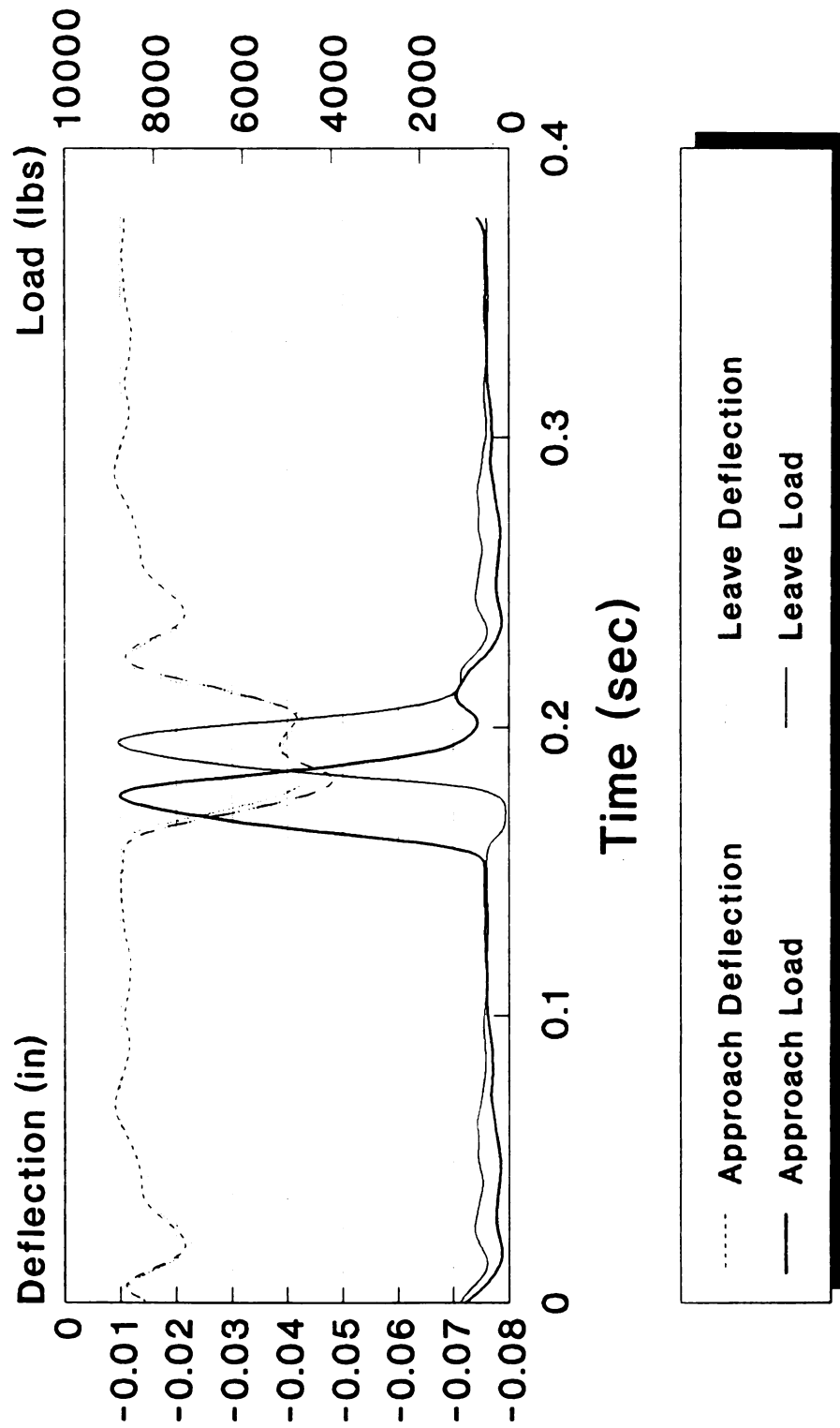
Figure A-33: Load and deflection curves for 17A virgin gravel after cycle # 1,000.
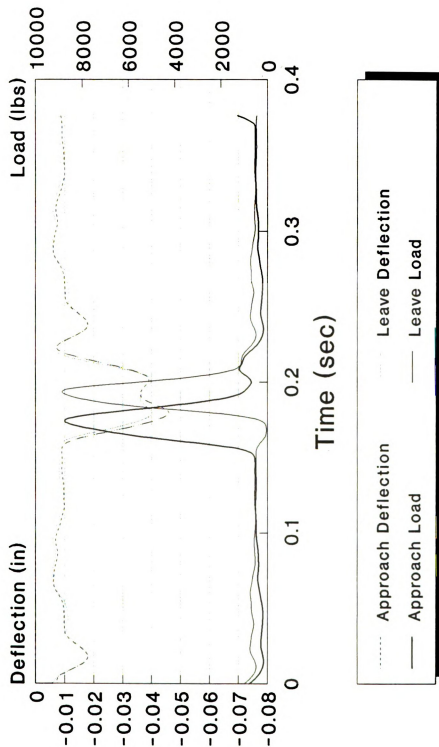
Figure A-34: Load and deflection curves for 17A virgin gravel after cycle # 2,000.

17A VIRGIN GRAVEL CYCLE # 5000
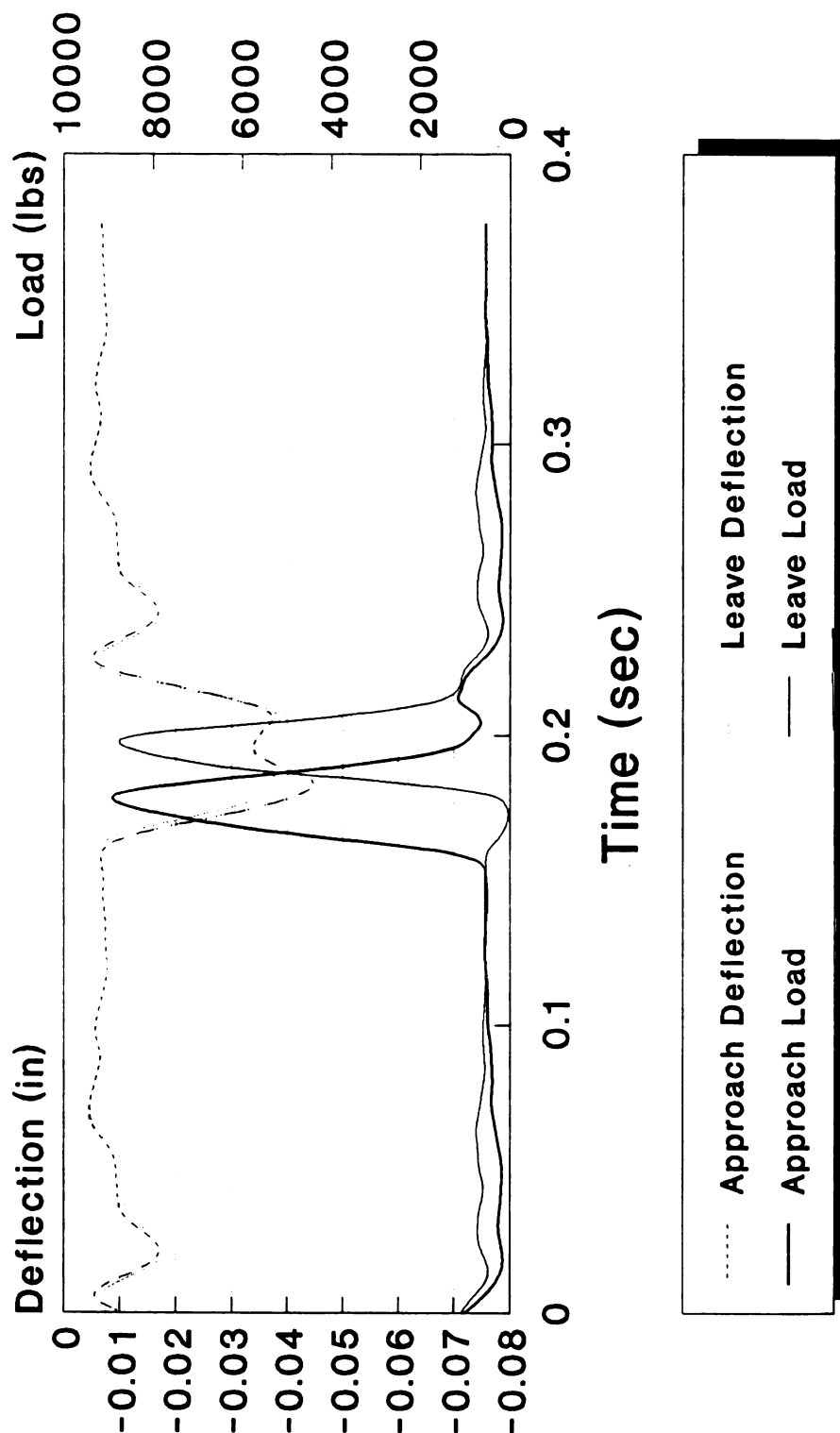
Figure A-35: Load and deflection curves for 17A virgin gravel after cycle # 5,000.
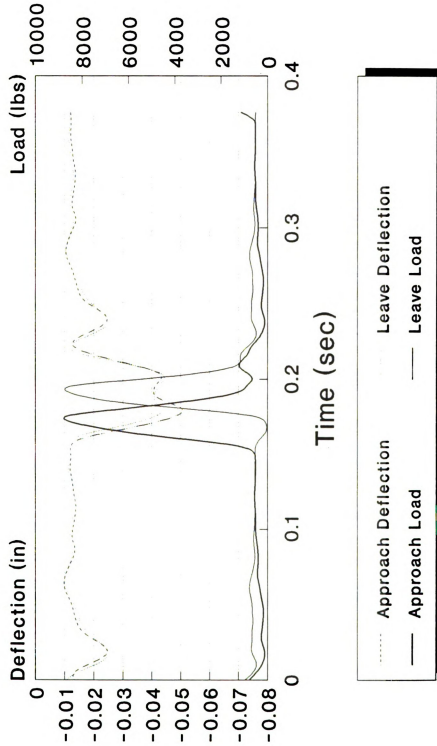
Figure A-36: Load and deflection curves for 17A virgin gravel after cycle # 10,000.

Figure A-37: Load and deflection curves for 17A virgin gravel after cycle # 20,000.

Figure A-38: Load and deflection curves for 17A virgin gravel after cycle # 50,000.

Figure A-39: Load and deflection curves for 17A virgin gravel after cycle # 100,000.

17A VIRGIN GRAVEL
CYCLE # 300000
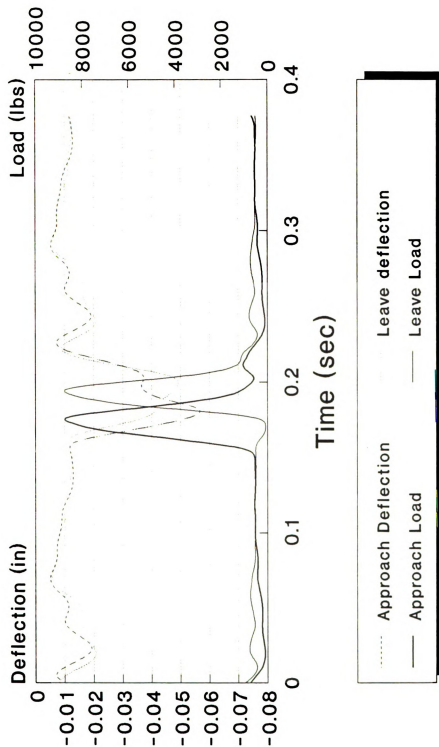
Figure A-40: Load and deflection curves for 17A virgin gravel after cycle # 300,000.
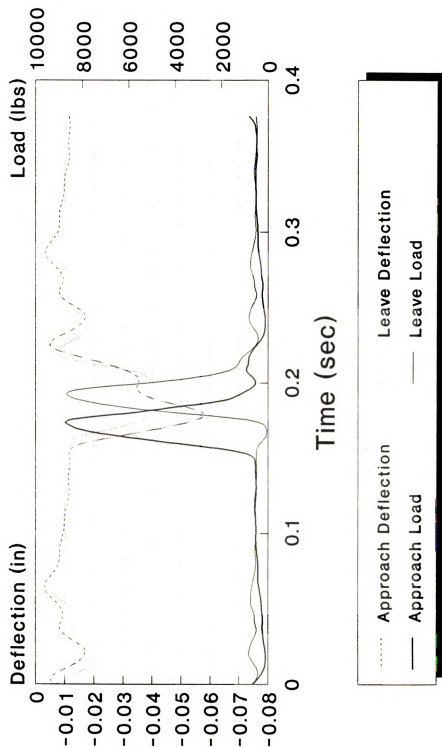
Figure A-41: Load and deflection curves for 17A virgin gravel after cycle # 600,000.
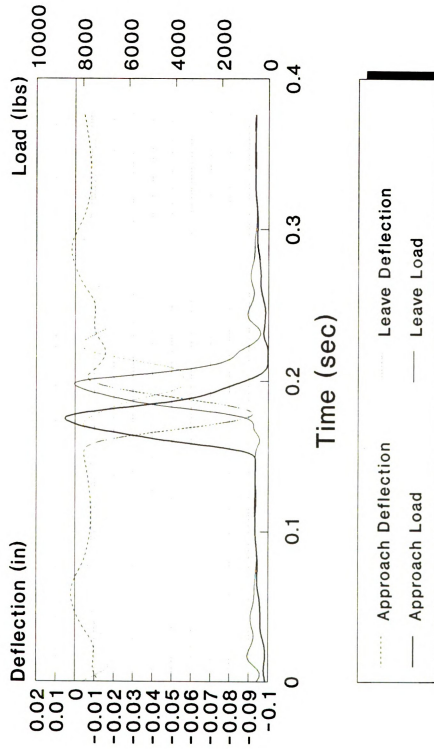
Figure A-42: Load and deflection curves for 17A virgin gravel after cycle # 900,000.

6A 100% RECYCLED GRAVEL
CYCLE # 1
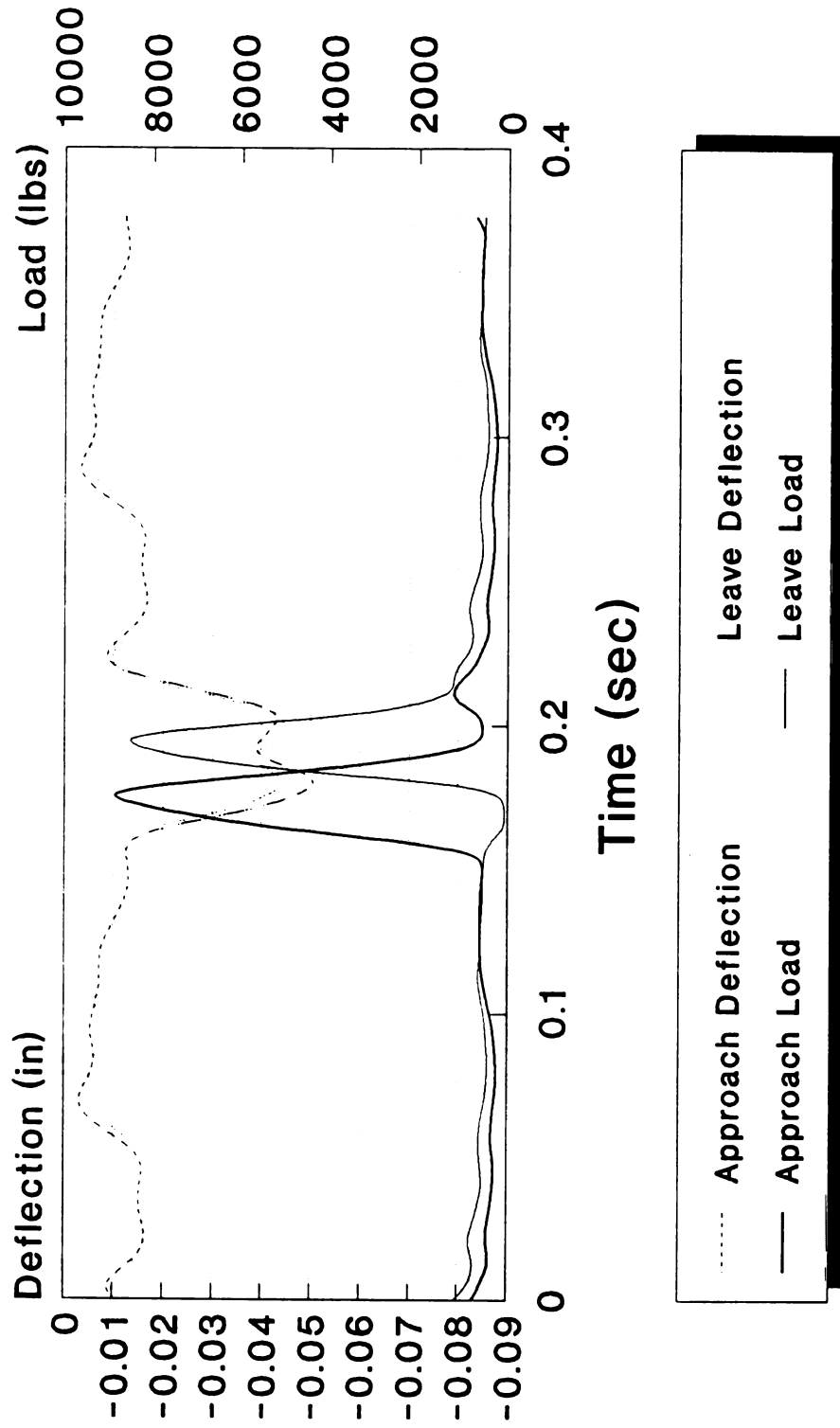
Figure A-43: Load and deflection curves for 6A 100% recycled gravel after cycle # 1.
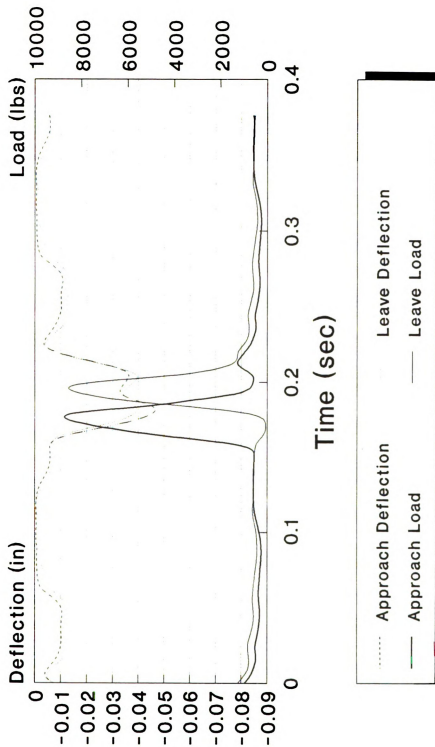
Figure A-44: Load and deflection curves for 6A 100% recycled gravel after cycle # 1,000.

182

6A 100% RECYCLED GRAVEL
CYCLE # 2000
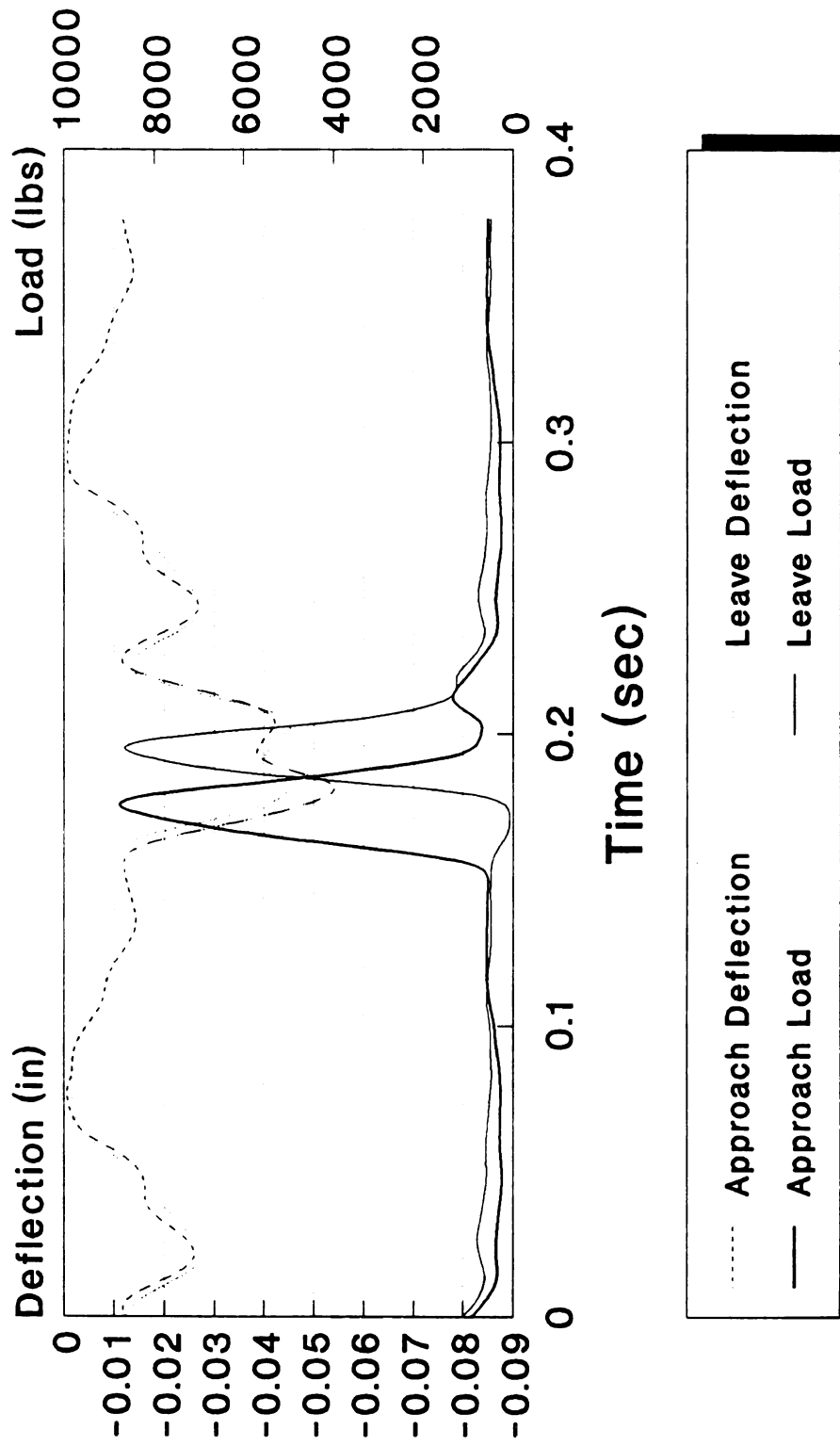
Figure A-45: Load and deflection curves for 6A 100% recycled gravel after cycle # 2,000.
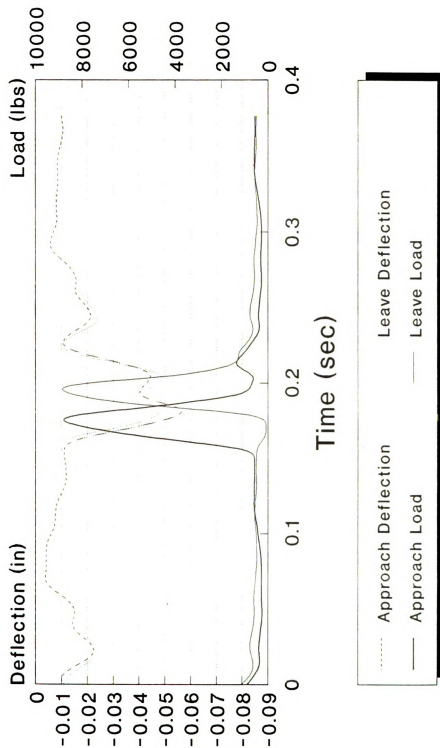
Figure A-46: Load and deflection curves for 6A 100% recycled gravel after cycle # 5,000.
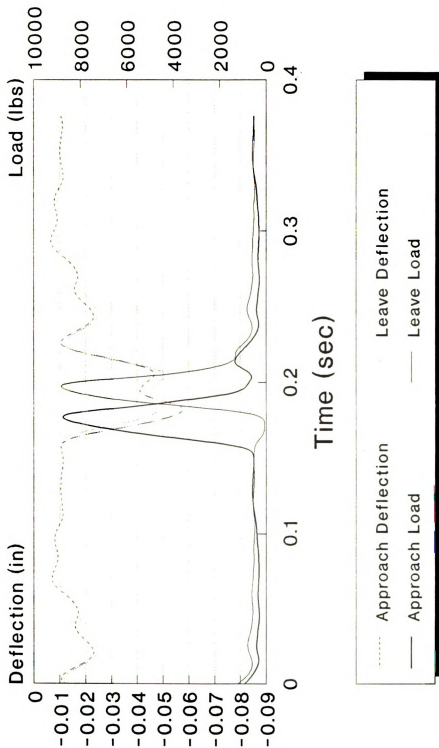
RECYCLED GRAVE

Figure A-47: Load and deflection curves for 6A 100% recycled gravel after cycle # 10,000.

6A 100% RECYCLED GRAVEL
CYCLE # 20000
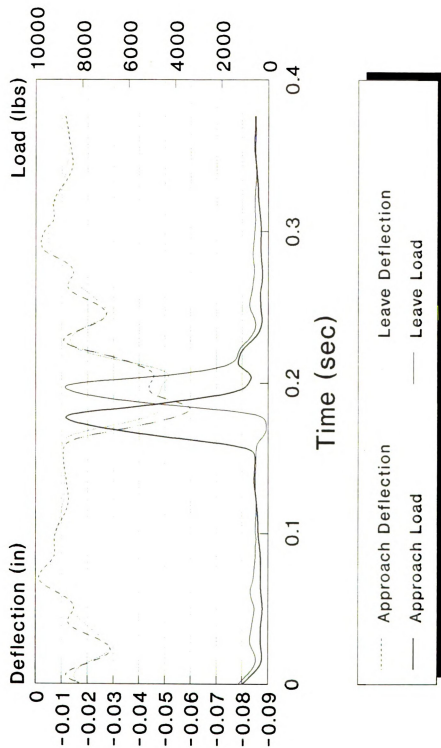
Figure A-48: Load and deflection curves for 6A 100% recycled gravel after cycle # 20,000.

186
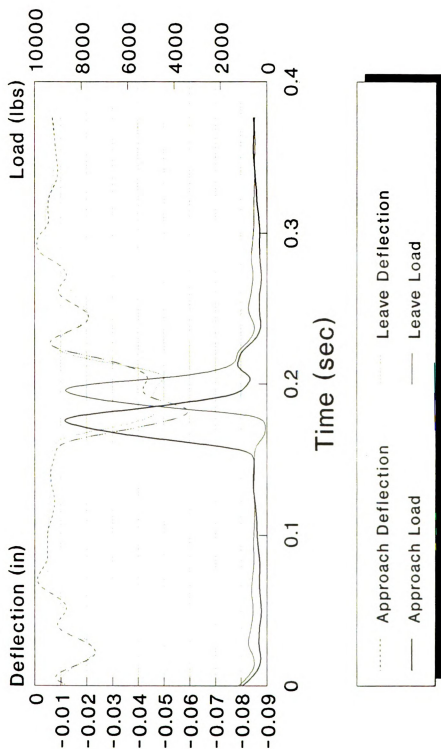
Figure A-49: Load and deflection curves for 6A 100% recycled gravel after cycle # 50,000.

6A 100% RECYCLED GRAVEL
CYCLE # 100000
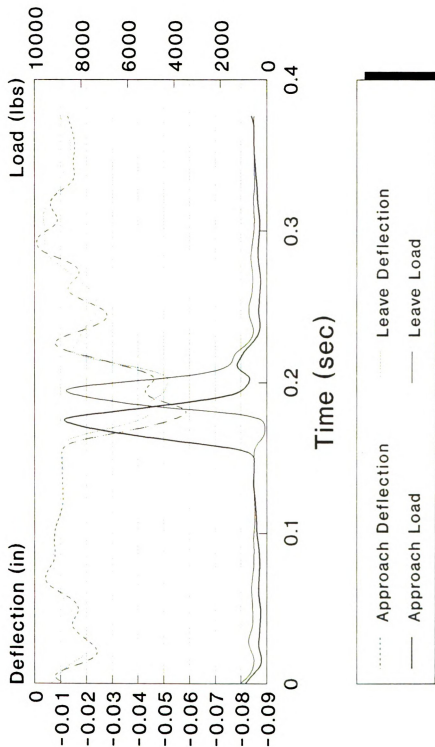
Figure A-50: Load and deflection curves for 6A 100% recycled gravel after cycle # 100,000.
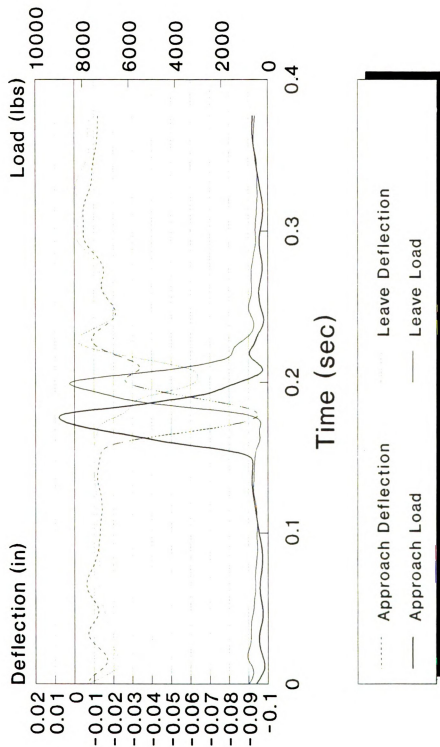
Figure A-51: Load and deflection curves for 6A 100% recycled gravel after cycle # 300,000.

Figure A-52: Load and deflection curves for 50-50 recycled blend after cycle # 1.

50-50 RECYCLE BLEND
CYCLE # 1000
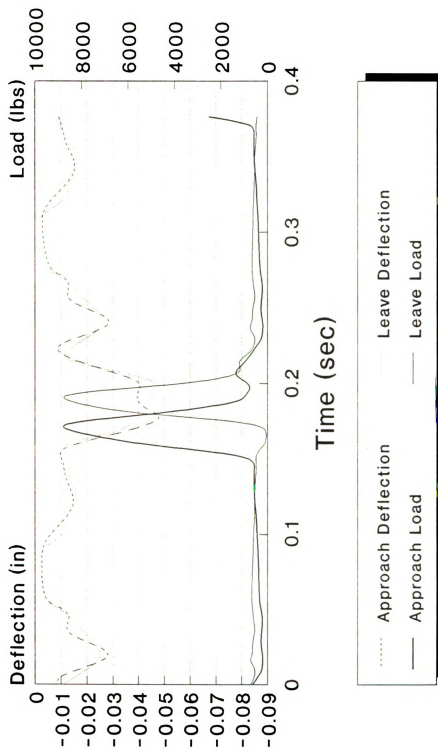
Figure A-53: Load and deflection curves for 50-50 recycled blend after cycle # 1,000.

50-50 RECYCLE BLEND
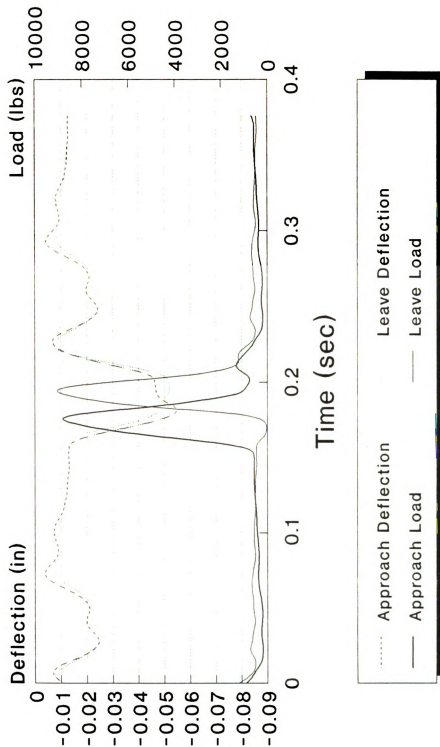
Figure A-54: Load and deflection curves for 50-50 recycled blend after cycle # 5,000.

50-50 RECYCLE BLEND
CYCLE # 10000

Deflection (in)

Load (lbs)

Time (sec)

Approach Deflection   Leave Deflection

Approach Load   Leave Load
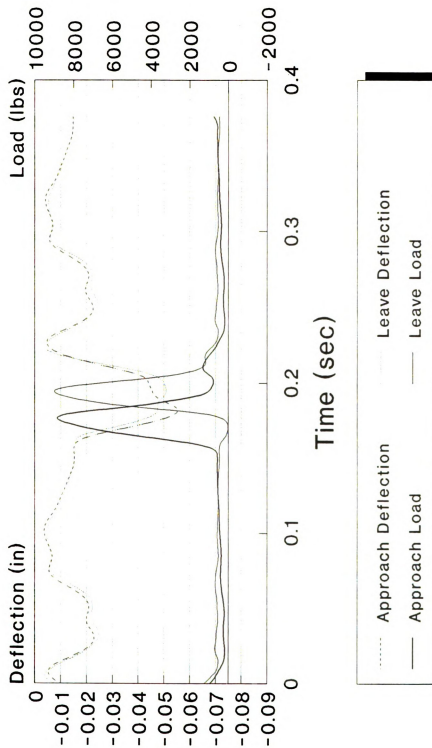
Figure A-55: Load and deflection curves for 50-50 recycled blend after cycle # 10,000.
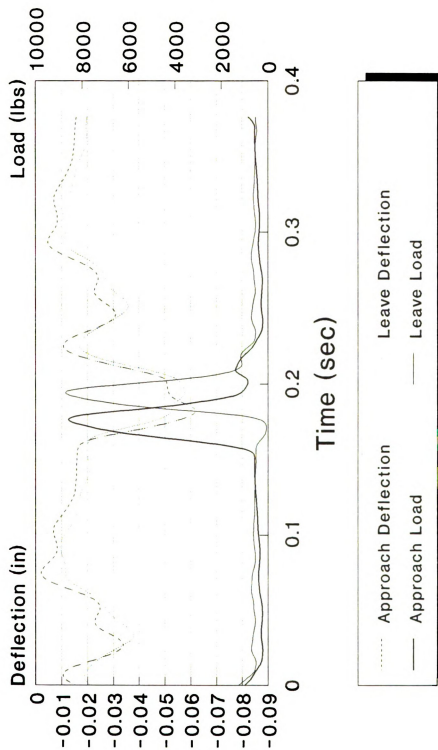
Figure A-56: Load and deflection curves for 50-50 recycled blend after cycle # 20,000.
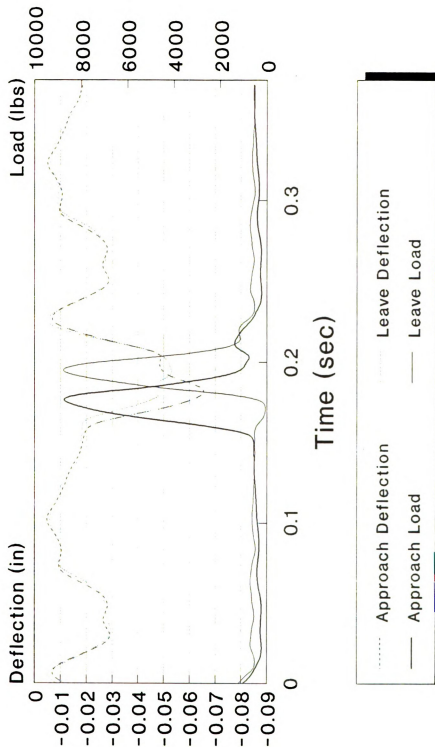
Figure A-57: Load and deflection curves for 50-50 recycled blend after cycle # 50,000.
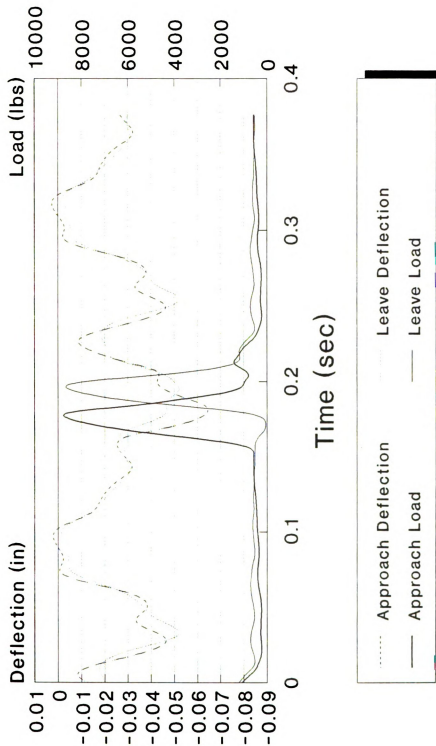
Figure A-58: Load and deflection curves for 50-50 recycled blend after cycle # 100,000.

Figure A-59: Load and deflection curves for 50-50 recycled blend after cycle # 300,000.

50-50 RECYCLE BLEND
CYCLE # 350000
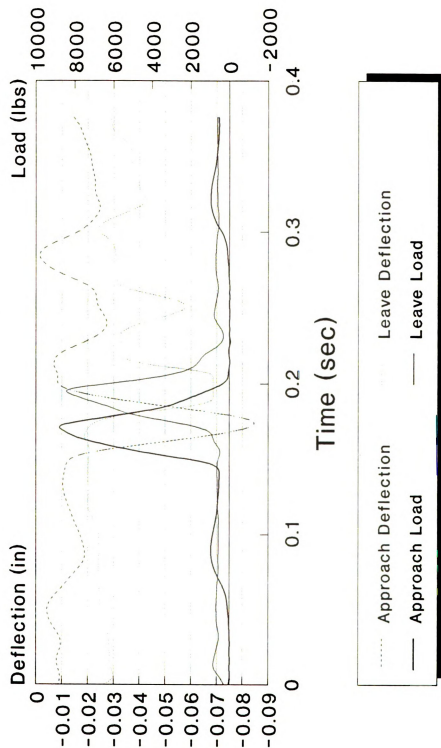
Figure A-60: Load and deflection curves for 50-50 recycled blend after cycle # 350,000.

APPENDIX B

LOAD-DEFLECTION HISTORIES OF TEST SPECIMENS

(DESIGN FACTORS)
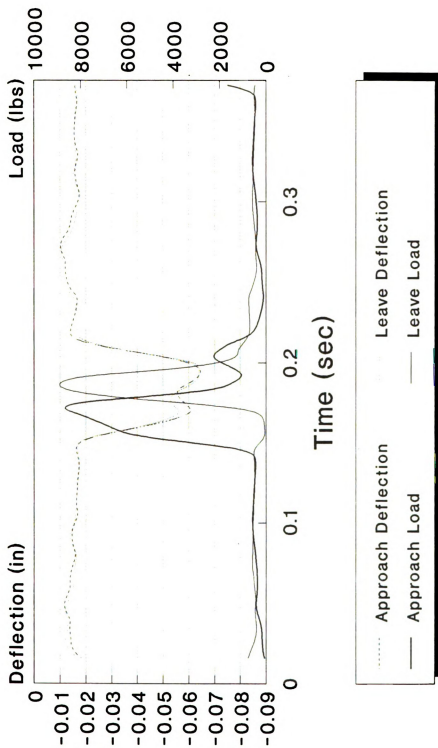
Figure B-1: Load and deflection curves for typical tension and 100 psi/in foundation modulus after cycle #1.
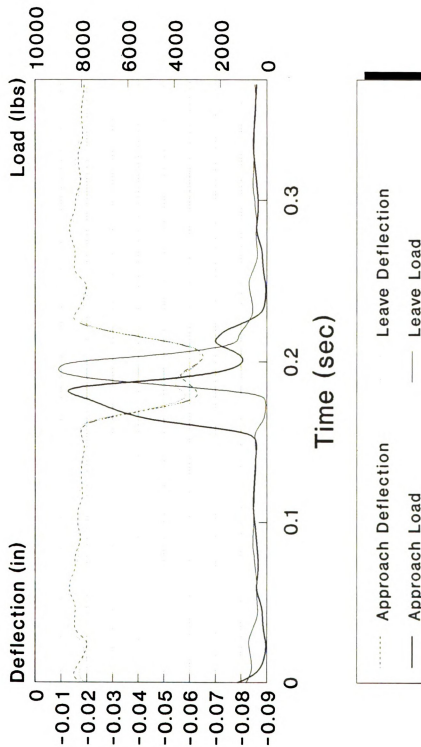
Figure B-2: Load and deflection curves for typical tension and 100 psi/in foundation modulus after cycle #1,000.

TYPICAL TENSION & SUPPORT
CYCLE # 2000
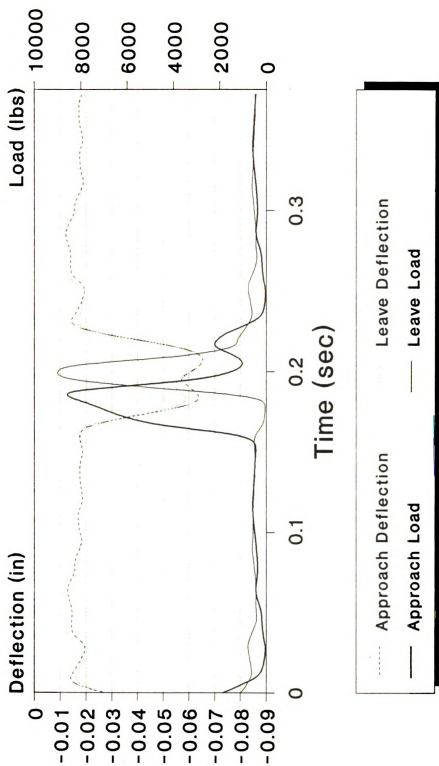
Figure B-3: Load and deflection curves for typical tension and 100 psi/in foundation modulus after cycle #2,000.
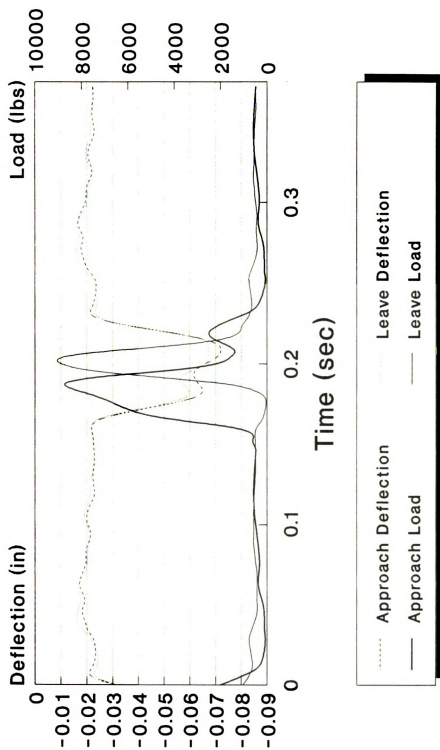
Figure B-4: Load and deflection curves for typical tension and 100 psi/in foundation modulus after cycle #5,000.

TYPICAL TENSION & SUPPORT
CYCLE # 10,000
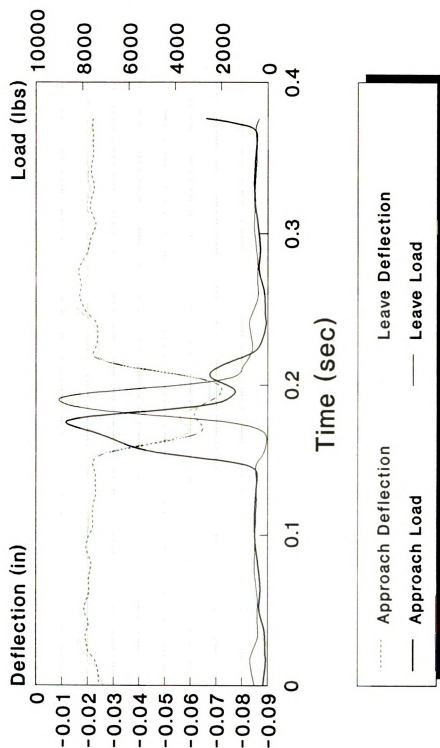
Figure B-5: Load and deflection curves for typical tension and 100 psi/in foundation modulus after cycle #10,000.

TYPICAL TENSION & SUPPORT
CYCLE # 20,000
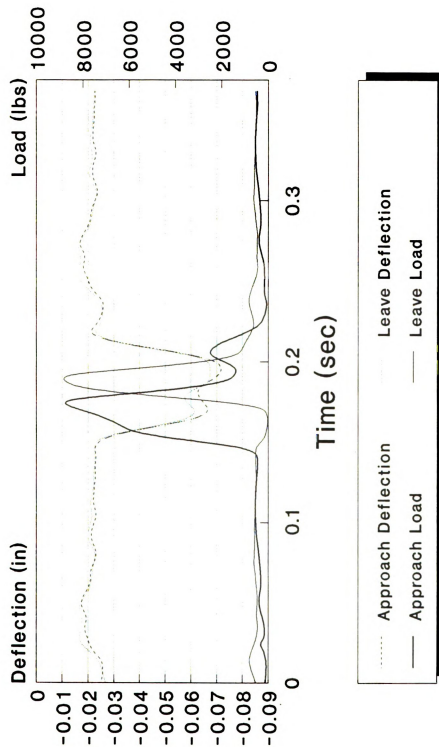
Figure B-6: Load and deflection curves for typical tension and 100 psi/in foundation modulus after cycle #20,000.
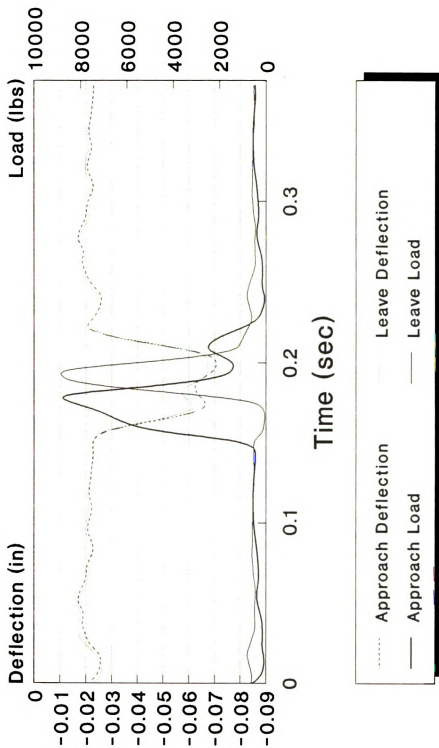
Figure B-7: Load and deflection curves for typical tension and 100 psi/in foundation modulus after cycle #50,000.

TYPICAL TENSION & SUPPORT
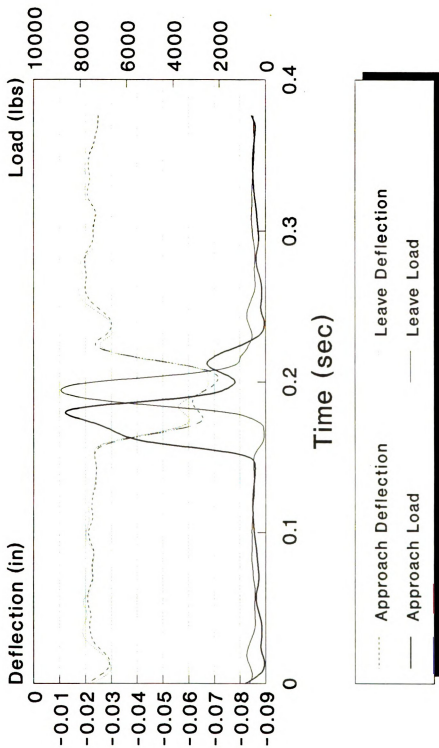
Figure B-8: Load and deflection curves for typical tension and 100 psi/in foundation modulus after cycle #100,000.
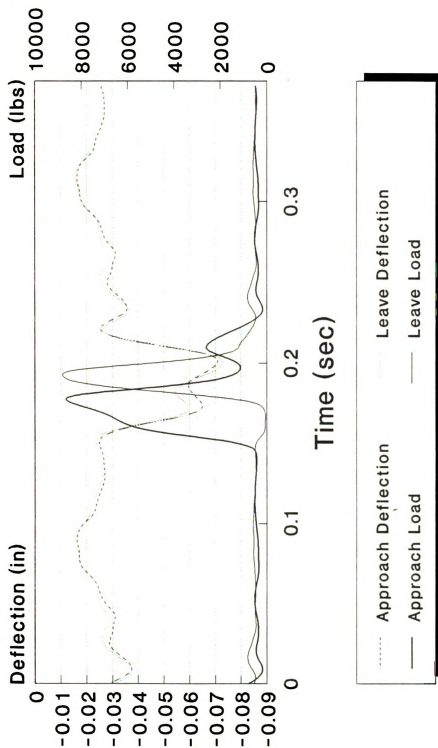
Figure B-9: Load and deflection curves for typical tension and 100 psi/in foundation modulus after cycle #300,000.
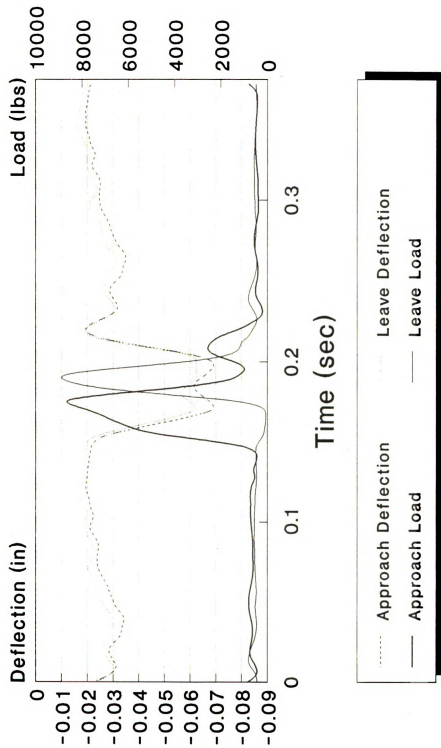
Figure B-10: Load and deflection curves for typical tension and 100 psi/in foundation modulus after cycle #600,000.

Figure B-11: Load and deflection curves for typical tension and 100 psi/in foundation modulus after cycle #1200,000.

TYPICAL TENSION & SUPPORT
CYCLE # 1800,000
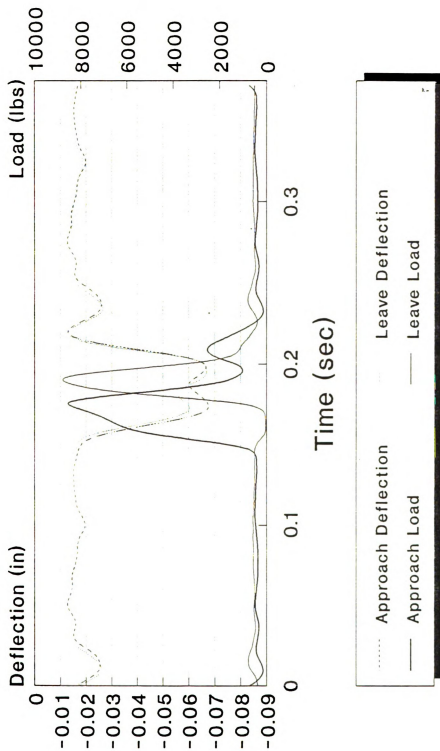
Figure B-12: Load and deflection curves for typical tension and 100 psi/in foundation modulus after cycle #1800,000.
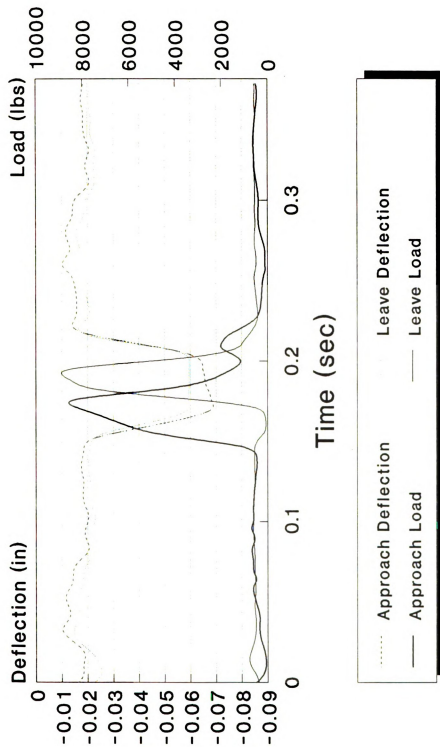
Figure B-13: Load and deflection curves for typical tension and 100 psi/in foundation modulus after cycle #2400,000.
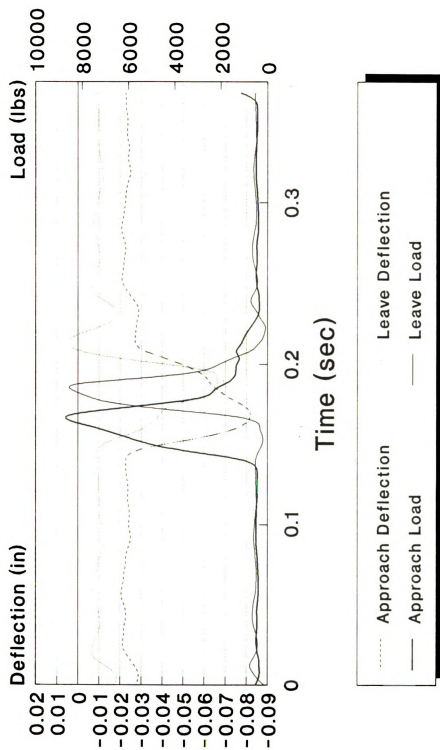
Figure B-14: Load and deflection curves for typical tension and 100 psi/in foundation modulus after cycle #2700,000.
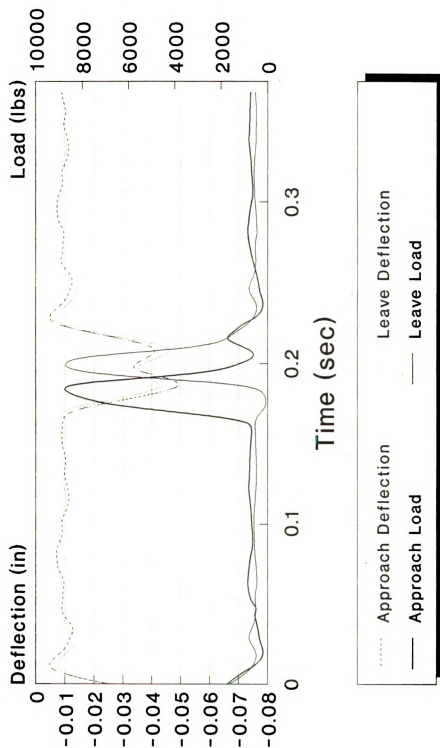
Figure B-15: Load and deflection curves for high tension slab after cycle #1.
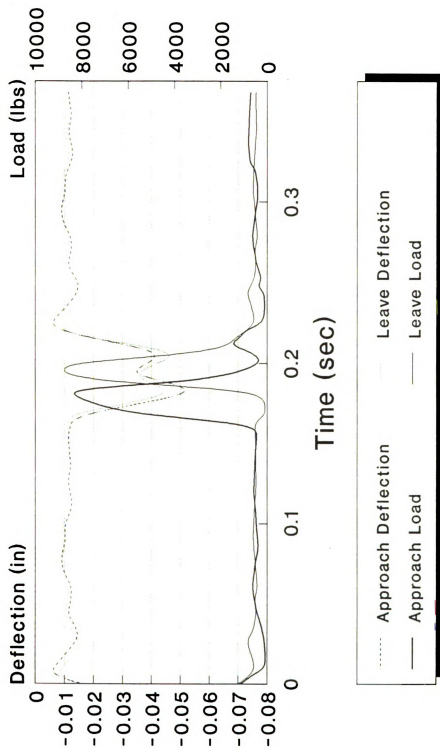
Figure B-16: Load and deflection curves for high tension slab after cycle #1,000.

HIGH TENSION
CYCLE # 2000

Deflection (in)

Load (lbs)

Time (sec)

Legend:
- ········ Approach Deflection
- ── Approach Load
- ── Leave Deflection
- ── Leave Load
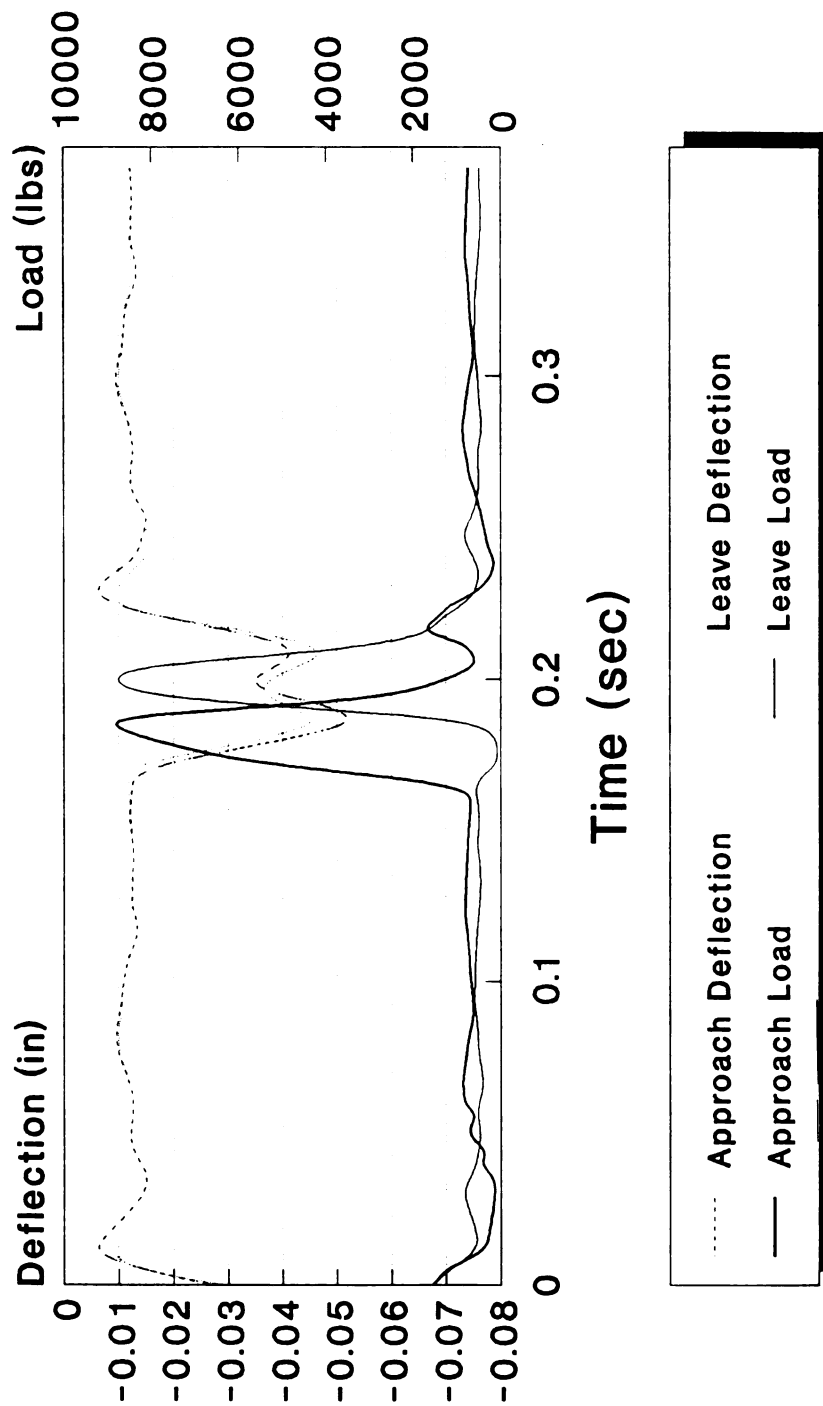
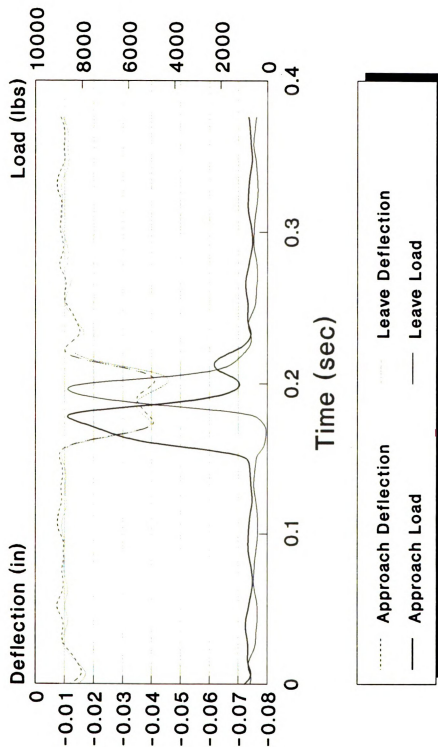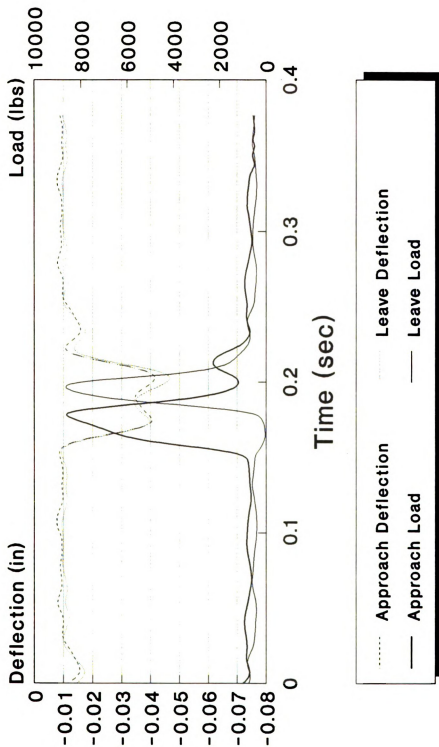**Figure B-17:** Load and deflection curves for high tension slab after cycle #2,000.
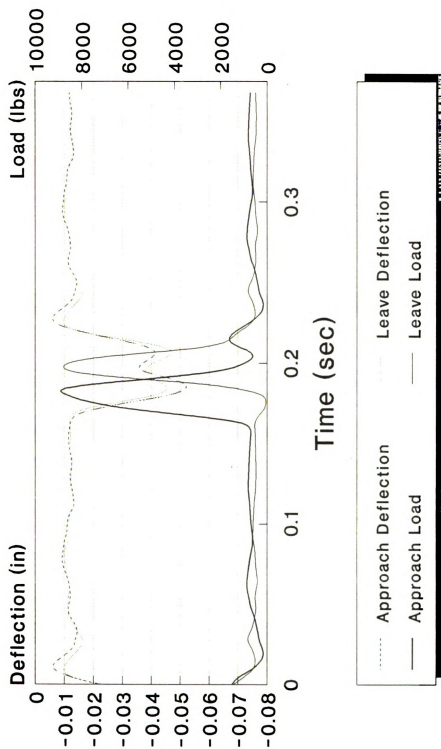
Figure B-18: Load and deflection curves for high tension slab after cycle #5,000.

HIGH TENSION
CYCLE # 10,000
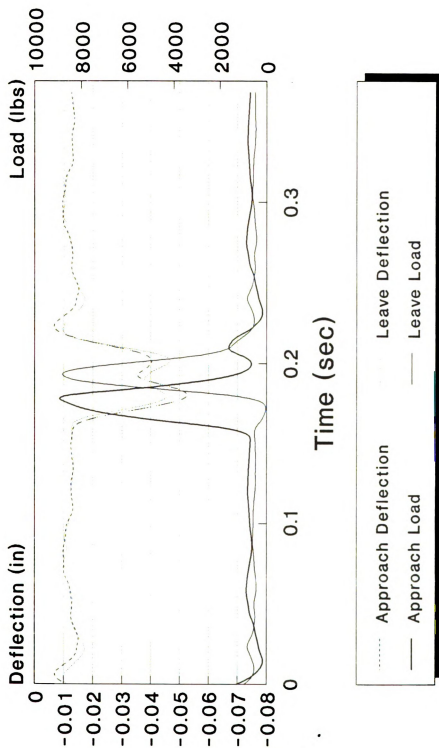
Figure B-19: Load and deflection curves for high tension slab after cycle #10,000.
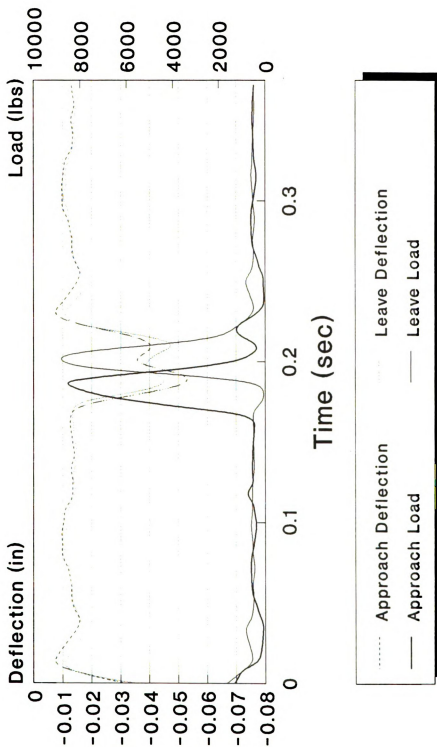
Figure B-20: Load and deflection curves for high tension slab after cycle #20,000.
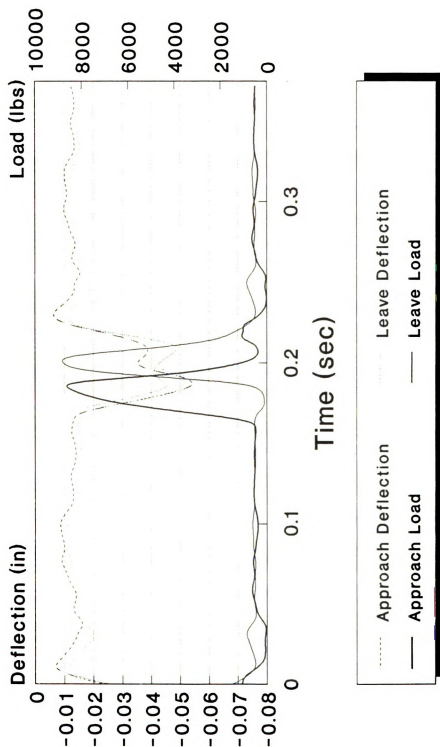
Figure B-21: Load and deflection curves for high tension slab after cycle #50,000.

HIGH TENSION
CYCLE # 100,000
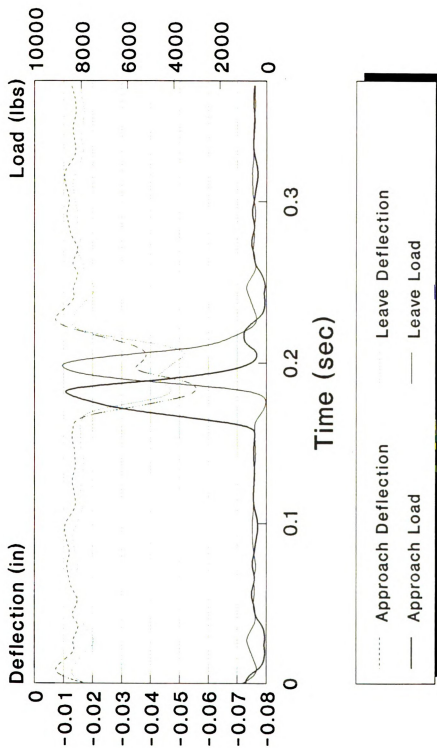
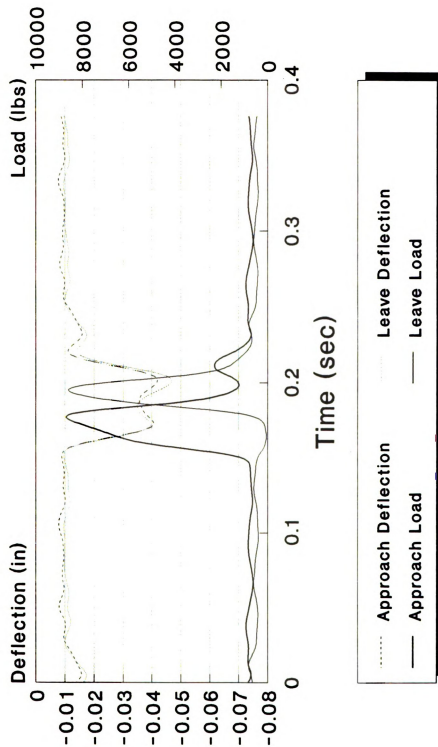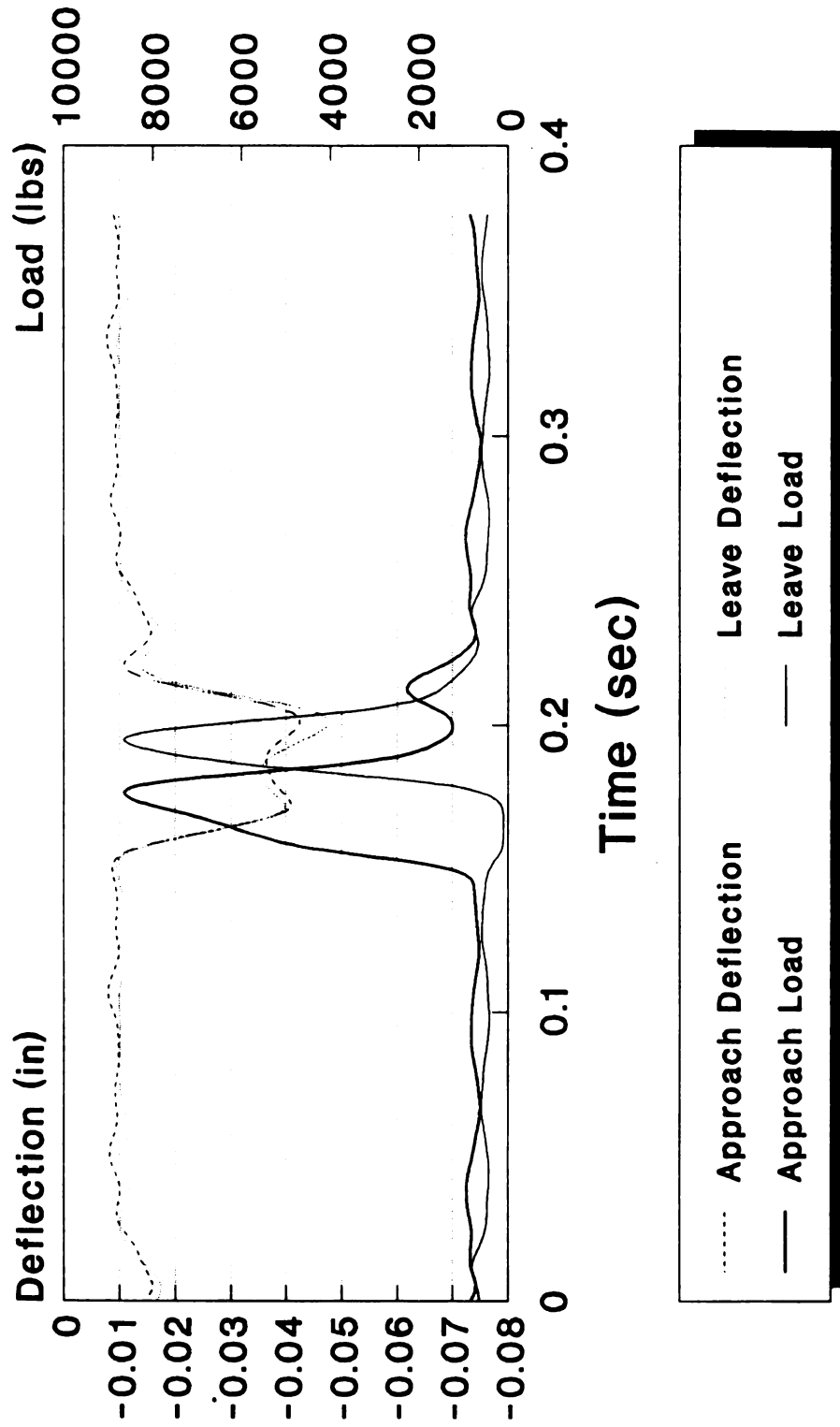Figure B-22: Load and deflection curves for high tension slab after cycle #100,000.
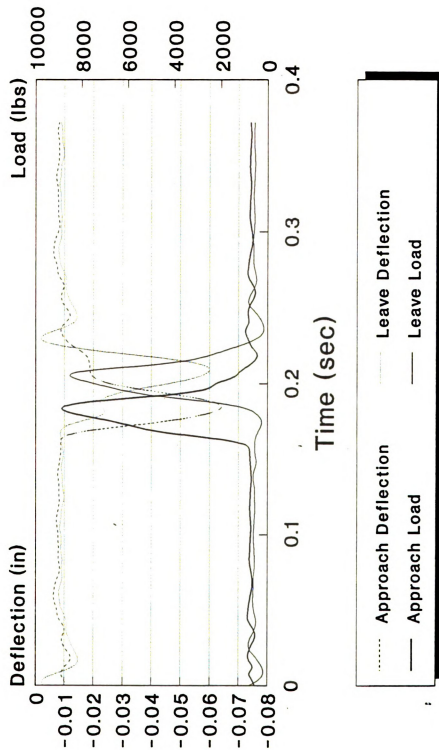
Figure B-23: Load and deflection curves for high tension slab after cycle #250,000.

HIGH FOUNDATION
CYCLE # 1
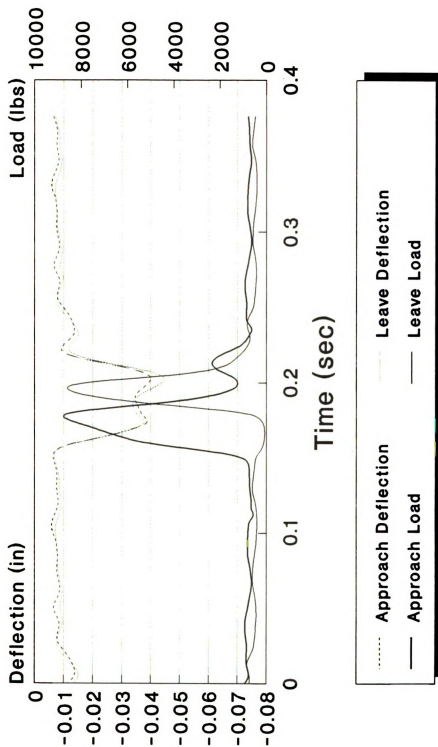
Figure B-24: Load and deflection curves for high foundation slab after load cycle #1.
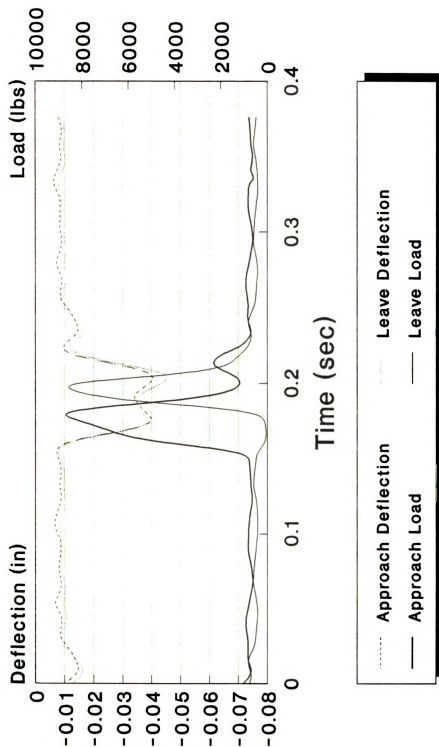
Figure B-25: Load and deflection curves for high foundation slab after load cycle #1,000.
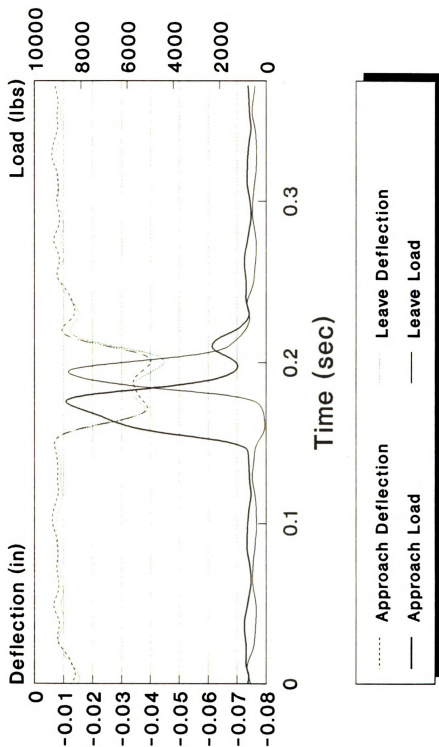
Figure B-26: Load and deflection curves for high foundation slab after load cycle #2,000.

Figure B-27: Load and deflection curves for high foundation slab after load cycle #5,000.

Figure B-28: Load and deflection curves for high foundation slab after load cycle #10,000.

Figure B-29: Load and deflection curves for high foundation slab after load cycle #20,000.

Figure B-30: Load and deflection curves for high foundation slab after load cycle #50,000.
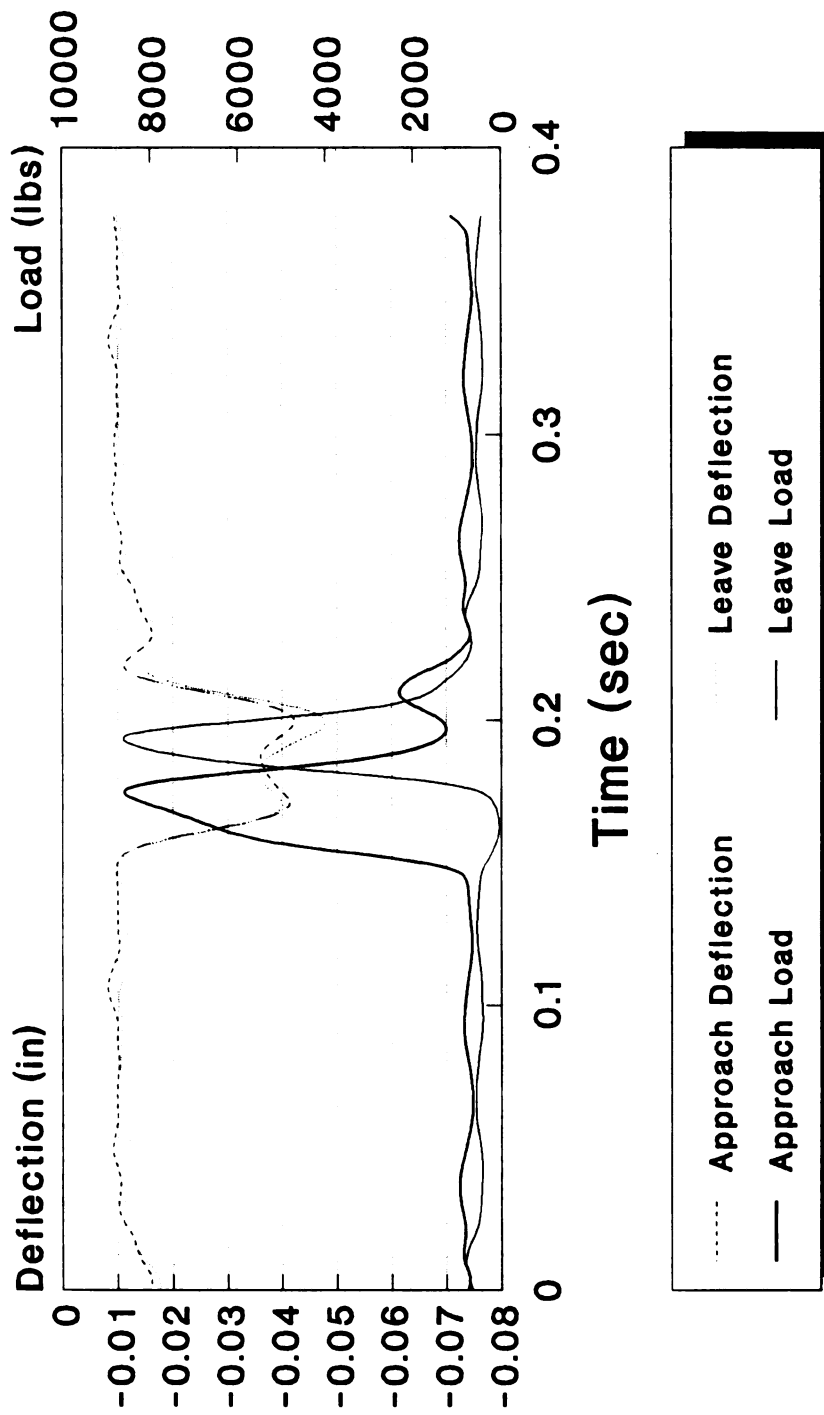
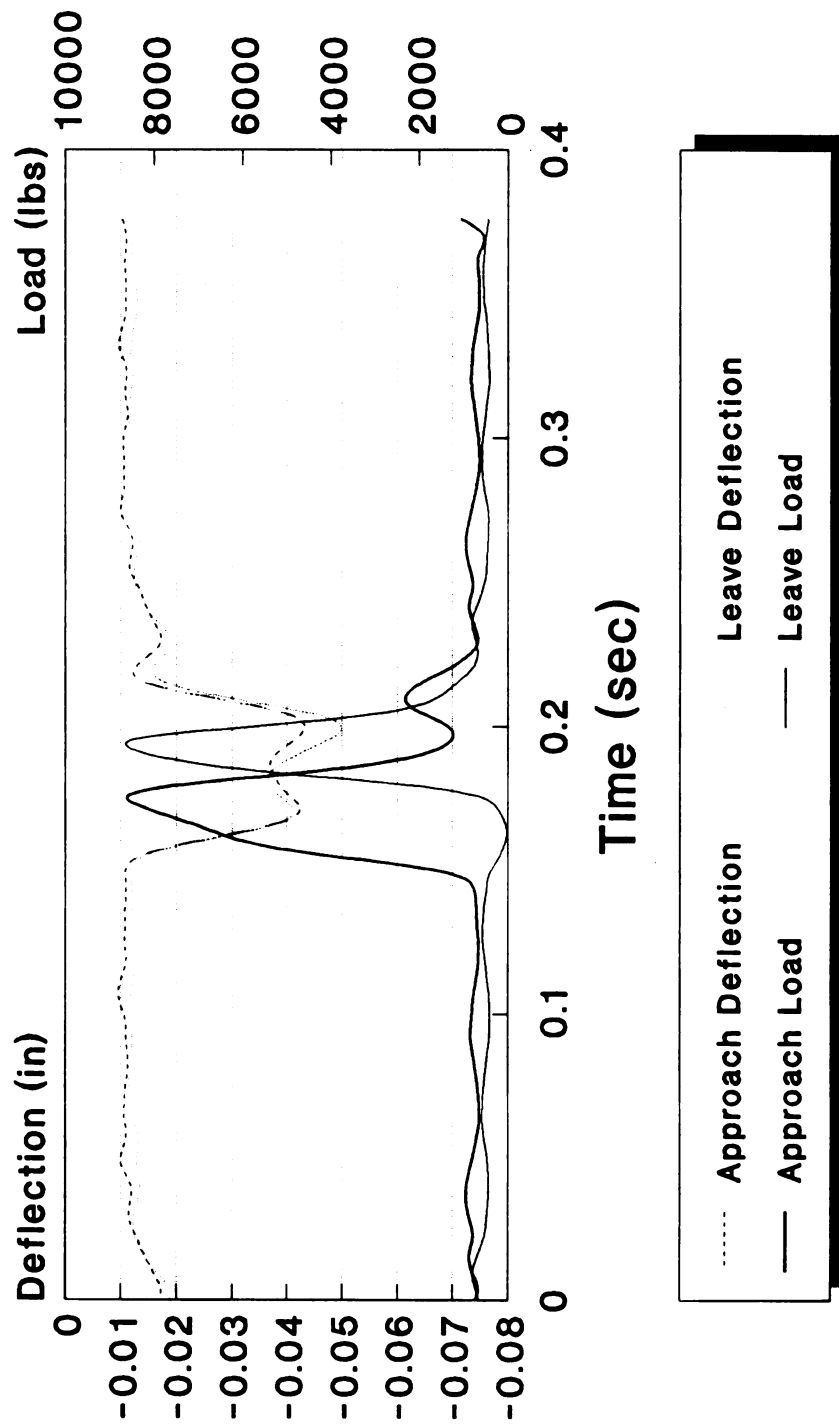Figure B-31: Load and deflection curves for high foundation slab after load cycle #100,000.

229

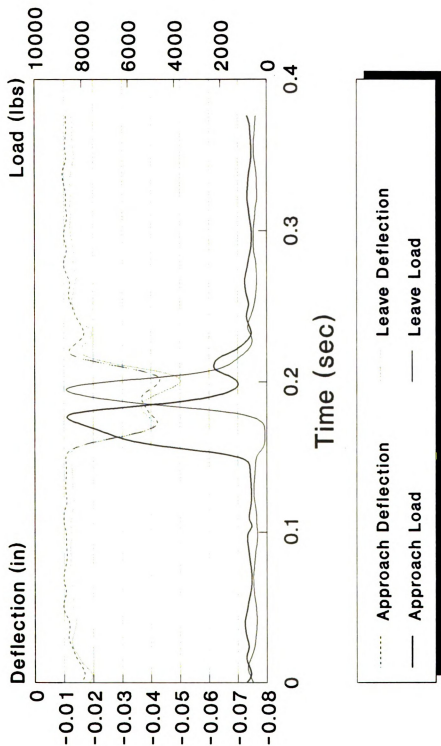Figure B-32: Load and deflection curves for high foundation slab after load cycle #300,000.

Figure B-33: Load and deflection curves for high foundation slab after load cycle #600,000.

Figure B-34: Load and deflection curves for high foundation slab after load cycle #1200,000.

Figure B-35: Load and deflection curves for high foundation slab after load cycle #1800,000.

233
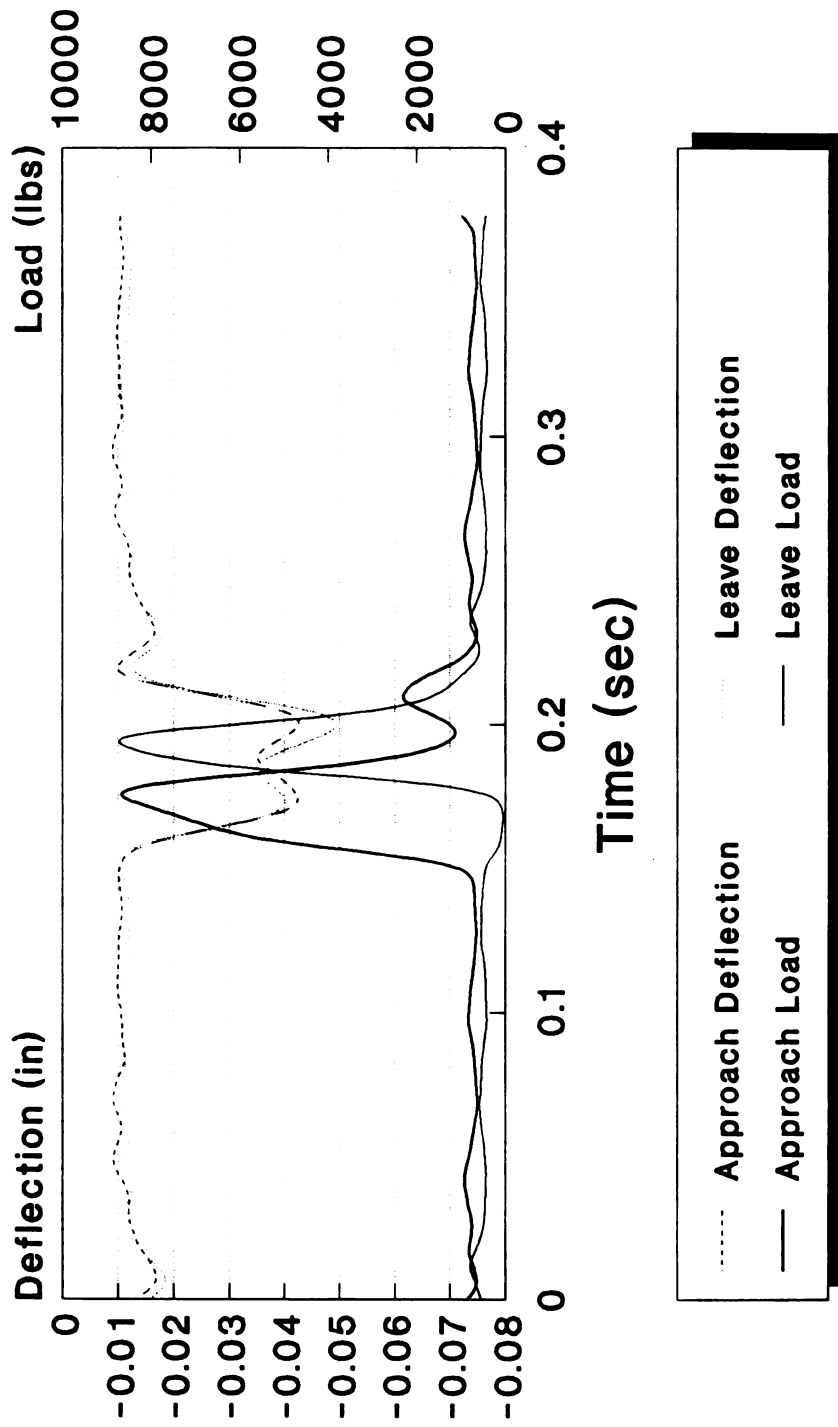

Figure B-36: Load and deflection curves for high foundation slab after load cycle #2400,000.

Figure B-37: Load and deflection curves for high foundation slab after load cycle #3000,000.

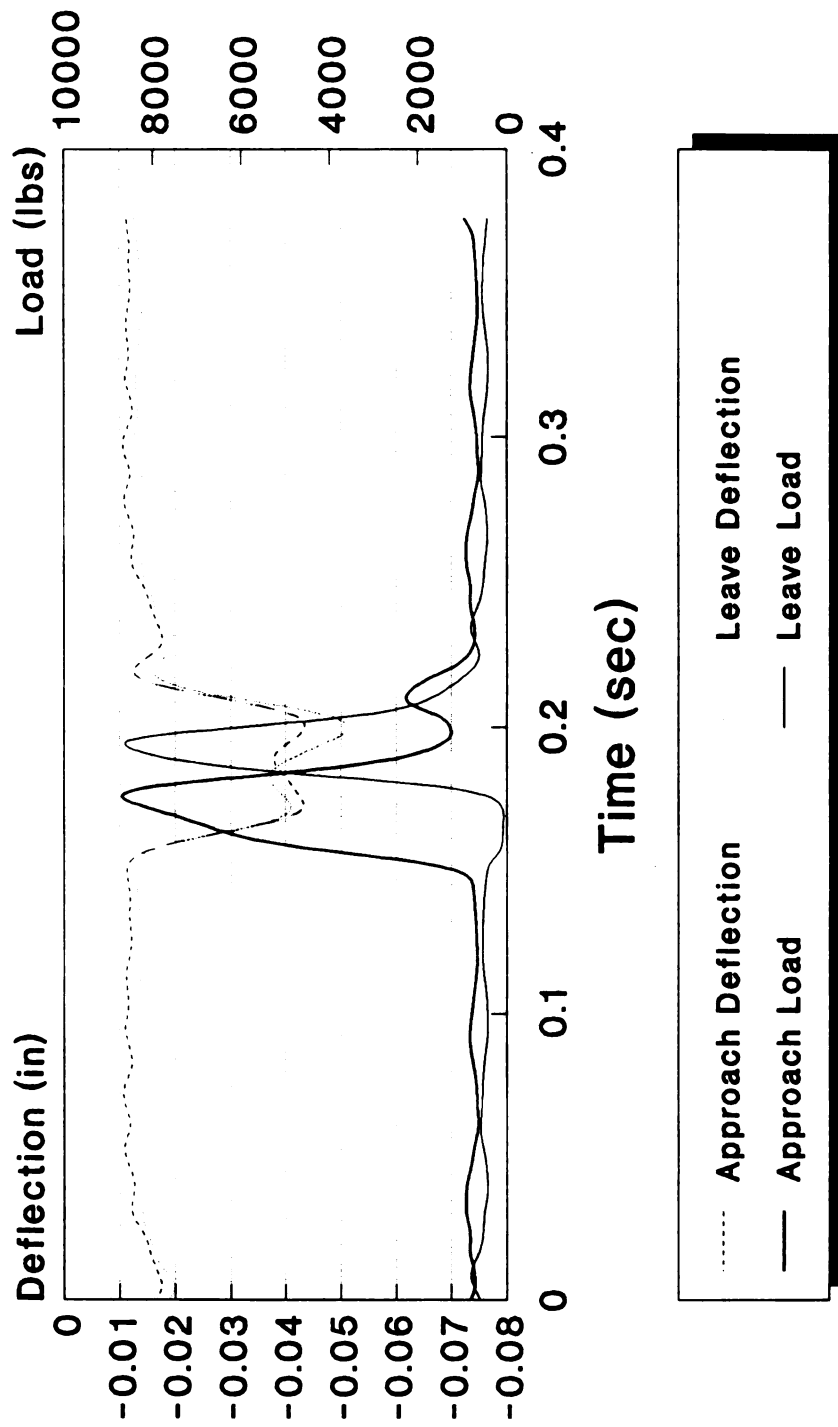Figure B-38: Load and deflection curves for high foundation slab after load cycle #3600,000.
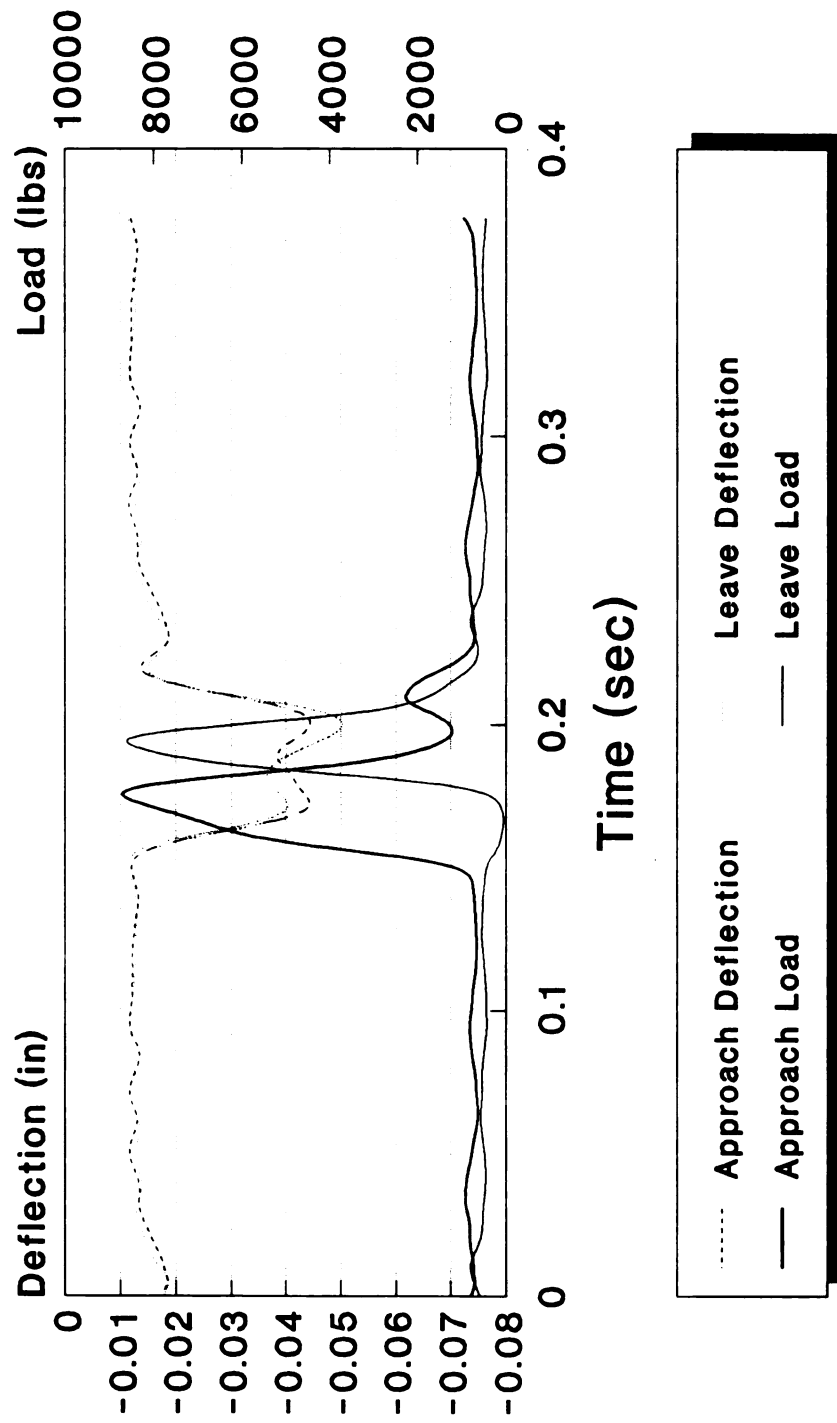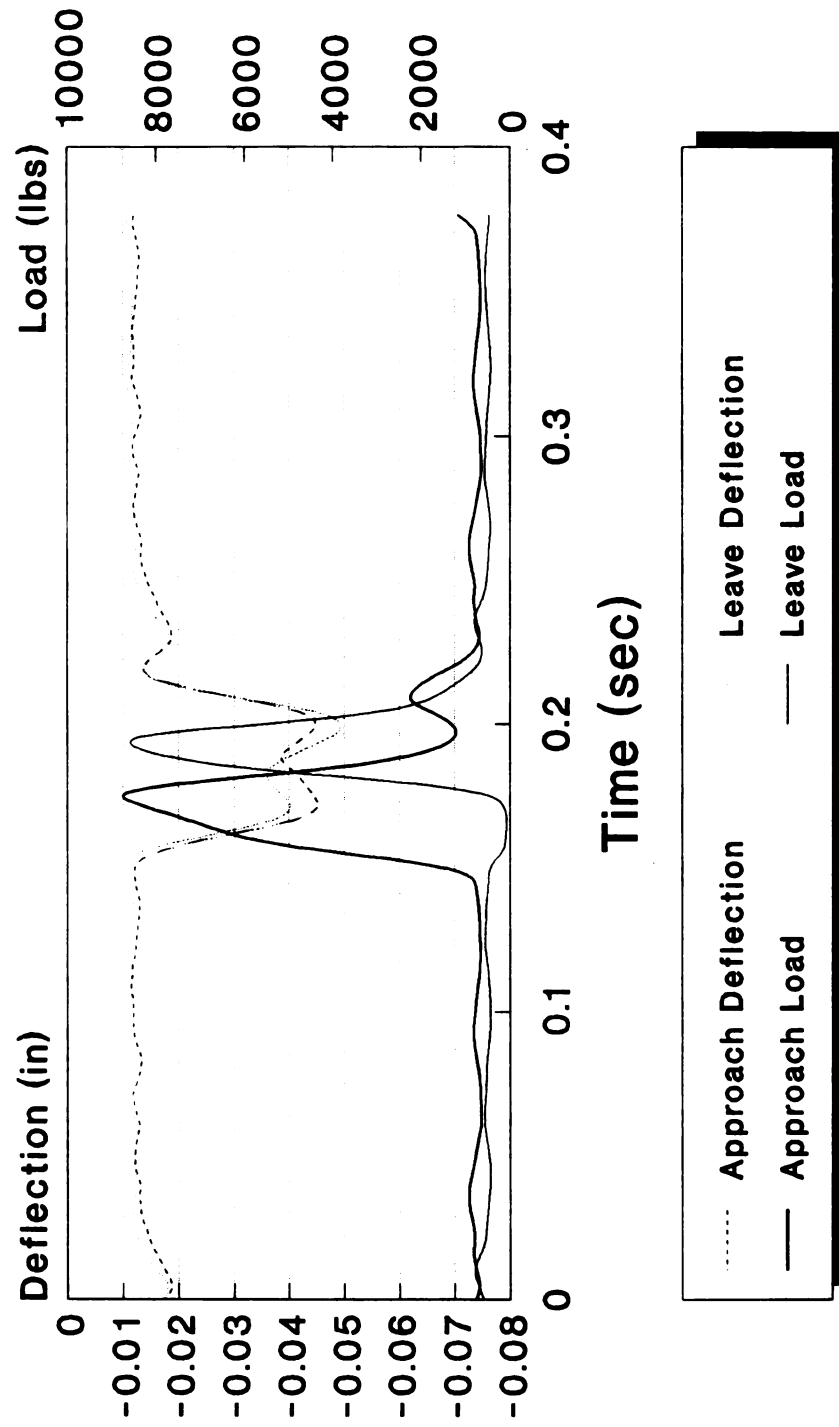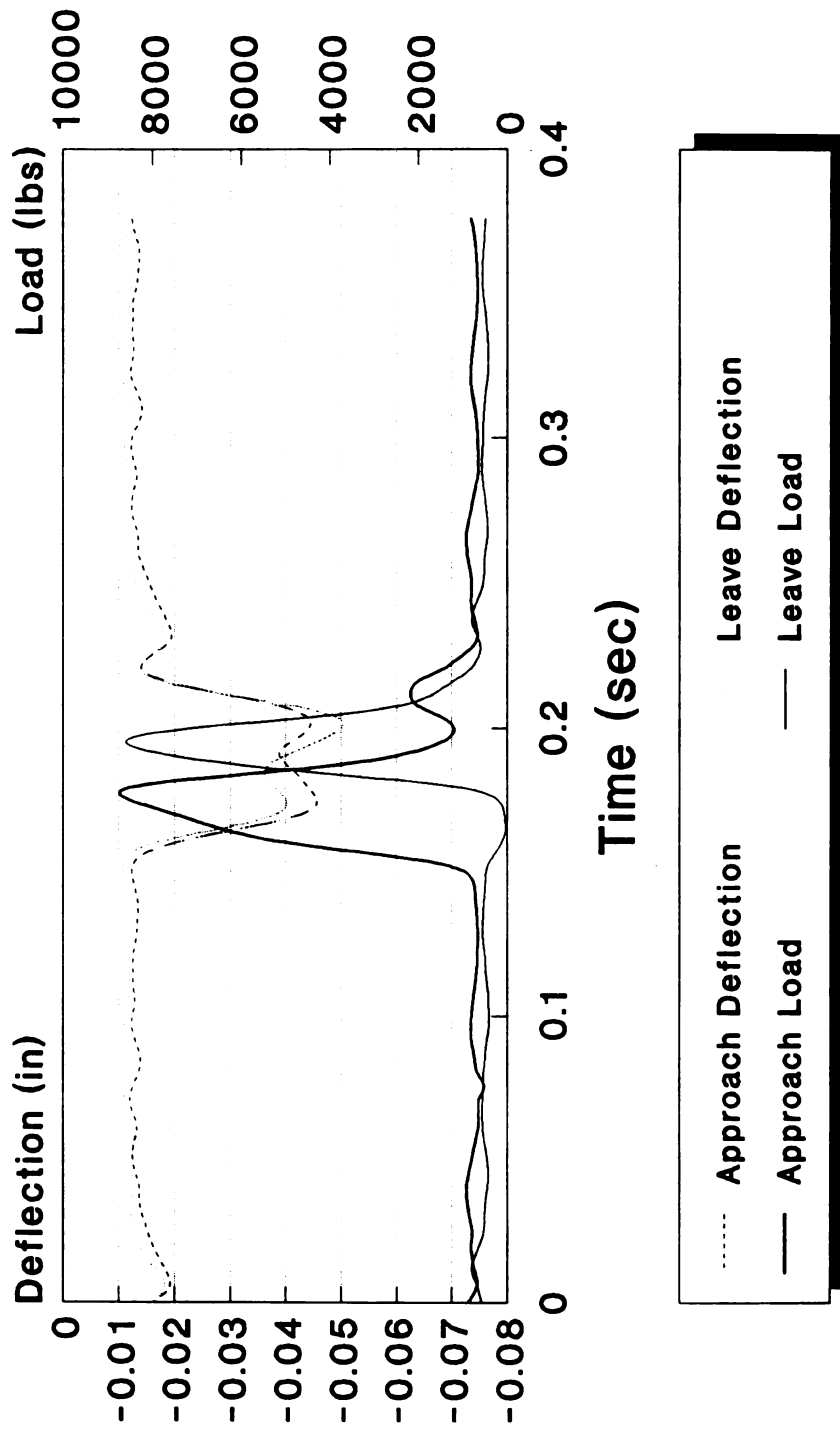
Figure B-39: Load and deflection curves for high foundation slab after load cycle #4200,000.

HIGH FOUNDATION
CYCLE # 4800,000
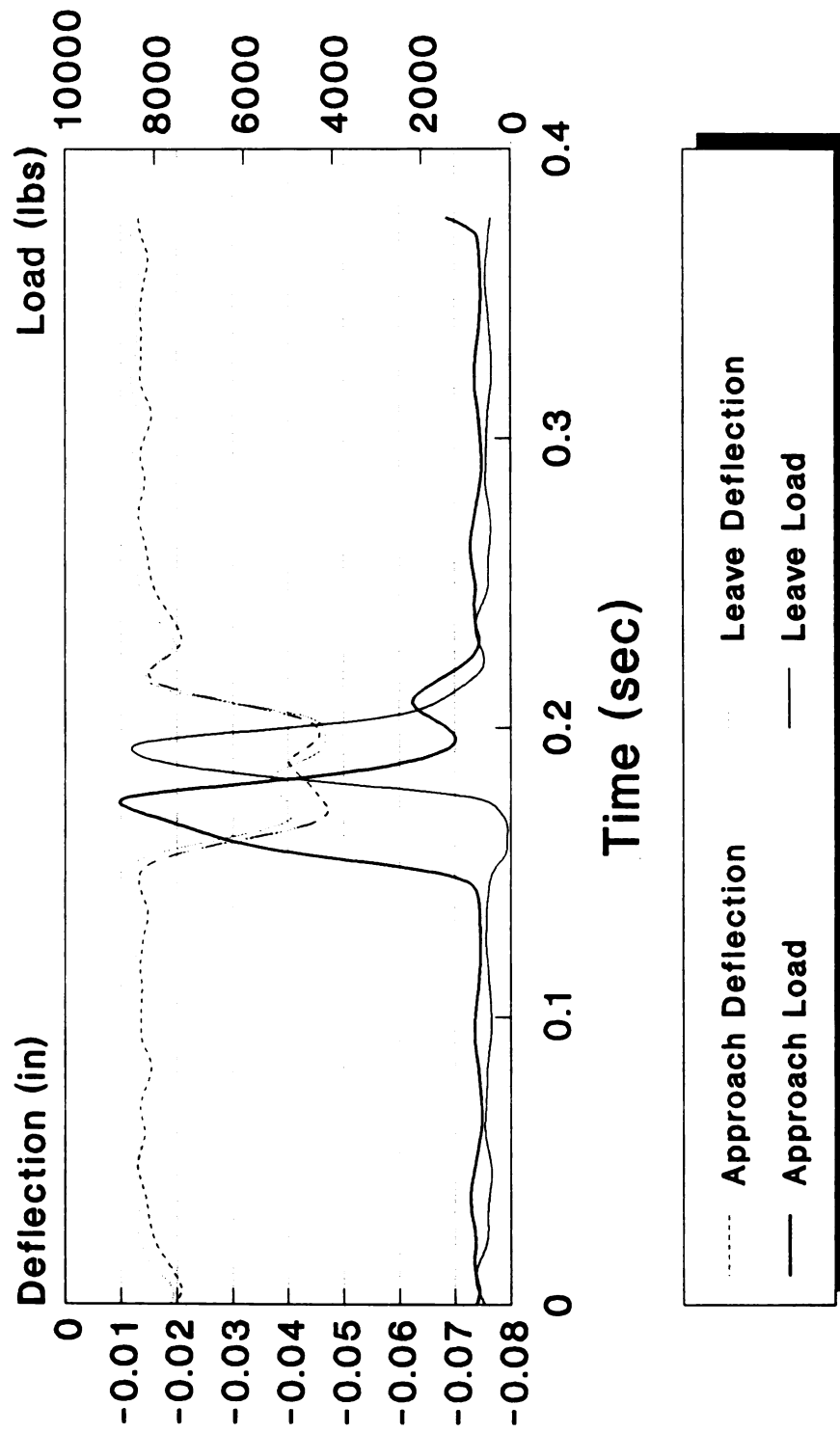
Figure B-40: Load and deflection curves for high foundation slab after load cycle #4800,000.
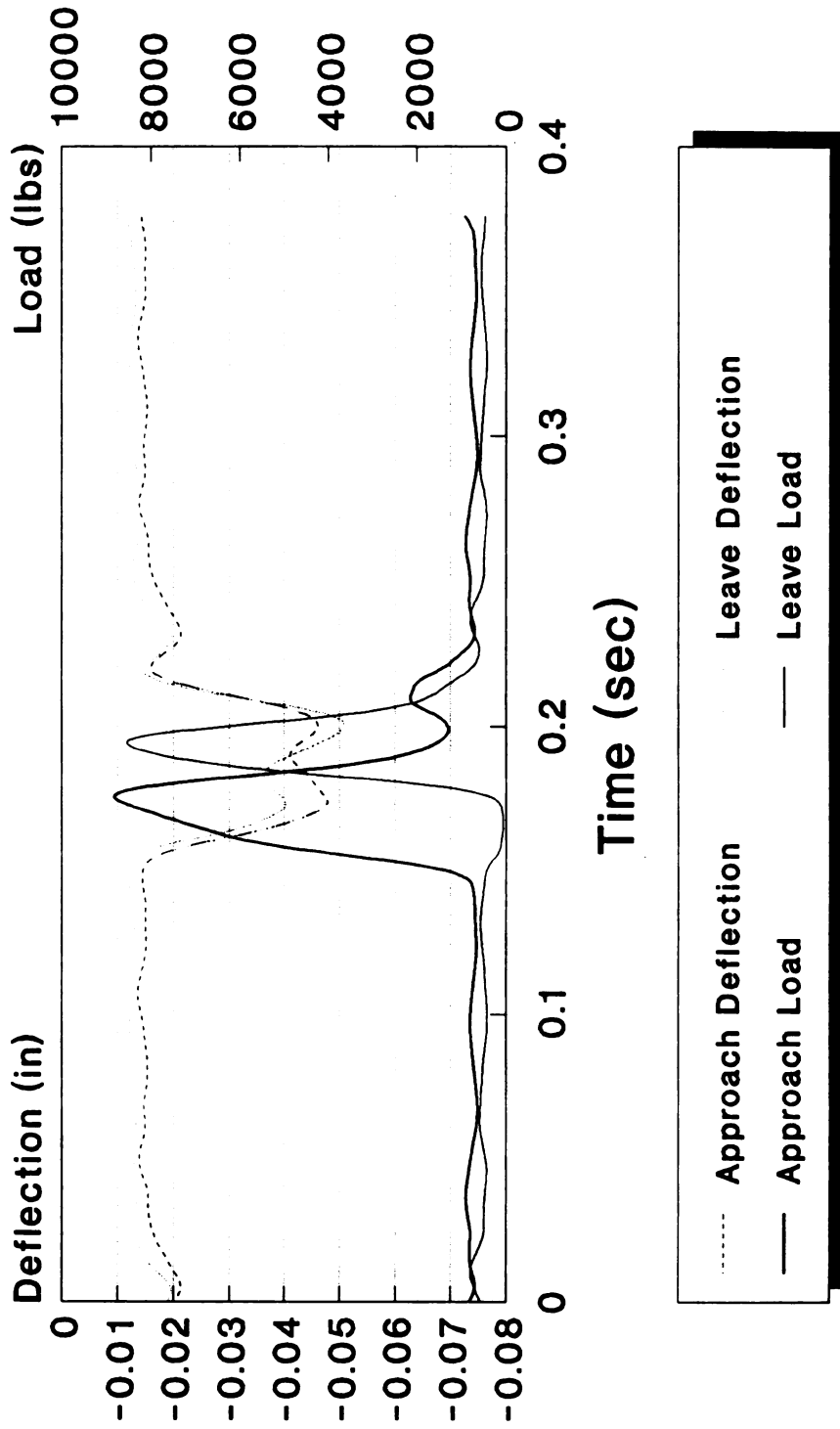
Figure B-41: Load and deflection curves for high foundation slab after load cycle #5400,000.
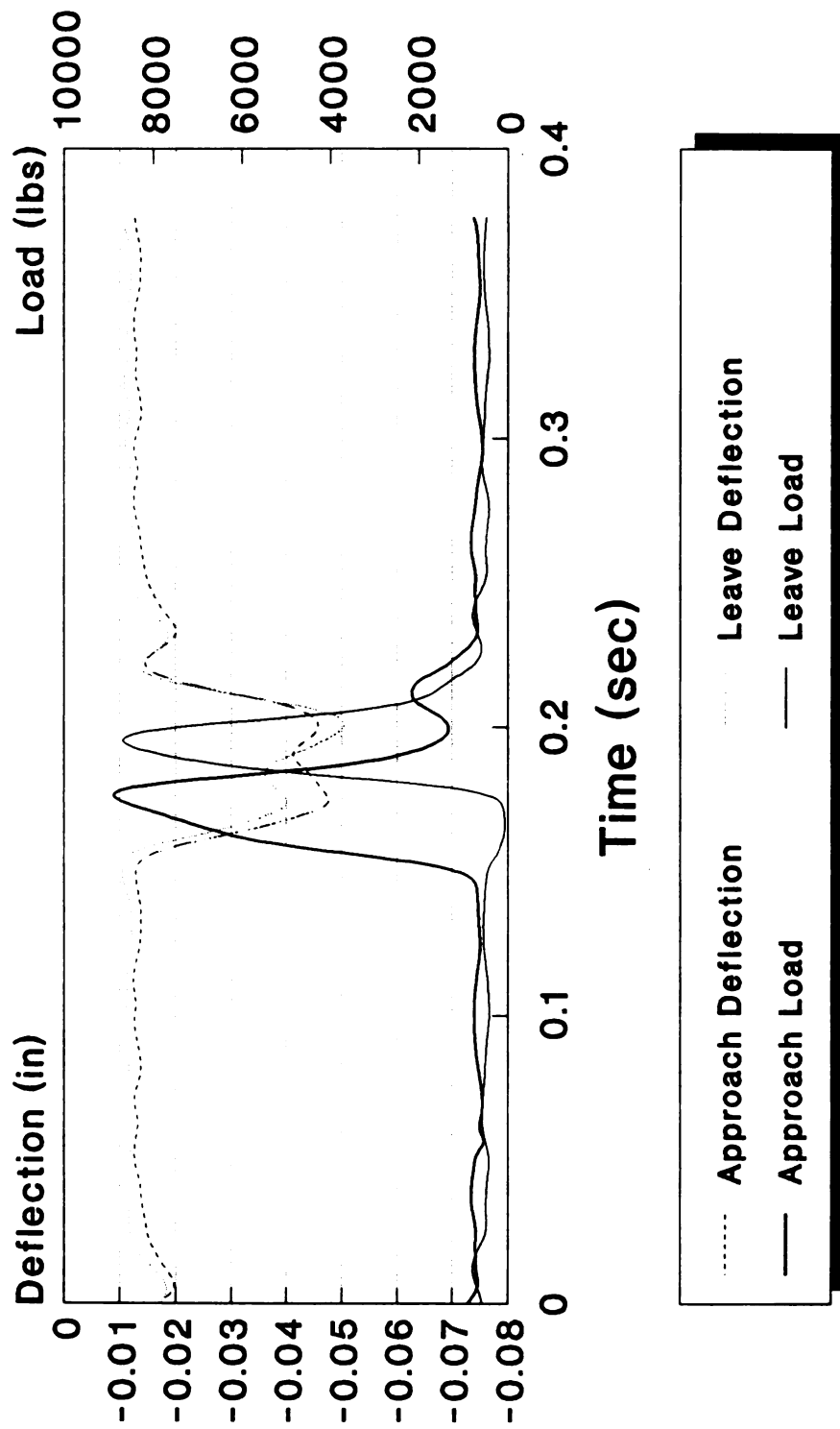
Figure B-42: Load and deflection curves for high foundation slab after load cycle #6000,000.
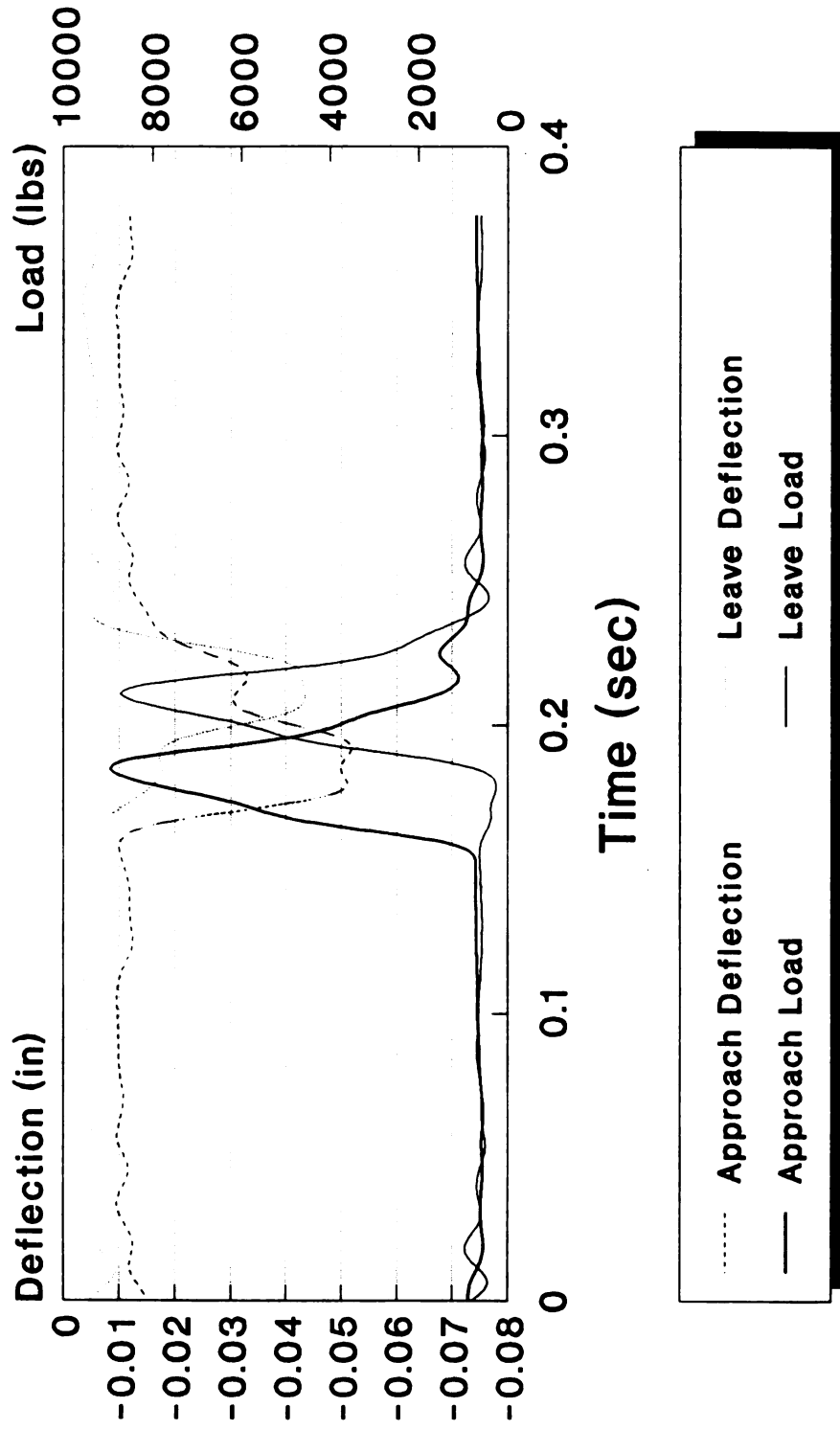
Figure B-43: Load and deflection curves for high foundation slab after load cycle #6600,000.

Figure B-44: Load and deflection curves for 6A virgin gravel slab (replicate) after cycle #1.

REPLICATE
CYCLE # 1000

Deflection (in)

Load (lbs)

0
-0.01
-0.02
-0.03
-0.04
-0.05
-0.06
-0.07
-0.08
-0.09

10000
8000
6000
4000
2000
0

Time (sec)

0.1
0.2
0.3

0

······· Approach Deflection ········ Leave Deflection

——— Approach Load ——— Leave Load

Figure B-45: Load and deflection curves for 6A virgin gravel slab (replicate) after cycle #1,000.

Figure B-46: Load and deflection curves for 6A virgin gravel slab (replicate) after cycle #2,000.

Figure B-47: Load and deflection curves for 6A virgin gravel slab (replicate) after cycle #5,000.

REPLICATE
CYCLE # 10000

Figure B-48: Load and deflection curves for 6A virgin gravel slab (replicate) after cycle #10,000.

Figure B-49: Load and deflection curves for 6A virgin gravel slab (replicate) after cycle #20,000.

Figure B-50: Load and deflection curves for 6A virgin gravel slab (replicate) after cycle #50,000.

REPLICATE CYCLE # 100000

Figure B-51: Load and deflection curves for 6A virgin gravel slab (replicate) after cycle #100,000.
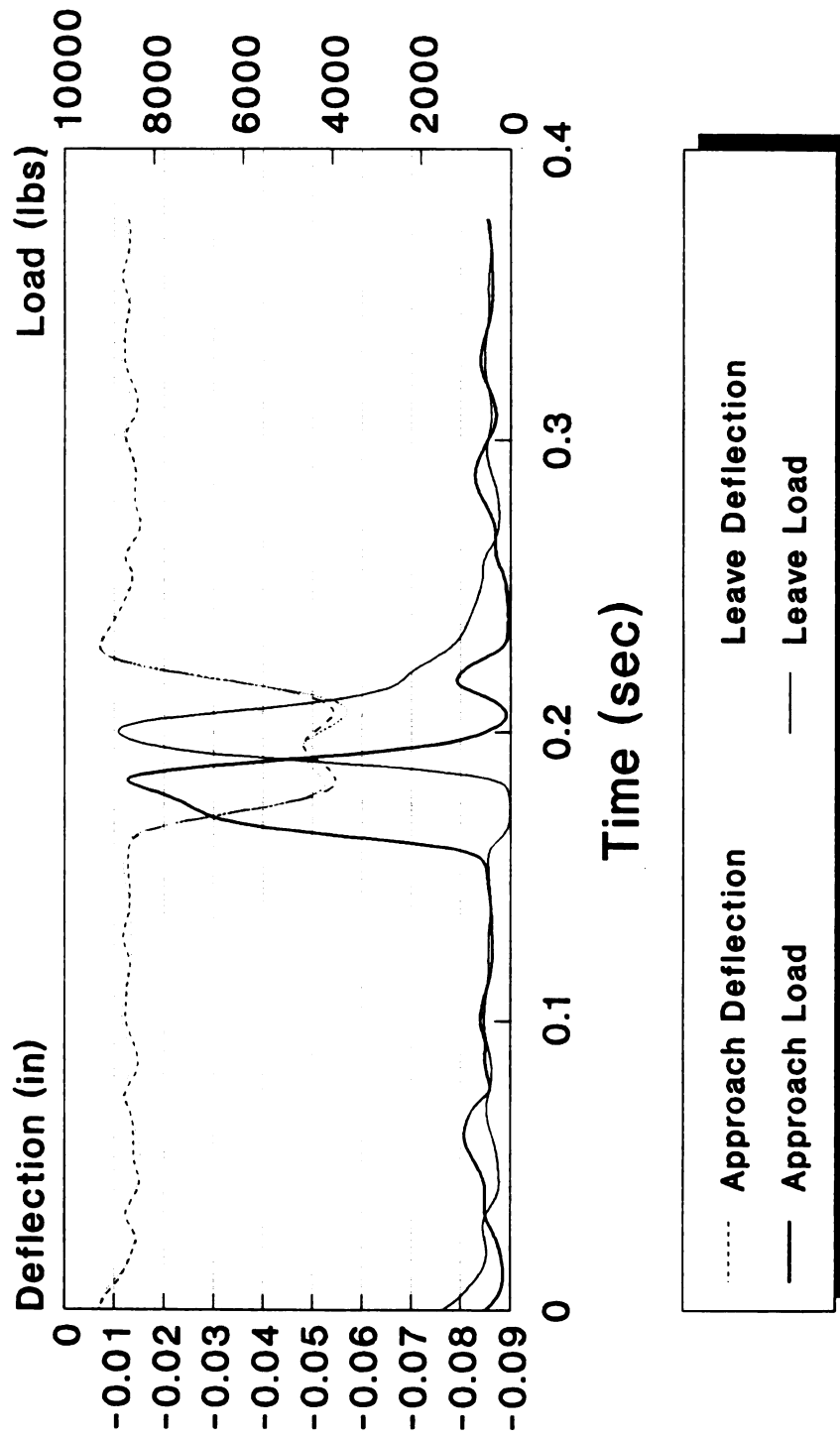
Figure B-52: Load and deflection curves for 6A virgin gravel slab (replicate) after cycle #300,000.

REPLICATE
CYCLE # 600000
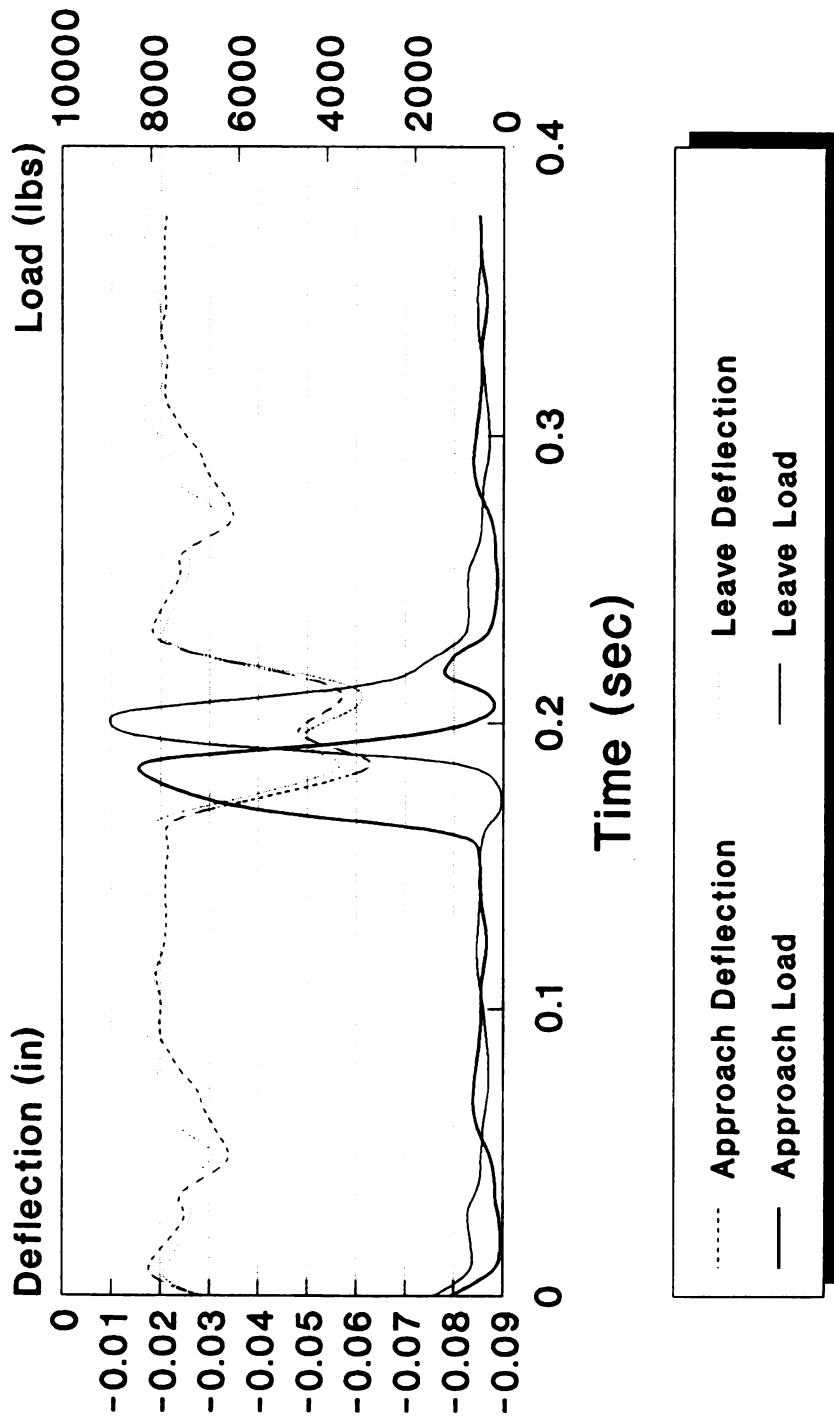
Figure B-53: Load and deflection curves for 6A virgin gravel slab (replicate) after cycle #600,000.
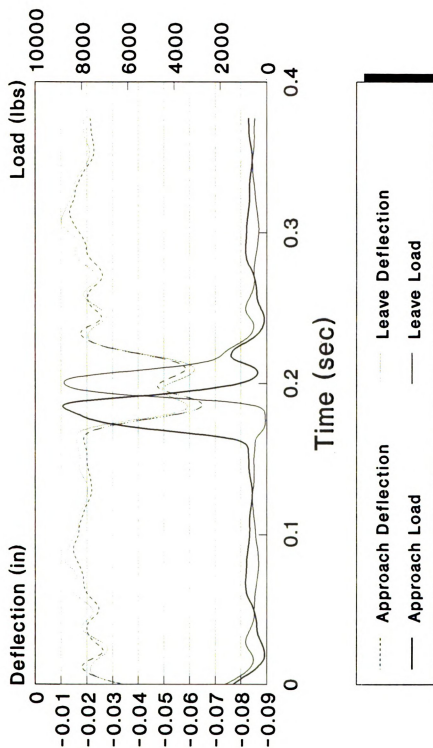
Figure B-54: Load and deflection curves for 6A virgin gravel slab (replicate) after cycle #1200,000.
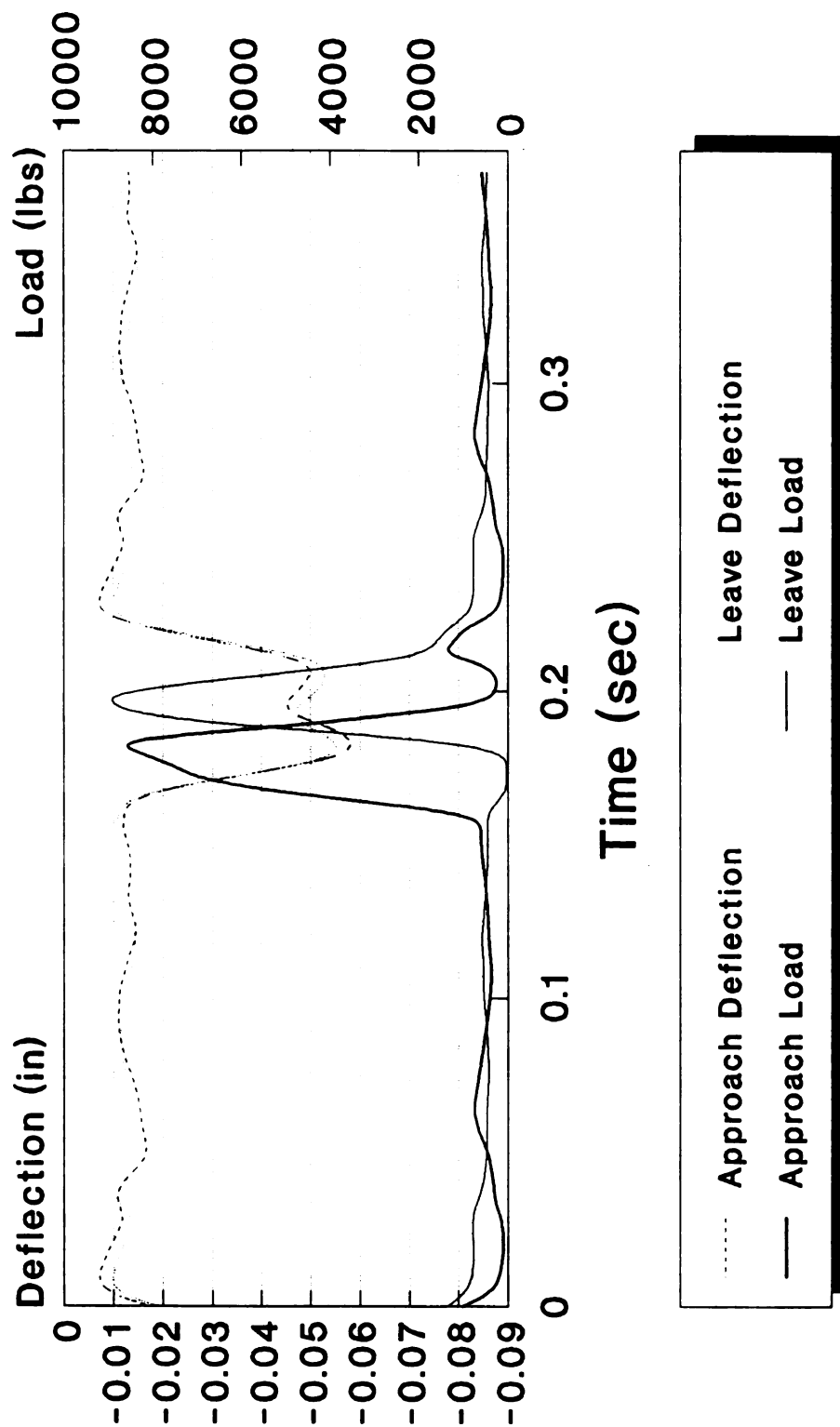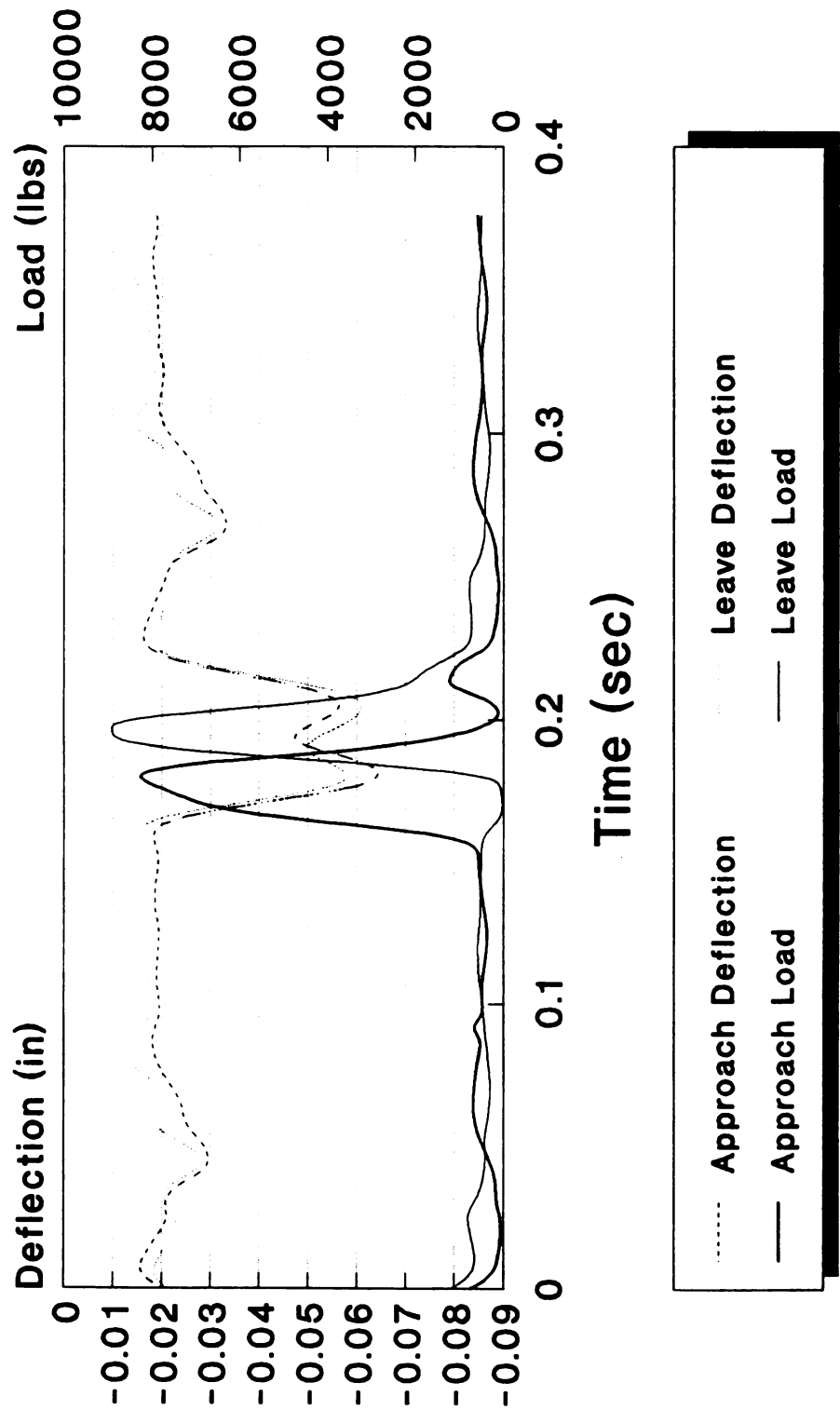
Figure B-55: Load and deflection curves for 6A virgin gravel slab (replicate) after cycle #1800,000.
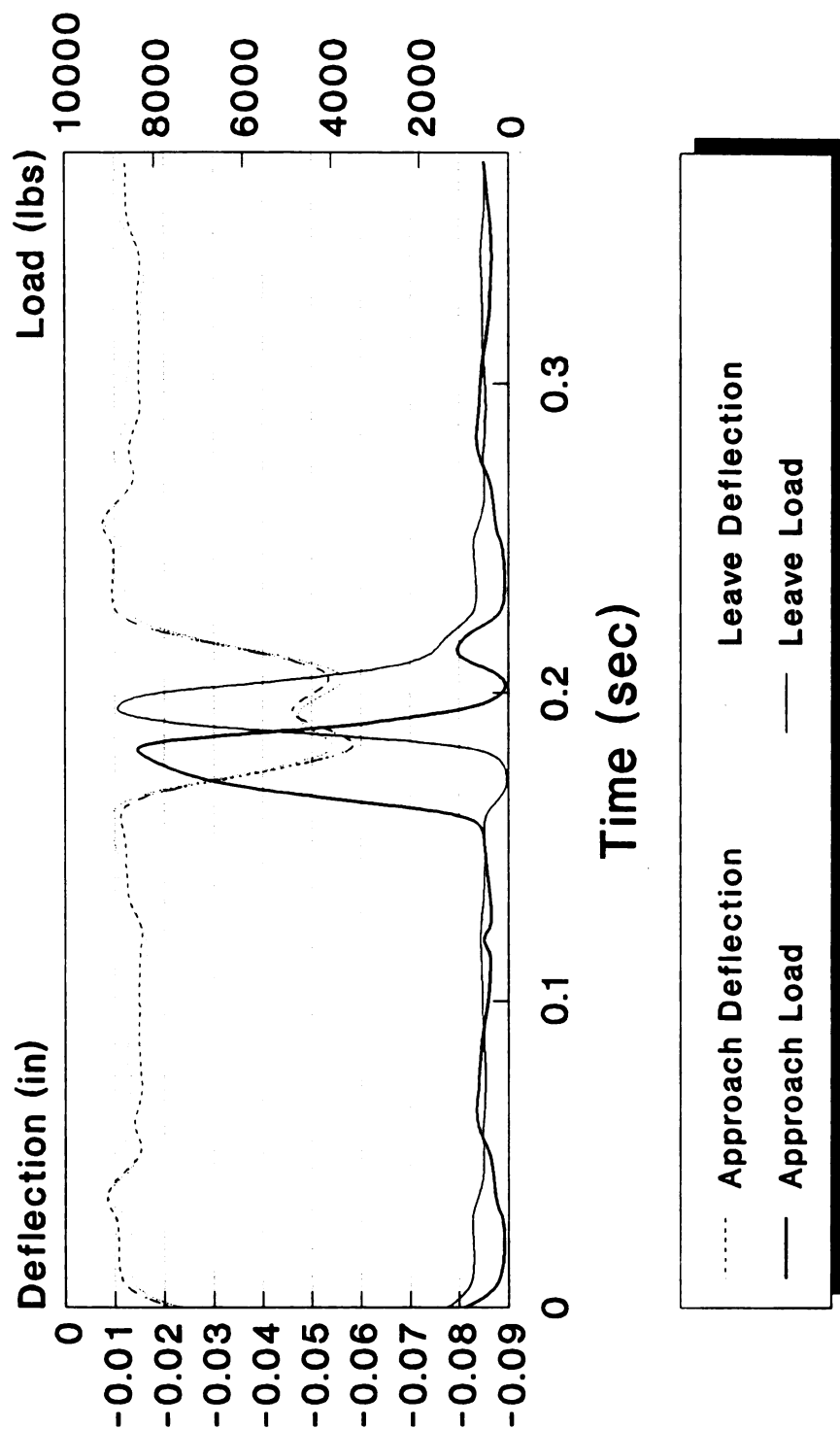
REPLICATE
CYCLE # 2400000
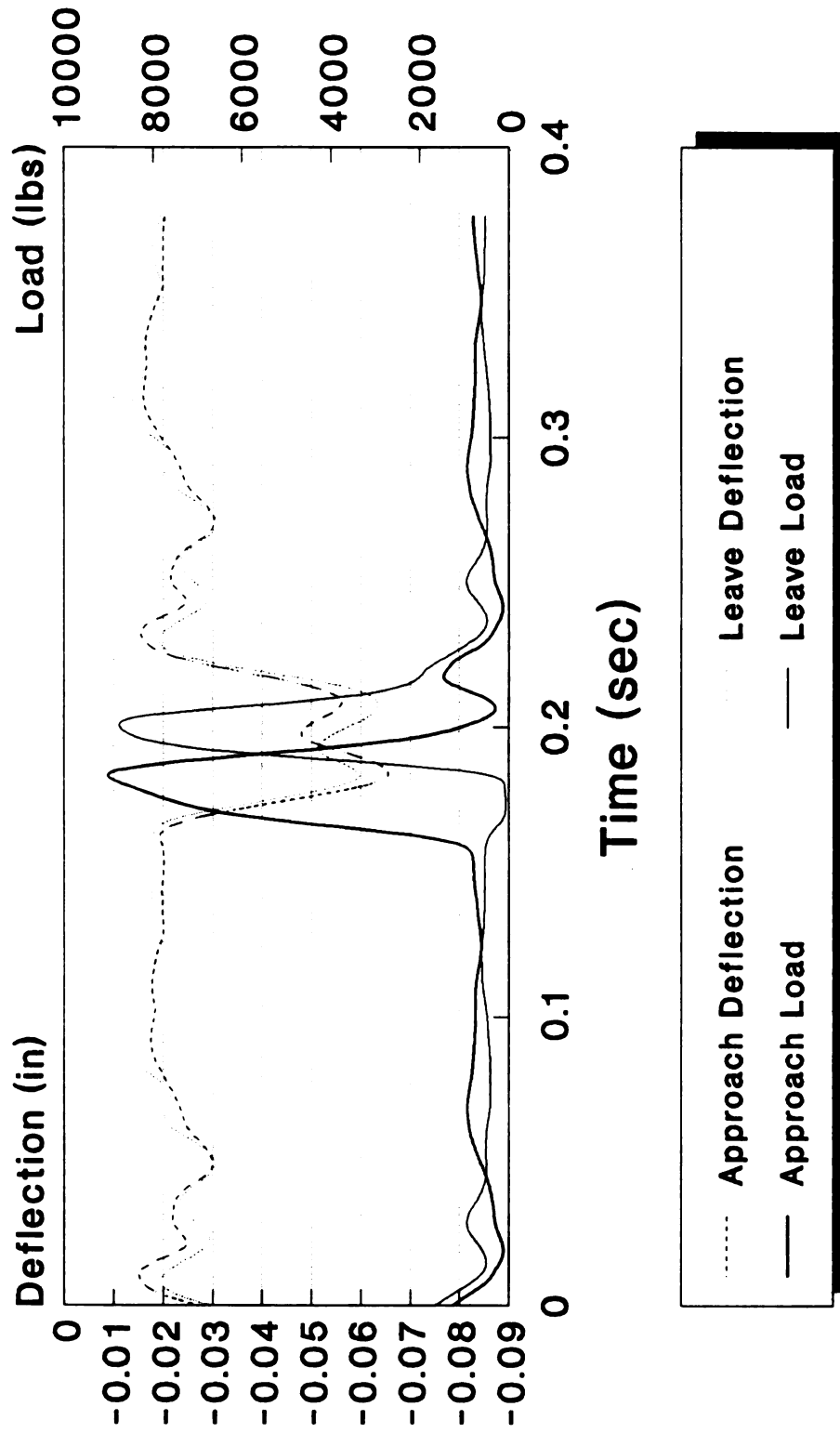
Figure B-56: Load and deflection curves for 6A virgin gravel slab (replicate) after cycle #2400,000.
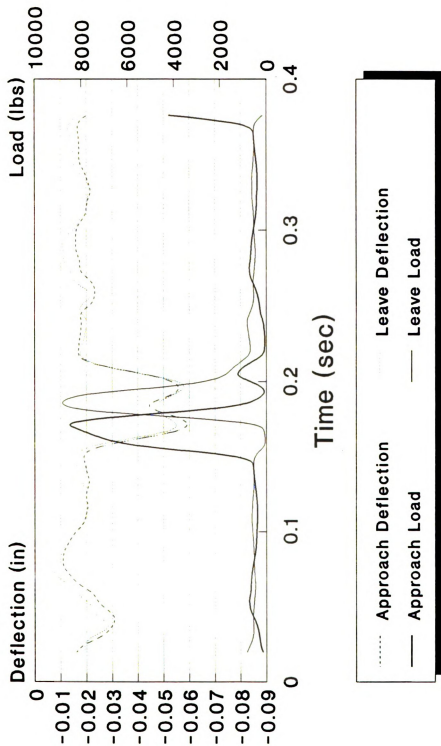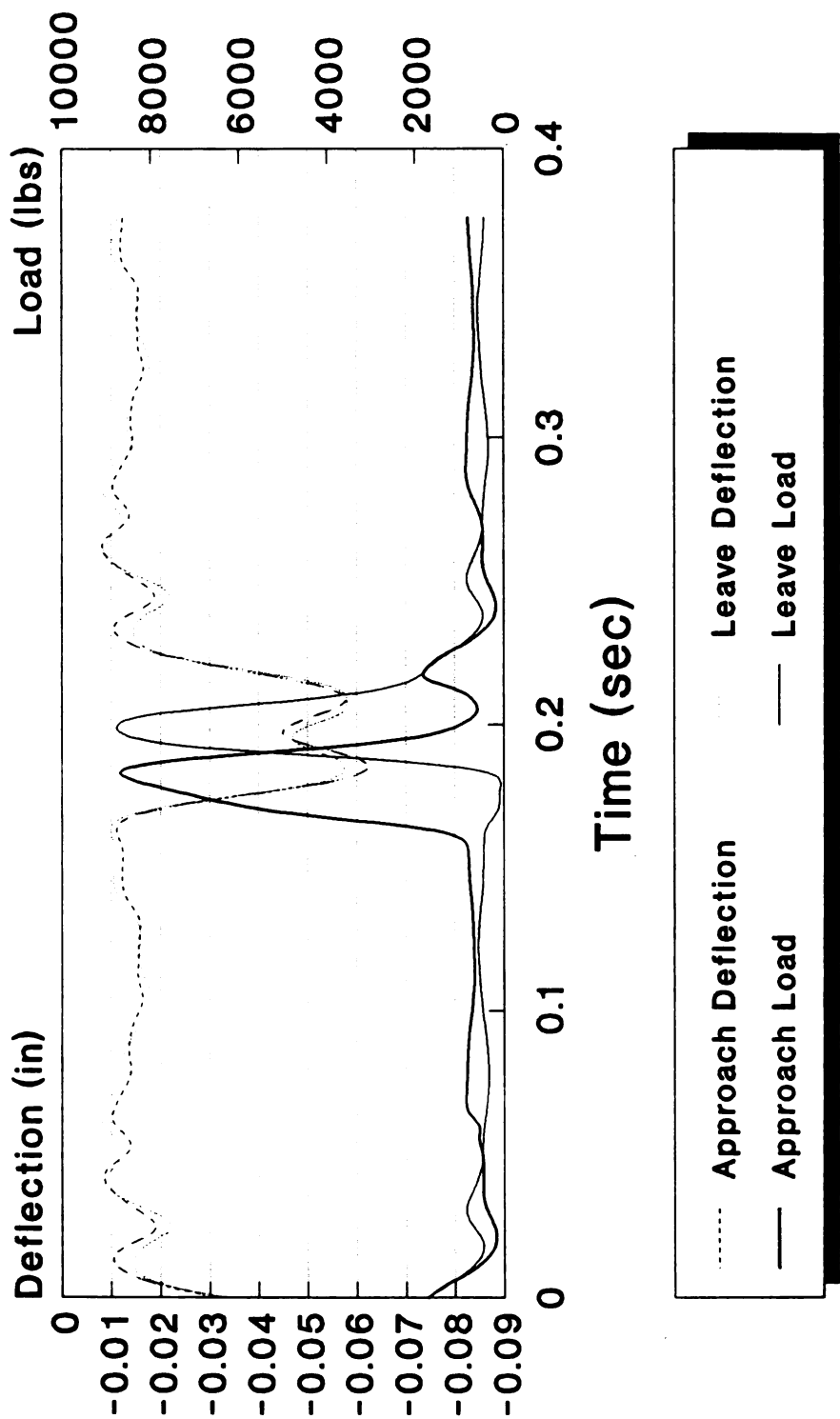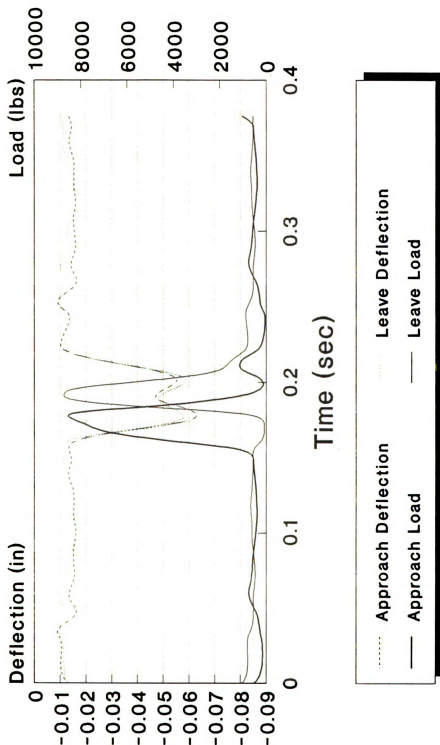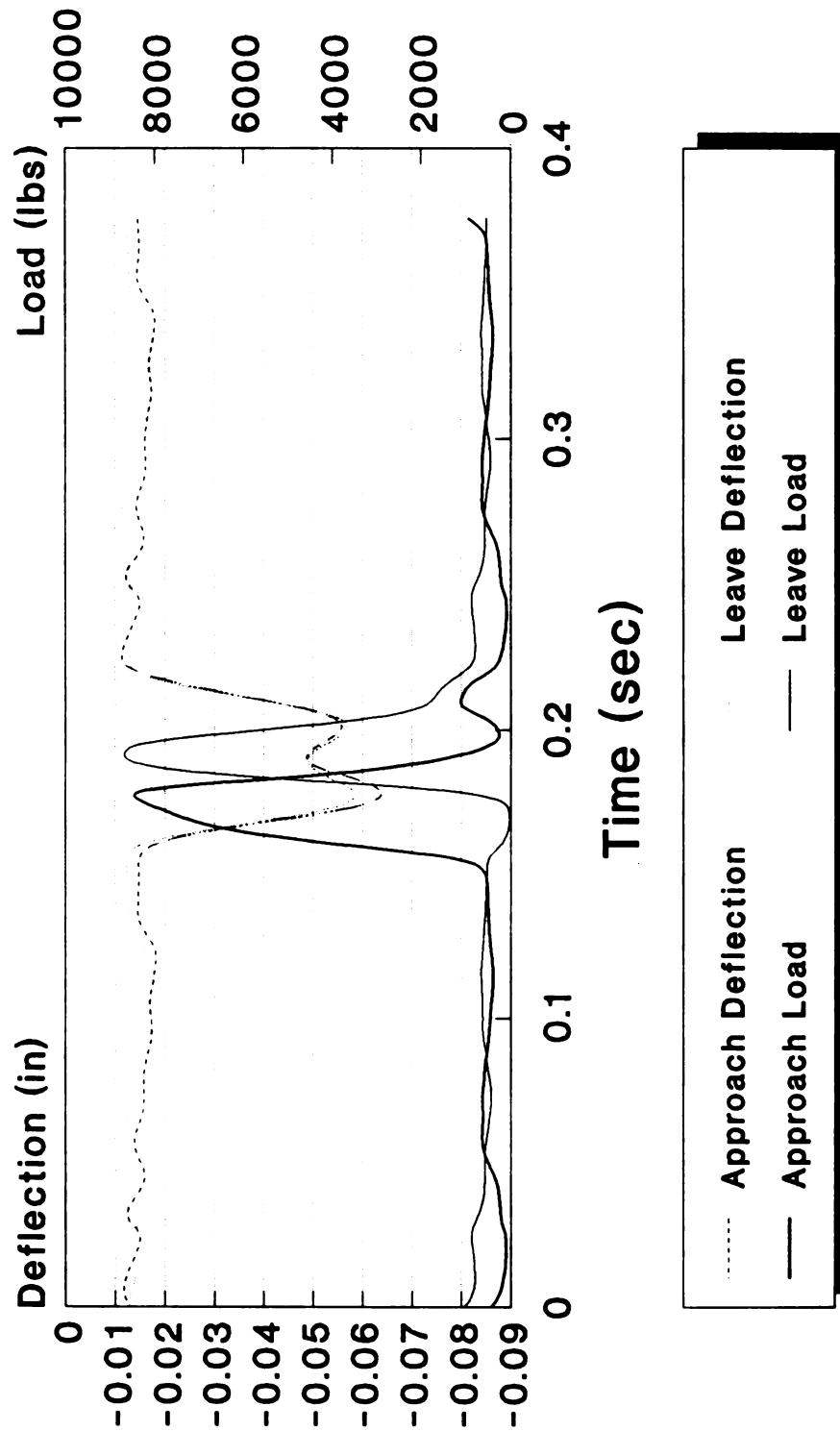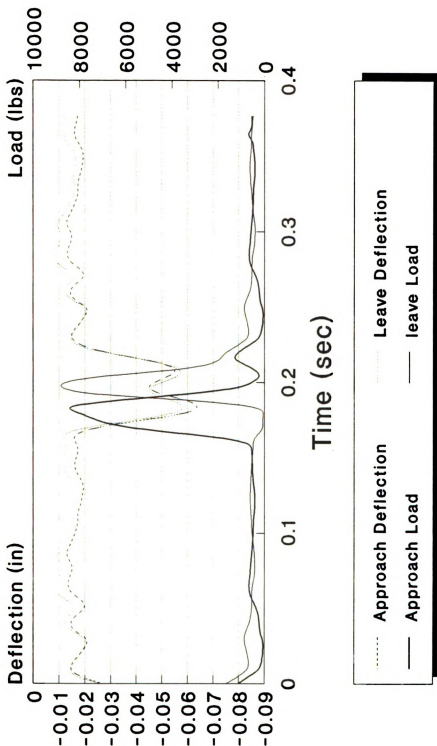
REPLICATE
CYCLE # 3000000
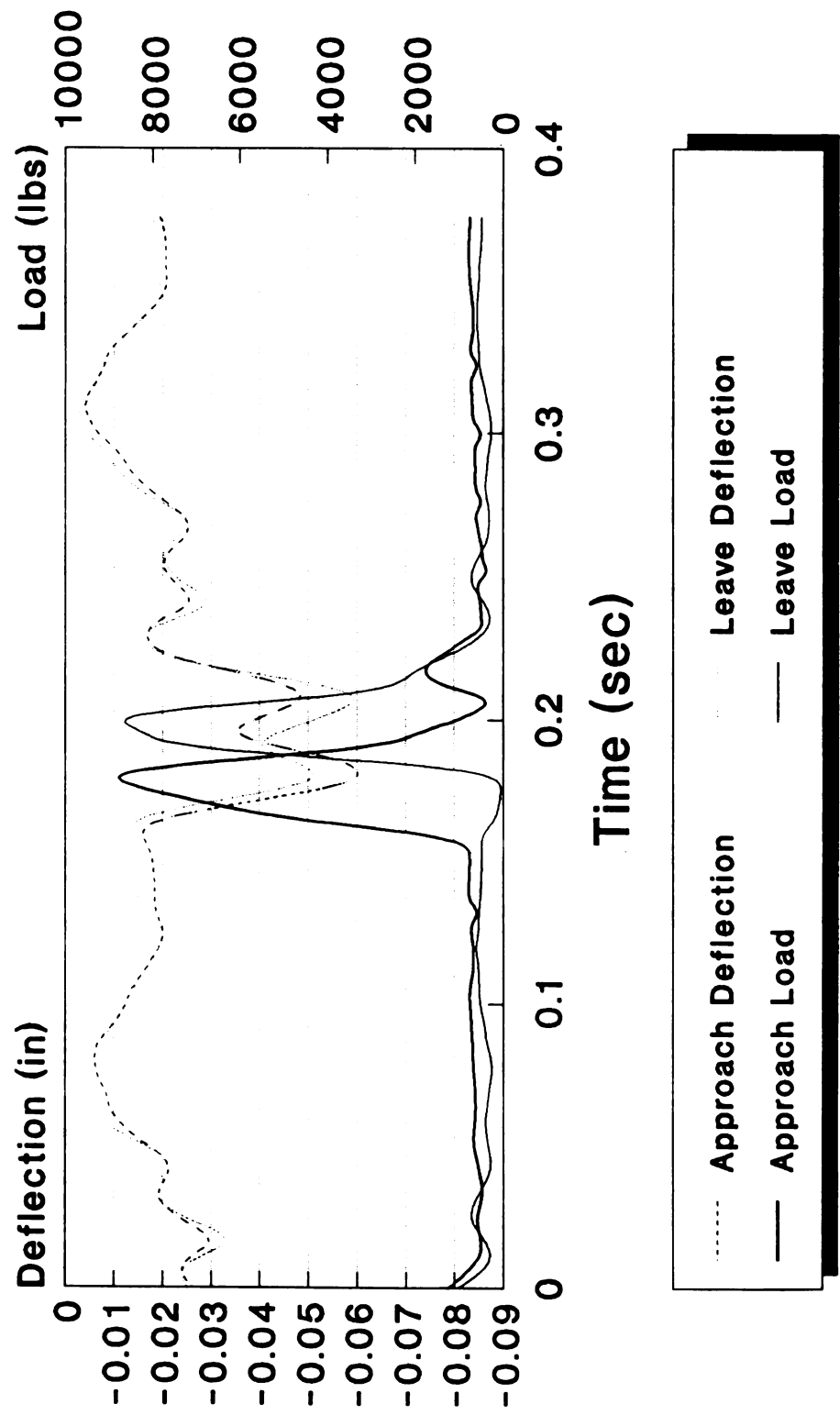
Figure B-57: Load and deflection curves for 6A virgin gravel slab (replicate) after cycle #3000,000.
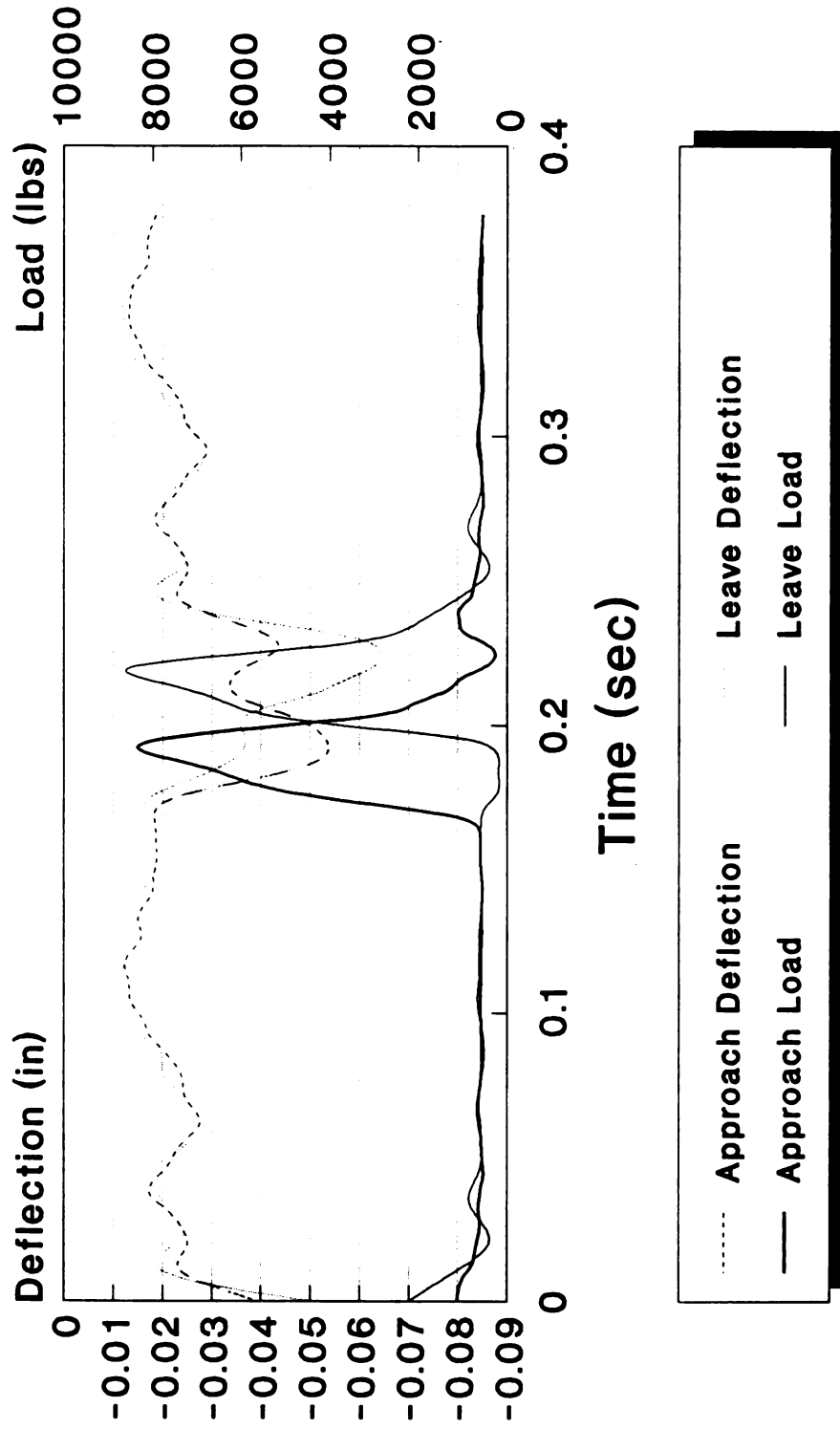
Figure B-58: Load and deflection curves for 6A virgin gravel slab (replicate) after cycle #3300,000.

APPENDIX C

PRELIMINARY STATISTICAL ANALYSIS

APPENDIX C

PRELIMINARY STATISTICAL ANALYSIS

C.1 EXPERIMENTAL DESIGN

The general concept of the study involved the application of repeated loads (simulating the passage of heavy truck traffic) across transverse cracks that have been induced in a series of large-scale reinforced concrete slab test specimens and the collection and analysis of load transfer data at several points during the testing of each specimen.

The effects of three material factors (coarse aggregate type, coarse aggregate gradation, and coarse aggregate treatment) and two design factors (amount of slab tension and foundation support) on aggregate interlock load transfer characteristics of transverse cracks in JRCP were investigated (detailed description is given in chapter 4).

As stated earlier, this research was sponsored by the MDOT and the Great Lakes Truck Center for Transportation

Research (GLCTTR). According to the terms of the contract only material factors (six test specimens) were to be tested under year 1 of the project. It was decided that two replicates of the 6A Virgin Gravel (control cell) and some additional variables (design factors) will be tested in year 2, under an extension to the original contract.

C.2 Test Setup Modifications

A test stand capable of simulating field shear and tension loading conditions was designed and constructed specially for this research work. However, during year 1 testing excessive vibrations of the test stand were observed. Year 2 work began by designing and installing some modifications to the test stand to eliminate unwanted vibration and reduce test noise. Moreover, some modifications were also made to improve specimen handling procedures. These modifications resulted in a more stable and stiffened test stand. Consequently, test specimens were able to endure significantly more number of load repetitions to failure compared to year 1 specimens, as shown by the results of the two replicates of the control cell run (6A virgin gravel) under year 2 conditions. Thus, change in test conditions resulted in a block effect. This blocking was not anticipated, and it caused a loss of one degree of freedom in the estimate of pure error.

C.3 **Estimate of Variability**

The block effect (as described-above) and limited number of replications (due to financial and time restraints) somewhat limits the scope of statistical analyses of the test data. However, a gross estimate of test variability and accuracy of test results (using a linear statistical model) is presented below.

C.3.1 *Test Results*

The test results converted to $\log_{10}$ are presented below:

RESULT	TYPE A	GRADATION B	TREATMENT C	FOUNDATION D	TENSION E
			YEAR 1		
5.95	Gravel	Coarse	Virgin	100 psi/in	Typical
6.18	Limestone	Coarse	Virgin	100 Psi/in	Typical
5.40	Slag	Coarse	Virgin	100 psi/in	Typical
5.95	Gravel	Fine	Virgin	100 psi/in	Typical
5.54	Gravel	Coarse	Blend	100 psi/in	Typical
5.48	Gravel	Coarse	Recycled	100 psi/in	Typical
			YEAR 2		
6.43	Gravel	Coarse	Virgin	100 psi/in	Typical
6.52	Gravel	Coarse	Virgin	100 psi/in	Typical
5.40	Gravel	Coarse	Virgin	100 psi/in	High
6.82	Gravel	Coarse	Virgin	250 psi/in	Typical

C.3.2 *Model and Assumptions*

The following general linear regression model in terms of X variables was used in the analyses of the test results:

$$Y = \beta_0 X_0 + \beta_1 X_1 + \beta_2 X_2 + \beta_3 X_3 + \beta_4 X_4 + \beta_5 X_5 + \beta_6 X_6 + \beta_7 X_7 + \beta_8 X_8 + \varepsilon$$

where

$X_0 = 1$

$X_1 = 1$ Block 2

     $= 0$ Block 1

$X_2 = 1$ Limestone

     $= 0$ Gravel

$X_3 = 1$ Slag

     $= 0$ Gravel

$X_4 = 1$ Fine Gradation

     $= 0$ Coarse Gradation

$X_5 = 1$ Recycled Blend

     $= 0$ Virgin

$X_6 = 1$ 100% Recycled

     $= 0$ Virgin

$X_7 = 1$ High Tension

     $= 0$ Typical Tension

$X_8 = 1$ High Foundation (k = 250 psi/in)

     $= 0$ Low Foundation (k = 100 psi/in)

and $\beta_0, \beta_1, \ldots, \beta_8$ are parameters

The model assumes uncorrelated normal data and additive effects.

C.3.3 *Matrix Expressions and Normal Equations*

The above model can be presented in matrix terms as follows:

$$
\textbf{Vector of Observations} = \vec{Y} =
\begin{bmatrix}
5.95 \\
6.18 \\
5.40 \\
5.95 \\
5.54 \\
5.48 \\
6.43 \\
6.52 \\
5.40 \\
6.82
\end{bmatrix}
\quad \textbf{10X1}
$$

Design Matrix = X =

$$
\begin{bmatrix}
1 & 0 & 0 & 0 & 0 & 0 & 0 & 0 & 0 \\
1 & 0 & 1 & 0 & 0 & 0 & 0 & 0 & 0 \\
1 & 0 & 0 & 1 & 0 & 0 & 0 & 0 & 0 \\
1 & 0 & 0 & 0 & 1 & 0 & 0 & 0 & 0 \\
1 & 0 & 0 & 0 & 0 & 1 & 0 & 0 & 0 \\
1 & 0 & 0 & 0 & 0 & 0 & 1 & 0 & 0 \\
1 & 1 & 0 & 0 & 0 & 0 & 0 & 0 & 0 \\
1 & 1 & 0 & 0 & 0 & 0 & 0 & 0 & 0 \\
1 & 1 & 0 & 0 & 0 & 0 & 0 & 1 & 0 \\
1 & 1 & 0 & 0 & 0 & 0 & 0 & 0 & 1
\end{bmatrix}
$$

10X9

Vector of Parameters = $\hat{\beta}$ =

$$
\begin{bmatrix}
\hat{\beta}_0 \\
\hat{\beta}_1 \\
\hat{\beta}_2 \\
\hat{\beta}_3 \\
\hat{\beta}_4 \\
\hat{\beta}_5 \\
\hat{\beta}_6 \\
\hat{\beta}_7 \\
\hat{\beta}_8
\end{bmatrix}
$$

9X1

X'X =

$$
\begin{bmatrix}
10 & 4 & 1 & 1 & 1 & 1 & 1 & 1 & 1 \\
4 & 4 & 0 & 0 & 0 & 0 & 0 & 1 & 1 \\
1 & 0 & 1 & 0 & 0 & 0 & 0 & 0 & 0 \\
1 & 0 & 0 & 1 & 0 & 0 & 0 & 0 & 0 \\
1 & 0 & 0 & 0 & 1 & 0 & 0 & 0 & 0 \\
1 & 0 & 0 & 0 & 0 & 1 & 0 & 0 & 0 \\
1 & 0 & 0 & 0 & 0 & 0 & 1 & 0 & 0 \\
1 & 1 & 0 & 0 & 0 & 0 & 0 & 1 & 0 \\
1 & 1 & 0 & 0 & 0 & 0 & 0 & 0 & 1
\end{bmatrix}
$$

9X9

$$\mathbf{X'Y} = \begin{bmatrix} 59.67 \\ 25.17 \\ 6.18 \\ 5.40 \\ 5.95 \\ 5.54 \\ 5.48 \\ 5.40 \\ 6.82 \end{bmatrix}_{9X1}$$

The least square normal equations for the general linear regression model are:

$$(\mathbf{X'X})\hat{\beta} = \mathbf{X'Y}$$

where $\hat{\beta}$ is the least square estimator

Therefore,

$$10\hat{\beta}_0 + 4\hat{\beta}_1 + \hat{\beta}_2 + \hat{\beta}_3 + \hat{\beta}_4 + \hat{\beta}_5 + \hat{\beta}_6 + \hat{\beta}_7 + \hat{\beta}_8 = 59.67 \qquad (1)$$

$$4\hat{\beta}_0 + 4\hat{\beta}_1 \qquad\qquad\qquad\qquad \hat{\beta}_7 + \hat{\beta}_8 = 25.17 \qquad (2)$$

$$\hat{\beta}_0 \qquad \hat{\beta}_2 \qquad\qquad\qquad\qquad\qquad = 6.18 \qquad (3)$$

$$\hat{\beta}_0 \qquad\qquad \hat{\beta}_3 \qquad\qquad\qquad\qquad = 5.40 \qquad (4)$$

$$\hat{\beta}_0 \qquad\qquad\qquad \hat{\beta}_4 \qquad\qquad\qquad = 5.95 \qquad (5)$$

$$\hat{\beta}_0 \qquad\qquad\qquad\qquad \hat{\beta}_5 \qquad\qquad = 5.54 \qquad (6)$$

$$\hat{\beta}_0 \qquad\qquad\qquad\qquad\qquad \hat{\beta}_6 \qquad = 5.48 \qquad (7)$$

$$\hat{\beta}_0 + \hat{\beta}_1 \qquad\qquad\qquad\qquad \hat{\beta}_7 \qquad = 5.40 \qquad (8)$$

$$\hat{\beta}_0 + \hat{\beta}_1 \qquad\qquad\qquad\qquad\qquad \hat{\beta}_8 = 6.82 \qquad (9)$$

The solution of the above equations yields the following estimates:

$$\hat{\beta}_0 = 5.95$$

$$\hat{\beta}_1 = +0.53 \quad \text{(block effect)}$$

$$\hat{\beta}_2 = +0.23 \quad \text{(limestone vs gravel)}$$

$$\hat{\beta}_3 = -0.55 \quad \text{(slag vs gravel)}$$

$$\hat{\beta}_4 = 0.00 \quad \text{(17A gradation vs 6A gradation)}$$

$$\hat{\beta}_5 = -0.41 \quad \text{(50-50 recycled vs virgin gravel)}$$

$$\hat{\beta}_6 = -0.47 \quad \text{(100\% recycled vs virgin gravel)}$$

$$\hat{\beta}_7 = -1.08 \quad \text{(high tension vs typical tension)}$$

$$\hat{\beta}_8 = +0.34 \quad \text{(high foundation vs low foundation)}$$

We see that the best linear unbiased estimates for effects are (*):

$$\hat{\beta}_1 = 1/2 (Y_7 + Y_8) - Y_1$$

$$\hat{\beta}_2 = Y_2 - Y_1$$

$$\hat{\beta}_3 = Y_3 - Y_1$$

$$\hat{\beta}_4 = Y_4 - Y_1$$

$$\hat{\beta}_5 = Y_5 - Y_1$$

$$\hat{\beta}_6 = Y_6 - Y_1$$

$$\hat{\beta}_7 = Y_9 - 1/2 (Y_7 + Y_8)$$

$$\hat{\beta}_8 = Y_{10} - 1/2 (Y_7 + Y_8)$$

C.3.4 *Student t-test*

The estimate of variance for 1-degree of freedom for the observed data is

```
mean = (6.43 + 6.52)/2 = 6.48
```

$$s^2 = [(6.43 - 6.48)^2 + (6.52 - 6.48)^2]/(2-1) = 0.004$$

$$s = 0.064 = \textit{estimate of } \sigma$$

From (*)

$$\text{Var}(\hat{\beta_1}) = \sigma^2 + (1/4)\sigma^2 + (1/4)\sigma^2 = (3/2)\sigma^2$$

$$\text{Var}(\hat{\beta_2}) = \sigma^2 + \sigma^2 = 2\sigma^2$$

$$\text{Var}(\hat{\beta_3}) = \quad " \quad = \quad "$$

$$\text{Var}(\hat{\beta_4}) = \quad " \quad = \quad "$$

$$\text{Var}(\hat{\beta_5}) = \quad " \quad = \quad "$$

$$\text{Var}(\hat{\beta_6}) = \quad " \quad = \quad "$$

$$\text{var}(\hat{\beta_7}) = \sigma^2 + (1/4)\sigma^2 + (1/4)\sigma^2 = (3/2)\sigma^2$$

$$\text{Var}(\hat{\beta_8}) = \sigma^2 + (1/4)\sigma^2 + (1/4)\sigma^2 = (3/2)\sigma^2$$

Standard error for $\hat{\beta_i}$ is given by

$$\text{SE}(\hat{\beta_i}) = 2\ s$$
$$i = 2,3,\ldots,6$$

Standard error for $\hat{\beta_1}$, $\hat{\beta_7}$ and $\hat{\beta_8}$ is given by

$$\text{SE}(\hat{\beta}_{1,7,8}) = 1.5\ s$$

t-statistics is given by

$$t = (\text{estimate})/(\text{SE})$$

The results are tabulated below:

Contrast	Estimate	SE	t	p-value
Block Effect	$\hat{\beta}_1$=+0.53	0.078	5.90	0.10**
Limestone vs Gravel	$\hat{\beta}_2$=+0.23	0.090	2.60	0.23
Slag vs Gravel	$\hat{\beta}_3$=-0.55	0.090	6.10	0.10**
17A Gradation vs 6A Gradation	$\hat{\beta}_4$=0.000	0.090	0.00	1.00
50-50 Recycled vs Virgin Gravel	$\hat{\beta}_5$=-0.41	0.090	4.60	0.14***
100% Recycled vs Virgin Gravel	$\hat{\beta}_6$=-0.47	0.090	5.22	0.12***
High Tension vs Typical Tension	$\hat{\beta}_7$=-1.08	0.078	12.5	0.05*
High Foundation vs Low Foundation	$\hat{\beta}_8$=+0.34	0.078	4.50	0.14***

 *   = statistically significant at α = 0.05

 ** = statistically significant at α = 0.10

 *** = statistically significant at α = 0.15

APPENDIX D

AREA UNDER CURVES OF TEST SPECIMENS

Figure D-1: Area under the curve for 6A virgin gravel slab used in the computation of EI

Figure D-2: Area under the curve for 6A virgin limestone slab used in the computation of EI
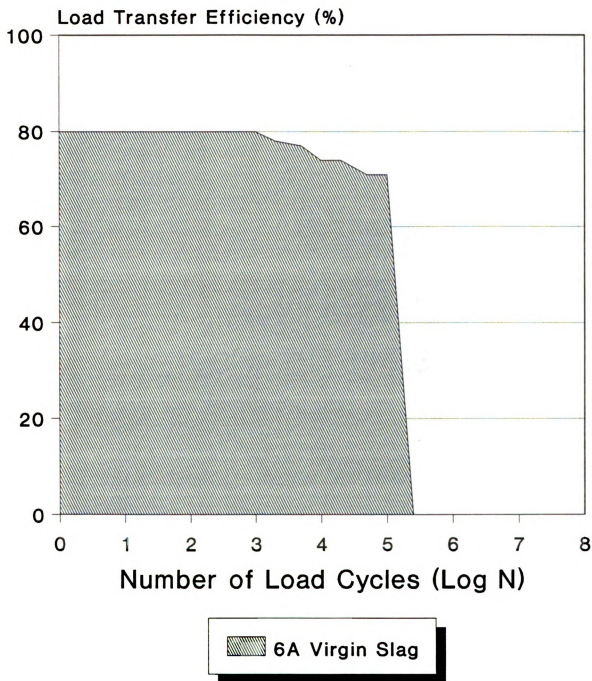
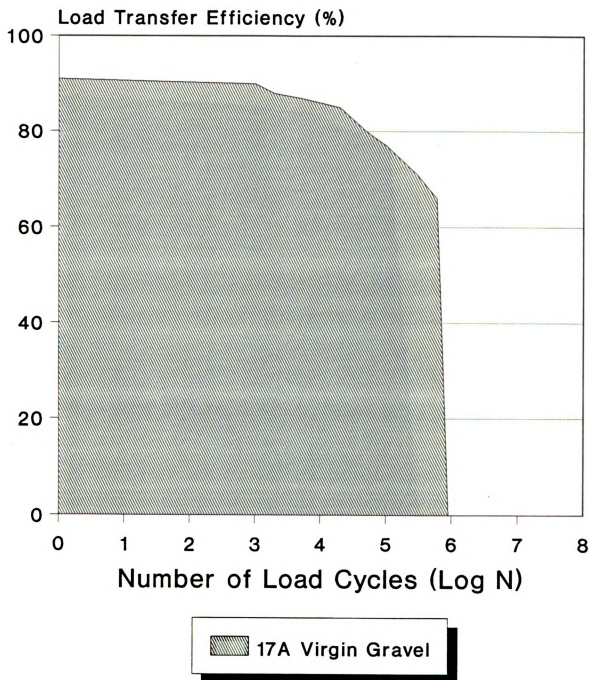**Figure D-3: Area under the curve for 6A virgin slag slab used in the computation of EI**

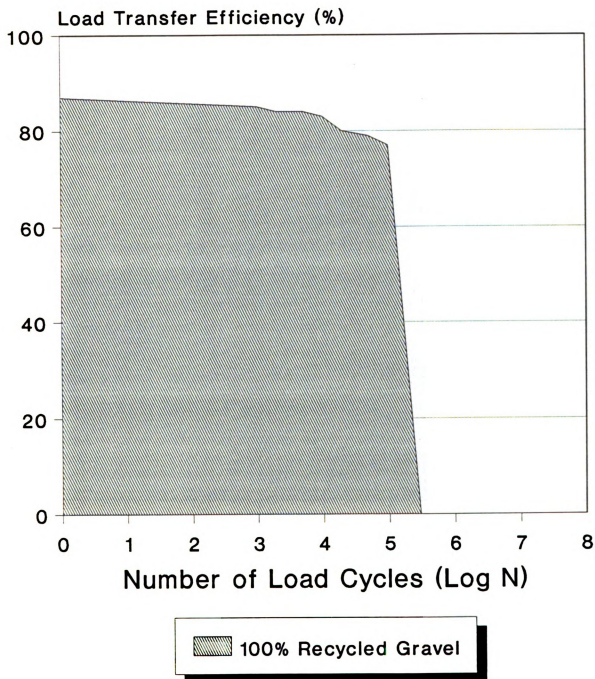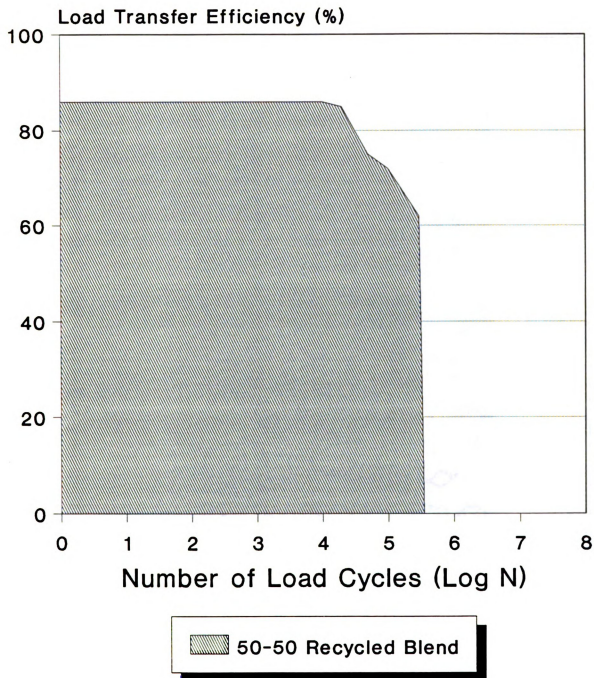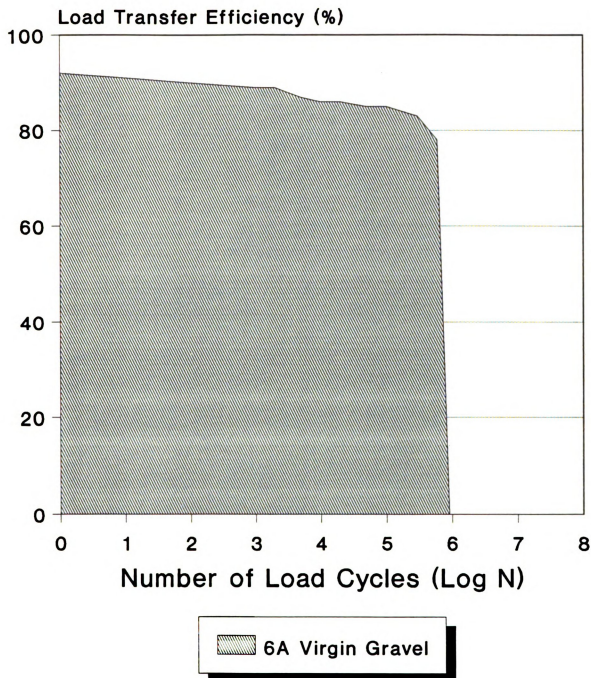Figure D-4: Area under the curve for 17A virgin gravel slab used in the computation of EI

Figure D-5: Area under the curve for 6A 100% recycled gravel slab used in the computation of EI

Figure D-6: Area under the curve for 50-50 recycled blend slab used in the computation of EI

mean = (6.43 + 6.52)/2 = 6.48

s^2 = [(6.43 - 6.48)^2 + (6.52 - 6.48)^2]/(2-1) = 0.004

s = 0.064 = *estimate of* σ

From (*)

$\text{Var}(\hat{\beta}_1) = \sigma^2 + (1/4)\sigma^2 + (1/4)\sigma^2 = (3/2)\sigma^2$

$\text{Var}(\hat{\beta}_2) = \sigma^2 + \sigma^2 = 2\sigma^2$

$\text{Var}(\hat{\beta}_3) = $ " $ = $ "

$\text{Var}(\hat{\beta}_4) = $ " $ = $ "

$\text{Var}(\hat{\beta}_5) = $ " $ = $ "

$\text{Var}(\hat{\beta}_6) = $ " $ = $ "

$\text{var}(\hat{\beta}_7) = \sigma^2 + (1/4)\sigma^2 + (1/4)\sigma^2 = (3/2)\sigma^2$

$\text{Var}(\hat{\beta}_8) = \sigma^2 + (1/4)\sigma^2 + (1/4)\sigma^2 = (3/2)\sigma^2$

Standard error for $\hat{\beta}_i$ is given by

$\text{SE}(\hat{\beta}_i) = 2\ s$

$i = 2,3,\dots,6$

Standard error for $\hat{\beta}_1$, $\hat{\beta}_7$ and $\hat{\beta}8$ is given by

$\text{SE}(\hat{\beta}_{1,7,8}) = 1.5\ s$

t-statistics is given by

t = (estimate)/(SE)

The results are tabulated below:

Contrast	Estimate	SE	t	p-value
Block Effect	$\hat{\beta}_1 = +0.53$	0.078	5.90	0.10**
Limestone vs Gravel	$\hat{\beta}_2 = +0.23$	0.090	2.60	0.23
Slag vs Gravel	$\hat{\beta}_3 = -0.55$	0.090	6.10	0.10**
17A Gradation vs 6A Gradation	$\hat{\beta}_4 = 0.000$	0.090	0.00	1.00
50-50 Recycled vs Virgin Gravel	$\hat{\beta}_5 = -0.41$	0.090	4.60	0.14***
100% Recycled vs Virgin Gravel	$\hat{\beta}_6 = -0.47$	0.090	5.22	0.12***
High Tension vs Typical Tension	$\hat{\beta}_7 = -1.08$	0.078	12.5	0.05*
High Foundation vs Low Foundation	$\hat{\beta}_8 = +0.34$	0.078	4.50	0.14***

$\ast$ = statistically significant at $\alpha = 0.05$

$\ast\ast$ = statistically significant at $\alpha = 0.10$

$\ast\ast\ast$ = statistically significant at $\alpha = 0.15$

APPENDIX D

AREA UNDER CURVES OF TEST SPECIMENS

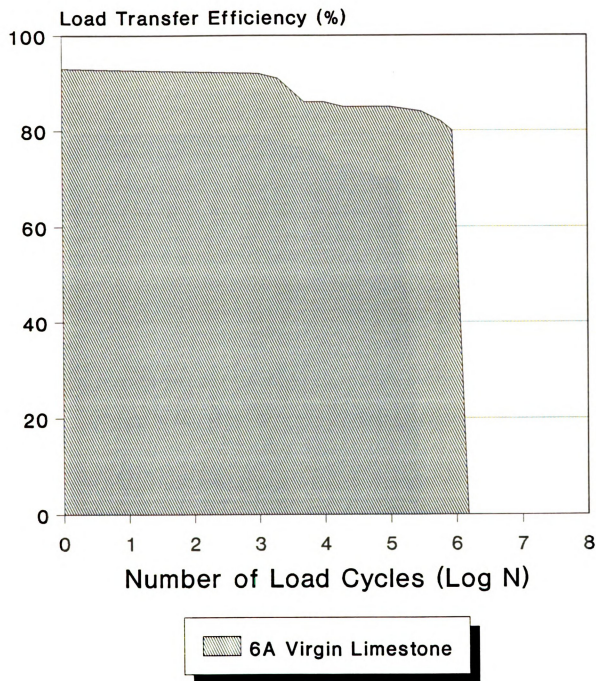**Figure D-1:** Area under the curve for 6A virgin gravel slab used in the computation of EI

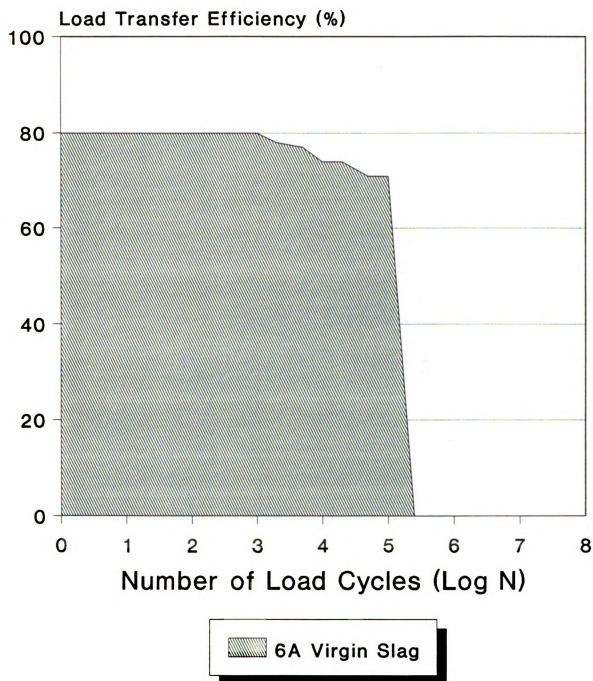Figure D-2: Area under the curve for 6A virgin limestone slab used in the computation of EI

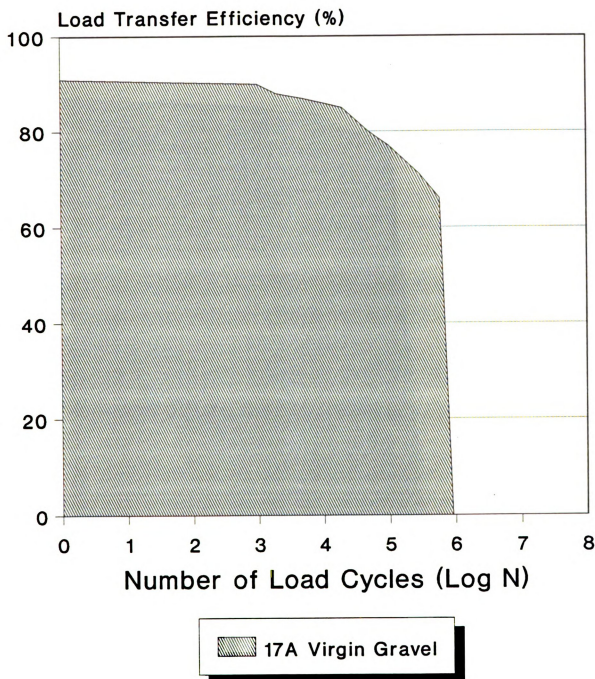Figure D-3: Area under the curve for 6A virgin slag slab used in the computation of EI

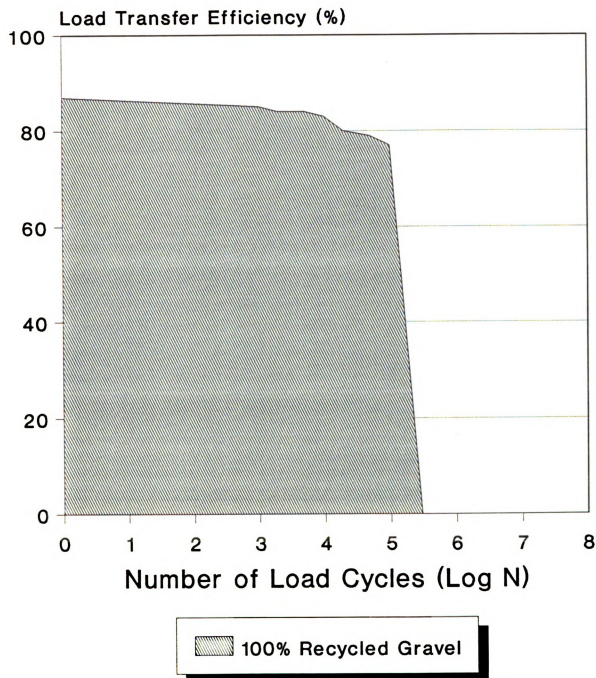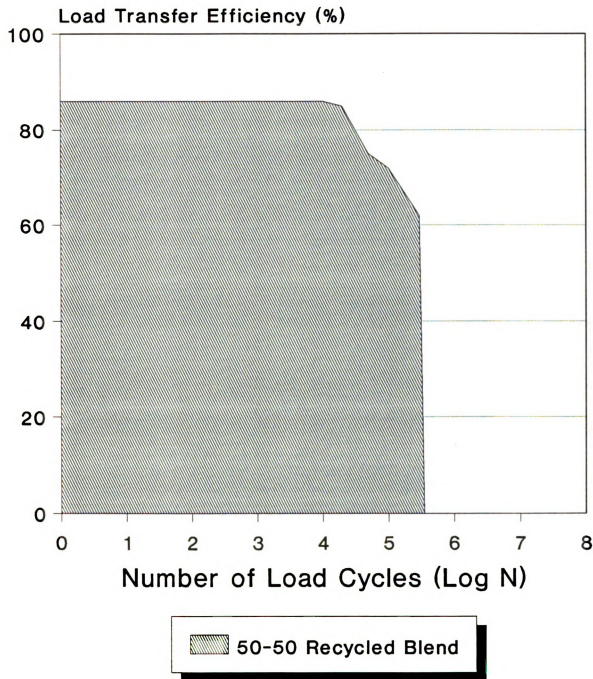Figure D-4: Area under the curve for 17A virgin gravel slab used in the computation of EI

Figure D-5: Area under the curve for 6A 100% recycled gravel slab used in the computation of EI

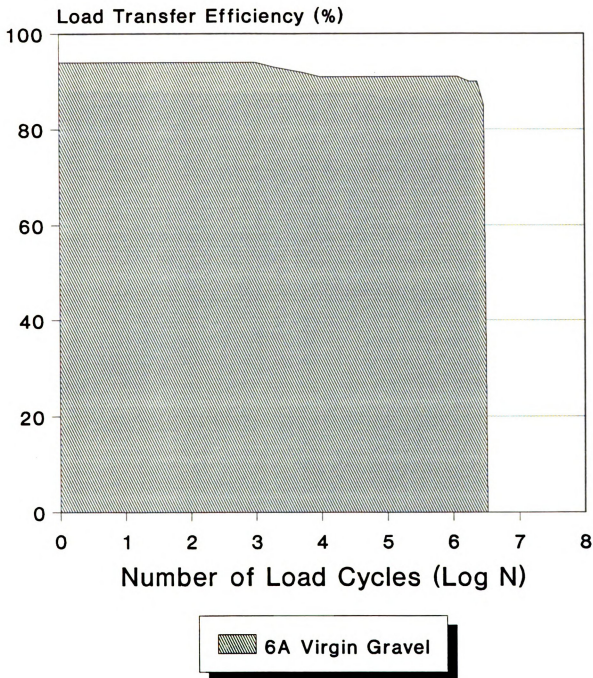Figure D-6: Area under the curve for 50-50 recycled blend slab used in the computation of EI

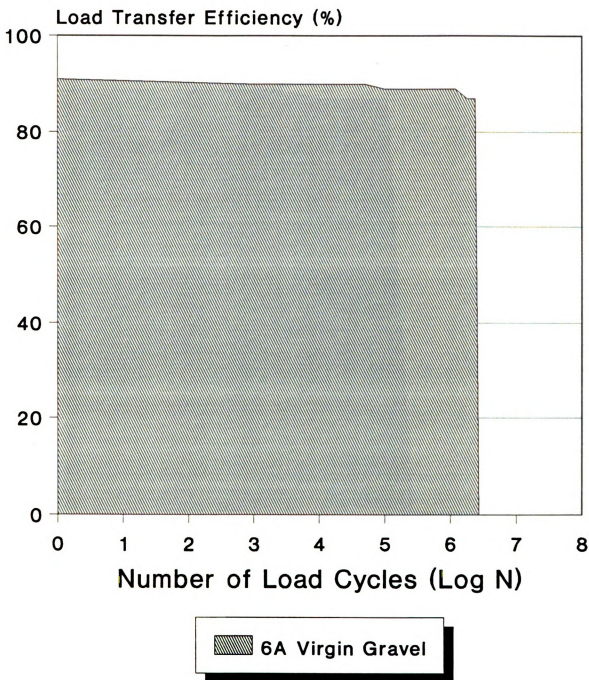Figure D-7: Area under the curve for 6A virgin gravel slab (year 2) used in the computation of EI

Figure D-8: Area under the curve for 6A virgin gravel slab (year 2) used in the computation of EI
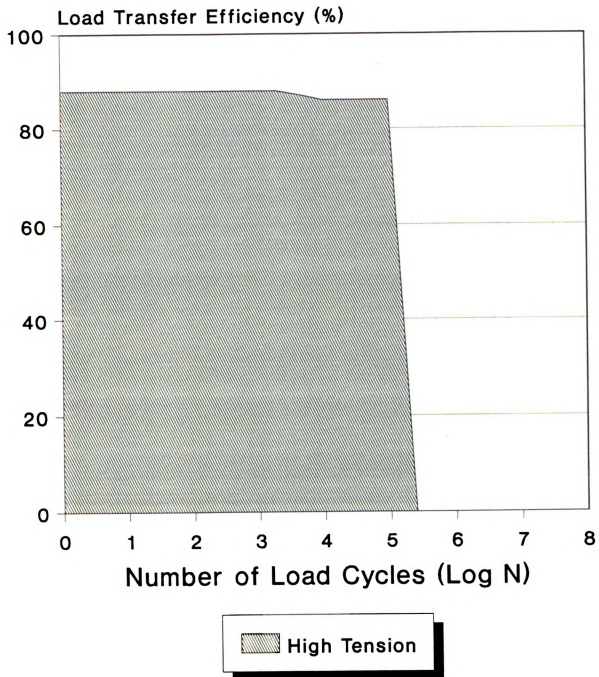
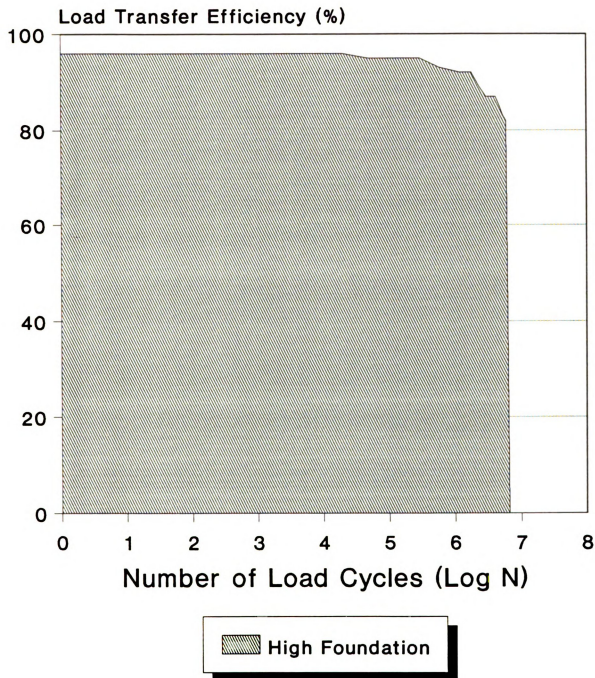Figure D-9: Area under the curve for High tension slab used in the computation of EI

Figure D-10: Area under the curve for high foundation slab used in the computation of EI